CHEM.

BULLETIN
OF THE
CHEMICAL SOCIETY OF JAPAN

CHEMISTRY HALL LIBRARY

Vol. 32 No. 7 July 1959

OHIO STATE UNIVERSITY
AUG 20 1959
LIBRARY

CONTENTS

General and Physical

S. IKEDA and T. ISEMURA: The Roles of Prolyl Residue in Polypeptide Monolayers. II. On the Surface Viscosity and Types of Monolayers. 659

C. V. SURYANARAYANA and K. M. SOMASUNDARAM: Role of Dielectric Constant at the Miscibility Point in the Ternary System 2-Propanol-Water and Carbon Tetrachloride. . . 666

T. KOBAYASHI, Y. TANIZAKI and N. ANDO: Absorption Spectra of Dyes. III. On the Composition of Complexes Formed in Mixtures of Chlorazol Sky Blue FF and *p*-Nitroaniline - γ Acid in Aqueous Solution 675

T. KOBAYASHI, Y. TANIZAKI and N. ANDO: Absorption Spectra of Dyes. IV. Absorption Spectra of Mixtures of Chlorazol Sky Blue FF and Dyes Prepared from Sulfanilic Acid and Cresidine 680

A. TSUJIOKA: The Volume Change on Neutralization of a Strong Acid with a Strong Base. 685

G. YAMAGUCHI and K. SAKAMOTO: Hydrothermal Reaction of Aluminumtrihydroxides. . . 696

K. NISHIMOTO and R. FUJISHIRO: A Convenient Method for the Calculation of the π-Electronic Structures of Aromatic Derivatives. 699

M. HIROTA and Y. URUSHIBARA: Isomerism and Polymorphism of Cinnamic Acids and Deuterated Allocinnamic Acids 703

M. TSUBOI and T. TAKENISHI: On the Difference between L-Forms and the Corresponding DL-Forms of Amino Acids in their Solid-State Infrared Spectra. 726

H. KURODA: Studies on the Graphitization. III. The Sub-Structure of Heat-Treated Coke. 728

S. NAGAKURA and J. TANAKA: Theoretical Study on the Mechanism of the Aromatic Substitution 734

Y. KINOSHITA, I. MATSUBARA and Y. SAITO: The Crystal Structure of Bis(succinonitrilo)-copper(I) Nitrate 741

K. KUCHITSU: Electron Diffraction Investigation on the Molecular Structure of *n*-Butane. . 748

Analytical and Inorganic

T. ISHIMORI and E. NAKAMURA: Distribution of Neptunium between TBP and Some Mineral Acids 713

S. YAMADA and R. TSUCHIDA: Spectrochemical Study of Microscopic Crystals. XIX. The Structure and Absorption Spectra of Fremy's Salt. 721

(Continued on inside cover)

Published by the Chemical Society of Japan

THE CHEMICAL SOCIETY OF JAPAN

(NIPPON KAGAKUKAI)

Founded in 1948

Successor to the former Chemical Society of Japan founded in 1878 and to the Society of Chemical Industry, Japan founded in 1898.

OFFICERS

Munio KOTAKE, *President*, Osaka University, Osaka
Jurô HORIUTI, *Vice-President*, Hokkaido University, Sapporo
Teiji ICHIKAWA, *Vice-President*, Hiroshima University, Hiroshima
Eiichi IWASE, *Vice-President*, Institute of Physical and Chemical Research, Tokyo
Kenichi YAMAMOTO, *Vice-President*, Waseda University, Tokyo

BULLETIN OF THE CHEMICAL SOCIETY OF JAPAN

Editor: Yoshiyuki URUSHIBARA, The University of Tokyo, Tokyo
Assistant Editor: Saburo NAGAKURA, The University of Tokyo, Tokyo
Editorial Board:

Toshio ANDO	Kei MATSUZAKI	Tadao SHIBA
Genjiro HAZATO	Koji NAKANISHI	Osamu SIMAMURA
Kenichi HONDA	Shigeo OKUMURA	Tadashi SUEHIRO
Isao ICHISHIMA	Kazuo SAITO	Kenzi TAMARU
Masaji KUBO	Naoyasu SATA	Takeo WATASE
Hisao KUROYA	Tetsuro SEIYAMA	Tsuneo YOSHINO

(*Continued from outside cover*)

Organic and Biological

S. MURAHASHI, S. NOZAKURA and M. SUMI: Stereoregular Polymers. II. Polymerization of Alkenyltrimethylsilanes with Ziegler Catalyst. 670

Y. KAWASE: Reactions of Active Methylene Compounds. VI. A New Synthesis of Coumestrol, 6,7'-Dihydroxycoumarino(3',4':3,2)coumarone 690

M. SHIGEMITSU: Syntheses of Chlorinated Copper Phthalocyanines from Chlorophthalic Anhydrides 691

M. OHTA and H. KATO: Non-benzenoid Aromatic Heterocycles. I. Reactions of 4-Pyrone, 4-Thiopyrone, and their Pyrylium Salts with Active Methylene Compounds. 707

K. SUGA, J. ISHII and S. WATANABE: Synthesis of 1,8(9)-*p*-Menthadien-10-yl-carbinol . . . 711

Applied

M. SHIGEMITSU: Color Characteristics of Copper Phthalocyanine and its Chlorinated Derivatives. 693

Short Communications

K. HIROTA and Y. NAKAI: Far Infrared Spectrum of Gaseous Formic Acid 769

K. NAGAI, M. KOBAYASHI and E. NAGAI: Poly-*p*-halostyrenes. I. Preparation of Crystalline Poly-*p*-chlorostyrene 771

H. AKAMATU and M. KINOSHITA: On the Magnetic Susceptibility of Hexabenzocoronene and Triphenylene 773

N. KATSUI: Isodelphinine, a New Alkaloid from Aconitum miyabei, Nakai. 774

T. ABE: Visible Absorption Spectra of Colored Solutions Produced by Adding Alkali to Nitro-, Dinitro- and Trinitro-substituted Benzenes in Acetone 775

CHEMISTRY ROLL LIBRARY

The Roles of Prolyl Residue in Polypeptide Monolayers. II. On the Surface Viscosity and Types of Monolayers

By Shoichi IKEDA and Toshizo ISEMURA

(Received November 17, 1958)

In the preceding paper[1] we have described the effects of prolyl residue in polypeptide monolayers revealed in the surface pressure and potential behavior and deduced their roles in the chain configuration, chain flexibility and intrachain interaction in the polypeptide monolayers. It was found that, as for the polypeptides examined, the presence of prolyl residues makes the monolayers more expanded as their content becomes increased, in spite of the peptide carbonyl groups having the same orientation at the interface. (However, the carbonyl groups in poly-L-proline film are oriented in a different manner.) This expanded nature of monolayer was attributed to the flexible chain configuration of polypeptide arising mainly from the decrease in number of hydrogen bonds. Conversely, the ordinary non-electrolytic polypeptide forms a monolayer of condensed type due to its rigidly held configuration with the strong intrachain hydrogen bonds.

In the study of monolayer the measurement of surface viscosity also gives information concerning its structure and other characteristics. Cumper and Alexander[2], and also Isemura and Hamaguchi[3] established the β-configuration in monolayers of non-electrolytic polypeptides from the surface viscosity measurement. Later, it was noticed[4] that in the monolayer of an amphoteric polypeptide the surface viscosity rises even at the area of low surface pressure if the pH of the aqueous subphase is near the isoelectric point, while the surface viscosity rises at the area of high surface pressure on either side of this pH. Generally, the former behavior appears to be observed in the monolayer of condensed type and the latter in that of expanded type. Such aspects of surface viscosity may be expected in the monolayers of polypeptides with the various proportions and arrangements of prolyl residues and may be related to their chain configuration, chain flexibility and intrachain hydrogen bonding.

In this paper we will report the results of surface viscosity measurements for poly-DL-alanine, poly-L-prolyl-L-leucylglycine and copoly-1:1:1-(L-proline, L-leucine, DL-alanine) and give a further confirmation of inferences obtained from the surface pressure and potential measurements.

Experimental

Materials.—The polypeptide samples were poly-DL-alanine, poly-L-prolyl-L-leucylglycine and copoly-1 : 1 : 1-(L-proline, L-leucine, DL-alanine) which were the same as those reported in the preceding paper[1]. Their degrees of polymerization and spreading solvents were as follows:

	D. P.	Spreading solvent dichloroacetic acid-benzene
Poly-DL-alanine	300	1 : 9
Poly-L-prolyl-L-leucylglycine	13	1 : 4
Copoly-1:1:1-(L-proline, L-leucine, DL-alanine)	129	1 : 4

Methods.—The lower portion of surface pressure was measured by a surface balance of float type and the higher portion (for the other two polypeptides) by a surface balance of hanging plate type. The surface pressures measured by these two balances were ascertained to be identical in the cases of the latter two polypeptides.

Surface viscosity was measured by the damped rotatory oscillation of a disk, utilizing the relation

$$\eta = \frac{2.303 I \cdot \Delta\lambda}{2\pi P}\left(\frac{1}{a^2} - \frac{1}{b^2}\right)$$

where I is the moment of inertia of the disk, P the period of oscillation, $\Delta\lambda$ the difference between logarithmic decrements of oscillation in the presence of film and in its absence, a the radius of disk and b the distance between the center of disk and the edge of trough. Usually an outer edge concentric with the disk is put on the aqueous surface in order to calculate surface viscosity by means of the above formula, but its

1) T. Isemura and S. Ikeda, This Bulletin, **32**, 178 (1959).
2) C. W. N. Cumper and A. E. Alexander, *Trans. Faraday Soc.*, **46**., 235 (1950).
3) T. Isemura and K. Hamaguchi, This Bulletin, **27**, 125 (1954).
4) T. Isemura and K. Hamaguchi, ibid,. **27**, 339 (1954).

use makes the reproducibility of measurement unsatisfactory for the monolayer of condensed type such as poly-DL-alanine, because it is difficult for it to flow into the annular region under high compression and it makes a heterogeneous film. It was found that substantially equal values of surface viscosity can be obtained for monolayers of expanded type such as copoly-1 : 1 : 1-(L-proline, L-leucine, DL-alanine) whether the concentric edge is put on or not. Hence, all the measurements were carried out on the surface without concentric edge. In the present apparatus, I was measured to be 43.45 g. cm^2, P 7.50 sec., a 1.28 cm. and b 7.00 cm. and the measurable range of surface viscosity was 10^{-3} to 2×10^{-1} surface poise, where the flow was Newtonian.

To regulate the temperature, a glass serpentine coil was put in the trough, through which water at constant temperature was passed from a thermostat.

Results

The surface pressure-area (*II-A*) and surface viscosity-area (η-*A*) curves of poly-DL-alanine are shown in Fig. 1. The monolayer is of condensed type. Surface

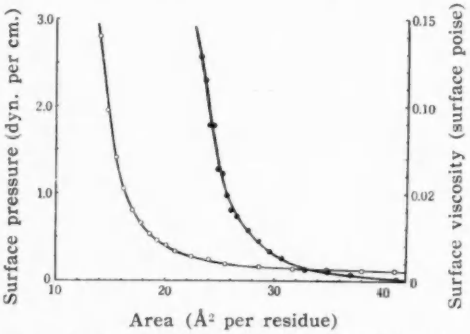

Fig. 1. The surface pressure-area (○) and surface viscosity-area (●) curves of poly-DL-alanine at 9°C.

viscosity begins to rise at the area of 42 Å^2 per residue and gelates at 22 Å^2 per residue and at the surface pressure lower than 0.3 dyn. per cm. Surface viscosity of poly-DL-alanine could be readily measured at room temperature. It appears to be slightly affected by temperature and to increase with the rise of temperature. However, its temperature dependence was not reproducible.

The *II-A* and η-*A* curves of polyl-L-prolyl-L-leucylglycine and copoly-1 : 1 : 1-(L-proline, L-leucine, DL-alanine) are shown in Figs. 2 and 3, respectively. Both films are of expanded type. While their close-packed areas are 57 and 46 Å^2 per three amino acid residues, respectively, both surface

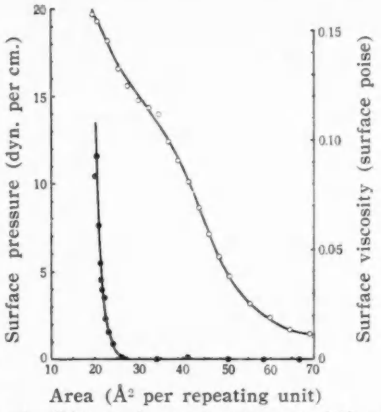

Fig. 2. The surface pressure-area (○) and surface viscosity-area (●) curves of poly-L-prolyl-L-leucylglycine at 16.7°C.

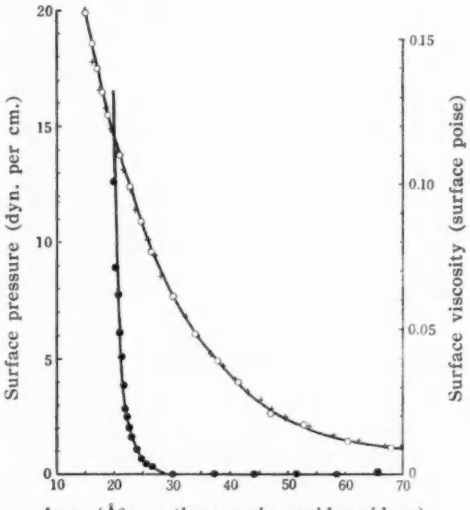

Fig. 3. The surface pressure-area curve (○, at 10.8°C; +, at 26.4°C) and the surface viscosity-area curve (●, at 16.7°C) of copoly-1:1:1-(L-proline, L-leucine, DL-alanine).

viscosities rise at the area less than about 29 Å^2 per three amino acid residues. The corresponding surface pressures range over 15 to 21 dyn. per cm. for the former polypeptide and over 10 to 16 dyn. per cm. for the latter, as the latter film is more expanded than the former. Thus these two polypeptides show almost the same behavior in surface viscosity, irrespective of their different behaviors in surface pressure.

It should be added here that surface

viscosities of these two polypeptides rise at such a small area that films can not occupy an area large enough to spread as complete monolayers. They were initially spread on the surface with an area therefore of about 80 Å^2 per three amino acid residues which is not a sufficiently large area compared with the close-packed areas, and the *II-A* curves in Figs. 2 and 3, therefore, shift to a smaller area than those obtained when spread on larger areas. The film of copoly-1 : 1 : 1-(L-proline, L-leucine, DL-alanine) was readily compressed even in the high surface pressure region, but the film of poly-L-prolyl-L-leucylglycine required some minutes after compression to establish the final surface pressure.

Surface viscosities of poly-L-prolyl-L-leucylglycine and copoly-1 : 1 : 1-(L-proline, L-leucine, DL-alanine) were found to be markedly dependent of temperature. They were quite reproducible and, to some extent, reversible for compression and expansion. The variation of η-*A* curves with temperature are shown in Figs. 4 and 5, for the respective polypeptide. The higher the temperature is, the lower is the surface viscosity. Both values of surface viscosity and their temperature dependence are almost identical for these two polypeptides. However, as illustrated in Fig. 3, surface pressure was not changed by temperature.

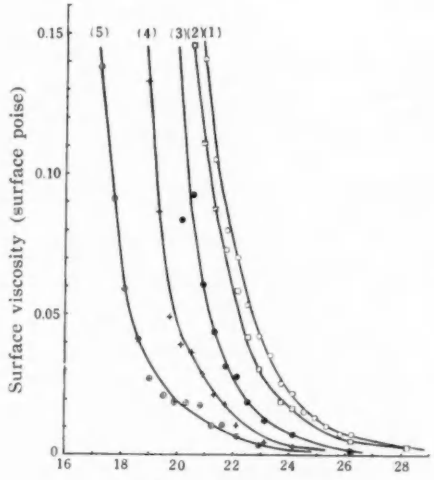

Fig. 4. The variation of surface viscosity-area curves of poly-L-prolyl-L-leucylglycine with temperature. Curves (1) 6.9°, (2) 10.0°, (3) 16.7°, (4) 21.5° and (5) 30.4°C.

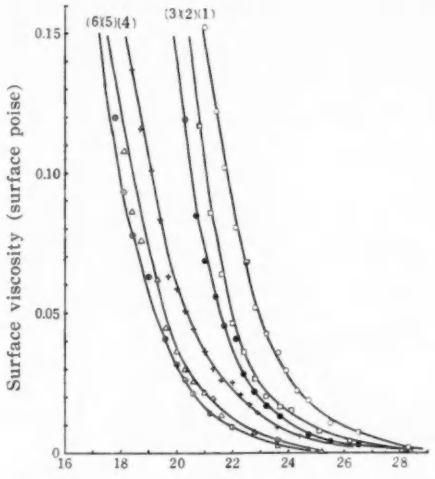

Fig. 5. The variation of surface viscosity-area curves of copoly-1 : 1 : 1-(L-proline, L-leucine, DL-alanine) with temperature. Curves (1) 4.7°, (2) 10.7°, (3) 16.7°, (4) 20.5°, (5) 25.6° and (6) 29.9°C.

Discussion

Surface Viscosity as a Function of Surface Pressure. — It was noticed that surface viscosity of poly-DL-alanine film is already high at the area where surface pressure is sufficiently low and surface viscosities of the other two polypeptide films are detected at the area where surface pressures are considerably high. In other words, surface viscosity of condensed film is actually measured for the monomolecular layer, but that of expanded film is presumably for folded monolayer. Such a difference in surface viscosity was already pointed out by Isemura and Hamaguchi[4] for the film of an electrolytic copolypeptide. It may be attributed to

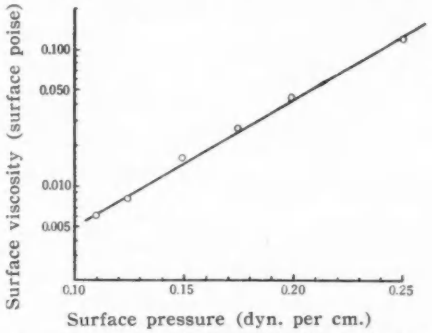

Fig. 6. The log η-Π curve of poly-DL-alanine.

the difference in chain configurations of spread polypeptides.

The monolayer of poly-DL-alanine is of condensed type. It was found that for the condensed films of fatty acids[5] and their mixtures[6] the logarithm of surface viscosity is in a linear relation to surface pressure. As shown in Fig. 6, the poly-DL-alanine monolayer follows the same relation as fatty acid films over the region of temperature, 8 to 12°C, and of area, 24 to 34 Å^2 per residue, although the surface pressure at which surface viscosity was measured is much lower. This relation is expressed by

$$\log \eta = \log K + c\Pi \qquad (1)$$

where $\log K$ and c are constants, the values of which are shown in Table I.

TABLE I

	$\log K$	c	B
Poly-DL-Ala	-3.2_3	9.24	0
Poly-L-Pro-L-Leu-Gly	−22.5	0.46	3560
Copoly-(L-Pro, L-Leu, DL-Ala)	−17.3	0.33	3370

On the other hand, poly-L-prolyl-L-leucylglycine and copoly-1 : 1 : 1-(L-proline, L-leucine, DL-alanine) give monolayers of expanded type. It was observed[7] that for the expanded monolayer of polyvinyl acetate the logarithm of surface viscosity changes also linearly with surface pressure at constant temperature. Joly[8] has tabulated the values of surface viscosity as a function of surface pressure for various protein films. These films are probably of expanded type, as they are spread on 0.01 N hydrochloric acid and will be ionized completely. If these values are plotted on a semilogarithm scale, again linear relations are obtained, particularly for the film of gliadin. As shown in Figs. 7 and 8, the films of the two polypeptides also follow the linear relation over the region of temperature, 5 to 30°C, and of area, 21 to 24 Å^2 per three amino acid residues. The relation is written as

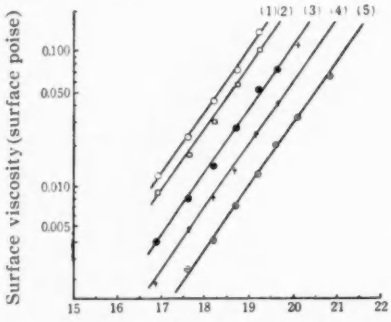

Fig. 7. The $\log \eta$-Π curves of poly-L-prolyl-L-leucylglycine at various temperatures. Curves (1) 6.9°, (2) 10.0°, (3) 16.7°, (4) 21.5° and (5) 30.4°C.

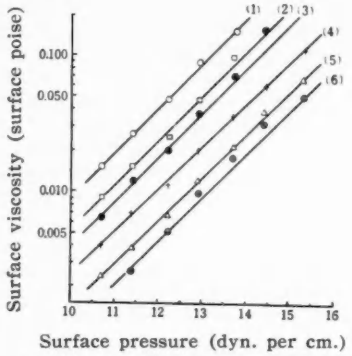

Fig. 8. The $\log \eta$-Π curves of copoly-1 : 1 : 1-(L-proline, L-leucine, DL-alanine) at various temperatures. Curves (1) 4.7°, (2) 10.7°, (3) 16.7°, (4) 20.5°, (5) 25.6° and (6) 29.9°C.

TABLE II

Poly-L-Pro-L-Leu-Gly			
T (°C)	$\log \mu$	c	
30.4	−10.80	0.46_4	
21.5	−10.54	0.45_7	$\log K = -22.7_0$
16.7	−10.21	0.46_3	$B = 3610$
10.0	−9.89	0.46_1	
6.9	−9.76	0.46_8	
Copoly-(L-Pro, L-Leu, DL-Ala)			
T (°C)	$\log \mu$	c	
29.9	−6.29	0.32_4	
25.6	−6.09	0.32_2	
20.5	−5.80	0.31_7	$\log K = -17.2_7$
16.7	−5.76	0.33_3	$B = 3340$
10.7	−5.48	0.32_0	
4.7	−5.42	0.33_5	

$$\log \eta = \log \mu + c\Pi \qquad (2)$$

where c is a constant but $\log \mu$ is a function of temperature, as seen in Table II. Further, the temperature dependence of $\log \mu$ is found to be given by

$$\log \mu = \log K + B/T \qquad (3)$$

where $\log K$ and B are constants, the

5) G. E. Boyd and W. D. Harkins, *J. Am. Chem. Soc.*, **61**, 1188 (1939).
6) G. E. Boyd and F. Vaslow, *J. Colloid Sci.*, **13**, 275 (1958).
7) T. Isemura and K. Fukuzuka, *Mem. Inst. Sci. Ind. Res., Osaka Univ.*, **13**, 137 (1956).
8) M. Joly, "Surface Chemistry", But-terworths Scientific Publications, London (1949), p. 157.

values of which are also shown in Table II.

Surface Viscosity as a Function of Temperature. — As mentioned before, surface viscosity of poly-DL-alanine monolayer scarcely varies with temperature but tends to increase slightly as temperature is raised. This appears to be a general aspect of the monolayer of condensed type.

For the films of poly-L-prolyl-L-leucylglycine and copoly-1 : 1 : 1-(L-proline, L-leucine, DL-alanine) surface viscosities diminish as temperature rises and it was found that plots of logarithm of surface viscosity against the inverse of temperature are linear over the region of temperature, 5 to 30°C, and of areas, 21 to 24 Å^2 per three amino acid residues, as illustrated in Figs. 9 and 10. That is, the relation is fitted to the Andrade equation

$$\log \eta = \log \nu + B/T \qquad (4)$$

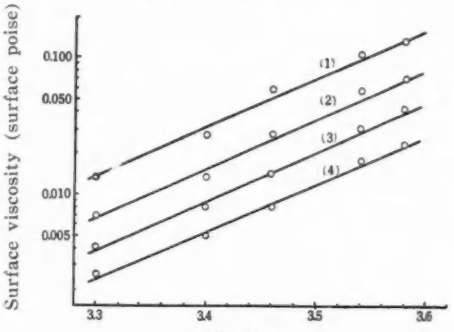

Fig. 9. The $\log \eta - 1/T$ curves of poly-L-prolyl-L-leucylglycine at various areas (at various surface pressures). Curves (1) 21.0 Å^2, (2) 22.0 Å^2, (3) 23.0 Å^2 and (4) 24.0 Å^2.

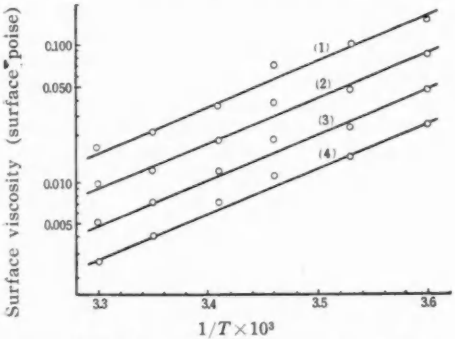

Fig. 10. The $\log \eta - 1/T$ curves of copoly-1 : 1 : 1-(L-proline, L-leucine, DL-alanine) at various areas (at various surface pressures). Curves (1) (21.0Å^2, (2) 22.0 Å^2, (3) 23.0 Å^2 and (4) 24.0 Å^2.

TABLE III

Poly-L-Pro-L-Leu-Gly

Π(dyn./cm.)	$\log \nu$	B	
19.2	−13.61	3520	
18.7	−13.92	3580	$\log \nu = -22.4_9$
18.2	−14.12	3610	$c = 0.46$
17.6	−14.38	3500	

Copoly-(L-Pro, L-Leu, DL-Ala)

Π(dyn./cm.)	$\log \nu$	B	
13.7	−12.88	3320	
12.9	−13.14	3370	$\log \nu = -17.3_0$
12.4	−13.41	3390	$c = 0.32$
11.4	−13.66	3390	

where B is a constant but $\log \nu$ depends on surface pressure. This has already been established for films of polyvinyl acetate[9] and 6-nylon[10], although the dependence of $\log \nu$ on surface pressure is not explicitly indicated. The values of B and $\log \nu$ are given in Table III. It can be seen that $\log \nu$ is represented by

$$\log \nu = \log K + c\Pi \qquad (5)$$

as a function of surface pressure, where both $\log K$ and c are constants the values of which are also shown in Table III.

From the data given in Tables II and III, numerical coincidences may be noticed between $\log K$ in Eqs. 3 and 5, between c in Eqs. 2 and 5 and between B in Eqs. 3 and 4. Consequently, the surface viscosity equation is reduced to

$$\log \eta = \log K + c\Pi + B/T \qquad (6)$$

for the films of poly-L-prolyl-L-leucylglycine and copoly-1 : 1 : 1-(L-proline, L-leucine, DL-alanine). Values of constants are listed in Table I. The values of B for these two polypeptides are found to be almost equal to each other, which should be the necessary condition for the equal temperature coefficient of surface viscosity.

Configuration and Flexibility of Polypeptide Chains. — In comparing the close-packed area with the area where surface viscosity was measured, it will be evident that surface film in this region corresponds to liquid or melt in bulk rather than to dilute solution, and accordingly, surface viscosity to viscosity of liquid or melt. It is generally accepted that a transition takes place at the glass temperature or the second-order transition temperature for polymers, below which the segmental motion becomes frozen-in. The segmental motion is exhibited in the behavior of

9) T. Isemura and K. Fukuzuka, *Mem. Inst. Sci. Ind. Res., Osaka Univ.*, **14**, 169 (1957).
10) K. Inokuchi, This Bulletin. **28**, 453 (1955).

melt viscosity[11]. At the transition temperature melt viscosity decreases markedly with the rise of temperature. While above the transition temperature melt viscosity alters with temperature in such a way as expressed by the Andrade equation, below that temperature it is not influenced by temperature very much but rather depends on other complicated factors[12]. The temperature at which such freezing-in of the segmental motion will occur depends on the structural factors such as inter- or intrachain interaction, chain flexibility or steric effect. Then at a given temperature a polymer will behave as liquid or glass whether that temperature is higher or lower than the glass temperature. This idea can be adequately applied to explain the observed behavior of surface viscosity of monolayer. Thus the monolayers of expanded type and condensed type might be correlated reasonably with a melt and glassy state in bulk, respectively. In other words, a spread polymer which gives a film of expanded type will behave as an ordinary liquid at the temperature where film properties are measured, since the segmental interaction is weak and the molecular chain is flexible; also the segmental motion of a spread polymer in a film of condensed type is inhibited at that temperature, since the chain is rigidly held owing to the strong segmental interaction. The difference is revealed most distinctly in surface viscosity behavior.

Eyring et al.[13,14] derived the surface viscosity equation by a simple analogy with liquid viscosity, regarding monolayer as a two-dimensional liquid. According to them, surface viscosity is expressed by

$$\eta = \frac{\boldsymbol{h}}{A_f} \exp\left(\frac{\Delta F^*}{\boldsymbol{k}T}\right) \tag{7}$$

where $\boldsymbol{h}$ is the Planck constant, $\boldsymbol{k}$ the Boltzmann constant and A_f is the area occupied by a unit of flow. The free energy of activation for flow per unit, ΔF^*, is given by

$$\Delta F^* = \Delta E^* + \Pi \Delta A^* - T\Delta S^* \tag{8}$$

where ΔE^* and ΔS^* are the energy and the entropy of activation per unit, respectively, and ΔA^* is the increment of area in the activated state over that of the initial state. Substituting Eq. 8 into Eq. 7, the final equation becomes

$$\ln \eta = \ln \frac{\boldsymbol{h}}{A_f} - \frac{\Delta S^*}{\boldsymbol{k}} + \frac{\Delta A^*}{\boldsymbol{k}T}\pi + \frac{\Delta E^*}{\boldsymbol{k}T} \tag{9}$$

This equation has the same form as Eqs. 1 and 6. From their comparison it can be seen that

$$\Delta E^* = 2.303\,\boldsymbol{k}B \tag{10}$$

$$\Delta A^* = 2.303\,\boldsymbol{k}Tc \tag{11}$$

$$\frac{\boldsymbol{h}}{A_f} \exp\left(-\frac{\Delta S^*}{\boldsymbol{k}}\right) = K \tag{12}$$

Thus ΔE^* and ΔA^* may be calculated from the data in Table I. Although the value of ΔS^* can not be determined uniquely from a single experimental value of $\log K$, its approximate value may be assigned, as it is not very sensitive for the choice of values of A_f. Table IV shows these data for the polypeptide films studied in the present investigation.

TABLE IV

	ΔE^* (kcal./mol.)	ΔA^* (Å²)	ΔS^{**} (e. u.)
Poly-DL-Ala	0	8000	−110∼−120
Poly-L-Pro-L-Leu-Gly	16.3	420	−21∼ −29
Copoly-(L-Pro, L-Leu, DL-Ala)	15.4	300	−45∼ −50

* Values when A_f is assumed to be 10 Å² to ΔA^*

For the monolayer of poly-DL-alanine, ΔE^* was found to be nearly zero. This suggests that the flow mechanism is different from that in liquid state and the polypeptide molecules flow under shear by breaking the entanglement or linkages such as van der Waals or hydrogen bonds between them. This may be expected from the discussion above that such a flow occurs for the film of polypeptide in which the segmental interaction is strong and the rigidity of the chain is high. This result is consistent with that deduced for the condensed nature of this film in the previous paper[1]. Further support is provided by estimating the value of ΔA^*, which was found to be about 8000 Å² per flow unit. Since the close-packed area of poly-DL-alanine is 15 Å² per residue, the area obtained above is occupied by about 500 residues. Taking account of the ambiguity concerning the degree of polymerization of material, 300, it may be roughly assumed that a unit of flow is composed of a poly-DL-alanine molecule. In addition, a large

11) T. Alfrey, G. Goldfinger and H. Mark, *J. Appl. Phys.*, **14**, 700 (1943); E. Jenkel, *Kolloid-Z.*, **120**, 160 (1951).
12) K. Ueberreiter and H. J. Orthmann, ibid., **126**, 140 (1952).
13) E. J. Moore and H. Eyring, *J. Chem. Phys.*, **6**, 391 (1938).
14) S. Glasstone, K. J. Laidler and H. Eyring, "The Theory of Rate Processes", McGraw-Hill Co., New York (1941), p. 561.

negative value for ΔS^*, -120 e. u., was assigned to the polypeptide. In view of the deduction concerning dependence of the entropy of activation for flow in bulk on chain length of polymers[15] and the result on surface viscosity of polyvinyl acetate[7], the entropy of activation for flow in film might be scarcely influenced by the degree of polymerization of polymers, that is, the term involving the degree of polymerization contributes to the entropy only a few e. u. Then the large negative value for ΔS^* should be characteristic of the monolayer of poly-DL-alanine. It might be attributed to the highly disordered configuration of flow unit or molecule of poly-DL-alanine at the interface. Probably the spread molecule is coiled and held together in monolayer.

On the other hand, for the films of poly-L-prolyl-L-leucylglycine and copoly-1 : 1 : 1-(L-proline, L-leucine, DL-alanine) values of ΔE^* are not zero but 16.3 and 15.4 kcal. per mole, respectively, and nearly equal to each other. These are of comparable order of magnitude with those reported, namely, 12.7 kcal. per mole for the film of polyvinyl acetate[9] and 6.4 kcal. per mole for the film of 6-nylon[10], although the sizes of their unit of flow will be different from one another. But the larger values for these two polypeptides than the other might come from the additional energy necessary for breaking (more) hydrogen bonds when units of flow move. The values of ΔA^* were 420 and 300 Å^2 per three amino acid residues, respectively. The size of flow units can not be estimated in the same way as above, as the viscous flow takes place at such small areas that they do not always correspond to a monomolecular layer. The polypeptide chains are probably in a folded configuration partly submerged into the aqueous subphase in these areas. The small negative values of ΔS^*, -25 and -50 e. u., respectively, would be an indication of the relatively regular configuration of chains. Both the mechanism of flow through the activation process and the regular folding of chains under compression favor the weak interaction and the flexibility of chains. This supports the results obtained in the previous paper[1].

All the differences in surface viscosity behavior between poly-DL-alanine and the other two polypeptides are based on the types of monolayers, namely, the nature of condensation and expansion of films. The types of monolayers depend on the structural factors defined by the proportion and arrangement of prolyl residues in polypeptide chains. But the surface viscosities and their temperature dependences were found to be equal to each other for poly-L-prolyl-L-leucylglycine and copoly-1 : 1 : 1-(L-proline, L-leucine, DL-alanine), which will originate from their identical chain configurations, irrespective of their different amino acid sequences in chains. The fact that the surface pressure of the former polypeptide is higher than that of the latter and shows some time effect. will mean that the former chain folds itself by compression with greater difficulty, as described in the preceding paper[1].

15) W. Kauzmann and H. Eyring, *J. Am. Chem. Soc.*, 62, 3113 (1940). See also Ref. 14, p. 501.

Summary

To investigate the roles of prolyl residue in polypeptide monolayers, surface viscosity was measured for the monolayers of poly-DL-alanine, poly-L-prolyl-L-leucylglycine and copoly-1 : 1 : 1-(L-proline, L-leucine, DL-alanine).

For the monolayer of poly-DL-alanine which is of condensed type, the surface viscosity was found to rise at the area larger than the close-packed area and scarcely to be dependent of temperature. This result was correlated with that observed in the glassy state of polymers in bulk and interpreted by assuming that the polypeptide chain is rigid owing to the strong interaction. For the films of the other two polypeptides which are of expanded type appreciable surface viscosities were manifested at the areas much smaller than their close-packed areas and temperature exerted marked influence on surface viscosities. Their chain configurations were considered to be flexible owing to the weak interaction, since the flows in films occur as in melt of polymers in bulk.

Further evidence for this inference was obtained from the results on dependences of surface viscosity on surface pressure and temperature. The dependences were found to follow Eyring's equation of surface viscosity. It was found that in the monolayer of poly-DL-alanine a unit of flow is roughly composed of a molecule and its chain is rather coiled at the interface, but the chains of the other two polypeptides are in a regularly folded configuration partly submerged into the

aqueous phase when compressed, as they are flexible.

The difference in surface viscosity behavior between poly-DL-alanine and the other two polypeptides was related to the condensed and expanded nature of films, which is defined by the content and distribution of prolyl residues in polypeptide chains. It was, however, observed that poly-L-prolyl-L-leucylglycine and copoly-1 : 1 : 1-(L-proline, L-leucine, DL-alanine) exhibit the same surface viscosity behavior, irrespective of their different distribution of prolyl residues in chains, while the former has a higher surface pressure than the latter.

All the results obtained were found to confirm the view deduced from the surface pressure and potential measurements.

The authors are indebted to Dr. H. Tani and Dr. S. Sakakibara of the Faculty of Science, Osaka University, to Dr. J. Kurtz of the Weizmann Institute of Science in Israel and to Professor J. Noguchi of Kanazawa University for the supply of valuable samples. This work was partly supported by a grant given by the Ministry of Education, to which the authors' thanks are also due.

Institute of Scientific and Industrial Research, and Institute for Protein Research
Osaka University, Sakai, Osaka

Role of Dielectric Constant at the Miscibility Point in the Ternary System 2-Propanol–Water and Carbon Tetrachloride

By C. V. SURYANARAYANA and K. M. SOMASUNDARAM

(Received December 26, 1958)

Two liquids are known[1] to be miscible in all proportions when both are sufficiently alike to obey Raoult's law. Only when the internal forces are quite unlike, separation of two liquid phases is known to occur. The fundamental question underlying all problems relating to solubility is the nature and the strength of intermolecular forces. The thermodynamic condition for equilibrium in any system is that the total free energy should be a minimum. If separation into two layers minimises the free energy of the system, it will happen so. Deviations from ideal behavior occur either owing to lowering the temperature or by choosing components more unlike in attractive forces. Either of these changes, when pursued far enough, can bring about a separation into two liquid phases.

A new outlook is developed in the following investigations. The work of Coomber[2] and McC. Lewis[3] shows that dielectric constant of a liquid system is related to its internal pressure. To an inhomogeneous mixture of two liquids progressive addition of a third component which happens to mix with both the liquids entails in a distribution of the added component between the two layers. With successive additions of the third component there is to be expected, as a result of the distribution between the two phases a progressive variation of the physico-chemical properties in the two layers. Just at the miscibility point these properties in the respective layers should tend to a limit at which the phase boundary just disappears forming a homogeneous system. Since internal pressure is connected with the dielectric constant (loc. cit.), at the transition when the phase boundary disappears, we may expect a quantitative relationship among the values of dielectric constant of the solution and those of the three pure components. The ternary system 2-propanol–water–carbon tetrachloride has been studied from the above point of view. We have reported[4] earlier our results on the ternary system 1-propanol–water–toluene.

1) E. Washburn, *Trans. Am. Electrochem. Soc.*, **22**, 330 (1912).
2) D. I. Coomber, *Trans. Faraday Soc.*, **35**, 304 (1939).
3) W. C. McC. Lewis, *Phil. Mag.*, **28**, 104, (1914).
4) K. M. Somasundaram and C. V. Suryanarayana, This Bulletin, **31**, 838 (1958).

TABLE I. 2-PROPANOL-WATER-CARBON TETRACHLORIDE

Mole fraction			Density	Viscosity in centipoises	Dielectric constant
2-Propanol x_1	Water x_2	CCl_4 x_3			
0.4397	0.2385	0.3222	1.1650	1.047	8.09
0.4345	0.3362	0.2291	1.0810	1.114	10.80
0.4101	0.4149	0.1752	1.0480	1.223	13.50
0.3853	0.4788	0.1355	1.0170	1.319	16.05
0.3431	0.5584	0.0986	0.9940	1.452	20.52
0.3057	0.6323	0.0622	0.9625	1.570	24.87
0.2844	0.6591	0.0565	0.9636	1.629	28.01
0.2349	0.7283	0.0364	0.9515	1.723	33.00
0.1939	0.7872	0.0188	0.9380	1.672	40.70

TABLE II

$\sum_3 P_3x_3$	$P_{1,2,3}$	% deviation from the mean value	$\sum_3 L_3x_3$	$L_{1,2,3}$	% deviation from the mean value
42.211	48.48	6.911	0.6946	0.7030	0.6009
40.948	47.73	7.647	0.7572	0.7656	0.5516
39.190	45.45	7.396	0.7967	0.8065	0.6113
37.545	43.14	6.937	0.8259	0.8337	0.4700
35.112	39.97	6.471	0.8559	0.8666	0.6212
32.913	36.32	4.920	0.8847	0.8886	0.2200
31.811	35.26	5.142	0.8908	0.9003	0.5304
29.196	31.54	3.860	0.9097	0.9141	0.2413
27.010	28.49	2.667	0.9264	0.9298	0.1832

TABLE III. 2-PROPANOL-WATER

Mole fraction		Density	Viscosity in centipoises	Dielectric constant
2-Propanol x_1	Water x_2			
—	1.0000	0.9941	0.7225	72.94
0.0232	0.9770	0.9813	0.947	71.00
0.0514	0.9486	0.9692	1.248	66.25
0.0956	0.9044	0.9499	1.639	58.22
0.1578	0.8422	0.9226	1.954	49.72
0.1914	0.8086	0.9097	2.040	45.98
0.2619	0.7381	0.8857	2.116	38.62
0.3526	0.6474	0.8618	2.095	32.47
0.4829	0.5171	0.8354	1.938	26.51
0.6797	0.3203	0.8072	1.699	20.70
0.8819	0.1183	0.7866	1.529	18.35
1.0000	—	0.7736	1.550	17.50

TABLE IV

$\sum_2 P_2x_2$	$P_{1,2}$	% deviation from the mean value	$\sum_2 L_2x_2$	$L_{1,2}$	% deviation from the mean value
—	17.42	—	—	0.9610	—
18.551	18.57	0.0512	0.9586	0.9590	0.0209
19.908	19.90	0.0201	0.9552	0.9559	0.0366
22.051	22.05	0.0023	0.9503	0.9504	0.0053
25.070	25.17	0.1991	0.9432	0.9419	0.0690
26.690	26.86	0.3174	0.9393	0.9376	0.0906
30.130	30.38	0.4130	0.9317	0.9262	0.2960
34.510	34.77	0.3753	0.9212	0.9128	0.4580
40.825	41.05	0.2748	0.9065	0.8948	0.6204
50.368	50.12	0.2468	0.8843	0.8680	0.9303
60.274	59.73	0.4533	0.8617	0.8523	0.5484
—	65.91	—	—	0.8484	—

TABLE V. 2-PROPANOL-CARBON TETRACHLORIDE

Mole fraction		Density	Viscosity in centipoises	Dielectric constant
2-Propanol x_1	CCl_4 x_2			
—	1.0000	1.5652	0.7942	2.205
0.1721	0.8279	1.4500	0.8910	2.84
0.3180	0.6820	1.3460	0.8742	3.84
0.4248	0.5752	1.2680	0.8710	5.09
0.5556	0.4444	1.1680	0.8828	7.04
0.6238	0.3762	1.1110	0.9042	8.60
0.8251	0.1749	0.9389	1.0300	13.10
0.8748	0.1252	0.8919	1.0510	14.30
0.9326	0.0674	0.8390	1.1090	15.68
0.9623	0.0377	0.8168	1.1350	16.27
1.0000	—	0.7736	1.5500	17.80

TABLE VI

$\sum_2 P_2 x_2$	$P_{1,2}$	% deviation from the mean value	$\sum_2 L_2 x_2$	$L_{1,2}$	% deviation from the mean value
—	28.66	—	—	0.2865	—
34.66	36.13	2.077	0.3832	0.3802	0.393
40.19	44.79	5.413	0.4654	0.4863	2.196
44.20	51.87	7.984	0.5252	0.5769	4.690
49.13	57.66	7.989	0.5988	0.6680	5.463
51.69	61.49	8.660	0.6367	0.7169	5.926
59.29	65.24	4.779	0.7499	0.8013	3.313
61.15	65.69	3.582	0.7777	0.8160	2.403
63.36	65.73	1.836	0.8105	0.8305	1.219
64.48	65.12	0.491	0.8272	0.8358	0.517
—	65.91	—	—	0.8484	—

Experimental

Preparation of solutions, measurements of dielectric constant, density and viscosity were done as given in our previous paper (loc. cit., this bulletin).

Purification of the Components.—E. Merck's purest 2-propanol was refluxed[5,6] with an excess of freshly burnt calcium oxide and distilled. The distillate was dried over small pieces of magnesium ribbon and fractionally distilled. The fraction boiling at 82.4°C was collected and stored in a pyrex bottle. E. Merck's pro analysi carbon tetrachloride was distilled, the distillate boiling at 76.8°C was collected and stored in a Pyrex bottle. Conductivity water was distilled once more in a Pyrex outfit and this was preserved free from carbon dioxide. A dielectric constant check was made now and then. This was used throughout the investigation.

All the experiments were performed at 35°C. Results obtained are given in Tables I to VI.

Discussion

In our previous publication in this bulletin[1] on the ternary system 1-propanol–water–toluene we had derived the equation

$$\sum_k L_k x_k = L_{1,2\cdots k} \qquad (1)$$

where L_k is the volume polarization of the k-th component, $L_{1,2\cdots k}$, that of the mixture of k components and x_k, the mole fraction. This derivation was made on the usual assumption of isomegethic solutions as done in some theories of solutions which means that

$$\bar{v}_1 = \bar{v}_2 = \cdots\cdots = \bar{v}_k \qquad (2)$$

On this assumption,

$$V_k = \frac{v_k}{\sum v_k} = \frac{n_k \cdot \bar{v}_k}{\sum n_k \cdot \bar{v}_k} = \frac{n_k}{\sum n_k} = x_k$$

But the above assumption 2 is not correct with real solutions. We rarely meet with solutions wherein the molecules of the components have the same molar volume. We shall now consider the consequences of this assumption.

Turning to the experimental values, Table II shows that Eq. 1 holds excellently well at the point of disappearance of the phase boundary, whereas the well known equation.

$$\sum_k P_k \cdot x_k = P_{1,2\cdots k} \qquad (3)$$

fails thoroughly.

5) A. I. Vogel, "Practical Organic Chemistry", Longmans, 2nd Ed., London (1951), p. 168.
6) A. A. Maryott, *J. Am. Chem. Soc.*, **63**, 3079 (1941).

Comparison of Tables IV and VI shows that in the case of 2-propanol–water system both Eq. 1 and 3 hold excellently, whereas with 2-propanol–carbon tetrachloride system both the Eq. 1 and 3 are inapplicable. Akerlöf[7] determined the dielectric constants of mixtures of 2-propanol–water at 25°C. Our data in Table III were collected at 35°C.

In this laboratory[8] the general observation made was that in about thirteen ternary systems investigated so far, Eq. 3 fails thoroughly while Eq. 1 succeeds just at the point of disappearance of the phase boundary. Further in polar-polar binary mixtures both Eqs. 1 and 3 are applicable, whereas in polar-nonpolar binary combinations both Eqs. 1 and 3 fail. From these observations one conclusion can be drawn, that Eq. 1 is in now way better than Eq. 3 in general but the former seems to be holding excellently at the transition of disappearance of the phase boundary.

We have pointed out above that the derivation of Eq. 1 assumes that the molar volumes of the participating species of molecules must be the same, which is not really so, as far as the three components 2-propanol, water and carbon tetrachloride are concerned. Even then, if Eq. 1 should hold good specially at the transition of disappearance of the phase boundary, one has to conclude that at the transition when the two phases should disappear, conversely one should obtain the condition that the molar volumes of the different species of molecules must be the same. That means condition 2 is satisfied at the transition. This may perhaps mean that for two phases to become homogeneous condition 2 is to be satisfied.

Let us examine the implication of condition 2 being satisfied at the transition of the disappearance of the phase boundary. Usually we obtain the molar volume of a substance by dividing the molecular weight by the macroscopic bulk density. The molar volume thus obtained is actually due to the molecules as well as the voids. Obviously such a computation is no indication of the actual size of the molecules. Molar volume thus obtained may be written as $(V_{ma}+\phi_v)$, where V_{ma} is the actual volume due to the molecules and ϕ_v that due to the voids. In this context, if Eq. 1 holds good at the transition of the disappearance of the phase boundary, by converse the condition

$$(V_{ma}+\phi_v)_1=(V_{ma}+\phi_v)_2=(V_{ma}+\phi_v)_3 \quad (4)$$

is valid. Of course ϕ_v is a characteristic constant for a given liquid at a particular temperature. In other words satisfaction of condition 4 seems to be a precondition for liquid-liquid miscibility. Relation 4 seems to imply that just at the transition when a phase boundary disappears to form a homogeneous system, there seems to be occurring an equipartition of space by the different species of molecules, irrespective of their sizes, constituting the homogeneous system resulting from the disappearance of the phase boundary. For a successful theory of liquid–liquid miscibility the future seems to revolve on a thorough understanding of the ϕ_v factor in Eq. 4 in all its qualitative and quantitative aspects.

In the binary system 2-propanol-carbon tetrachloride the viscosity variation is anomalous. A plot of viscosity against mole per cent of 2-propanol shown in the graph exhibits a minimum at about 45 mole per cent of 2-propanol. Sugden[9] explained a similar phenomenon of negative viscosity in aqueous solutions as due to the strong dipole action of one of the constituents in the solution having the effect of depolymerizing the associated molecules of the other constituent entailing in a decrease of viscosity. But in this binary system carbon tetrachloride molecule is not a dipole. Sometimes a shortening of the length of the associated polymers is given as an explanation for lowering of viscosity. But then this presupposes a length of the associated polymer of the alcohol more than that due to two molecules. Of course, we can not assume a long chain formation of a compound between 2-propanol and carbon tetrachloride. The situation, therefore, leaves us in doubt as to what is the causative factor for such a decrease in viscosity.

Summary

To understand why a heterogeneous system of two immiscible liquids so exists without mixing we have made a new approach of studying the physical properties of the system just at the transition of the disappearance of the phase

7) G. Akerlöf, ibid., **54**, 4125 (1932).
8) K. M. Somasundaram, Ph. D. thesis, Annamalai University (1958).
9) J. N. Sugden, *J. Chem. Soc.*, **1926**, 183.

boundary after the addition of an optimum amount of a third component which is freely miscible with the two heterogeneous components thus resulting in the formation of a ternary system. At the transition of the disappearance of the phase boundary we have found that $\sum_3 L_3 x_3 = L_{1,2,3}$, wherein L represents volume polarization and x the mole fraction, holds good. The implications of the validity of the above equation have been discussed.

Physico-Chemical Laboratory
Annamalai University
Annamalainagar
South India

---

*Stereoregular Polymers. II. Polymerization of Alkenyltrimethylsilanes with Ziegler Catalyst**

By Shunsuke MURAHASHI, Shun'ichi NOZAKURA and Masao SUMI

(Received November 17, 1958)

Isotactic polymers of normal α-olefins have been known to have a maximum melting point at polypropylene (165°C), a minimum value at polyhexene-1 (−55°C), and after that show a gradual increase of melting points with the higher members[1,2]. On the other hand, isotactic polymers of branched α-olefins, which are shown in Table I by the general formulae II and III, have considerably higher melting points than those of the corresponding polymers of normal olefins.

The present study was undertaken to see if (i) the polymerization of alkenyltrimethylsilanes with Ziegler catalyst could lead to crystalline polymers and (ii) the similar melting behaviors could be expected in the case of polyalkenyltrimethylsilane having the same structure of monomer as type III of branched olefins.

A survey of the literature of the subject reveals that the polymers of alkenyltrimethylsilanes hitherto obtained are all liquid polymers of low molecular weight. Kanazashi[3] studied the polymerization of vinyltrimethylsilane with peroxide catalysts at 120°C and with Friedel-Crafts catalysts at 150°C, and obtained oily polymer in the former case and no polymer in the latter case. Polymerization of allyltrimethylsilane was attempted by Sommer[4] with Friedel-Crafts catalysts and also by Petrov[5] and Polyakova[6] at 130°C under a high pressure in the presence of peroxide catalysts. However, in both the cases the product was viscous liquid polymers. Polymerization of 3-butenyltrimethylsilane was also carried out by the latter author[6] to yield only a viscous liquid.

The present authors have prepared three alkenyltrimethylsilanes of the general formula $CH_2=CH(CH_2)_nSi(CH_3)_3$ ($n=0, 1$ and 2), i.e., vinyl-, allyl-, and 3-butenyltrimethylsilane, and subjected them to polymerization by means of Ziegler catalyst. It was found from the experiments that the alkenyltrimethylsilanes could polymerize to high polymeric products having high melting points and, furthermore, the polymers were proved to be highly crystalline by X-ray investigation**.

Polymerization. — Polymerization was carried out in *n*-heptane in the presence of Ziegler catalyst, that is, triethylaluminum and titanium tetrachloride. Considering the question from the results of the preceding paper[7], a method which had given a good yield of isotactic polystyrene was adopted in the present study;

* Presented at the 11th Meeting of Chem. Soc. of Japan in Tokyo, April 4, 1958. A brief description of this work was published in *Annual Report of the Institute of Fiber Research (Japan)* (*Sen'ikagaku Kenkyusho Nenpo*), **11**, 23 (1958).

1) F. P. Reding, *J. Polymer Sci.*, **21**, 547 (1956).
2) G. Natta, *Angew. Chem.*, **68**, 393 (1956).
3) M. Kanazashi, This Bulletin, **28**, 44 (1955).
4) L. H. Sommer, L. J. Tyler, F. C. Whitmore, *J. Am. Chem. Soc.*, **70**, 2872 (1948).
5) A. D. Petrov et al., *Doklady Akad. Nauk S. S. S. R.*, **99**, 785 (1954).
6) A. M. Polyakova, et al., *Izvest. Akad. Nauk S. S. S. R., Otdel Khim. Nauk*, **1956**, 978.

** Quite recently Natta and his collaborators have presented a letter and we have learned that they succeeded to prepare the crystalline polymers of allylsilane and of allyltrimethylsilane. G. Natta et al., *J. Polymer Sci.*, **31**, 181 (1958).

TABLE I. MELTING POINTS OF ISOTACTIC POLY-α-OLEFINS

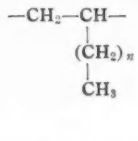

(I)

n	m. p., °C
0	165, 165*
1	128, 120*
2	80, 70*
3	−55*
4	−40*
5	−38*
9	45*
15	70*

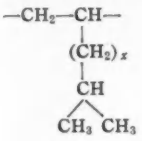

(II)

x	m. p., °C
0	245, 300*
1	205, 235*
2	130

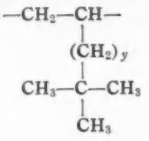

(III)

y	m. p., °C
1	320

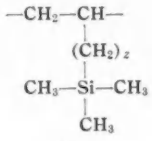

(IV)

z	m. p., °C
0	340
1	258
2	206

The values with asterisks are reported by Reding[1] and the others except the type IV are reported by Natta[2]. The values of type IV are presented by the present authors.

TABLE II. POLYMERIZATION OF ALKENYLTRIMETHYLSILANES WITH ZIEGLER CATALYSTS AT 70°C[a]

$AlEt_3$, g.	$TiCl_4$, g.	Monomer	Wt., g.	Polymn. time, hr.	Conversion, %
0.66	0.47	Vinyltrimethylsilane	2.77	5.5	2.4
0.44	0.27	Allyltrimethylsilane	5.54	9.0	30.2
0.34	0.23	3-Butenyltrimethylsilane	2.76	6.0	44.6

a) Twenty ml. of *n*-heptane were used as a solvent in each run.

TABLE III. SEPARATION OF CRYSTALLINE POLYMERS FROM CRUDE POLYMERS

Polymer	Extracting solvent	Fraction, %	Analysis of fractions					
			C, %		H, %		Si, %	
			Found	Calcd.	Found	Calcd.	Found	Calcd.
Polyvinyltrimethylsilane	Hot toluene	Extract, 44	80.26	85.6[a]	12.49	14.4[a]		
		Residue, 55	58.94	59.91	11.83	12.07	29	28.02
Polyallyltrimethylsilane	Toluene	Extract, 23	64.89	63.14	12.70	12.69	23.03	24.59
		Residue, 72	63.70		12.43		24.19	
Poly-3-butenyltrimethylsilane	Hot ether	Extract, 26	65.93	65.57	12.48	12.49	21.20	21.90
		Residue, 70	65.90		12.66		21.47	

a) Calcd. for $(C_2H_4)_n$, polyethylene.

that is, the catalysts were prepared without stirring and polymerizations were carried out also without stirring.

The conversions of both allyl- and 3-butenyltrimethylsilane were moderately high, but the conversion of vinyltrimethylsilane was very low (Table II).

Separation of Crystalline Polymers. — In the polymerizate of vinylmethylsilane, the existence of polyethylene was recognized from the analytical data and X-ray diffraction pattern. The separation of the polyethylene was effected by extraction with hot toluene. The occurrence of the polyethylene is considered to be due to the polymerization of ethylene which evolved during the preparition of the heterogeneous catalyst[7]. Polyvinyltrimethylsilane is insoluble in most organic solvents.

The amorphous polymer in the polymerizate of allyltrimethylsilane could be separated from the crystalline part by extraction with toluene. It was found that the crystalline part is soluble only in hot high-boiling solvents such as α-methylnaphthalene and dioctylphthalate.

In the case of 3-butenyltrimethylsilane, the separation of amorphous polymer was effected by hot extraction with ether, and also the extraction with cold *n*-heptane was found to be effective, wherein the

7) S. Murahashi, S. Nozakura, M. Sumi and K. Hatada, This Bulletin, in press.

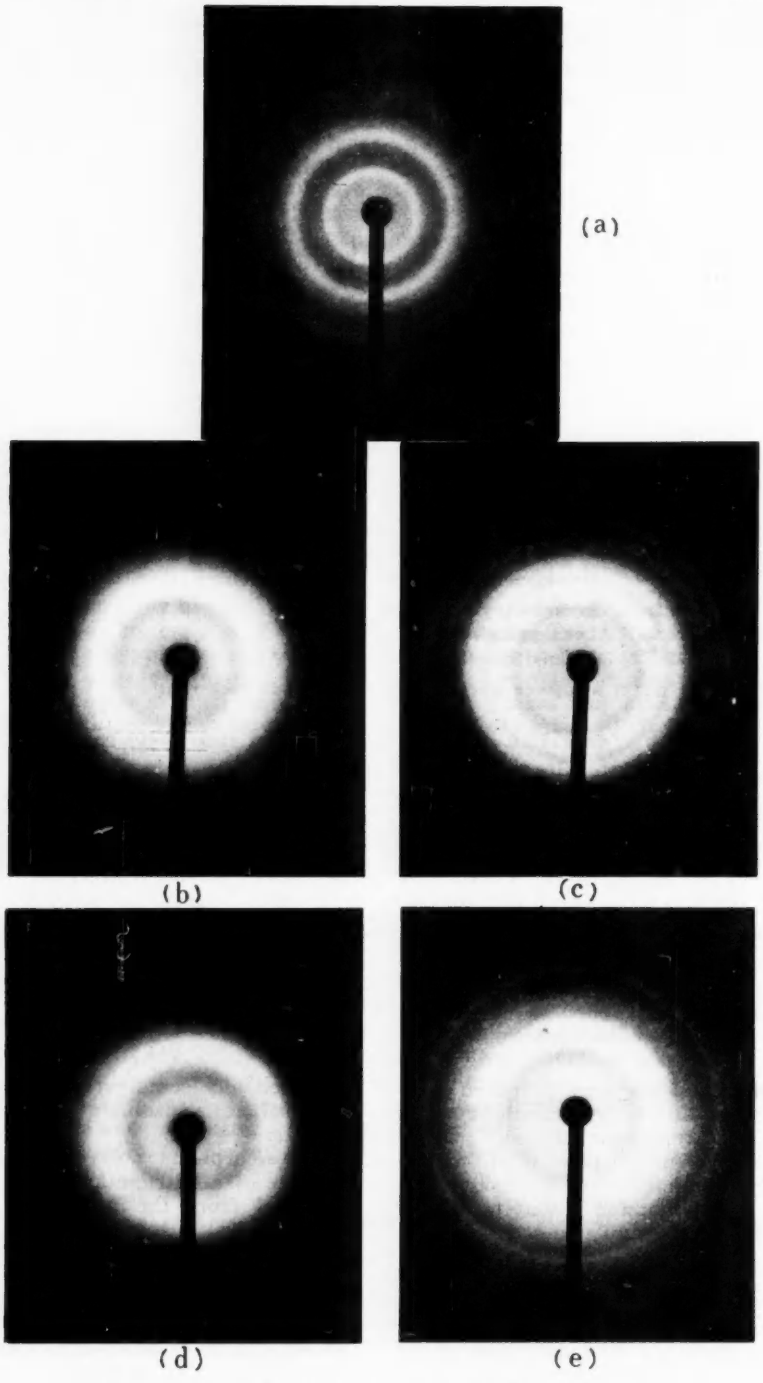

Fig. 1. X-ray diffraction patterns of polyalkenylsilanes.
(a) Polyvinyltrimethylsilane, the insoluble part in hot toluene.
(b) Polyallyltrimethylsilane, the soluble part in toluene.
(c) Polyallyltrimethylsilane, the insoluble part in toluene.
(d) Poly-3-butenyltrimethylsilane, the soluble part in hot ether.
(e) Poly-3-butenyltrimethylsilane, the insoluble part in hot ether.

TABLE IV. SOME PROPERTIES OF POLYALKENYLTRIMETHYLSILANES

Polymer		m. p., °C	*Tg*, °C	Density[a]	Appearance
Polyvinyltrimethylsilane		340[b]	—	0.95	White powder
Polyallyltrimethylsilane	amorph.	—	114	—	Soft solid
	cryst.	258	—	0.895	Hard and brittle
Poly-3-butenyltrimethylsilane	amorph.	—	132	—	Soft solid
	cryst.	206	—	0.889	Hard and brittle

a) Measured at room temperature by flotation method.
b) Upon being heated on a free flame in a nitrogen atmosphere the polymer decomposed to a volatile liquid.

crystalline part was insoluble. It was found to be soluble in decalin and hot tetralin. The experimental results of extraction and the analytical data of both the amorphous and crystalline fractions were summarized in Table III.

Physical Properties.—The X-ray photograph of the extraction residue of polyvinyltrimethylsilane showed a sharp Debye reflection, indicating the highly crystalline nature of the polymer. The photographs of the fractions of polyvinyl-, polyallyl-, and poly-3-butenyltrimethylsilane were presented in Fig. 1. In all the cases the residual part of solvent extraction showed marked crystalline patterns, while the extracts showed only minor extents of crystallinity. From the crystalline part of poly-3-butenyltrimethylsilane an extruded filament was obtained, which could be drawn at 100°C to several times of its original length, and gave a fine X-ray fiber diagram. From the analysis of the fiber diagram, a helical structure containing three monomeric units per identity period was established as follows***.

Rhombic $\begin{cases} a = 10.97\ \text{Å} \\ b = 20.02\ \text{Å} \\ c = 6.46\ \text{Å (fiber axis)} \end{cases}$

No. of monomeric unit in unit cell = 6

ρ(X-ray) = 0.902 g./cm^3

ρ(obsd.) = 0.889 g./cm^3

The crystalline polymers of other monomers than 3-butenyltrimethylsilane considered to be isotactic by analogy to the case of poly-3-butenyltrimethylsilane, but their fiber diagrams could not be obtained because of the difficulty of drawing.

Melting points and glass transition temperatures were determined dilatometrically on the amorphous as well as the crystalline parts of the polymers. The results and other properties are shown together in Table IV. As was expected, the melting points of the crystalline parts are very high in all cases and the polymer with the larger branch has the lower melting points. Particularly, the first member of this series, polyvinyltrimethylsilane has an extremely high melting point and was completely insoluble in all organic solvents examined.

*** Details of the structural annalysis of the polymer will be published elsewhere by Mr. Y. Chatani of Nitta's laboratory. We are very grateful to him for the X-ray data.

Experimental

Monomers. — Vinyltrimethylsilane was synthesized through two different ways. One is the methylation of vinyltrichlorosilane by methylmagnesium bromide[8]. Refluxing the ethereal reaction mixture for 6 hr. gave 58% of the product, b. p. 55.0~55.2°C. The other way is the Wurtz-Wittig's reaction between trimethylchlorosilane and vinylchloride[9]. The yield was 55.6% based on trimethylchlorosilane used, b. p. 55.0~55.2°C.

Allyltrimethylsilane was also synthesized through two alternating methods. One is the methylation of allyltrichlorosilane**** by methylmagnesium bromide[10] and the other is the reaction of allylmagnesium bromide on trimethylchlorosilane[5]. The former yielded 53% of allyltrimethylsilane calculated from allyltrichlorosilane used and the latter yielded only 19.3% of the product after refluxing the ethereal solution for 8.5 hr.

3-Butenyltrimethylsilane was synthesized according to Petrov's method: that is the reaction between allylbromide and trimethylsilylmethylmagnesium chloride[5]. After refluxing the ether solution for 5 hr., 35.2% of the product was obtained, b. p. 118.5~111.7°C.

Materials.—Triethylaluminum was the product of Mitsui Chem. Ind. Co. Thirty percent solution in *n*-heptane was prepared in a modified Schlenk's apparatus and separated in small portions into sealed ampoules.

8) R. Nagel and H. W. Post, *J. Org. Chem.*, **17**, 1379 (1952).
9) M. Kanazashi, This Bulletin, **26**, 493 (1953).
**** Allyltrichlorosilane was kindly offered by Dr. R. Okawara at Faculty of Engineering, Osaka University.
10) C. A. Burkhard, *J. Am. Chem. Soc.*, **72**, 1078 (1950).

Titanium tetrachloride was the product of Osaka Titanium Co. and 21% solution in *n*-heptane was used.

n-Heptane was purified by shaking with fuming sulfuric acid, washing with water and aqueous sodium hydroxide, and was dried over calcium chloride, distilled and stored over sodium chips.

Polymerization. — Polymerization was carried out in the same apparatus as in the preceding paper[7]. The solution of $AlEt_3$ was added first to *n*-heptane and mixed thoroughly, and the solution of $TiCl_4$ was dropped slowy along the wall of the vessel without stirring. The solid brown mass was observed to form at the bottom of the flask. Finally the monomer was added and the polymerization was carried out without stirring.

Polymerization was stopped by adding 2 ml. of methanol and 0.3 ml. of concentrated hydrochroric acid, and the reaction mixture was poured onto about 100 ml. of methanol. After being kept overnight, the polymer was collected and washed thoroughly with methanol. The results of polymerization were given in Table II.

Separation of Crystalline Polymers from Crude Products. — When the crude polyvinyltrimethylsilane was extracted with hot toluene, a precipitate was obtained from the cooled extract. The precipitate was ascertained to be polyethylene from the analytical data and X-ray powder pattern. The insoluble part was nearly pure polyvinyltrimethylsilane.

Crude polyallyltrimethylsilane was refluxed gently with a large volume of toluene for several hours. After being cooled, the insoluble part was separated from the solution by a centrifuge. The intrinsic viscosity of the amorphous part in toluene was 0.087 at 30°C.

In the case of poly-3-butenyltrimethylsilane, the separation was effected by hot extraction with ether using a modified Soxhlet apparatus. The separation could also be done by cooling the hot solution of the crude polymer in *n*-heptane; only the crystalline polymer was precipitated when being cooled, while the amorphous polymer still remained in solution. Intrinsic viscosities of the amorphous and the crystalline part in decalin were 0.169 and 1.21 at 30°C, respectively.

Analysis of Silicon. — Analysis of silicon in the polymers was carried out by wet digestion using fuming sulfuric acid in a platinum crucible. The ignited silica was ascertained by treating with 60% hydrofluoric acid.

Properties. — Melting points and glass transition temperatures were determined dilatometrically. The polymer was melted in vacuum to form a small rod prior to measurement.

Density was measured by the flotation method at room temperature using the mixtures of carbon tetrachloride and alcohol.

Summary

Vinyl-(I), allyl-(II), and 3-butenyl-trimethylsilane(III) were polymerized at 70°C in *n*-heptane with the heterogeneous catalyst of Ziegler's type. The monomer I gave only a small yield of polymer, while the monomers II and III gave moderate amounts of polymers.

The amorphous and crystalline polymers of these monomers were separated by extraction with appropriate solvents. As regards the crystalline polymers, solubility property, density, dilatometrical melting point, and X-ray spectra were described. Glass transition temperatures of the amorphous polymers are also determined.

The authors wish to thank Mitsui Chemical Industry Co. for the supply of triethyltitanium aluminum and Osaka Titanium Co. for tetrachloride.

Department of Chemistry
Faculty of Science
Osaka University
Kita-ku, Osaka

Absorption Spectra of Dyes. III[1]. *On the Composition of Complexes Formed in Mixtures of Chlorazol Sky Blue FF and p-Nitroaniline→γ Acid in Aqueous Solution**

By Teruaki KOBAYASHI, Yoshié TANIZAKI and Noboru ANDO

(Received November 22, 1958)

The fact that complexes are formed between some kinds of dyes in aqueous solution has been revealed by means of spectroscopic measurements[2-4], and the mixtures of some direct dyes have been measured qualitatively in order to investigate the composition of the complexes formed[3,4].

The authors reported in the previous paper[1] that the mixtures of Chlorazol Sky Blue FF and some acid dyes, *p*-X-aniline→γ acid (X=H, CH_3, OCH_3, Cl or NO_2), did not show additive spectra in aqueous solution at room temperature, and that, of these mixtures, a pair of Chlorazol Sky Blue FF and *p*-nitroaniline →γ acid underwent the greatest change in spectrum. In the present paper the authors selected the combination of Chlorazol Sky Blue FF with *p*-nitroaniline→γ acid and investigated its spectrum at 620 mμ where the most remarkable change was seen in the whole region measured, in order to obtain some information about the composition of the complexes formed.

Experimental

Materials.—All the dyes used are the same as those used in the previous paper[1].

Preparation of Samples.—The dye solutions were prepared by using conductivity water whose specific conductivity was about 3.5×10^{-7} mho. All of the concentrations were determined by weight.

Absorption Spectra.—All the absorption spectra of the dyes in aqueous solution were measured by means of the Shimadzu QB-50 or QR-50 spectrophotometer at room temperature. Absorption cells were about 0.2 to 5 cm. thick.

Results

Hereafter Sky Blue will stand for Chlorazol Sky Blue FF, and NO_2-α for the acid dye made by coupling diazotized *p*-nitroaniline with γ acid in acid, and NO_2-β for the same in alkali.

It has already been shown[1] that the absorption spectrum of the mixture of Sky Blue and NO_2-α or NO_2-β in aqueous solution does not coincide with the sum of the spectra of individual dye, and this non-additivity is the most remarkable in the neighborhood of 620 mμ in wavelength. This spectral change is characterized by a marked decrease in optical density, with a slight shift of absorption maxima to longer wavelengths. For example, the absorption spectra of solutions containing

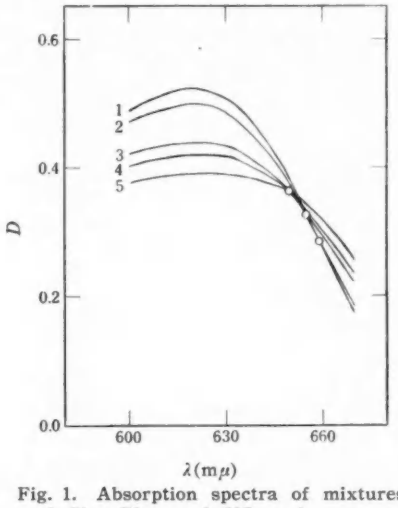

Fig. 1. Absorption spectra of mixtures of Sky Blue and NO_2-α in aqueous solution at room temperature. The concentration of Sky Blue is 1.41×10^{-5} mol./l., and that of NO_2-α is $1=2.72\times10^{-6}$, $2=6.98\times10^{-6}$, $3=2.11\times10^{-5}$, $4=3.51\times10^{-5}$ and $5=8.36\times10^{-5}$ mol./l. The absorption of NO_2-α alone is subtracted from each curve.

1) Part II of this series, Y. Tanizaki, T. Kobayashi and N. Ando, This Bulletin, **32**, 119 (1959).

* This was represented before the 11th Annual Meeting of the Chemical Society of Japan, April 1958.

2) S. M. Neale and W. A. Stringfellow, *J. Soc. Dyers Col.*, **59**, 241 (1943).

3) D. R. Lemin and T. Vickerstaff, *Trans. Faraday Soc.*, **43**, 491 (1947).

4) A. N. Derbyshire and R. H. Peters, *J. Soc. Dyers Col.*, **72**, 268 (1956).

a given amount of Sky Blue and different amounts of NO_2-α are illustrated in Fig. 1, in which each absorption of NO_2-α alone is subtracted from that of the corresponding mixture. The figure shows that the spectra obviously indicate no isobestic point and the intersections of the adjacent curves are gradually shifted to shorter wavelengths. Therefore, it is clear that the formation of only a 1:1 complex does not adequately explain the data over the whole concentration range measured. Plotting the observed optical density, D, of this mixture at 620 mμ in relation to the concentration of NO_2-α, we obtain the curves as shown in Fig. 2, where the concentrations of Sky Blue indicated by the curves I and II are 6.02×10^{-6} and 1.41×10^{-5} mol./l., respectively. Inspection of these curves shows that in either case the optical density decreases with the concentration of NO_2-α to the amount about four times as great as that of Sky Blue, and then increases with the further increase of NO_2-α. The same

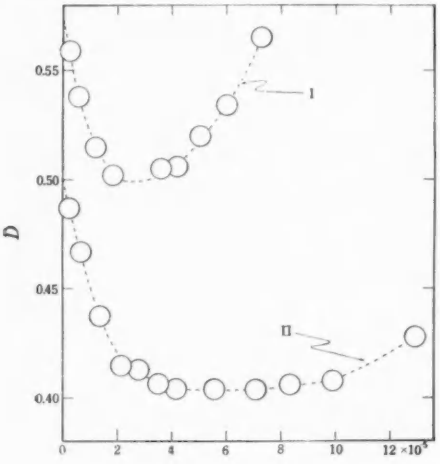

[NO_2-α], mol./l.

Fig. 2. The relation between the observed optical density of the combination of Sky Blue with NO_2-α and the concentration of NO_2-α at 620 mμ.

	The concentration of Sky Blue (mol./l.)	Cell (cm.)
I	6.02×10^{-6}	1
II	1.41×10^{-5}	0.399

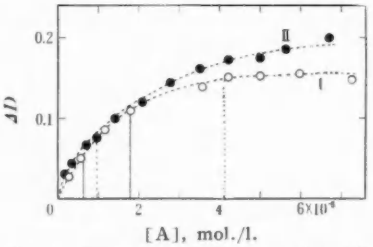

[A], mol./l.

Fig. 3. The relation between the difference in density, ΔD, and the concentrations of the acid dyes at 14~16°C. 1 cm. cell, λ=620 mμ. I: The mixture of NO_2-α and Sky Blue of 6.02×10^{-6} mol./l. II: The mixture of NO_2-β and Sky Blue of $7.15\times^{-6}$ mol./l.

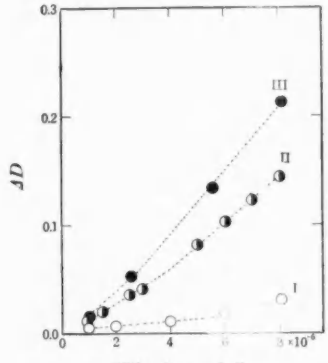

[Blue], mol./l.

Fig. 4. The relation between the difference in density, ΔD, of the combination of Sky Blue with NO_2-α and the concentration of Sky Blue at 14~16°C. 1 cm. thick, λ=620 mμ. The concentration of NO_2-α is I=2.00×10^{-6}, II=2.02×10^{-5} and III=6.41×10^{-5} mol./l.

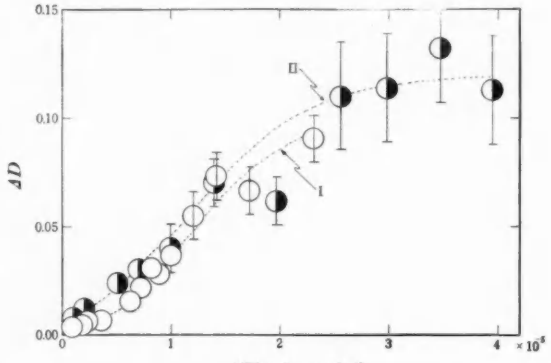

[Blue], mol./l.

Fig. 5. The relation between the difference in density, ΔD, of the combination of Sky Blue with NO_2-α and the concentration of Sky Blue at 20~22°C. 1 cm. thick, λ=620 mμ. The concentration of NO_2-α is I=4.0×10^{-6} and II=5.97×10^{-6} mol./l.

tendency was also observed in the mixture of Sky Blue and NO_2-β.

Now, let us consider the difference between the sum of densities of its components and that of the mixture, ΔD. The relation between ΔD and the concentration of NO_2-α or of NO_2-β for a given concentration of Sky Blue is shown in Fig. 3. Both the curves in the figure curve upwards in the whole region and are inclined to approach certain values.

On the other hand, corresponding series of measurements were also carried out with mixtures containing various amounts of Sky Blue and given amounts of NO_2-α, and the results are shown in Figs. 4 and 5. Here celles were selected so as to make values of density fall in 0.3 to 0.7, but all the observed values were converted into those for 1 cm. cell. Similarly, Fig. 4 indicates the relation between ΔD at 620 mμ and the concentration of Sky Blue, where the curves I, II and III correspond to the concentration of NO_2-α 2.00×10^{-6}, 2.02×10^{-5} and 6.41×10^{-4} mol./l., respectively. Fig. 5 shows the same relation as that in Fig. 4, but the curves I and II correspond to the concentrations of NO_2-α, 4.0×10^{-6} and 5.97×10^{-6} mol./l. The optical densities were measured at about 21°C unlike the former case (at about 15°C). It will be seen at once from these curves that the higher the concentration of acid dye, the more remarkable the difference (Figs. 4 and 5), and that each curve bends downwards and upwards relatively to the low and high concentrations of Sky Blue, respectively (Fig. 5). Moreover, its point of inflexion moves towards a smaller value of concentration of Sky Blue in accordance with an increase in that of NO_2-α. These are distinctly different from the case of the curves of ΔD-concentration of NO_2-α or ΔD-concentration of NO_2-β.

Discussion

Lemin and Vickerstaff[3] showed by the spectroscopic measurement that Chlorazol Sky Blue FF and Durazol Red 2B formes a 1:1 complex in aqueous solution at room temperature. On the other hand, Derbyshire and Peters[4] examined the mixture of Chlorazol Sky Blue FF and Chrysophenine G in aqueous solution by the spectroscopic and calorimetric measurements and concluded that the formation of a 1:1 complex occurs to an appreciable extent even at 90°C, while higher complexes are formed to a certain extent in the presence of an excess of Chrysophenine G. Now, as for the present case, it was stated in the last section that the formation of a 1:1 complex does not explain all the spectral change, judging from the fact that the absorption spectra of solutions containing Sky Blue and NO_2-α showed no isosbestic point anywhere over the region measured (Fig. 1).

The fact that most direct dyes aggregate more or less in aqueous solution and that this aggregation is increased by adding neutral salts has been confirmed by measuring conductivity, absorption spectra, etc.[5] And it has also been recognized that the absorption spectrum of Sky Blue in aqueous solution does not obey Beer's law[3]. In addition, it can safely be considered as a matter of course that another dye added to Sky Blue solution exerts such a salt effect on this dye. In spite of these facts, however, it will be assumed here that the effect of the self-aggregation of the individual dye, which is induced by its increased concentration or by the addition of another dye, can be disregarded as compared with the effect of the complex formation, because the change in optical density of either component caused by increasing its concentration was of comparatively small magnitude compared with that produced by mixing**. Further the change in density of Sky Blue produced by the salt effect of the acid dyes can also be disregarded on account of the fact that an addition of sodium

TABLE I. VARIATION OF MOLAR EXTINCTION COEFFICIENT OF CHLORAZOL SKY BLUE FF IN AQUEOUS SOLUTION AT ROOM TEMPERATURE
1 cm. thick, λ=620 mμ

Solution (mol./l.)	Molar extinction coefficient
5.10×10^{-6}	$9.3_9\times10^4$
9.97×10^{-6}	9.5_2 〃
1.99×10^{-5}	9.3_0 〃
2.99×10^{-5}	9.3_0 〃
3.97×10^{-5}	9.1_1 〃

5) C. Robinson and J. L. Moilliet, *Proc. Roy. Soc.* (*London*), **A143**, 630 (1934); E. Valkó, *Trans. Faraday Soc.*, **31**, 230 (1935); C. Robinson, *Proc. Roy. Soc.* (*London*), **A148**, 681 (1935); N. Ando, *J. Chem. Soc. Japan, Pure Chem. Sec.* (*Nippon Kagaku Zasshi*), **64**, 1192, 1431 (1943); Y. Tanizaki and N. Ando, ibid., **78**, 343 (1957).

** The variation of the molar extinction coefficient of Sky Blue with respect to its concentration is shown in Table I. The measurement was carried out at 620 mμ over a range of concentration up to 3.97×10^{-5} mol./l. This table shows that the deviation from Beer's law is negligible. On the other hand, the aggregation of the acid dye itself, even if it occurs, could be disregarded, because its absorption at 620 mμ is very small.

TABLE II. OPTICAL DENSITY OF CHLORAZOL SKY BLUE FF (6.66×10^{-6} mol./l.) IN SODIUM CHLORIDE SOLUTION AT ROOM TEMPERATURE
1 cm. thick, $\lambda=620$ mμ

Sodium chloride (mol./l.)	Optical density
0	0.62_3
5.23×10^{-6}	0.61_6
1.00×10^{-5}	0.62_1
5.02×10^{-5}	0.61_6
1.02×10^{-4}	0.62_3

chloride to Sky Blue solution, in a range of concentrations comparable to those of the acid dyes used here, showed no significant change in optical density of Sky Blue***. Based on these assumptions, the observed result will be discussed as follows.

Now, in order to investigate the composition of the complexes formed, let us suppose m mol. of Sky Blue, B, and n mol. of any acid dye, A, have produced one mole of complex, C, in solution, that is,

$$m\mathrm{B} + n\mathrm{A} \rightleftarrows \mathrm{C}$$

According to the law of mass action, we can rewrite this as follows:

$$K=[\mathrm{C}]/([\mathrm{B}]-m[\mathrm{C}])^m([\mathrm{A}]-n[\mathrm{C}])^n \quad (1)$$

where [C], [B] and [A] mean the concentration in mol./l. of the complex and the initial concentrations of Sky Blue and the acid dye, respectively; and K is the equilibrium constant. When the absorption layer is regarded as unity, the observed optical density, D_{obs}, at any wavelength of a mixture will be

$$D_{obs}=([\mathrm{B}]-m[\mathrm{C}])\varepsilon_B + ([\mathrm{A}]-n[\mathrm{C}])\varepsilon_A + [\mathrm{C}]\varepsilon_C$$

where ε_B, ε_A and ε_C signify the molar extinction coefficients of Sky Blue, the acid dye and the complex, respectively. On the other hand, the sum of optical densities of the components, D_{sum}, is

$$D_{sum}=[\mathrm{B}]\varepsilon_B+[\mathrm{A}]\varepsilon_A$$

so the difference, ΔD, becomes

$$\Delta D=(m\varepsilon_B+n\varepsilon_A-\varepsilon_C)[\mathrm{C}] \quad (2)$$

Since the molar extinction coefficients may be assumed to be unvarying, ($m\varepsilon_B+n\varepsilon_A-\varepsilon_C$) can be described as a constant, k, provided that m and n are not changed in the entire concentration range of the dyes. As [C] is a function of [B] and [A] (Eq. 1), ΔD can be expressed as a function of them. According to the usual method[3], K and k can be determined. A calculated value of K by making use of the observed values of optical density indicated by full lines in Fig. 3 was 8.0×10^4 for the mixture of Sky Blue and NO_2–α when $m=n=1$. K values calculated by various observed optical densities were not so different from one another. Now, in order to investigate the relation between ΔD and the concentration of NO_2–α, curves were drawn in accordance with Eq. 2. The results are shown in Fig. 6, in which the full lines indicate the calculated ones

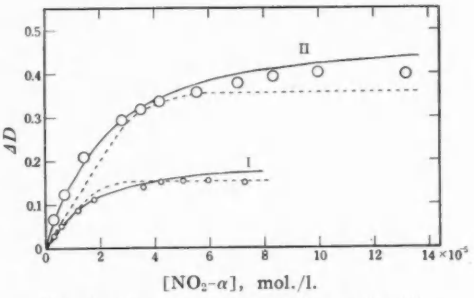

Fig. 6. The comparison between the differences observed and calculated by Eq. 2 for the mixtures of Sky Blue and NO_2–α at 15°C. 1 cm. thick, $\lambda=620$ mμ. The concentration of Sky Blue is I $=6.02\times10^{-6}$ and II $=1.41\times10^{-5}$ mol./l. The full lines signify calculated 1 : 1 curves ($K=8.0\times10^4$), the dotted lines 1 : 2 curves ($K=7.1\times10^{10}$) and the circles the corresponding observed values.

and the circles the corresponding observed values. From the figure it will be seen at once that the curves of $m=n=1$, namely of a 1 : 1 complex, suit the observed values comparatively well. A minute observation shows, however, that the calculated values are somewhat greater than the observed ones where the concentration of NO_2–α is higher than that of Sky Blue. As Derbyshire and Peters reported[4], while Chlorazol Sky Blue FF and Chrysophenine G form a 1 : 1 complex in aqueous solution, they form higher complexes richer in Chrysophenine G in presence of an excess of this dye. If this happens in the present case and higher complexes richer in the acid dye are formed, a curve of $m=1$ and $n=2$,

*** As is shown in Table II, the effect of sodium chloride on Sky Blue solution in a range of concentrations comparable to those of the acid dyes used here is not so great as can be observed, so we leave the salt effect by the acid dye out of consideration.

namely of a 1:2 complex, should fit the observed values better than the 1:1 curve in the higher concentration region of the acid dye. The 1:2 curves ($K=7.1\times10^{10}$ which was calculated by making use of the observed values of optical density shown by the dotted lines in Fig. 3) are indicated by the dotted lines in Fig. 6. These curves differ extremely from the observed ones in the region where the 1:1 curve was rather suitable, but they are more suitable in the higher concentration range of the acid dye where the 1:1 complex curve has not fitted well. These facts suggest that a 1:1 complex is formed first and then higher complexes richer in the acid dye are formed with an increase of its concentration. If this is the case, the region of low concentration of the acid dye in the mixtures containing a given amount of Sky Blue should correspond to that of high concentration of Sky Blue in the mixtures containing a given amount of the acid dye. Actually, the curves of ΔD-concentration of Sky Blue (Figs. 4 and 5) are obviously different in shape from the curves of ΔD-concentration of NO_2-α, and become similar to the 1:1 curve in a region of high concentration of Sky Blue. Probably all the experimental results would be explained by a combination of a 1:1, a 1:2 and other complexes, or by a combination of several complexes different in their compositions. Exactly the same result has been obtained in the mixture of Sky Blue and NO_2-β. It is concluded here that one kind of complex does not explain all the exprimental data, and the comparison between the calculated and observed curves shows that a 1:1 complex occurs to a greater extent over a range of relatively low concentration of acid dye and that higher complexes richer in the acid dye may be formed in the presence of an excess of it.

Summary

1. The change in spectrum at 620 mμ of the mixture of Chlorazol Sky Blue FF and *p*-nitroaniline→γ acid in aqueous solution was measured in detail at room temperature, by varying the concentration of the component dyes.

2. On the assumption that the spectral change is due to the complex formation, the composition of complexes was discussed by comparing the observed and the calculated difference in optical density.

3. It may be supposed that a 1:1 complex occurs to a great extent over a range of low concentration of *p*-nitroaniline→γ acid as compared with that of Chlorazol Sky Blue FF, and that higher complexes are formed in the presence of an excess of the acid dye.

Laboratory of Physical Chemistry
Tokyo Institute of Technology
Meguro-ku, Tokyo

Absorption Spectra of Dyes. IV[1]. *Absorption Spectra of Mixtures of Chlorazol Sky Blue FF and Dyes Prepared from Sulfanilic Acid and Cresidine*

By Teruaki KOBAYASHI, Yoshié TANIZAKI and Noboru ANDO

(Received December 19, 1958)

In the previous papers the authors have reported that binary mixtures of Chlorazol Sky Blue FF and certain monoazo acid dyes in aqueous solution show non-additivity in absorption spectrum at room temperature, explained qualitatively the spectral change assuming the formation of loose complexes[2], and then discussed their compositions[1]. In the present paper, absorption spectra of the binary mixtures in aqueuos solution of Chlorazol Sky Blue FF, as the one component, and dyes prepared from sulfanilic and cresidine, as the other, were analyzed, and the result obtained was examined.

Experimental

Dyes.—Chlorazol Sky Blue FF (called Sky Blue) is the same as used before[1,2]. SC_1 and SC_2 will signify the dye obtained by coupling diazotized sulfanilic acid with cresidine and that obtained by coupling diazotized SC_1 with cresidine. Their structures are as follows:

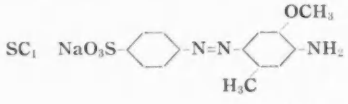

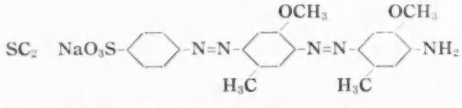

Both of them are carefully prepared from purified intermediates. SC_1 was purified by the recrystallization from water and SC_2 by the Robinson and Mills' method until no change in spectrum was observed. It was noticed that the solubility of SC_2 in water is extremely dependent on pH, and that its flocculent precipitate was easily produced by carbon dioxide from the air. The dye solutions, therefore, were once heated in order to remove carbon dioxide.

Measurements of Absorption Spectra.—All the absorption spectra of the dyes in aqueous solution were measured by means of the Shimadzu QR-50 spectrophotometer at room temperature. Absorption cells used were 0.2, 0.5 and 1 cm. thick. All the experimental values were converted into those corresponding to 1 cm. cell.

Results

The absorption spectrum of a mixture of Sky Blue (7.44×10^{-6} mol./l.) and SC_1 (3.58×10^{-5} mol./l.) is shown by a full line in Fig. 1, together with each spectrum of Sky Blue (curve I) and of SC_1 (curve II). The sum (curve III) of curves I and II coincides completely with the observed one (curve IV) in the whole region measured. The additivity in spectrum, however, does not come into being in the mixtures containing a great excess of SC_1. The results are given in Fig. 2, where the dotted line shows the absorption spectrum of Sky Blue alone (7.42×10^{-6} mol./l.) and curves I and II those of mixtures containing Sky Blue and SC_1 49.4 and 137 times as much as Sky Blue, respectively. In this wavelength region, SC_1 does not absorb light. As this change in spectrum is similar to that of certain benzidine disazo dyes like Sky Blue caused by the salt effect[3], it is supposed that it may be due to the self-aggregation of Sky Blue. Then the variation in optical density at 620 mμ of Sky Blue (7.42×10^{-6} mol./l.) in sodium chloride solution was examined, in order to investigate whether or not the change

TABLE I. VARIATION OF OPTICAL DENSITY OF CHLORAZOL SKY BLUE FF (7.42×10^{-6} mol./l.) IN SODIUM CHLORIDE SOLUTION AT 27°C. 1 cm. cell, λ=620 mμ

Sodium chloride (mol./l.)	Ratio of sodium chloride to Sky Blue	Optical density
0	0	0.73_4
4.05×10^{-4}	54.6	0.73_1
1.01×10^{-3}	136	0.73_0
1.05×10^{-2}	1415	0.70_9

1) Part III of this series, T. Kobayashi, Y. Tanizaki and N. Ando, This Bulletin, **32**, 675 (1959).

2) Y. Tanizaki, T. Kobayashi and N. Ando, ibid., **32**, 119 (1959).

3) Y. Tanizaki and N. Ando, *J. Chem. Soc. Japan, Pure Chem. Sec.* (*Nippon Kagaku Zasshi*), **78**, 343 (1957).

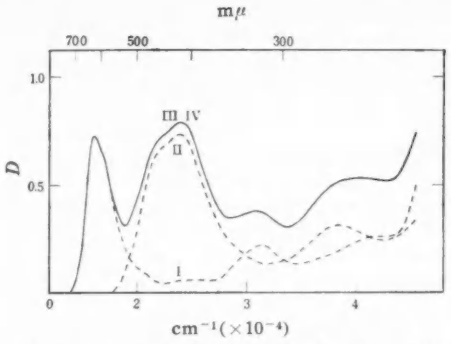

Fig. 1. Absorption spectra of Sky Blue, SC_1 and their mixture in aqueous solution at room temperature (27°C). 1 cm. cell.
I: Sky Blue (7.44×10^{-6} mol./l.)
II: SC_1 (3.58×10^{-5} mol./l.)
III: Sum of curves I and II
IV: Mixture

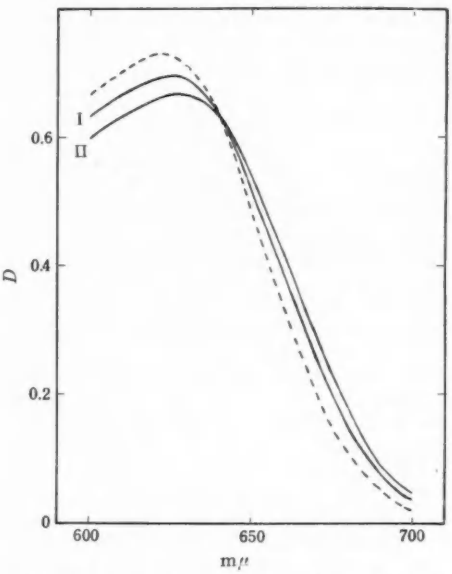

Fig. 2. Absorption spectra of mixtures of Sky Blue (7.42×10^{-6} mol./l.) and SC_1 in aqueous solution at room temperature (27°C). 1 cm. cell.
Dotted line: Sky Blue alone
I: The ratio of concentrations of Sky Blue and SC_1 is 49.4
II: The ratio is 137

is due to the salt effect of SC_1. The results are shown in Table I. It shows clearly that no significant departure from Beer's law is observed, even though the amount of sodium chloride becomes 140 times as much as that of Sky Blue. Therefore, we must consider that the spectral change shown in Fig. 2 is not due to the self-aggregation of Sky Blue caused by the salt effect of SC_1 added, but due to the interaction between the two dyes. It will be seen that the spectra pass through an isosbestic point at about 640 mμ, where the absorption of SC_1 does not appear (Fig. 1). This suggests that one Sky Blue molecule interacts with SC_1 molecules, or that $1:n$ complexes are formed. But the number n of SC_1 component in one complex molecule has not been known. These results mean that even if the additive spectrum appears in an equimolar or nearly equimolar mixture, the spectrum of the same mixture will often become non-additive with an increase of one component, and the interaction between the two components will occur.

The absorption spectrum of a mixture of Sky Blue and SC_2 is given in Fig. 3, where curves I and II show each absorption spectrum of Sky Blue and of SC_2, curve III the sum of them, and curve IV the observed one of the mixture. Inspection of them shows that the observed curve is weaker in intensity than the resultant curve both in the neighborhood of 620 mμ (the first band of Sky Blue) and at absorptions in the ultraviolet region, but stronger in the neighborhood of the first band of SC_2 (505 mμ).

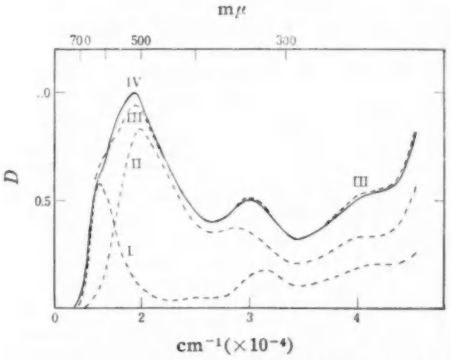

Fig. 3. Absorption spectra of Sky Blue, SC_2 and their mixture in aqueous solution at room temperature (30°C). 1 cm. cell.
I: Sky Blue (5.90×10^{-6} mol./l.)
II: SC_2 (3.01×10^{-5} mol./l.)
III: Sum of curves I and II
IV: Mixture

This spectral change was more systematically examined by varying the concentration of SC_2 and keeping that of Sky

Blue constant (5.90×10^{-6} mol./l.). The results are shown in Fig. 4, in which each absorption of SC_2 is subtracted from the corresponding observed curve. The curves in the figure pass through a well-defined isosbestic point at about 650 mμ; this means that one Sky Blue molecule interacts with a molecule or molecules of SC_2.

On the other hand, the relation between the concentration of SC_2 added and the

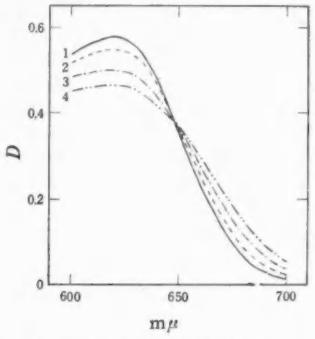

Fig. 4. Absorption spectra of mixtures of Sky Blue and SC_2 in aqueous solution at room temperature (30.5°C), where each absorption of SC_2 is subtracted from the corresponding mixture curve. 1 cm. cell.
Concentration of SC_2 is 1: zero, 2: 6.08×10^{-6}, 3: 3.01×10^{-5} and 4: 1.20×10^{-4} mol./l. that of Sky Blue is 5.90×10^{-6} mol./l;

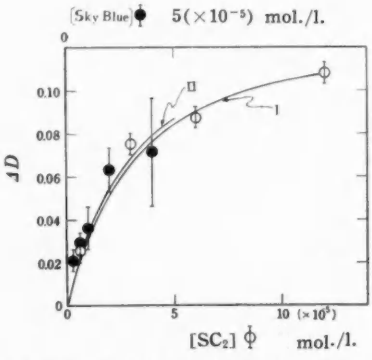

Fig. 5. The relation between the difference in density, ΔD, of the combination of Sky Blue with SC_2 and the concentration of SC_2 or of Sky Blue. 1 cm. cell, $\lambda=620$ mμ. $K=3.8\times10^4$ (at 30.5°C).
I: Calculated difference when the concentration of Sky Blue is constant (5.90×10^{-6} mol./l.); the white circles are corresponding observed values at 30.5°C.
II: Calculated difference when the concentration of SC_2 is constant (6.07×10^{-6} mol./l.); the black circles are representing observed values at 28.2°C.

difference between the sum of optical densities of the components and that of the mixture, ΔD, at 620 mμ is plotted by white circles in Fig. 5. Now, if a 1:1 complex is assumed to be formed in the solution, and if the mass action law is applied to it, an equilibrium constant, K, will be obtained by the method mentioned before[1]. Thus the obtained value of K was 3.8×10^4 at 30.5°C. Here were used the observed values of ΔD, when the concentrations of Sky Blue and of SC_2 are 5.90×10^{-6} mol./l. and up to 1.20×10^{-4} mol./l., respectively. Curve I in the figure was drawn by making use of this value of K. It will be seen at once from the figure that the observed values (white circles) well fit the calculated curve; this means the formation of a 1:1 complex. If a 1:1 complex is formed, the curve of ΔD should show the same feature when the concentration of Sky Blue is varied, while that of SC_2 is kept constant, because of the symmetry of the equation. The curve of ΔD-concentration of Sky Blue is also shown in Fig. 5, where the black circles denote the observed values and curve II the calculated. These two also well fit each other within an experimental error. Therefore, the formation of a 1:1 complex of Sky Blue and SC_2 would well explain all the results obtained.

The absorption spectrum of the 1:1 complex of Sky Blue and SC_2 will, therefore, be obtained experimentally by making use of the equilibrium constant*.

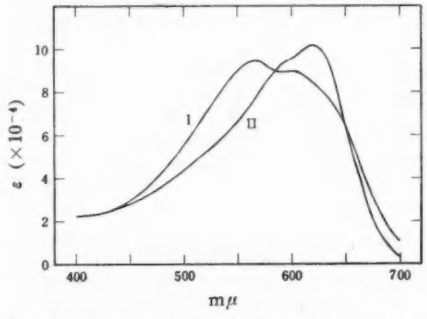

Fig. 6. Absorption spectrum of the 1:1 complex of Sky Blue and SC_2.
I: Complex
II: Sum of absorptions of the components (both 2.9×10^{-6} mol./l.)

* If the equilibrium constant is known, the concentration of the complex corresponding to given amounts of the components can be calculated and then that of the components free from the complex formation will be known. Therefore, the absorption of the complex will be obtained by subtracting absorptions of the free components from that of the mixture.

The absorption spectrum of the complex (curve I) obtained from the experimental results shown in Fig. 3 is indicated in Fig. 6, together with the sum of those of the components (curve II). The figure shows clearly that the absorption of the complex is weaker in intensity than that indicated by the resultant curve at the first absorption band of Sky Blue (620mμ), but stronger at that of SC_2.

Discussion

It has been reported before[1] that Sky Blue and certain monoazo acid dyes (*p*-nitroaniline $\rightarrow\gamma$ acid) form higher complexes richer in the acid dyes in presence of an excess of these dyes, when mixed in water[4]. Though SC_1 and *p*-nitroaniline $\rightarrow\gamma$ acid are both monoazo acid dyes, only the former shows an isosbestic point in spectra when mixed with Sky Blue (Fig. 2). It seems that such a difference has relation to the fact that the substantivity of dyes increases with the length of the conjugated double bonds chain connecting their auxochromes[5], and that at the same time they come to associate with themselves easily[6].

According to measurements of the conductivity of SC_1 and SC_2[6], the association of SC_1 with itself is not noticed over a range of concentrations $(3\sim60)\times10^{-4}$ mol./l., while the formation of ion-micelles of SC_2 is clearly observed. From these results, Ando considered, according to the substantivity theory, that the length of the conjugated double bonds was closely related to the aggregation of SC_1 and SC_2**. It has also been known that, of dyes with various substituents, similar to Congo Red in constitution, those which have the stronger substantivity show the greater spectral change caused by their association[3]. Therefore, though it is impossible to explain briefly the fact that a larger quantity is needed for SC_1 than for SC_2 to cause a change in spectrum when mixed with Sky Blue***, it may be said that this is partly due to the difference in the substantivity of SC_2 and of SC_1.

Derbyshire and Peters[7] obtained experimentally the absorption spectrum of a 1:1 complex of Sky Blue and Chrysophenine G. To be compared with the present result (Fig. 6, curve I), their spectra are shown in Fig. 7, in which curve I shows the absorption of the 1:1 complex and curve II the sum of those of the components. Inspection of these figures shows that the absorption of each mixture corresponding to the first band of the dye combined with Sky Blue shifts to longer wavelengths with an increase in intensity. On the other hand, the absorption corresponding to the peak of the first band of Sky Blue (620 mμ) shifts to longer wavelengths, with a peak getting more distinct, in the complex of Chrysophenine G, while it disappears in the complex of SC_2. Derbyshire and Peters[7] consider that Sky Blue and Chrysophenine G can approach in parallel with each other and form a complex, because while Sky Blue has its charged groups at the ends of the linear molecule, the corresponding groups of Chrysophenine G are near the centre, so the repulsion between them is small. On the other hand, if SC_2, which has its charged group at an end of the molecule, forms a complex in parallel with Sky Blue, it may be repelled by the charged groups of Sky Blue. The difference between the spectra of the two complexes and their stabilities may be related to the fact just mentioned. Further, the fact

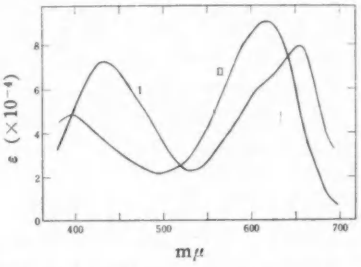

Fig. 7. Absorption spectrum of the 1:1 complex of Sky Blue and Chrysophenine G (quoted from the result of Derbyshire and Peters).
I: Complex
II: Sum of absorptions of the components

4) This fact has been recently confirmed by dyeing measurements from mixtures of the same pairs of dyes. [Y. Horiki, Y. Tanizaki and N. Ando, This Bulletin, to be published.]

5) E. Schirm, *J. prakt. Chem.*, **144**, 69 (1935).

6) N. Ando, *J. Chem. Soc. Japan, Pure Chem. Sec.* (*Nippon Kagaku Zasshi*), **64**, 1305 (1943).

** The number of sulfonic groups per molecular weight of SC_2 is smaller than that of SC_1, and the former is more insoluble in water. This may be one of the reason why SC_2 more easily associates with itself.

*** If a complex is formed from two dyes, the extent of the change in spectrum of the mixture also depends on wavelengths of corresponding absorptions of the component dyes and the relative direction of their transitions (Ref. 2).

7) A. N. Derbyshire and R. H. Petes, *J. Soc. Dyers Col.*, **72**, 268 (1956).

that the increasing order of length of the conjugated chain connecting the auxochromes is SC_2<Sky Blue<Chrysophenine G may also be related to the difference between the spectra, according to the following reason. The first absorption band of a dye has close relation to the electron donating power of its auxochromes containing lone paired electrons[8], which are more easily affected by outer conditions than other π electrons under consideration. It will be seen that if both of the components approach in parallel with each other to form a complex, the auxochromes at both ends of Sky Blue get out of place from the π electron system of SC_2 or only one of them approaches it, though they draw near that of Chrysophenine G.

From the above discussion, it may be considered that the pair of Chrysophenine G and Sky Blue has a smaller intermolecular distance in a complex than that of SC_2 and Sky Blue. The amount of delocalization energy of π electrons between two components in a complex formed from molecules containing no lone pair electrons has been estimated[9]. If this idea can be applied to the present discussion, it will turn out that the pair of Chrysophenine G and Sky Blue is more stable than that of SC_2 and Sky Blue, and that the spectral change of the former is also larger; that is, in case of the former the electron transition corresponding to the first absorption band of Sky Blue will change more remarkably with larger intermolecular charge transfer (probably through auxochromes) than in case of the latter. Thus the character of the absorption spectra of the complexes can be explained qualitatively.

The above discussion will be applied to the difference between spectral characters of the pairs of SC_1 and Sky Blue and of SC_2 and Sky Blue.

8) J. Tanaka and S. Nagakura, *J. Chem. Soc. Japan, Pure Chem. Sec.* (*Nippon Kagaku Zasshi*), **78**, 1200 (1957).
9) K. E. Shuler, *J. Chem. Phys.*, **20**, 1865 (1952).

Summary

1. The absorption spectra of the binary mixtures in aqueous solution of Chlorazol Sky Blue FF and sulfanilic acid → cresidine and sulfanilic acid → cresidine → cresidine were measured at room temperature.

2. The mixture of Chlorazol Sky Blue FF and sulfanilic acid → cresidine shows the additive spectrum when the ratio of the two dyes is about 1:5 but the non-additive one when it is about 1:40. From this fact the authors pointed out that even if an equimolar or nearly equimolar mixture shows the additive spectrum, it often exhibits the additive one with a relative increase of one component, due to the interaction between the components. That the spectra of the mixture pass through an isosbestic point means that a Sky Blue molecule interacts with n molecules of sulfanilic acid → cresidine (n is unknown).

3. It was indicated that the mixture of Chlorazol Sky Blue FF and sulfanilic acid → cresidine → cresidine showed the non-additive spectrum, and that this was well explained by assuming the formation of a 1:1 complex over the range of concentrations measured.

4. The authors discussed qualitatively the characters of the spectra and the stability of these complexes, comparing them with the complex of Sky Blue and Chrysophenine G, etc.

The intermediates used were presented by the Sumitomo Kagaku Kogyo Co. Ltd. through Dr. S. Arikawa and Dr. M. Okazaki. The authors wish to express their gratitude to them.

Laboratory of Physical Chemistry
Tokyo Institute of Technology
Meguro-ku, Tokyo

The Volume Change on Neutralization of a Strong Acid with a Strong Base[1]

By Akira TSUJIOKA

(Received November 23, 1958)

A method of calculation has been proposed by which we may evaluate the changes of volume on neutralization of various acids and bases at a constant temperature. The values of volume change fraction on neutralization of hydrochloric acid with sodium hydroxide solution at 20°C have been calculated. These calculated values have shown a good agreement with the observed ones. We have, on the other hand, shown that the volume change fraction of the reaction between a strong acid and a strong base of equal concentrations is represented by a simple function of the initial concentration.

It was noticed in an early period that there is an expansion on the neutralization of a strong acid with a strong base[2], but there are only a few data[3]. In particular, there are few data regarding the volume change on neutralization of an acid and a base of unequal concentrations. No investigation has as yet been made to correlate quantitatively the change of volume with concentration. Therefore we devised a method of calculation by which still more data can easily be provided, and then derived the relationship between the volume change on neutralization and the concentration of an acid or a base.

Now, if the density of a salt solution produced by neutralization is obtained, the volume change which occurs in this case can readily be evaluated. Then we have evaluated the density of the salt solution from the density table. That is, the weight per cent concentration of the resulting salt solution can be evaluated from the initial concentrations, so the density of this solution may be obtained by interpolation from the density table. The densities of electrolyte solutions have been fully known at intervals of one or two per cent concentration, so this interpolation does not cause any appreciable errors, as will be dealt with later.

The method mentioned above can be applied to the neutralization not only of a strong acid and a strong base, but also of both weak electrolytes or a strong electrolyte and a weak one.

Calculations

In considering the volume changes on neutralization of various acids and bases, we shall deal with both 1–1 strong electrolytes. In the other cases, we may deal with them in the manner described below.

If V_a ml. of a C_a mol./l. acid (the density, d_a) is neutralized with V_b ml. of a C_b mol./l. solution of a base (the density, d_b) at constant temperature, the volume change can be calculated as follows.

The weight per cent concentration of the resulting salt solution, denoted by a, is represented by the equation,

$$a = M_s/10(d_a/C_a + d_b/C_b) \tag{1}$$

where M_s is the molecular weight of the salt. If the density of this solution is denoted by d_s, the apparent molar volume of the acid by Φ_a, that of the base by Φ_b and that of the salt by Φ_s, these apparent molar volumes are defined by the following equations, respectively.

$$\Phi_a = \{1000 - (1000d_a - C_aM_a)/d_w\}/C_a \tag{2}$$

$$\Phi_b = \{1000 - (1000d_b - C_bM_b)/d_w\}/C_b \tag{3}$$

$$\Phi_s = 1000(d_a/C_a + d_b/C_b)(1/d_s - 1/d_w) + M_s/d_w \tag{4}$$

where d_w is the density of water, M_a, the molecular weight of the acid and M_b, that of the base.

Then it may be presumed that the volume change on neutralization is due to the change in the apparent molar volume of the solute, so that the volume change denoted by ΔV ml. is given by

1) A part of this paper was presented at the 11th Annual Meeting of the Chemical Society of Japan, held in Tokyo in April, 1958.

2) J. R. Partington, "An Advanced Treatise on Physical Chemistry", Vol. 2, 1st Ed., Longmans, Green and Co., London (1951), p. 33.

3) J. D'Ans and E. Lax, "Taschenbuch für Chemiker und Physiker", 2nd Ed., Springer Verlag, Berlin (1949), p. 821; Landolt-Börnstein, "Physikalisch-Chemische Tabellen", Erg. B. II, Springer Verlag, Berlin (1931), p. 274.

$$\Delta V = (\Phi_s + \Phi_w - \Phi_a - \Phi_b) C_a V_a / 1000 \quad (5)$$

where Φ_w is the apparent molar volume of water, equal to M_w/d_w (M_w is the molecular weight of water). In Eq. 5, ΔV has been defined as a positive value when there is an expansion in total volume.

On the other hand, ΔV may be directly represented by means of the equation,

$$\Delta V = (d_a V_a + d_b V_b)/d_s - (V_a + V_b) \quad (6)$$

We may choose between Eqs. 5 and 6 to evaluate ΔV, because substitution of Eqs. 2, 3 and 4 into Eq. 5 gives Eq. 6.

Neutralization at Equal Concentrations. —The equations by which we may evaluate the volume change on neutralization of a C mol./l. acid, which occupies a volume V ml., with a base of an equal concentration can be derived by replacing V_a and V_b in Eqs. 5 and 6 by V, and C_a and C_b in Eqs. 1—5 by C.

The weight per cent concentration of the resulting salt solution is obtained by

$$a^* = M_s C / 10(d_a + d_b) \quad (7)$$

Therefore, in the case of neutralization of an acid with a base of equal concentration, the increase in total volume is

$$\Delta V^* = (\Phi_s^* + \Phi_w - \Phi_a - \Phi_b) C V / 1000 \quad (8)$$

where

$$\Phi_s^* \doteq 1000(d_a + d_b)(1/d_s^* - 1/d_w)/C + M_s/d_w$$

or by an alternative formula (using Eq. 6).

$$\Delta V^* = \{(d_a + d_b)/d_s^* - 2\} V \quad (9)$$

The subscripts refer to salt, water, acid and base, respectively, and the asterisk indicates that the salt concentration is a^* %.

Then replacing $(\Delta V^*/2V) \times 10^3$ by Ψ in Eqs. 8 and 9, we have

$$\Psi = (\Phi_s^* + \Phi_w - \Phi_a - \Phi_b) C/2 \quad (10)$$

$$\Psi = \{(d_a + d_b)/2d_s^* - 1\} \times 10^3 \quad (11)$$

Now we will for convenience' sake call Ψ, which represents the rate of change of the volume upon neutralization, "Volume Change Fraction". The numerical value of Ψ represents the change in the total volume observed on mixing the acid, which amounts to 500 ml., with an equi-volume of the base, of which the concentration is equal to that of the acid. The value of Ψ has the same sign as ΔV^*, so it is positive when the total volume expands on mixing the two solutions.

Results and Discussion

The values of volume change fraction on neutralization of a hydrochloric acid with a sodium hydroxide solution of equal concentration at 20°C have been calculated by the method mentioned in the previous section.

The weight per cent concentration of the resulting sodium chloride solution has been evaluated by Eq. 7, so the density of this solution has been obtained by interpolation from the density data of the "International Critical Tables"[4].

Therefore, the value of Ψ has been calculated by Eq. 11. The results obtained here are shown in Table I. In this table the values of the fifth column are those observed by Saslawsky et al.[5] and those in the last column are those calculated by Eq. 24, which will be derived later.

In Table II are shown volume changes

TABLE I. VOLUME CHANGE FRACTIONS ON NEUTRALIZATION OF HYDROCHLORIC ACID WITH SODIUM HYDROXIDE AT 20°C

Initial concn.	Final concn.	Density of NaCl. aq.	Volume change fraction		
C (mol./l.)	a^* (%)	d_s^*	$\Psi_{calc.}$	$\Psi_{obs.}$	$\Psi_{eq.(24)}$
1	2.841	1.01849	10.02	9.8	9.9
2	5.530	1.03787	18.16	18.0	18.2
3	8.093	1.05658	25.37	25.1	25.5
4	10.544	1.07475	31.74	31.8	31.9
5	12.895	1.09246	37.42	37.6	37.7
6	15.159	1.10975	42.51	42.8	42.8
7	17.346	1.12677	46.91	47.2	47.3
8	19.459	1.14349	50.80	51.3	51.3
9	21.514	1.16002	54.14	54.6	54.8
10	23.504	1.17632	57.02	57.3	57.8
11	25.448	1.19254	59.35	59.0	60.4

4) "International Critical Tables", Vol. III, McGraw-Hill Book Co., New York (1928), p. 79.

5) J. J. Saslawsky aad E. G. Standel, *Z. anorg. Chem.*, **186**, 171 (1930).

TABLE II. VOLUME CHANGES ON NEUTRALIZATION OF HYDROCHLORIC ACID WITH SODIUM HYDROXIDE OF UNEQUAL CONCENTRATION AT 20°C

HCl		NaOH		NaCl		Vol. change	Vol. change per mole
Concn. (mol./l.) C_a	Vol. (l.) V_a	Concn. (mol./l.) C_b	Vol. (l.) V_b	Concn. (%) a	Density d_s	ΔV ml.	
1	1	2	0.5	3.756	1.02505	18.17	18.17
2	0.5	1	1	3.753	1.02503	19.68	19.68
2	1	4	0.5	7.266	1.05052	31.63	15.82
4	0.5	2	1	7.246	1.05038	35.93	17.97
4	1	8	0.5	13.725	1.09876	50.46	12.62
8	0.25	2	1	8.582	1.06019	34.97	17.49
8	0.5	4	1	13.628	1.09802	62.58	15.65
8	0.75	6	1	16.983	1.12392	84.88	14.15

on neutralization at unequal concentrations, which are calculated by Eqs. 1 and 6.

The Degree of Inaccuracy in Ψ.—Whether or not the values of Ψ in Table I and ΔV^* in Table II are nearly the same as those obtained by a strict experiment depends upon the extent to which an error is made in evaluating the density of the resulting solution by interpolation. Therefore, we will discuss the error in density caused by interpolation[6].

In the case of sodium chloride, the maximum error in density caused by interpolation at intervals of four per cent concentration is 0.007~0.015 per cent in each range of concentration. It is proved by a mathematical calculation that the error in density caused by interpolation at intervals of two per cent concentration is less than one fourth of that at intervals of four per cent concentration, so that it would be rightly considered that the maximum of the errors which would be expected by interpolation at intervals of two per cent concentration is less than 0.004 per cent. If the density data are given at intervals of one per cent concentration, it is needless for us to consider the error in density caused by interpolation.

On the other hand, an error of 0.001 per cent in density would cause an inaccuracy of about 0.01 in Ψ. It is derived from Eq. 11 or deduced from the inaccuracy in Φ (cf. Eq. 10)[7]. Therefore, each of the calculated values of Ψ in Table I may be slightly less than the corresponding true value of Ψ, but the difference between the two does not exceed 0.04.

It is of course true that the above-mentioned discussion can be applied not only to Ψ in Table I, but also to ΔV^* in Table II.

Further, densities of the solutions of acids and bases at 20°C shown in Table III have been evaluated by the following equations, which have been suggested by Root[8].

$$d_{HCl} = 0.99823 + 0.01870\,C - 0.00087\,C^{3/2} \quad (12)$$

$$d_{NaOH} = 0.99823 + 0.04744C - 0.00454C^{3/2} \quad (13)$$

where C is the concentration in mol./l. of the electrolyte solution. These equations have been derived by using the values of Φ^0 and S_v for each electrolyte shown in Table IV.

TABLE III. DENSITIES OF HYDROCHLORIC ACIDS AND SODIUM HYDROXIDE SOLUTIONS AT 20°C

Concn. (mol./l.)	Density	
C	d_{HCl}	d_{NaOH}
1	1.01606	1.04113
2	1.03317	1.08027
3	1.04981	1.11696
4	1.06607	1.15167
5	1.08200	1.18467
6	1.09769	1.21615
7	1.11302	1.24623
8	1.12814	1.27502
9	1.14304	1.30261
10	1.15772	1.32906
11	1.17219	1.35444

TABLE IV. VALUES OF THE PARAMETERS OF EQS. 14, 15 AND 16 AT 20°C

Electrolyte	Φ^0	S_v
HCl	17.80	0.87
NaOH	−7.45	4.55
NaCl	15.82	2.32

6) It has been fully discussed in "Changes of Volume of Mixing Electrolytic Solutions with Water", presented at the 10th Annual Meeting of the Chemical Society of Japan, held in Tokyo in April, 1957; A. Tsujioka, *Proc. of Faculty of Eng., Keio Univ.*, **10**, 47 (1957).

7) H. S. Harned and B. B. Owen, "The Physical Chemistry of Electrolytic Solutions", 2nd Ed., Reinhold Publishing Co., New York (1950), p. 251.

8) W. C. Root, *J. Am. Chem. Soc.*, **55**, 850 (1933).

At this point, therefore, the errors other than those caused by interpolation would be introduced in the values of Ψ and ΔV^* shown in Tables I and II, because they were evaluated by using the data in Table III. In conclusion, the values of Ψ and ΔV^* shown in Tables I and II appear to leave more or less room for doubt at 2 places of decimals. Nevertheless, the agreement between our data and Saslawsky's data has been found very satisfactory in Table I.

Relationships between the Volume Change Fraction and the Concentration.—Since the discovery by Masson[9] that the apparent molar volume of a dissolved salt is a linear function of the square root of the volume concentration, several investigators[10,11] have made extensive tests of the applicability of this relationship. It was found valid for a number of electrolytes over a surprisingly large concentration range. In the range of high dilution, however, the apparent molar volumes Φ_v of strong electrolytes in solution confirm the limiting law derived from the Debye-Hückel theory[12,13]. That is, the function $\Phi_v - S_v C^{1/2}$ is linearly related to the volume concentration C, where S_v is the universal limiting slope. (The experimental limiting slopes determined from the results above 0.25 N are specific[14].)

Therefore, the following Masson's linear relationships hold over a wide range of concentration except at high dilution.

$$\Phi_a = \Phi_a^0 + S_a\sqrt{C} \tag{14}$$

$$\Phi_b = \Phi_b^0 + S_b\sqrt{C} \tag{15}$$

$$\Phi_s^* = \Phi_s^0 + S_s\sqrt{C_s^*} \tag{16}$$

where Φ_a^0, Φ_b^0, Φ_s^0, S_a, S_b and S_s are constants, and C_s^* is the concentration in mol./l. of the salt solution, of which the concentration has been denoted by a^* % in the above section, obtained on neutralization of an acid with a base of equal concentration, C mol./l. Accordingly Eq. 10 for Ψ can be reduced to

$$\Psi = \{(\Phi_s^0 + \Phi_w - \Phi_a^0 - \Phi_b^0) + S_s\sqrt{C_s^*} - S_a\sqrt{C} - S_b\sqrt{C}\}C/2 \tag{17}$$

The resulting salt solution has a volume $(2V + \Delta V^*)$ ml., as has been indicated in the previous section. Hence the following equation:

$$C_s^* = C/2(1 + 10^{-3}\cdot\Psi) \tag{18}$$

Where Ψ, equal to $(\Delta V^*/2V)\times 10^3$, is the volume change fraction. Substituting Eq. 18 in Eq. 17 and then putting it in order by the binomial formula, we find the following equation.

$$\Psi = [(\Phi_s^0 + \Phi_w - \Phi_a^0 - \Phi_b^0) + (S_s\sqrt{2C/2}) \times\{1 + \sum_{r=1}^{\infty}\binom{-1/2}{r}(10^{-3}\cdot\Psi)^r\} - S_a\sqrt{C} - S_b\sqrt{C}\,]C/2 \tag{19}$$

In this equation, the terms $\sum_{r=1}^{\infty}\binom{-1/2}{r}(10^{-3}\cdot\Psi)^r$ are small and can usually be ignored[15], so that we may write,

$$\Psi = \{(\Phi_s^0 + \Phi_w - \Phi_a^0 - \Phi_b^0) + (S_s\sqrt{2C/2})(1 - \Psi/2000) - S_a\sqrt{C} - S_b\sqrt{C}\}C/2 \tag{20}$$

Solving this equation with respect to Ψ, we may readily derive the following equation.

$$\Psi = \{(\Phi_s^0 + \Phi_w - \Phi_a^0 - \Phi_b^0) + \sqrt{C}(\sqrt{2}S_s/2 - S_a - S_b)\}(1 - \sqrt{2}\,S_s C^{3/2}/8000)C/2 \tag{21}$$

Consequently we obtain the following equation for Ψ.

$$\Psi = K_1C + K_2C^{3/2} - K_3C^{5/2} - K_4C^3 \tag{22}$$

where
$$K_1 = (\Phi_s^0 + \Phi_w - \Phi_a^0 - \Phi_b^0)/2$$
$$K_2 = (\sqrt{2}\,S_s - 2S_a - 2S_b)/4$$
$$K_3 = (\sqrt{2}\,S_s/8000)K_1$$
$$K_4 = (\sqrt{2}\,S_s/8000)K_2$$

In most cases K_3 and K_4 are small and can be ignored, so that Eq. 22 is approximately represented by means of the following equaiion.

$$\Psi = K_1C + K_2C^{3/2} \tag{23}$$

As an example, we shall deal with the reaction between a hydrochloric acid and a sodium hydroxide solution. Values of the parameters of Eqs. 14, 15 and 16 at 20°C obtained by the present writer are shown in Table IV[16]. The limiting law of the apparent molar volume has been

9) D. O. Masson, *Phil. Mag.*, **8**, 218 (1929).
10) W. Geffcken and D. Price, *Z. physik. Chem.*, **B26**, 81 (1934).
11) A. F. Scott, *J. Phys. Chem.*, **35**, 2315 (1931).
12) B. B. Owen and S. R. Brinkley, Jr., *Ann. N. Y. Acad. Sci.*, **51**, 753 (1949).
13) O. Redlich and J. Bigeleisen, *J. Am. Chem. Soc.*, **64**, 758 (1942).
14) See Ref. 7, p. 523.

15) The largest one of these terms, $\binom{-1/2}{2}(10^{-3}\cdot\Psi)^2$, is generally less than 0.001. So it would be rightly considered that the contribution of these terms to the value of Ψ does not exceed 0.1 per cent.
16) These values were not evaluated from data at high dilution.

confirmed for aqueous solutions of sodium chloride up to 0.75 N and of hydrochloric acid up to 0.2 N[12,13]. Therefore the empirical equations, which will be derived below, should not be extrapolated to lower concentrations. Again for aqueous solutions of a few acids (i. e., perchloric acid and sulfuric acid) the apparent molar volume show an unusual dependence on the concentration[17-19].

It appears to be the same for aqueous solutions of hydrogen halides[20]. For hydrochloric acid, however, this deviation from Masson's rule is negligibly small[21,22], so we have not taken it into consideration.

By using the data in Table IV, the coefficients K_1, K_2, K_3 and K_4 in Eq. 22 have been calculated as follows.

$$K_1=11.76,\ K_2=-1.89,\ K_3=4.8\times10^{-3},$$
$$K_4=-7.7\times10^{-4}$$

In this case, therefore, we obtain

$$\Psi=11.76\,C-1.89\,C^{3/2} \qquad (24)$$

The correctness of this equation has been found very satisfactory in Fig. 1 and Table I. In Fig. 1, values of $2\Psi/C$ have been plotted against the square root of the concentration. The numerical value of $2\Psi/C$ represents the volume change in ml. on neutralization of an acid and a base of equal concentrations, C mol./l., which occupy the equal volume, v ml.,

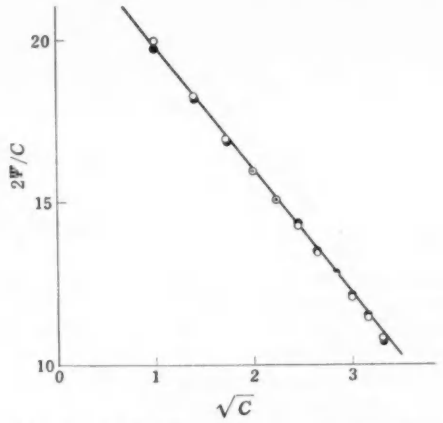

Fig. 1. Dependence of the volume change per mol., on neutralization of hydrochloric acid with sodium hydroxide of equal concn., upon concentration, at 20°C.
——, Calculated by Eq. 24, i.e., $2\Psi/C=23.52-3.78\sqrt{C}$;
○, Tsujioka's data; ●, Saslawsky's data

where v is the volume of the solution, expressed in ml., containing one mole of the solute[23].

On the other hand, in the case of volume changes on neutralization of acids and bases of unequal concentrations, it has been shown in Table II that the expansion in total volume on neutralization gets larger as the range of concentration gets lower, and that the volume change which occurs when hydrochloric acid is more concentrated than sodium hydroxide is larger than that in the reverse case, and so on. These facts, together with the discussion of Eq. 24, may be explained by considering the volume change on dilution. It will be reported in this bulletin shortly.

The Chemical Laboratory, Keio University
Hiyoshi, Yokohama

17) J. Bigeleisen, *J. Phys. and Colloid Chem.*, **51**, 1369 (1947).
18) H. E. Wirth and F. N. Collier, Jr., *J. Am. Chem. Soc.*, **72**, 5292 (1950).
19) I. M. Klotz and C. F. Eckert, ibid., **64**, 1878 (1942).
20) A. Tsujioka, *J. Chem. Soc. Japan, Pure Chem. Sec. (Nippon Kagaku Zasshi)*, in contribution.
21) H. E. Wirth, *J. Am. Chem. Soc.*, **62**, 1128 (1940).
22) T. F. Young and M. B. Smith, *J. Phys. Chem.*, **58**, 716 (1954).
23) Then C is equal to $10^3/v$, and the volume change fraction Ψ is equal to $(\Delta v/2v)\times10^3$, as has been defined in the previous section, where Δv is the volume change in ml. on neutralization. Therefore it follows that $\Delta v=2\Psi/C$.

Reactions of Active Methylene Compounds. VI. A New Synthesis of Coumestrol, 6,7'-Dihydroxycoumarino (3',4':3,2) coumarone

By Yoshiyuki KAWASE

(Received December 13, 1958)

It has been reported that naturally occurring wedelolactone[1](I) and coumestrol[2](II) are 5,5',6-trihydroxy-7'-methoxy and 6,7'-dihydroxy derivatives of coumarino (3',4':3,2)coumarone, respectively.

The synthesis of coumarino(3',4':3,2) coumarones has been achieved by the action of hydrobromic acid[3] or pyridine hydrochloride[4] on 3-(2'-methoxyphenyl)-4-hydroxycoumarin derivatives; wedelolactone trimethylether[3,4], from which wedelolactone[5] was derived, was prepared by this method, and coumestrol has recently been synthesized by the action of aniline hydrochloride or hydriodic acid on 3-(2',4'-dimethoxyphenyl)-4, 7-dihydroxycoumarin[6].

Another synthetic route to coumarino-(3',4':3,2)coumarone was reported by Chatterjea and Roy, which involves the action of hydrobromic acid on 2-methoxybenzoyl-2-methoxyphenylacetonitrile[7].

The author also has achieved independently the synthesis of 3-phenyl-4-hydroxycoumarins[8] and coumarino (3',4':3,2)coumarones[9] from methoxy derivatives of benzoyl-phenylacetonitrile or corresponding ester by the action of hydrobromic or hydriodic acid or pyridine hydrochloride or anhydrous aluminum chloride.

Now, the synthesis of coumestrol has been carried out by the action of pyridine hydrochloride or hydriodic acid on 2,4 dimethoxybenzoyl-2, 4-dimethoxyphenyl-acetonitrile(III). The acetate of coumestrol thus obtained, m. p. 227~228°C (uncorrected), was identical with the sample, m .p. 227~228°C (uncorrected), which was kindly sent by Dr. Emerson.

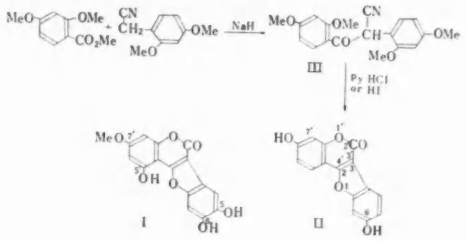

Experimental[10]

Ester Condensation.—To a solution of methyl 2,4-dimethoxybenzoate (3.5 g.) and 2,4-dimethoxyphenylacetonitrile (3 g., prepared by azlactone-method[11]) in anhydrous benzene (100 cc.), sodium hydride (ca. 0.6 g.) was added, and the mixture was heated on an oil bath (ca. 95~100°C) for 4 hr. under anhydrous condition, most of the benzene having been distilled off in the meantime. After being well cooled, the mixture was treated with a small amount of ethanol to destroy the excessive sodium hydride, and then diluted with water. Insoluble starting materials being extracted with ether (from the residue of the ether solution, 1.5 g. of the nitrile was recovered through crystallization from methanol), the alkaline solution was acidified and the separated product was collected, washed with aqueous sodium bicarbonate solution and recrystallized from ethanol to give III in colorless needles, m. p. 97~98°C; yield 2.4 g. or 40% (yield was raised to 70% when recovery of the nitrile was taken into account).

Anal. Found: C, 67.01; H, 5.72; N, 4.25. Calcd. for $C_{19}H_{19}O_5N$: C, 66.85; H, 5.61; H, 4.10%.

Coumestrol.—*(a) By pyridine hydrochloride.*—A mixture of III (0.7 g.) and anhydrous pyridine hydrochloride (3.5 g.) was refluxed for 40 min.

1) T. R. Govindachari et al., *J. Chem. Soc.*, **1956**, 629; ibid., **1957**, 545.
2) E. M. Bickoff et al., *Science*, **126**, 969 (1957); *J. Agr. Food Chem.*, **6**, 536 (1958); *J. Am. Chem. Soc.*, **80**, 3969 (1958).
3) W. J. Bowyer, A. Robertson and W. Whalley, *J. Chem. Soc.*, **1957**, 542.
4) T. R. Govindachari et al., ibid., **1957**, 548.
5) N. R. Krishnaswamy and T. R. Seshadri, *J. Sci. Ind. Research (India)*, **16B**, 268 (1957); [*Chem. Abstr.*, **52**, 376 (1958)].
6) O. H. Emerson and E. M. Bickoff, *J. Am. Chem. Soc.*, **80**, 4381 (1958).
7) J. N. Chatterjea and S. K. Roy, *J. Indian Chem. Soc.*, **34**, 98 (1957); [*Chem. Abstr.*, **51**, 16445 (1957)]; cf. J. N. Chatterjea and S. K. Roy, *J. Indian Chem. Soc.*, **34**, 155 (1957); [*Chem. Abstr.*, **52**, 1987 (1958)].
8) Y. Kawase, This Bulletin, **31**, 440 (1958); ibid., **32**, 9, 11 (1959); *Experientia*, **14**, 435 (1958).
9) A report will appear in this bulletin afterwards.
10) Melting points are uncorrected.
11) P. C. Mitter and S. S. Maitra, *J. Indian Chem. Soc.*, **13**, 236 (1936).

on an oil bath (ca. 220~230°C) in a carbon dioxide atmosphere under anhydrous condition. The cooled mixture was warmed with dilute hydrochloric acid on a steam bath for 30 min. The separated precipitates were crystallized from ethanol to give light brown microcrystals (m. p. of this was very high); yield ca. 0.2 g.

Anal. Found: C, 67.35; H, 3.18. Calcd. for $C_{15}H_8O_5$: C, 67.17; H, 3.01%.

The acetate prepared by pyridine-acetic anhydride method was colorless needles (from acetic acid), m. p. 227~228°C, and was identical with the sample from Dr. Emerson, m. p. 227~228°C (corrected m. p. is reported to be 235~236°C).

Anal. Found: C, 64.51; H, 3.59. Calcd. for $C_{19}H_{12}O_7$: C, 64.77; H, 3.43%.

(*b*) ***By hydriodic acid.*** — A mixture of III (0.8 g.), hydriodic acid (d=1.7, 15 cc.), acetic acid (7.5 cc.) and acetic anhydride (7.5 cc.) was refluxed for 2 hr. on an oil bath (ca. 140°C) under a carbon dioxide atmosphere. The cooled solution was diluted with dilute aqueous sodium bisulfite solution, and the precipitates were crystallized from ethanol to give a red product (ca. 0.1 g.), the acetate, m. p. 225.5~226.5°C, which was identical with the other sample.

The author wishes to express his hearty thanks to Professor K. Fukui for his helpful advice, to Dr. O. H. Emerson of the United States Department of Agriculture for the sample of coumestryl acetate, and the members of the Agricultural Department of Kyoto University for microanalyses.

Faculty of Literature and Science
Toyama University
Hasumachi, Toyama

Syntheses of Chlorinated Copper Phthalocyanines from Chlorophthalic Anhydrides

By Masahiro SHIGEMITSU

(Received December 16, 1958)

As a method of synthesis of copper phthalocyanine, the urea-method[1] resorting to the condensation of phthalic anhydride, urea and copper salts prevails. Chlorinated copper phthalocyanines can be obtained by the use of chlorophthalic anhydrides instead of phthalic anhydride. However, since chlorinated copper phthalocyanines are manufactured by chlorinating copper phthalocyanine, little work has been done upon the syntheses of them from chlorophthalic anhydrides.

The author carried out the syntheses of chlorinated copper phthalocyanines by the urea-method, using chlorophthalic anhydrides instead of phthalic anhydride and studied the effect given by the chlorine atoms of starting materials.

Experimental

Materials.—***Phthalic anhydride*** (I).—Commercial phthalic anhydride was used with further purification (m. p. 130~131°C).

Monochlorophthalic anhydrides. — By the improved V. Villiger's method[2,3], phthalic anhydride was chlorinated with chlorine gas at 50~55°C in an iron closed vessel, using oleum as solvent and iodine as catalyst. From the mixture of monochlorophthalic anhydrides thus prepared, were separated 3-monochlorophthalic anhydride (II), m. p. 121~122°C (reported m. p. 122°C[4]) (*Anal.* Found: Cl, 19.47%) and 4-monochlorophthalic anhydride (III), m. p. 97~98°C (reported m. p. 98°C[4]) (*Anal.* Found: Cl, 19.44%) by repeating recrystallization with toluene-ethanol (1 : 1) solvent.

Dichlorophthalic anhydrides. — From the mixture of dichlorophthalic anhydrides prepared by the same procedure as above, were separated 3,4-dichlorophthalic anhydride (IV), m. p. 120~121°C (reported m. p. 120~121°C[4]) (*Anal.* Found: Cl, 32.68%), 3,6-dichlorophthalic anhydride (V), m. p. 190~191°C, (reported m. p. 190~191°C[4]) (*Anal.* Found: Cl, 32.71%) and 4,5-dichlorophthalic anhydride (VI), m. p. 185.5~186.5°C (reported m. p. 185~187°C[4]) (*Anal.* Found: Cl, 32.66%) with toluene-ethanol (1:1) solvent.

1) U. S. Pat. 2,197,458 (1940).

2) V. Villiger, *Ber.*, **42**, 3538 (1909).

3) M. Shigemitsu, *J. Chem. Soc. Japan, Ind. Chem. Sec.* (*Kogyo Kagaku Zasshi*), **62**, 110 (1959). (Presented at the Autumnal Joint Meeting of Chemical Society of Japan with other Societies, Tokyo, 1957).

4) V. Villiger, *Ber.*, **42**, 3532 (1909).

Trichlorophthalic anhydrides.—From the mixture of trichlorophthalic anhydrides prepared by the same procedure as above, were separated 3,4,6-trichlorophthalic anhydride (VII), m. p. 147.5~148.5°C (reported m. p. 148°C[5]) (*Anal.* Found: Cl, 42.19%) and 3,4,5-trichlorophthalic anhydride (VIII), m. p. 155.5~156.5°C (reported m. p. 157°C[6]) (*Anal.* Found: Cl, 42.20%) with toluene-ethanol (1:1) solvent.

Tetrachlorophthalic anhydride (IX).—By N. Juvalta's method[7], phthalic anhydride was chlorinated with chlorine gas at 50~60°C and thereafter 200°C in oleum, using iodine as catalyst, and the product was recrystallized with toluene-ethanol (1:1) solvent; m. p. 255~256.5°C (reported m. p. 255~256.5°C[8]) (*Anal.* Found: Cl, 49.22%).

Methods.—Into a three-necked flask of 300 cc. capacity equipped with a stirrer, a thermometer and a reflux condenser were placed 4:20:1 mol. ratio mixture of phthalic anhydride or its chlorinated derivatives, urea and cuprous chloride as indicated in Table I, and 150 g. of trichlorobenzene used as solvent.

The mixture was stirred at room temperature for 30 min., and then heated to 175°C for 1 hr. at a uniform rate and finally at 175~180°C for 3 hr. After the reaction was complete, trichlorobenzene was removed by steam distillation and the product was heated with 5% hydrochloric acid and then with 2% caustic soda, filtered, washed with water and ethanol and dried at 95~100°C.

In the case of tetrachlorophthalic anhydride, the reaction was conducted with the addition of ammonium molybdate[9], boric acid[1], zirconium tetrachloride[10] and titanium tetrachloride[10] as catalysts of condensation.

Results and Discussion

Results of condensation of phthalic anhydride or its chlorinated derivatives with urea and cuprous chloride are given in Table I.

Phthalic anhydride easily reacts with urea and cuprous chloride and forms copper phthalocyanine. However, when the chlorine content of phthalic anhydride increases, the yield of the product decreases.

The yields obtained in Experiments 3, 6 and 8 are all larger than those obtained in Experiments 2, 5 and 7. Experiment 4 shows the yield between those obtained in Experiments 5 and 6. It is recognized from the above experiments that chlorinated copper phthalocyanines are formed from chlorophthalic anhydrides more easily when chlorine atoms are in 4,5-positions of phthalic anhydride than when they are in its 3,6-positions.

Although copper hexadecachlorophthalocyanine should be obtained in Experiment 9, the chlorine content of the product coincides with that of copper dodecachlorophthalocyanine. The author further studied this matter as follows.

Ammonium molybdate, boric acid, zirconium tetrachloride and titanium tetrachloride are used as catalysts to increase the yield of phthalocyanine formed in

TABLE I. CONDENSATION OF PHTHALIC ANHYDRIDE OR ITS CHLORINATED DERIVATIVES WITH UREA AND CUPROUS CHLORIDE

Expt.	Starting material	Urea	Cuprous chloride	Product				
				Wt.	Yield	Cl (%)		
	(g.)	(g.)	(g.)	(g.)	(%)	Found	Calcd.	
1	I, 10.0	19.3	1.7	A, 8.6	89	0.09	0	($C_{32}H_{16}N_8Cu$)
2	II, 10.0	13.7	1.4	B, 7.4	76	19.76	19.87	($C_{32}H_{12}N_8Cl_4Cu$)
3	III, 10.0	13.7	1.4	C, 8.3	85	19.80	〃	〃
4	IV, 10.0	11.6	1.2	D, 7.3	75	33.19	33.24	($C_{32}H_8N_8Cl_8Cu$)
5	V, 10.0	11.6	1.2	E, 6.9	70	33.22	〃	〃
6	VI, 10.0	11.6	1.2	F, 7.8	80	33.18	〃	〃
7	VII, 10.0	9.9	1.0	G, 5.9	60	42.98	43.02	($C_{32}H_4N_8Cl_{12}Cu$)
8	VIII, 10.0	9.9	1.0	H, 6.8	69	43.01	〃	〃
9	IX, 10.0	8.8	0.9	I, 4.1	42	43.04	50.34	($C_{32}N_8Cl_{16}Cu$)

A, Copper phthalocyanine.
B, Copper tetra-(3)-chlorophthalocyanine.
C, Copper tetra-(4)-chlorophthalocyanine.
D, Copper octa-(3,4)-chlorophthalocyanine.
E, Copper octa-(3,6)-chlorophthalocyanine.
F, Copper octa-(4,5)-chlorophthalocyanine.
G, Copper dodeca-(3,4,6)-chlorophthalocyanine.
H, Copper dodeca-(3,4,5)-chlorophthalocyanine.
I, To be discussed later.

5) C. Graebe and S. Rostowzew, ibid., **34**, 2108 (1901).
6) Ad. Claus and H. Kautz, ibid., **18**, 1370 (1885).
7) D. R. Pat. 50,177 (1889).
8) D. S. Pratt and G. A. Perkins, *J. Am. Chem. Soc.*, **40**, 204 (1918).
9) U. S. Pat. 2,214,477 (1940).
10) U. S. Pat. 2,549,842 (1951).

TABLE II. CONDENSATION OF TETRACHLOROPHTHALIC ANHYDRIDE WITH UREA AND CUPROUS CHLORIDE

Expt.	IX	Urea	Cuprous chloride	Catalyst	Product		
	(g.)	(g.)	(g.)	(g.)	Wt. (g.)	Yield (%)	Cl (%)
10	10.0	8.8	0.9	A, 0.5	4.6	47	43.25
11	10.0	8.8	0.9	B, 0.5	4.9	50	43.51
12	10.0	8.8	0.9	C, 0.5	5.9	60	45.95
13	10.0	8.8	0.9	D, 0.5	5.4	55	44.73

A, Ammonium molybdate. B, Boric acid.
C, Zirconium tetrachloride. D, Titanium tetrachloride.

urea-method. Using these compounds as catalysts and under the reaction conditions in Table I, IX was condensed with urea and cuprous chloride. The results are given in Table II.

In Table II, the yield in Experiment 12 is the largest, but it is only 60%. The larger the yield, the larger the chlorine content is. However, all the chlorine contents in Table II are smaller than that of copper hexadecachlorophthalocyanine and close to that of copper dodecachlorophthalocyanine.

As it was considered that dechlorination reaction might possibly occur in the formation of phthalocyanine, the product obtained in Experiment 9 (Table I) was examined. Based on the method in Ref. 11, 3 g. of the product was decomposed by oxidation with ceric sulfate, which gave 2.0 g. of 3,4,5-trichlorophthalic anhydride, m. p. 156~157°C (reported m. p. 157°C[6]) (*Anal.* Found: Cl, 42.17%). It was evident from the above experiments that the chlorine atom at 6-position of IX separated and condensed with urea and cuprous chloride.

11) R. P. Linstead el al., *J. Chem. Soc.*, **1939**, 1823.

Summary

Syntheses of chlorinated copper phthalocyanines from various chlorophthalic anhydrides were conducted. Formation of phthalocyanine depends upon the contents and positions of chlorine atoms of chlorophthalic anhydrides.

The author extends his sincere thanks to Dr. Ryozo Goto, Professor of Kyoto University, for his kind guidance. Thanks are also due to Dr. Takahisa Nakamura and Dr. Wataru Ishikawa, Toyo Ink Manufacturing Company, for their help.

Central Research Laboratory
Toyo Ink Mfg. Co.
Sumida-ku, Tokyo

Color Characteristics of Copper Phthalocyanine and its Chlorinated Derivatives

By Masahiro SHIGEMITSU

(Received December 16, 1958)

Copper phthalocyanine pigments range in shade from blue to green, and are very strong and bright. Arranged in order of increasing greenness or of decreasing redness, they are listed as follows:

(1) Copper phthalocyanine (β-form)
(2) Copper phthalocyanine (α-form)
(3) Copper semichlorophthalocyanine
(4) Copper polychlorophthalocyanine

They are used as coloring matters dispersed in various vehicles such as polymerized linseed oil, nitrocellulose and miscellaneous synthetic resins.

In order to study the effects of the crystal structures, the numbers and positions of chlorine atoms and the pigment contents on the variation of color, the author formulated coloring matter with polymerized linseed oil used as the vehicle, and measured the reflectance curves.

Experimental

Materials.—*α-Form* (I) *and β-form* (II) *copper phthalocyanines.*—A mixture of phthalic anhydride, urea and cuprous chloride was heated in trichlorobenzene at about 190°C for 3 hr[1]. The reaction product was treated with 5% hydrochloric acid and 2% caustic soda, filtered off, washed with water and ethanol, and dried.

The crystal structure of copper phthalocyanine thus prepared was α-form (I)[2,3]. It was pulverized in a ball mill by the method described in Ref. 4.

To transform it into β-form (II), it was dissolved in 98% sulfuric acid, poured into water and deposited as fine crystals[5].

Copper octa-(4,5)-chlorophthalocyanine (III) *and copper octa-(3,6)-chlorophthalocyanine* (IV).—First, from the mixture of dichlorophthalic anhydrides prepared by chlorinating phthalic anhydride in oleum by the improved V. Villiger's method[6,7], 4,5-dichlorophthalic anhydride, m. p. 185.5~186.5°C (reported m. p. 185~187°C[8]) (*Anal.* Found: Cl, 32.66%) and 3,6-dichlorophthalic anhydride, m. p. 190~191°C (reported m. p. 190~191°C[8]) (*Anal.* Found: Cl, 32.71%) were separated with toluene-ethanol (1:1) solvent.

III (*Anal.* Found: Cl, 33.21%) and IV (*Anal.* Found: Cl, 33.23%) were synthesized respectively from 4,5- and 3,6-dichlorophthalic anhydrides by the urea-method[1]. They were respectively dissolved in chlorosulfonic acid and poured into ice water and reprecipitated as fine crystals.

Copper hexadecachlorophthalocyanine (V).—V was prepared by chlorinating copper octa-(3,6)-chlorophthalocyanine (*Anal.* Found: Cl, 50.33%)[7]. It was dissolved in chlorosulfonic acid, poured into ice water and reprecipitated as fine crystals. Particle size distributions of these materials were obtained with an electron microscope[9]. The diameters of these particles were 200~400 mμ and the mean value was about 250 mμ.

Methods.—A mixture of an equal quantity of each pigment and polymerized linseed oil was made into paste (A) by grinding 400 rounds in a Hoover automatic muller. A mixture of an equal quantity of aluminum hydroxide and polymerized linseed oil was made into paste (B) as above. A and B were mixed and pastes of each pigment, having pigment contents of 30, 25, 20, 15, 10, 7.5 and 5%, respectively, were prepared. These were applied 0.5 mm. in thickness on coated papers with a bladeoapplicator (Gardner Laboratory) and dried at room temperature. Reflectance curves of these samples were measured with a recording spectrophotometer (General Electric Co.) and C. I. E. Notations were obtained.

1) U. S. Pat. 2,197,458 (1940).
2) J. M. Robertson, *J. Chem. Soc.*, **1935**, 615; ibid., **1936**, 1195; ibid., **1937**, 219.
3) M. Shigemitsu, This Bulletin, **32**, 607 (1959).
4) U. S. Pat. 2,556,726 (1951); U. S. Pat. 2,556,727 (1951); U. S. Pat. 2556,728 (1951); U. S. Pat. 2,556,730 (1951).
5) G. von Susich, *Anal. Chem.*, **22**, 425 (1950).
6) V. Villiger, *Ber.*, **42**, 3538 (1909).
7) M. Shigemitsu, to be published in *J. Chem. Soc. Japan, Ind. Chem. Sec.* (*Kogyo Kagaku Zasshi*), **62**, 112 (1959), (presented at the Autumnal Joint Meeting of Chemical Society of Japan with other Societies, Tokyo, 1957).
8) V. Villiger, *Ber.*, **42**, 3532 (1957).
9) E. Suito et al., presented at the 58th Meeting of Electron Microscope Committee of Japan, 1951.

Results

Tables I, II, III, IV and V show the C. I. E. Notations of I, II, III, IV and V. In these tables, *Y* denotes luminosity, *Pe* purity and λ_D dominant wavelength.

TABLE I. C. I. E. NOTATIONS OF COPPER PHTHALOCYANINE (α-form)

Pig. cont. %	*Y* %	*Pe* %	λ_D mμ
30	8.42	50.2	465.5
25	9.10	51.0	466.0
20	10.62	51.8	470.2
15	12.40	51.0	471.9
10	16.60	49.1	475.4
7.5	18.28	47.1	476.4
5	25.08	40.2	478.2

TABLE II. C. I. E. NOTATIONS OF COPPER PHTHALOCYANINE (β-form)

Pig. cont. %	*Y* %	*Pe* %	λ_D mμ
30	7.64	50.0	463.0
25	8.52	52.5	464.1
20	9.44	52.0	466.2
15	10.37	51.2	469.4
10	15.10	47.5	472.4
7.5	17.49	44.8	474.8
5	23.18	38.4	476.2

TABLE III. C. I. E. NOTATIONS OF COPPER OCTA-(4,5)-CHLOROPHTHALOCYANINE

Pig. cont. %	*Y* %	*Pe* %	λ_D mμ
30	9.86	49.7	466.4
25	10.85	49.8	468.5
20	12.59	49.2	470.6
15	14.29	47.0	474.4
10	18.29	43.5	478.5
7.5	20.43	40.6	480.8
5	27.15	33.4	482.4

TABLE IV. C. I. E. NOTATIONS OF COPPER OCTA-(3,6)-CHLOROPHTHALOCYANINE

Pig. cont. %	*Y* %	*Pe* %	λ_D mμ
30	10.45	49.2	474.0
25	11.05	48.0	474.4
20	13.17	46.0	476.2
15	15.00	43.1	479.1
10	19.25	38.4	482.1
7.5	23.62	33.5	484.0
5	30.24	31.5	486.1

TABLE V. C. I. E. NOTATIONS OF COPPER HEXADECACHLOROPHTHALOCYANINE

Pig. cont. %	*Y* %	*Pe* %	λ_D mμ
30	10.14	49.4	479.0
25	10.45	46.3	479.2
20	12.50	42.9	480.5
15	15.06	39.1	483.0
10	20.84	34.4	486.8
7.5	25.56	30.5	489.3
5	34.24	28.5	492.0

In all cases, luminosities and dominant wavelengths decreased as the pigment contents increased, but variations of purities differed depending upon the kinds of pigments. I and II gave the maximum purities when their pigment contents were 20 and 25% respectively. On the other hand, purities of IV and V increased as their pigment contents increased. III showed a tendency similar to I and II. Fig. 1 shows the relation between purities and luminosities.

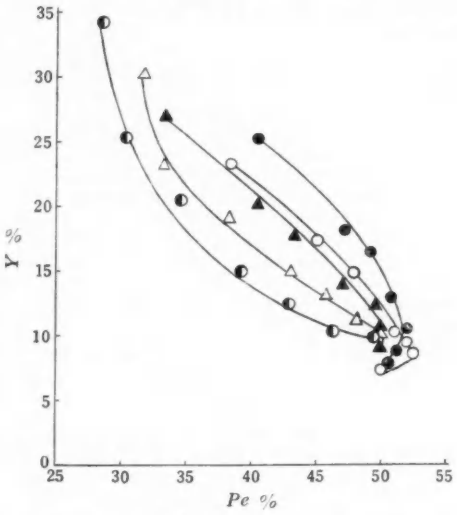

Fig. 1 Relation between purity and luminosity.
-●- Copper phthalocyanine (β-form).
-○- Copper phthalocyanine (α-form).
-▲- Copper octa-(4,5)-chlorophthalocyanine.
-△- Copper octa-(3,6)-chlorophthalocyanine.
-◐- Copper hexadecachlorophthalocyanine.

The purity of II was higher than that of I. The luminosities of I and II increased and decreased from the points of maximum purities with the variations in their purities, and the tendency in II was more conspicuous than in I. On the other hand, the luminosities of IV and V decreased with the increase in their purities.

Summary

The variation of color of copper phthalocyanine and its chlorinated derivatives in polymerized linseed oil was investigated.

The β-form of copper phthalocyanine is more conspicuous than the α-form in their variation of color.

Chlorine atoms at 3, 6- or 4, 5-positions of phthalocyanine nucleus give very different actions according to their variations of color, even if their chlorine contents are the same.

The author extends his sincere thanks to Dr. Ryozo Goto, Professor of Kyoto University, for his kind guidance. Thanks are also due to Dr. Takahisa Nakamura and Dr. Wataru Ishikawa, Toyo Ink Manufacturing Co., for their help.

Central Research Laboratory
Toyo Ink Mfg. Co.
Sumida-ku, Tokyo

Hydrothermal Reaction of Aluminumtrihydroxides

By Goro YAMAGUCHI and Kenichi SAKAMOTO

(Received December 17, 1958)

Recently, many studies of thermal transformation of the aluminumtrihydroxides have been reported[1] and we have got details of the mechanism of thermal change. Moreover, there are many experiments dealing with the digesting of gibbsite in an autoclave, but there is no consistent theory of the mechanism of the digesting reaction. The present authors studied and tried to explain the mechanism of hydrothermal reaction of aluminumtrihydroxides. Details are shown as follows.

Experimental

Materials. — The aluminumtrihydroxides employed in this experiment were gibbsite and bayerite. The gibbsite was a commercial product. It was washed with pure water. Ignition loss was 34.40%. The bayerites were prepared by three methods. The details of the methods had already been reported by the authors[2]. Three bayerites are named bayerite-*a*, -*b* and -*c*. In this study, the *a* was prepared by aging alumina-gel in ammonia water, the *b* was precipitated from sodium aluminate solution by means of a current of carbon dioxide, and the *c* was prepared by auto-precipitation from sodium aluminate solution. The main impurity was sodium oxide of 0.10～0.50%. The crystallinities of bayerites were quite different according to their processes of preparation. They were identified by X-ray analysis.

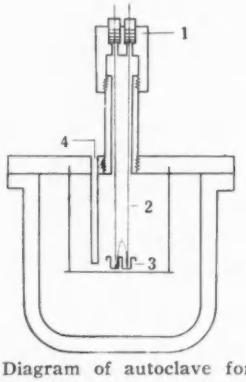

Fig. 1. Diagram of autoclave for DTA in saturated vapor.
(1) Teflon packing, (2) double thermocouples, (3) sample holders, (4) thermometer.

Apparatus and Procedure.—The authors devised an apparatus for differential thermal analysis in saturated vapor. The diagram is shown in Fig. 1. Air-tightness of the part 1 is kept by packing many thin Teflon sheets. This part is cooled in runs to protect the Teflon packings from thermal damage. Sample holders are silica vessels with 1 cm. diameter and 1.5 cm. depth.

The sample was about 1.5 g. in weight, and soaked with 1.5 cc. of water or alkali solutions of various concentrations. In some cases samples were mixed with boehmite. The reaction products were checked by X-ray diffraction.

TABLE I. GIBBSITE

The concn. of alkali added(%)	The contents of boehmite added(%)	Peak temp. (°C)	The breadth
—	—	218	5
0.5	—	217	6
5.0	—	212	8
20.0	—	207	8
—	5	210	9
—	10	205	9
—	20	203	10
—	30	200	17
	Bayerite-*a*		
—	—	190	14
0.5	—	167	14
5.0	—	153	12
20.0	—	145	10
—	30	185	13
	Bayerite-*b*		
—	—	205	8
0.5	—	202	10
5.0	—	192	11
20.0	—	190	11
—	30	194	11
	Bayerite-*c*		
—	—	206	6
0.5	—	200	8
5.0	—	187	10
20.0	—	185	9
—	30.0	194	6

1) A. S. Russell et al., Technical Paper No. 10, Aluminum Company of America, Pittsburgh, Pennsylvania (1956).
2) G. Yamaguchi, K. Sakamoto and K. Shirasuka, *J. Chem. Soc. Japan, Ind. Chem. Sec.* (*Kogyo Kagaku Zasshi*), **61**, 307 (1958).

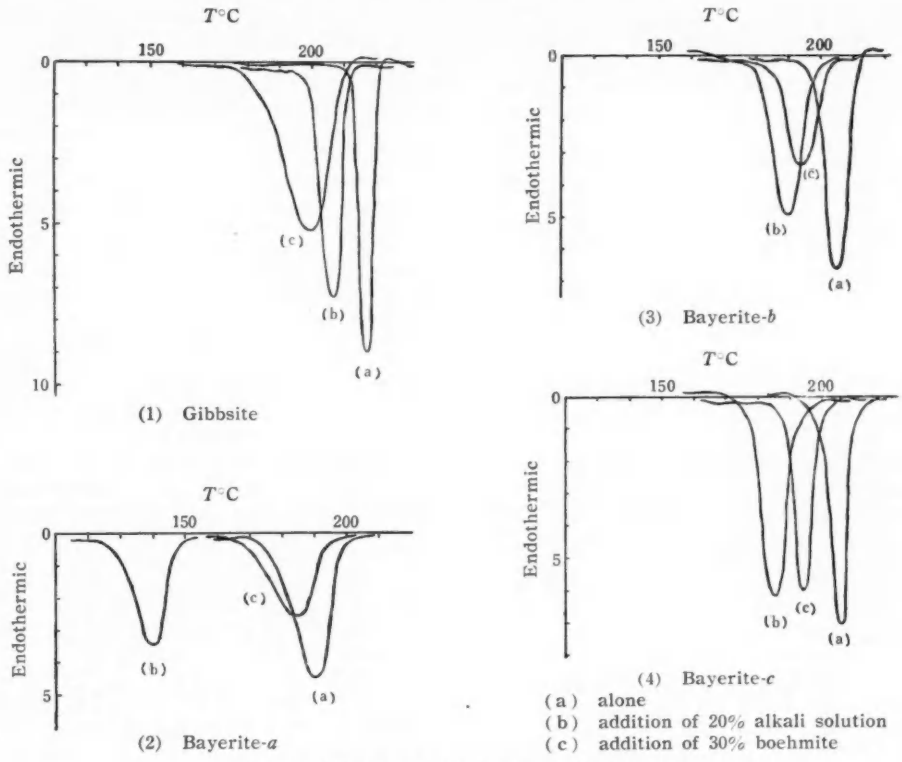

Fig. 2. DTA-curve of aluminumtrihydroxides.

Result

The results of the differential thermal analysis were shown in Fig. 2 and Table I. Gibbsite decomposes endothermally into boehmite. When gibbsite is immersed in alkali solution the peak temperature shifts to a lower point and the breadth at the half value of the endothermic peak becomes greater. The fall in peak temperature and the widening in breadth are very striking at the mixture of gibbsite and boehmite. In the case of 30%-boehmite, the peak temperature lowers to 200°C and the breadth becomes as wide as 17°C. These facts indicate that the alkalinity and the existence of boehmite lower the transformation temperature, that is, accelerate the transformation velocity.

About bayerites, it is clear that they have different stabilities according to the process of preparation. The bayerite-*a* exhibited the lowest peak temperature, and the temperature at the beginning of the transformation is also low. The peak temperature of DTA-curve is lowered remarkably by the addition of alkali. This indicates that this type of bayerite dissolves faster than it does in water. On the other hand, boehmite has only a little effect on the transformation of bayerite-*a*. Bayerite-*b* and -*c* showed similar characters. Added alkali lowers the peak temperature of these two bayerites, and makes the breadth wider. Boehmite lowers also the peak temperature of these bayerites, but has a different effect upon their width. The width of DTA-curve for bayerite-*c* is not effected by the addition of boehmite but the width for bayerite-*b*, becomes wider.

Consideration

Bauermeister and Fulda[3] and also Ginsberg and Koester[4] reported that the transformation of gibbsite to boehmite in an autoclave was accelerated by a small amount of alkali being added. Their

3) B. Bauermeister and W. Fulda, *Aluminum*, **25**, 97 (1953).
4) H. Ginsberg and M. Koester, *Z. anorg. u. allgem. Chem.*, **271**, 41 (1952).

results agree with the present results. Further Russell and his co-workers[5] reported that gibbsite transformed quickly to boehmite in a concentrated alkali solution. Bauermeister explained the transformation from gibbsite to boehmite as a dissolution change, but Ginsberg, and also Sato[6] supposed this reaction to be solid-decomposition. Now, the authors support the resolution reaction through which the transformation proceeds. This reaction consists of two steps; the dissolution of trihydroxides and the crystallization of boehmite. We can represent this reaction as follows:

$$Al(OH)_3 + (OH)^- \rightarrow Al(OH)_4^-$$

$$Al(OH)_4^- \rightarrow AlO(OH) + (OH)^- + H_2O$$

Thus, we can understand the effect of boehmite as the seed of the crystallization of boehmite. In this region boehmite is very stable, so it is unnatural to suppose that this boehmite reacts directly with aluminumtrihydroxide. This is quite analogous to the effect of gibbsite-seed in the Bayer-process.

About bayerites, it was found that their stabilities were quite different according to the process of their preparation. Also in reference to X-ray diffraction data, it is sure that stabilities of bayerites correspond to their crystallinities. So, the properties which bayerite-*a* exhibited, i.e., the low temperature of the beginning of the transformation and the broad width of the DTA-curve, are attributed to its poor crystallinity. This bayerite was prepared by aging an alumina gel in ammonia solution. So it is supposed that this bayerite consisted of components with different crystallinities. The stability of the composition with poor crystallinity is very small, so this part begins to change into boehmite at temperature as low as 165°C. When alkali solution was added to this bayerite the peak temperature lowered remarkably. This is explained as follows: The part with poor crystallinity dissolves faster in alkali solution than in water, then boehmite crystallizes quickly from this aluminate solution, so this boehmite acts as the seed for the following crystallization. Therefore, the peak temperature fell remarkably, and the width of the DTA-curve remained as before.

Finally, it is emphasized that the transition of aluminumtrihydroxides in saturated vapor does not proceed as an equilibrium transition but as the change from an unstable system to a stable one. This means that the transition velocity at the equilibrium state is very slow and the first phase exists unchanged. A sufficiently high temperature is necessary for rapid change of aluminumtrihydroxides. When this condition is fulfilled, the transition proceeds quickly and shows a sharp endothermic peak of DTA-curve. This was realized in the thermal analysis of trihydroxides without alkali and boehmite (Fig. 2). In this case, the endothermic peak is very sharp and seems to be the peak of a monovariant reaction. But this is attributed to the large velocities of dissolution of aluminumtrihydroxides and of crystallization of boehmite.

In general the change of the Gibbs free energy of any reaction is represented by the next formula

$$\Delta G = \Delta H - T\Delta S$$

In this experiment, the chemical change proceeds as follows:

$$Al(OH)_3 + (OH)^- \rightarrow Al(OH)_4^-$$

$$Al(OH)_4^- \rightarrow AlO(OH) + (OH)^- + H_2O$$

in short

$$Al(OH)_3 \rightarrow AlO(OH) + H_2O$$

Under this condition, of course, ΔG must be negative. ΔH was found to be positive, and the entropy change is positive, because entropy increases at dehydration reaction. When this entropy term overcomes the enthalpy term, then the reaction proceeds. Russell and his co-workers studied the equilibrium constants to form aluminate ion from gibbsite and boehmite and found the transition temperature from gibbsite to boehmite in pure water to be 27°C. Also they found that the trihydrates transformed rapidly to α-monohydrate at solution temperatures above 100°C. This is consistent with the present results.

Summary

In saturated vapor, the aluminumtrihydroxides dissolve in the water and the velocity of dissolution of the trihydroxides becomes larger as the temperature rises. When this solution is supersaturated over the solubility of boehmite, transformation proceeds. The alkalinity and the boehmite added to the hydroxides accelerate

5) A. S. Russell et al., *J. Metal*, 7, 1123 (1955).
6) T. Sato, Abstracts of the 11th Annual Meeting of Chemical Society of Japan, 296 (1958).

the transition. The former makes easy the dissolution of trihydroxides, and the latter acts as the seed and accelerates the velocity of the crystallization of boehmite.

Department of Applied Chemistry
Faculty of Engineering
The University of Tokyo
Hongo, Tokyo

A Convenient Method for the Calculation of the π-Electronic Structures of Aromatic Derivatives

By Kichisuke NISHIMOTO and Ryoichi FUJISHIRO

(Received January 12, 1959)

Theoretical investigations about the π-electronic structures of the aromatic derivatives based on the LCAO MO method have been carried out by many authors[1]. According to the results obtained by them, the molecular properties have been well correlated with their π-electronic structures, if the parameters appearing in the method have been properly chosen. But the actual calculation of the π-electronic structure of the molecule by means of the MO method is in general rather laborious. Therefore, it will be very convenient if one can find the method by which the calculation is simplified. In this paper we shall provide a convenient method using the set of vacant orbitals for the calculation and apply this method to the calculation of the molecular diagrams of the benzene hydroxy derivatives. In later discussions, we shall refer to this method as the "VO method" (vacant orbital method).

Method

The method is based on the framework of LCAO MO approximation, neglecting the differential overlap. When the molecule contains $2p\pi$ atomic orbitals (AO) in number of n, the molecular orbitals (MO), φ_i, are expressed by the linear combination of these AO's as follows:

$$\varphi_i = \sum_{\mu}^{n} \phi_\mu c_\mu \qquad (1)$$

where ϕ_μ is the μ-th $2p\pi$AO and c_μ is the coefficient to be determined by the variational method. When the following matrix notations which are the same as in Roothaan's paper[2] are used

$$\boldsymbol{\Phi} = (\varphi_1\varphi_2\cdots\cdots\varphi_n)$$

$$\boldsymbol{\phi} = (\phi_1\phi_2\cdots\cdots\phi_n)$$

$$\mathbf{C} = \begin{pmatrix} c_{11} & c_{12} & \cdots\cdots & c_{1n} \\ c_{21} & c_{22} & \cdots\cdots & c_{2n} \\ \vdots & \vdots & & \vdots \\ c_{\mu 1} & c_{\mu 2} & \cdots\cdots & c_{\mu n} \\ \vdots & \vdots & & \vdots \\ c_{n1} & c_{n2} & \cdots\cdots & c_{nn} \end{pmatrix}$$

we may write then for Eq. 1

$$\boldsymbol{\Phi} = \boldsymbol{\phi}\mathbf{C}$$

If we multiply the right-hand side by $\boldsymbol{\Phi}^*$ and the left-hand side by $\boldsymbol{\phi}^*\mathbf{C}^*$, then the following relation may be obtained,

$$\mathbf{C}^*\mathbf{C} = \mathbf{E}$$

or

$$\sum_{\mu}^{n} c_{\mu i}^* c_{\mu i} = 1 = \sum_{\mu}^{occ} c_{\mu i}^* c_{\mu i} + \sum_{\mu}^{vac} c_{\mu i}^* c_{\mu i}$$

$$\sum_{\mu}^{n} c_{\mu i}^* c_{\nu i} = 0 = \sum_{i}^{occ} c_{\mu i}^* c_{\nu i} + \sum_{i}^{vac} c_{\mu i}^* c_{\nu i} \qquad (2)$$

where $\sum_{i}^{occ}$ and $\sum_{i}^{vac}$ mean the summation over the set of occupied orbitals and that of vacant orbitals, respectively. According to the definitions, the charge density q_μ and the bond order $p_{\mu\nu}$ may be written as,

$$2\sum_{i}^{occ} c_{\mu i}^* c_{\mu i} = q_\mu$$

$$2\sum_{i}^{occ} c_{\mu i}^* c_{\nu i} = p_{\mu\nu}$$

1) See, e.g., B. Pullman and A. Pullman, "Les Theories Electroniques de la Chimie Organique", Masson et Cie, Paris (1952).

2) C. C. J. Roothaan, *Rev. Modern Phys.*, **23**, 69 (1951).

It is convenient to introduce q_μ^v and $p_{\mu\nu}^v$ as the corresponding quantities for the set of vacant orbitals, that is,

$$2\sum_i^{vac} c_{\mu i}^* c_{\mu i} = q_\mu^v$$

$$2\sum_i^{vac} c_{\mu i}^* c_{\nu i} = p_{\mu\nu}^v$$

Using these quantities, Eq. 2 can be rewritten as

$$(q_\mu - 1) = -(q_\mu^v - 1)$$

$$p_{\mu\nu} = -p_{\mu\nu}^v \qquad (3)$$

$(q_\mu - 1)$ represents the net charge at the position of the μ-th carbon atom belonging to the parent hydrocarbon system. As seen in Eq. 3, the set of vacant orbitals may become a mirror image of that of occupied orbitals. For the case of substituents which have only the lone pair orbitals, such as OH, NH_2, Cl, etc., the net charge must be expressed by $(q_\mu - 2)$ instead of $(q_\mu - 1)$. Therefore, in this case $-q_\mu^v$ may directly measure the net charge at the substituent. Using the relation 3, the calculation of the molecular diagram of the aromatic derivative may be considerably simplified, because

(1) the number of vacant orbitals is always less than that of occupied orbitals, and

(2) the vacant orbital and their energies differ only slightly from those of the reference system, since the large differences in orbital energies between the occupied and the vacant orbitals in the reference system may restrict the deformation of the vacant orbitals by conjugation to small extent. Here, we call the system in which the interactions between the parent hydrocarbon system and the substituents do not take place, as the reference system.

Pople's method for the LCAO SCF MO calculation tells us that the matrix elements of the Hartree-Fock Hamiltonian can be expressed by q_μ's, $p_{\mu\nu}$'s and the fundamental atomic integrals. Therefore, the SCF calculation based on his method may substantially expedited by the use of VO method, because

(1) the calculations of q_μ's and $p_{\mu\nu}$'s are easily carried out, and

(2) the rapid convergence to the SCF MO's may be expected, since the vacant orbitals may differ only slightly from those of the reference system.

When the square of the coefficient of the carbon atom to be bonded with the substituent in the lowest vacant orbital (frontier orbital) of the parent hydrocarbon system has considerably large value, the deformation for the lowest vacant orbital by conjugation may be greater than for others. Thus, in this case the frontier orbital will make the greatest contribution to the mirror image relations. Actually, it is well known[3] in many cases that the frontier orbital theory provides satisfactory information for the discussion of chemical reactions.

Next, we shall show a mirror image relation of orbital energies. The energy, ε_i, of the φ_i is determined by the solution of the secular determinant of n-th degree, that is,

$$\det|H_{\mu\nu} - \delta_{\mu\nu}\varepsilon| = 0$$

where $H_{\mu\nu}$ is the matrix element of the Hamiltonian, which is expressed by

$$H_{\mu\nu} = \int \phi_\mu^* H \phi_\nu \, dv$$

where H is the (effective or Hartree-Fock) Hamiltonian operator. According to the algebraic theory, the total sum of roots is equal to the negative value of the coefficient of ε^{n-1} term in the development of the secular determinant in terms of ε, that is,

$$\sum_i^n \varepsilon_i = \sum_\mu^n H_{\mu\mu} = \sum_i^{occ} \varepsilon_i + \sum_i^{vac} \varepsilon_i \qquad (4)$$

From this equation we obtain

$$2\sum_i^{occ} \varepsilon_i - \sum_\mu^n H_{\mu\mu} = -(2\sum_i^{vac} \varepsilon_i - \sum_\mu^n H_{\mu\mu}) \qquad (5)$$

For many purposes, only the extra delocalization energy, $\Delta\varepsilon$, arising from the delocalization of the $2p\pi$ electrons by substitution may be important. $\Delta\varepsilon$ is defined as follows:

$$\Delta\varepsilon = 2(\sum_i^{occ} \varepsilon_i - \sum_i^{occ} \varepsilon_i^0) \qquad (6)$$

where ε_i^0 is the orbital energy in the reference system. Similar relation to Eqs. 4 and 5 may also be obtained for the case of reference system, that is,

$$\sum_i^n \varepsilon_i^0 = \sum_\mu^n H_{\mu\mu}^0 = \sum_i^{occ} \varepsilon_i^0 + \sum_i^{vac} \varepsilon_i^0$$

$$2\sum_i^{occ} \varepsilon_i^0 - \sum_\mu^n H_{\mu\mu}^0 = -(2\sum_i^{vac} \varepsilon_i^0 - \sum_\mu^n H_{\mu\mu}^0) \qquad (7)$$

3) K. Fukui, T. Yonezawa and H. Shingu, *J. Chem. Phys.*, **20**, 722 (1952); K. Fukui, T. Yonezawa, C. Nagata and H. Shingu, ibid., **22**, 1433 (1954); K. Fukui, T. Yonezawa and C. Nagata, This Bulletin, **27**, 423 (1954).

TABLE I. MO'S AND MO ENERGIES

Orbital energy in β	MO
	Benzene
-2	$\varphi_1^v = 1/\sqrt{6}\,(\phi_1-\phi_2+\phi_3-\phi_4+\phi_5-\phi_6)$
-1	$\varphi_2^v = 1/\sqrt{12}(2\phi_1-\phi_2-\phi_3+2\phi_4-\phi_5-\phi_6)$
-1	$\varphi_3^v = 1/\sqrt{4}\,(\phi_2-\phi_3+\phi_5-\phi_6)$
	Catechol
-2.0497	$\varphi_1^v = 0.3978(\phi_1-\phi_4)-0.4365(\phi_2-\phi_3)-0.3790(\phi_6-\phi_5)+0.0861(\phi_7-\phi_8)$
-1.0897	$\varphi_2^v = 0.0462(\phi_1-\phi_4)+0.4651(\phi_2-\phi_3)-0.5155(\phi_6-\phi_5)-0.1256(\phi_7-\phi_8)$
-1.0346	$\varphi_3^v = 0.5663(\phi_1+\phi_4)-0.3076(\phi_2+\phi_3)-0.2783(\phi_6+\phi_5)+0.0849(\phi_7+\phi_8)$
	Resorcinol
-2.0480	$\varphi_1^v = 0.4125\phi_1-0.4224(\phi_2+\phi_6)+0.3943(\phi_3+\phi_5)-0.3850\phi_4+0.0833(\phi_7+\phi_8)$
-1.0987	$\varphi_2^v = 0.5129(\phi_2-\phi_6)-0.4668(\phi_3-\phi_5)-0.1381(\phi_7-\phi_8)$
-1.0313	$\varphi_3^v = 0.5258\phi_1-0.2711(\phi_2+\phi_6)-0.3389(\phi_3+\phi_5)+0.5791\phi_4+0.0752(\phi_7+\phi_8)$
	Hydroquinone
-2.0475	$\varphi_1^v = 0.4180(\phi_1-\phi_4)-0.3990(\phi_2-\phi_3-\phi_5+\phi_6)-0.0826(\phi_7-\phi_8)$
-1.1269	$\varphi_2^v = 0.5748(\phi_1+\phi_4)-0.2702(\phi_2+\phi_3+\phi_5+\phi_6)-0.1532(\phi_7+\phi_8)$
-1.0000	$\varphi_3^v = 0.5000(\phi_2-\phi_3+\phi_5-\phi_6)$
	Phloroglucinol
-2.0698	$\varphi_1^v = 0.4111(\phi_1+\phi_3+\phi_5)-0.3973(\phi_4+\phi_2+\phi_6)-0.0806(\phi_7+\phi_8+\phi_9)$
-1.0987	$\varphi_2^v = 0.2961(2\phi_1-\phi_3-\phi_5)+0.2695(2\phi_4-\phi_2-\phi_6)-0.0797(2\phi_7-\phi_8-\phi_9)$
-1.0987	$\varphi_3^v = 0.5129(\phi_3-\phi_5)-0.4668(\phi_2-\phi_6)-0.1381(\phi_8-\phi_9)$
	2, 3, 5, 6-Tetrahydroxybenzene
-2.0923	$\varphi_1^v = 0.3909(\phi_1-\phi_4)-0.4090(\phi_2-\phi_3-\phi_5+\phi_6)+0.0797(\phi_7-\phi_8-\phi_9+\phi_{10})$
-1.1827	$\varphi_2^v = 0.4838(\phi_2-\phi_3+\phi_5-\phi_6)-0.1261(\phi_7-\phi_8+\phi_9-\phi_{10})$
-1.0664	$\varphi_3^v = 0.5571(\phi_1+\phi_4)-0.2971(\phi_2+\phi_3+\phi_5+\phi_6)+0.0810(\phi_7+\phi_8+\phi_9+\phi_{10})$

We may now define $\Delta\varepsilon^v$ as follows:

$$\Delta\varepsilon^v = 2\left(\sum_i^{vac}\varepsilon_i - \sum_i^{vac}\varepsilon_i^0\right) \tag{8}$$

Then the following expression may be derived from above equations,

$$\Delta\varepsilon - \sum_i^n (H_{\mu\mu}-H_{\mu\mu}^0) = -\left[\Delta\varepsilon^v - \sum_\mu^n (H_{\mu\mu}-H_{\mu\mu}^0)\right] \tag{9}$$

When $H_{\mu\mu}=H_{\mu\mu}^0$, which is the case in the simple LCAO MO treatment neglecting the inductive effect, Eq. 9 becomes

$$\Delta\varepsilon = -\Delta\varepsilon^v$$

Thus the mirror image relation of orbital energies is established.

Calculation of the Molecular Diagrams

We shall apply VO method to the calculation of the molecular diagrams of benzene hydroxy derivatives. The method is based on the framework of simple LCAO AO method neglecting the inductive effect. The parameters used are the same as those of phenol[4]. All the hydroxy derivatives have only three vacant orbitals, since the reference systems have

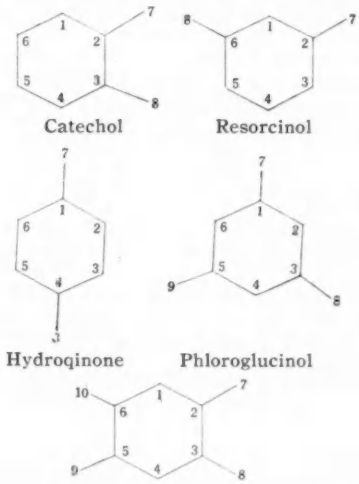

Fig. 1. Numbering of atoms.

4) K. Nishimoto and R. Fujishiro, This Bulletin, 31, 1036 (1958).

only three vacant orbitals, respectively. Therefore, the calculation based on the VO method is an easier task than that employing the set of occupied orbitals. The numbering of atoms is shown in Fig. 1. The calculated vacant MO's, ϕ_i^*, and their energies are collected in Table I, with those of a benzene molecule. Comparison of ϕ_1^*'s of hydroxy derivatives with that of benzene indicates that the former are polarized regularly along the direction toward the substituent; but their magnitudes are rather small. On the other hand, the frontier orbitals, φ_L^* and φ_{L+1}^*, seem to reflect roughly the characters of the ground states of the molecules. The molecular diagrams calculated are given in Fig. 2. When we try to plot the magnitude of the charge migration, Δe, from the substituents into the benzene ring, against the extra delocalization energy, $\Delta\varepsilon$, a linear relationship is obtained as shown in Fig. 3.

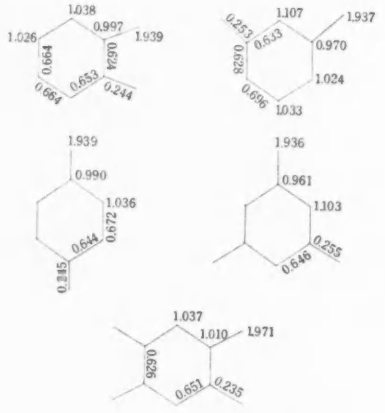

Fig. 2. Molecular diagrams.

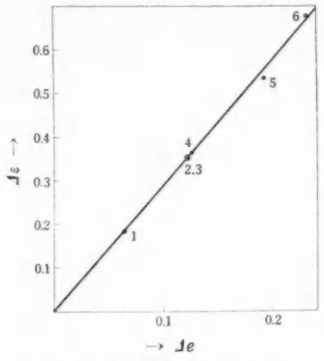

Fig. 3. Relation between $\Delta\varepsilon$ and Δe for benzene hydroxy derivatives.
1. Phenol
2. Catechol
3. Hydroquinone
4. Resorcinol
5. Phloroglucinol
6. 2,3,5,6-Tetrahydroxy benzene

Summary

It was shown that the set of vacant orbitals of the conjugated system would be a mirror image of that of occupied orbitals. Using this relation the calculations of the π-electronic structures of the aromatic derivatives are considerably simplified. As an example, the molecular diagrams of the benzene hydroxy derivatives were calculated.

Department of Chemistry
Institute of Polytechnics
Osaka City University
Kita-ku, Osaka

Isomerism and Polymorphism of Cinnamic Acids and Deuterated Allocinnamic Acids

By Minoru HIROTA and Yoshiyuki URUSHIBARA

(Received January 17, 1959)

Since the three polymorphic forms of allocinnamic acid were found and studied by Liebermann[1], by Paal[2], and by Biilmann[3], they have been the subject of many researches[4] including those on the dipole moment[5], the infrared absorption[6], other physical properties, and the transition between them[7].

In the course of the studies of the polymorphic behaviors of the compounds with group $C_6H_5CH=CHCO$[8], deuterated allocinnamic acids have been investigated in comparison with the ordinary allocinnamic acid, the powder X-ray diffraction and ultraviolet absorption spectra of α,β-d_2-allocinnamic acid and *O*-*d*-allocinnamic acid being measured. The X-ray diffraction patterns of the *O*-*d*-allocinnamic acid showed an expansion of the crystal lattice. No remarkable difference was found among the ultraviolet absorptions of three polymorphic forms of allocinnamic acid. In an experiment of catalytic hydrogenation of phenylpropiolic acid to allocinnamic acid, a new polymorphic form, m. p. 120°C, of (*trans*-)cinnamic acid was obtained by chance, and its transition to the stable form, m. p. 133°C, was observed.

Experimental

Partial Hydrogenation of Phenylpropiolic Acid.—Phenylpropiolic acid was prepared from commercial cinnamic acid according to the method of "Organic Syntheses"[9,10], and catalytically hydrogenated to allocinnamic acid. Palladium catalysts, e. g., Pd-$BaSO_4$[11] Pd-poly(vinyl alcohol)[12] and Pd-Na protalbinate[13], and the Urushibara catalysts[14,15], e. g., U-Ni-B and U-Co-A, were used in the partial hydrogenation and the latter catalysts were found useful for the purpose. The U-Ni-B catalyst gave the purest allocinnamic acid, while the palladium catalysts yielded hardly crystallizable products which had to be purified through the aniline salt[16]. The results of the catalytic hydrogenation with various catalysts are summarized in Table I.

The 58°-form[17] of allocinnamic acid was prepared by recrystallization of the hydrogenation products, the 68°-form through the aniline salt and the 42°-form by cooling suddenly the melt of the 58°-form or 68°-form in dry ice.

Preparation of Deuterated Allocinnamic Acids.—α,β-d_2-Allocinnamic acid was prepared by the catalytic deuteration of sodium phenylpropiolate with deuterium in a solution in 99.7% heavy water produced by the Norsk Hydro-Elektrisk Kvaelstofaktieselskab, Norway. The deuterium was generated by the electrolysis of the heavy water by using anhydrous sodium sulfate as the electrolyte, platinum electrodes, and an electric current of density 0.02~0.03 amp./cm^2 and 6~8 V. Palladium on barium sulfate, which was chosen on account of its small content of exchangeable hydrogen, was first deuterated in the heavy water and then employed for the catalytic deuteration. It was presumed without any determination that the α,β-d_2-allocinnamic acid contained nearly 100% deuterium in the α and β positions.

In order to deuterate the carboxylic hydrogen, allocinnamic acid was recrystallized once from 47.4% D_2O and then from 99.7% D_2O. The deuterium content of allocinnamic acid deuterated in this way was determined to be 80±5% of the carboxylic hydrogen.

Measurements of Absorption Spectra.—Ultraviolet absorptions were measured in ethanolic solution in the range of wavelengths 2100~4000 Å with a Beckman Model DU spectrophotometer. Infrared absorptions were measured with a Baird Model B infrared recording spectrophotometer in

1) C. Liebermann, *Ber.*, **23**, 515 (1890); **25**, 91 (1892).
2) C. Paal and W. Hartmann, ibid., **42**, 3931 (1909).
3) E. Biilmann, ibid., **43**, 573 (1910).
4) Cf. C. Weygand and H. Baumgärtel, ibid., **65**, 693 (1932); A. W. K. De Jong, *Rec. Trav. Chim. Pays-Bas*, **51**, 397 (1932).
5) F. Eisenlohr and W. Hass, *Z. physik. Chem.*, **A173**, 249 (1935).
6) J. Guy, *Ann. Phys.*, (12), **4**, 704 (1949).
7) F. Eisenlohr and A. Metzner, *Z. physik. Chem.*, A, **178**, 339 (1937).
8) F. Iimura, *J. Chem. Soc. Japan, Pure Chem. Sec.* (*Nippon Kagaku Zasshi*), **77**, 1851 (1956).
9) T. W. Abbott, "Organic Syntheses", Col. Vol. 2, John Wiley & Sons, New York (1948), p. 515.
10) T. W. Abbott and D. Althousen, ibid., Col. Vol. 2, (1948), p. 270.
11) R. Mozingo, ibid., Vol. 26, (1946), p. 77.
12) L. D. Rampino and F. F. Nord, *J. Am. Chem. Soc.*, **63**, 2745 (1941).
13) C. Paal and C. Amberger, *Ber.*, **38**, 1398 (1905).
14) Y. Urushibara and S. Nishimura, This Bulletin, **27**, 480 (1954).
15) Y. Urushibara, S. Nishimura and H. Uehara, ibid., **28**, 446 (1955).
16) C. Liebermann, *Ber.*, **27**, 2037 (1894).
17) "58°-Form" denotes the polymorphic form melting at 58°C and so on.

TABLE I. PARTIAL HYDROGENATION OF PHENYLPROPIOLIC ACID WITH VARIOUS CATALYSTS*

Catalyst	Conditions of hydrogenation	Forms of cinnamic acid obtained
U-Ni-B	Na salt in water	*cis*-58°**
U-Ni-A	Acid in ethanol	*cis*-58°
U-Co-A	Na salt in water	*cis*-58°, *cis*-68°
U-Co-A, then U-Ni-A	Acid in ethanol	*trans*-120°
U-Co-B	Na salt in water	*cis*-58°**
Pd-Na protalbinate (colloidal)	Na salt in water	Oil, *cis*-68° through aniline salt
Pd-charcoal	Na salt in water	Oil, *cis*-68° by recrystallization
Pd-$BaSO_4$	Na salt in water	*cis*-58°
Pd-poly(vinyl alcohol) (colloidal)	Na salt in water	Oil (*cis*-58°)**
U-Ni-B and active charcoal	Na salt in water	*cis*-68°, *cis*-58°

* Hydrogenation was stopped when one mole of hydrogen was absorbed.
** Phenylpropionic acid was obtained.

Nujol and in carbon tetrachloride solution when necessary.

Measurements of X-ray Diffraction Patterns. — The powder method was used with a Norelco X-ray diffractometer. The identity and the difference among polymorphic forms were determined by the diffraction patterns, the diffraction angles being mainly taken into consideration for the identification and the intensity of the diffracted beams being only auxiliarily respected.

Results and Discussion

Ultraviolet Absorption. Guy[18] observed that polymorphic forms of allocinnamic acid give different infrared spectra especially in the finger print region, and Urushibara, Iimura and Ikeda[8,19] showed that polymorphic forms of chalcones differ not only in infrared but also in ultraviolet spectra. The ultraviolet absorptions of cinnamic acid and allocinnamic acid have been reported with no notice of any difference in polymorphic forms[20].

TABLE II. ULTRAVIOLET ABSORPTION SPECTRA OF CINNAMIC ACIDS IN ETHANOL

	Form	λ_{max}(Å)	ε_{max}
Cinnamic acid	133°	2730	20500
(*trans*)	120°	2725	19000
Allocinnamic acid	58°	2670	9500
(*cis*)	68°	2660	9800
	42°	2630~2650	ca.10000

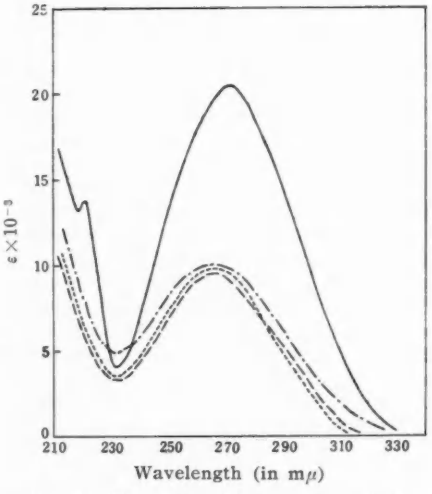

Fig. 1. The ultraviolet spectra of cinnamic acids.
Cinnamic acid 133°-form ———
Allocinnamic acid 42°-form —·—·—
58°-form ·····
68°-form ———

Ultraviolet absorption spectra in ethanol were measured with all the polymorphic forms of cinnamic acid and of allocinnamic acid with the results shown in Table II and Fig. 1. The three forms of allocinnamic acid gave similar absorption curves with no remarkable differences in either the locations or the intensities of the absorption maxima. Moreover, cinnamic acid and allocinnamic acid absorbed almost the same wavelength but the intensity of the former was roughly twice as strong as the latter.

18) J. Guy, *Ann. Phys.*, (12), **4**, 704 (1949).
19) Y. Urushibara, F. Iimura and K. Ikeda, *J. Chem. Phys.*, **22**, 1943 (1954); **23**, 759 (1955); F. Iimura, *J. Chem. Soc. Japan, Pure Chem. Sec.* (*Nippon Kagaku Zasshi*), **77**, 1846 (1956).
20) A. E. Gilam and E. S. Stern, "Introduction to Electronic Absorption Spectroscopy in Organic Chemistry", Edward Arnold Ltd., London (1954); H. M. Hershenson, "Ultraviolet and Visible Absorption Spectra, Academic Press Inc., New York (1956), p. 233.

Braude and his co-workers[21-23] have extensively studied the relations between the ultraviolet spectra and the steric hindrance in conjugated systems and concluded that, when the steric hindrance is not so large as to prevent the conjugation, the sterically hindered *cis*-isomer gives an absorption maximum almost at the same location as the unhindered *trans*-isomer but having a remarkably lower intensity. The appearance of polymorphism in a molecule with a partially hindered conjugated system is caused by the existence of metastable, rotationally hindered, forms conditioned by both the steric hindrance and the π-electron interaction between two parts of the molecule[24,25]. The interpretation that the polymorphism of cinnamic acids is based on such causes is supported by the different infrared spectra of the polymorphic forms.

The ultraviolet spectra of the deuterated allocinnamic acids revealed no isotope effect in any polymorphic forms.

Polymorphism of Deuterated Allocinnamic Acids.—Measurements of the powder X-ray diffraction with α,β-d_2-allocinnamic acid (II) and *O*-*d*-allocinnamic acid (III) in comparison with the ordinary allocinnamic acid (I) showed that the diffraction patterns of the polymorphic forms of *O*-*d*-allocinnamic acid deviate from those of the corresponding forms of the other

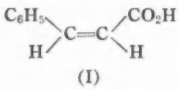

(I)

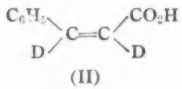

(II)

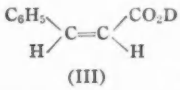

(III)

two, respectively. The deviations are comparatively remarkable, though small, in the two polymorphic forms melting at 58°C and at 68°C, and noticeably in the direction of smaller diffraction angles, suggesting a lattice expansion caused by deuteration. Deviations observed in the 42°-form permit to conclude neither a lattice expansion nor a lattice contraction.

The lattice expansion observed in the two forms of *O*-*d*-allocinnamic acid is supposed to be due to the deuterium bond which is weaker than the hydrogen bond in the corresponding forms of the ordinary allocinnamic acid. Such an isotope effect is known in oxalic acid[26] and other compounds[27] and explained on the basis of the weaker deuterium bond.

TABLE III. THE MELTING POINTS OF ALLOCINNAMIC ACIDS

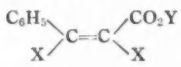

Form	I X=Y=H	II X=D, Y=H	III X=H, Y=D
68°	67.5~68.0°	67.0~68.0°	66.5~67.0°
58°	57.5~58.5°	55.0~57.5°	54.5~55.0°
42°	41.0~42.5°		41.5~42.0°

Some forms of the deuterated allocinnamic acids melted lower than the corresponding forms of the ordinary allocinnamic acid, as shown in Table III, and, since the melting point of either the 58°-form or the 68°-form of the ordinary allocinnamic acid was lowered by recrystallization from heavy water, it can be concluded that the lowering of the melting points of *O*-*d*-allocinnamic acid is connected with the lattice expansion.

Formation and Properties of the Metastable Form, m. p. 120°C, of Cinnamic Acid.—The new form of (*trans*-)cinnamic acid was obtained in an experiment to prepare allocinnamic acid from phenylpropiolic acid. The experimental sequence was as follows: When phenylpropiolic acid was hydrogenated with the U-Co-A catalyst, the reaction was too slow to be completed. Then U-Ni-A was added with an intension of finishing the partial hydrogenation to allocinnamic acid. After being left to stand for a day, the product was isolated from the reaction mixture, but it melted at 120°C and did not coincide with any form of allocinnamic acid. The product proved a new form of (*trans*-)cinnamic acid, since it gave an infrared absorption in solution quite similar to that of the known form (m. p. 133°C) of cinnamic acid except for a slight difference in the finger print region, and an ultraviolet absorption also similar to that of the 133°-form of cinnamic acid (120°-form: λ_{max} 2725 Å, ε_{max} 19000; 133°-form: λ_{max} 2730 Å, ε_{max} 20500). On the other hand,

21) E. A. Braude et al., *J. Chem. Soc.*, **1949**, 1890.
22) E. A. Braude and F. Sondheimer, ibid., **1955**, 3754.
23) E. A. Braude and C. J. Timmons, ibid., **1955**, 3766.
24) B. Eistert, F. Weygand and E. Csendes, *Ber.*, **84**, 745 (1951).
25) B. Eistert, F. Weygand and E. Csendes, ibid.. **85**, 164 (1952).
26) M. J. Robertson and A. R. Ubbelhde, *Proc. Roy. Soc.*, **A170**, 222 (1939).
27) Benzoic acid, succinic acid, sodium bicarbonate, etc.

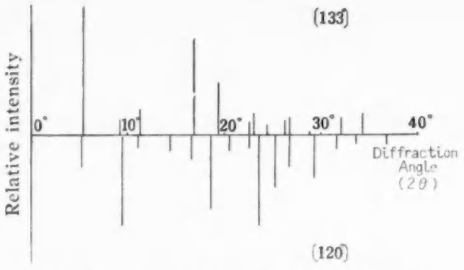

Fig. 2. The X-ray diffraction patterns of the 120°-form and the 133°-form of (*trans*-)cinnamic acid.

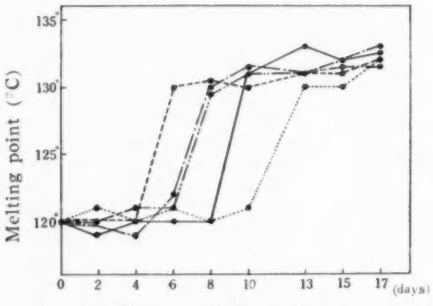

Fig. 3. Changes of the melting points of the 120°-form of cinnamic acid.

the X-ray diffraction pattern of the 120°-form is clearly different from that of the stable 133°-form of cinnamic acid, as shown in Fig. 2.

The formation of the new form of cinnamic acid in the hydrogenation of phenylpropiolic acid is explained by assuming that the allocinnamic acid formed by the catalytic hydrogenation was isomerized to a metastable form of the *trans*-isomer during its contact with the catalyst. The 120°-form was transformed into the 133°-form in one week or two, when it was kept in a dark place at room temperature. All attempts to repeat the preparation of the metastable form failed and the *cis*-isomer was always obtained instead. Further, it was observed that the transition of the metastable form to the stable form occurred abruptly when it once started by chance. Namely, when five portions of the metastable form were kept in a dark place at about 15°C, the melting points of these portions, determined every second or third day, changed suddenly but at different times, as shown in Fig. 3.

The authors wish to acknowledge their indebtedness to the late Dr. Iimura, and to express their thanks to Dr. Ōki and to Dr. Kobayashi, for their helpful discussions, to Dr. Nishimura and Dr. Sugimori for catalytic hydrogenation, and to Dr. Hayashi for measurements of the infrared spectra.

Department of Chemistry
Faculty of Science
The University of Tokyo
Hongo, Tokyo

Non-benzenoid Aromatic Heterocycles. I. Reactions of 4-Pyrone, 4-Thiopyrone, and their Pyrylium Salts with Active Methylene Compounds

By Masaki OHTA and Hiroshi KATO

(Received January 9, 1959)

It has been widely accepted that the –O– group is equivalent to the –CH=CH– group, thus 4-pyrone and 4-thiopyrone can be regarded as heterocyclic tropone analogues. The physical and chemical properties of these compounds can be more adequately explained in terms of formula Ia than in terms of the conventional formula Ib. In the same sense the pyrylium salts Ic derived from them can be considered as heterocyclic tropylium salt analogues.

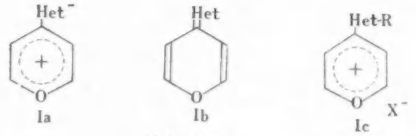

Het = O or S

In this respect, it is of interest to study some of their reactions. The concept that the carbonyl group of 4-pyrone behaves anomalously and does not react with most carbonyl reagents had long been accepted until Woods' report[1], where he has shown that 2,6-dimethyl-4-pyrone(II) undergoes condensation with malonitrile by refluxing in acetic anhydride. The present authors have tried further the condensation of II and 2,6-dimethyl-4-thiopyrone(III) with active methylene compounds aiming to show, to what extent the carbonyl or thiocarbonyl group of these compounds is active, and to distinguish the difference between these two compounds. 2,6-Dimethyl-4-pyrone(II) reacted with malonitrile, ethyl cyanoacetate, or rhodanine to give the corresponding condensation product IV~VI under the condition reported by Woods, but it failed to react with diethyl malonate, acetylacetone, cyclopentadiene, or nitromethane. Just the same result was obtained when III was treated with the above-cited compounds; this fact indicates essentially the same carbonyl character of these two compounds. The fact that the same condensation products are obtained starting from II or III unequivocally proves the structures of the condensation products. It is noteworthy that the condensation is not effected by the usual catalysts, e. g., sodium ethoxide or *tert.*-butoxide, sodium acetate, or piperidine. This fact suggests anomalous character of pyrone carbonyl group.

Woods reported that IV was hydrolyzed to the corresponding dicarboxylic acid, but in the authors' experiment, the corresponding nitrile-amide VII was the sole product. In this connection, it is worthy of note that malonic acid reacted with II or III by gently warming in acetic anhydride, but the reaction was accompanied by decarboxylation, and the product obtained in each case was black unpurifiable powder.

Recently, Dimroth et al.[2] have reported that 2,4,6-trialkylpyrylium borofluorides or perchlorates, when treated with potassium *tert*-butoxide in nitromethane, give the corresponding nitrobenzene derivatives. As 4-methoxy- or 4-methylmercaptopyrylium perchlorate, derived from II or III respectively, is structurally similar to trialkylpyrylium salts, the present authors predicted the reaction of the same type. This occurred as expected, and when 4-methoxy-2,6-dimethylpyrylium perchlorate (VIII) was treated with nitromethane and sodium *tert*-butoxide, 4-methoxy-2,6-dimethylnitrobenzene(IX)* was obtained. This compound IX was converted into 3,5-dimethyl-4-nitrophenol(X)* by refluxing

1) L. L. Woods, *J. Am. Chem. Soc.*, **80**, 1440 (1958).

2) K. Dimroth and D. Bräuniger, *Angew. Chem.*, **68**, 519 (1956); K. Dimroth, G. Bräuniger and G. Neubauer, *Chem. Ber.*, **90**, 1634 (1957); K. Dimroth, G. Neubauer, H. Möllenkamp and G. Oosterloo, ibid., **90**, 1668 (1957).

* Rowe et al.[3] prepared X in 2.4% yield by nitrating 3,5-dimethylphenol, and X was converted into IX by dimethyl sulfate.

3) F. M. Rowe, S. H. Bannister, R. R. Seth and R. C. Storey, *J. Soc. Chem. Ind.*, **49**, 469 (1930); *Chem. Abstr.*, **25**, 930 (1931).

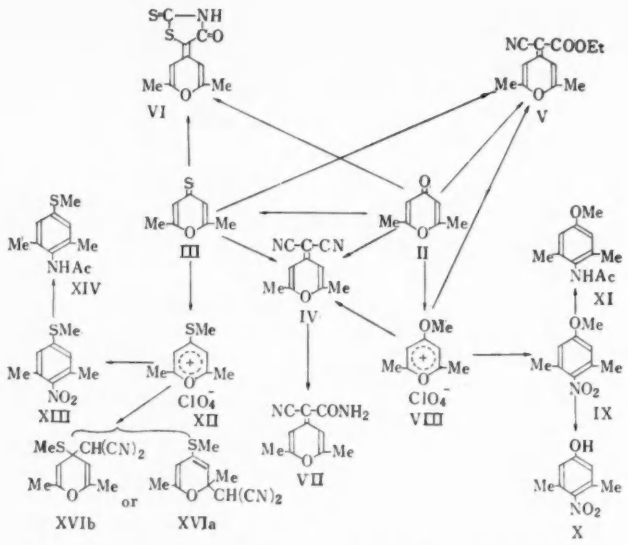

Fig. 1. Reactions of 2,6-dimethyl-4-pyrone and their derivatives with active methylene compounds.

with hydrobromic acid, and to 2,6-dimethyl-*p*-anisidine** by reduction with zinc and hydrochloric acid, which was identified as its acetyl derivative XI. Similarly, 4-methylmercapto-2,6-dimethylpyrylium perchlorate(XII) gave 4-methylmercapto-2,6-dimethylnitrobenzene(XIII) by the reaction with nitromethane and sodium *tert*-butoxide. This compound XIII was reduced, by zinc and hydrochloric acid to the corresponding amine, which was identified as an acetyl derivative(XIV)***. As Dimroth et al. have pointed out, these reactions are of value as a convenient preparatory method of the otherwise unobtainable or not easily accessible compounds. Moreover, the results of these reactions clearly reject the structure XVa which was once proposed for the salts****, and add an unambiguous proof of the widely accepted structure XVb.

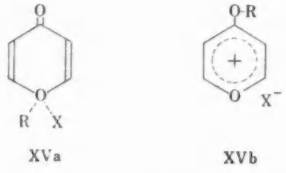

XVa XVb

Dimroth et al.[6] have briefly reported that the reaction of 2,4,6-trialkylpyrylium salts with ethyl cyanoacetate leads to benzonitrile derivatives. The present authors have expected the reaction of the same type with VIII, but in this case, the condensation at the position 4 of the salt VIII occurred, and gave exclusively 4-(ethoxycarbonylcyanomethylene)-2,6-dimethyl-4H-pyrane(V). Similarly, when VIII was treated with malonitrile, 4-(dicyanomethylene)-2,6-dimethyl-4H-pyrane (IV) was obtained. In the case of XII, the splitting up of methyl mercaptan did not occur, and the compound of the type XVIa or XVIb was obtained.

These reactions can be interpreted if the reaction mechanism shown in Fig. 2 is taken into account.

In Fig. 2, the key steps which determine the reaction routes are assumed to be steps A, B, C and D. The reactions with nitromethane take place smoothly by way of the steps A and C, but in the reaction with ethyl cyanoacetate, the step

** Bamberger et al.[4] prepared this compound by treating 2,6-dimethylphenylhydroxylamine with methanol in the presence of sulfuric acid.

4) E. Bamberger, *Ber.*, **36**, 2028 (1903).

*** This compound was prepared by Kloosterziel et al.[5], starting from 2,6-xylidine via thiocyano compound followed by reduction with lithium aluminum hydride and methylation.

**** Cf., for example, J. N. Collie and T. Tickle, *J. Chem. Soc.*, **1899**, 710; F. Kehrmann and A. Duttenhöfer, *Ber.*, **39**, 1299 (1906).

5) H. Kloosterziel and H. J. Backer, *Rec. trav. chim. Pays-Bas*, **72**, 655 (1953).

6) K. Dimroth and G. Neubauer, *Angew. Chem.*, **69**, 95 (1957).

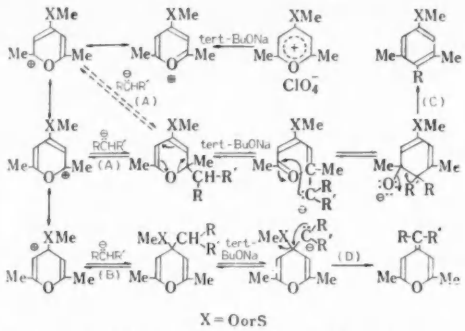

X = O or S

Fig. 2. Mechanism of the condensation reaction.

D (demethoxylation) is more favorable than the step C (decarbethoxylation), and the reaction leads to the condensation at the position 4. The same reaction mechanism can be assumed to the reaction with malonitrile. In the case of trialkylpyrylium salts, the step D corresponds to dealkylation which is hindered, thus the reaction proceeds thoroughly via the step C to give benzonitrile derivatives, as is observed in Dimroth's report.

As 4-pyrone perchlorate is believed to possess the structure of the pyrylium salt type, the reaction between this compound and malonitrile was tried in hopes of effecting a condensation reaction, but when 2,6-dimethyl-4-pyrone perchlorate was treated with malonitrile and sodium *tert*-butoxide, free 2,6-dimethyl-4-pyrone was obtained.

Experimental

2,6-Dimethyl-4-pyrone (II)[7].—Dehydroacetic acid (100 g.) was refluxed in concentrated hydrochloric acid (400 ml.) for an hour, and the solution was boiled for two hours to concentrate, and finally concentrated nearly to dryness under reduced pressure. The residue was dissolved in water, and the solution was washed with benzene, saturated with potassium carbonate and extracted with chloroform. The extract, after being dried with potassium carbonate, was evaporated and the residue was collected. Yield, 71 g. (97%); m. p. 130°C. The product was pure enough for use in the subsequent experiments.

2,6-Dimethyl-4-thiopyrone (III).—This compound was prepared by King's method[8].

Condensation of II or III with Active Methylene Compounds.—2,6-Dimethyl-4-pyrone (II) (1 g.) or -thiopyrone (III) (0.5 g.) and 1 mol. each of active methyl or methylene compounds were refluxed in acetic anhydride for an hour. Solvent was removed under reduced pressure, and the residue was collected, washed with ether and recrystallized.

The following results were obtained (Yield A refers that from II and Yield B that from III):
Malonitrile: pale yellow needles (from ethanol), m. p. 191°C[9]. Yield A, 90%; B, 33%.
Ethyl cyanoacetate: pale yellow needles (from ethanol), m. p. 184°C. Yield A, 31%; B, 44%.

Anal. Found: C, 65.51; H, 6.10; N, 6.67. Calcd. for $C_{12}H_{13}O_3N$ (V): C, 65.74; H, 5.98; N, 6.39%.

Rhodanine: yellow needles (washed with benzene and recrystallized from acetone), m. p. 260°C. Yield A, 32%; B, 59%.

Anal. Found: C, 49.93; H, 4.12; N, 5.17. Calcd. for $C_{10}H_9O_2NS_2$ (VI): C, 50.21; H, 3.79; N, 5.86%.

The products obtained from III were identified by their melting points, and by the failure of m. p. depressions on admixture with the specimens prepared from II.

These condensations could not be effected by sodium ethoxide or *tert*-butoxide, sodium acetate, or piperidine as catalyst.

In the case of diethyl malonate, acetylacetone, cyclopentadiene, or nitromethane, the reaction occurred neither with II nor with III, and the starting material was recovered unchanged.

When malonic acid (3 g.) was gently warmed in acetic anhydride (15 ml.) with II or III (3 g. each) a marked evolution of gas was observed and black unpurifiable powder (3 g.) was obtained after removal of the solvent. This substance was soluble in aqueous solution of sodium bicarbonate, but insoluble in most solvents.

Hydrolysis of IV.—A suspension of IV (7 g.) in a mixture of concentrated hydrochloric acid (40 ml.) and ethanol (40 ml.) was refluxed for twenty-four hours and then poured into water. The precipitate was collected and recrystallized from ethanol giving pale yellow amorphous powder with green fluorescence. (5 g.) m. p. 252°C (decomp.).

Anal. Found: C, 62.61; H, 5.35; N, 14.42. Calcd. for $C_{10}H_{10}O_2N_2$ (VII): C, 63.15; H, 5.30; N, 14.73%.

No dicarboxylic acid was obtained when refluxing was prolonged for another thirty hours.

4-Methoxy-2,6-dimethylpyrylium Perchlorate (VIII).—This compound was prepared by Baeyer's method[10].

4-Methylmercapto-2,6-dimethylpyrylium Perchlorate (XII).—This compound was prepared by Arndt's method[11].

4-Methoxy-2,6-dimethylnitrobenzene (IX).—A hot solution of sodium *tert*-butoxide (0.47 g. of metallic sodium in 30 ml. of *tert*-butanol) was added into a solution of VIII (2.4 g.) in nitromethane (10 ml.) under stirring and reflux. After refluxing for an hour, the mixture was

7) This is a modification of the procedure reported by Cornubert et al. (*Bull. soc. chim. France*, **1950**, 40) and by King et al.[8]
8) L. C. King et al., *J. Am. Chem. Soc.*, **73**, 300 (1951).
9) Woods[1] reports the m. p. 190~192°C.
10) A. Baeyer, *Ber.*, **43**, 2337 (1910).
11) F. Arndt and P. Nachtwey, ibid., **59**, 446 (1926).

poured into dilute hydrochloric acid (200 ml. containing 2 ml. of concentrated hydrochloric acid) and the solution was extracted with chloroform. The extract was dried with potassium carbonate, the viscous oily residue which remained after removal of the solvent was distilled under reduced pressure, and the fraction distilling at 129°C/8 mmHg was collected; it soon solidified to pale yellow needles (1 g.), m. p. 50°C [12].

Anal. Found: C, 59.68; H, 6.43; N, 7.67. Calcd. for $C_9H_{11}O_3N$ (IX): C, 56.66; H, 6.12; N, 7.73%.

4-Methylmercapto-2, 6-dimethylnitrobenzene (XIII).—A hot solution of sodium *tert*-butoxide (0.32 g. of metallic sodium in 30 ml. of *tert*-butanol) was added to a solution of XII (1.7 g.) in nitromethane (8 ml.), and was treated by essentially the same method as described above. A fraction which was distilled at 148~149°C/8 mmHg was collected, and it solidified to yellow needles (0.6 g.), m. p. 62~63°C.

Anal. Found: N, 7.39. Calcd. for $C_9H_{11}O_2NS$ (XIII): N, 7.10%.

3, 5-Dimethyl-4-nitrophenol (X).—A solution of IX (0.5 g.) in a mixture of hydrobromic acid (48%, 10 ml.) and acetic acid (5 ml.) was refluxed for three hours and the reaction mixture was extracted with chloroform. Removal of the solvent left yellow residue, which was recrystallized from ethanol giving yellow plates (0.4 g.), m. p. 107~108°C [13].

Anal. Found: N, 8.34. Calcd. for $C_8H_9O_3N$ (X): N, 8.38%.

***N*-Acetyl-2, 6-dimethyl-*p*-anisidine (XI).**—To a solution of IX (1 g.) in a mixture of hydrochloric acid (10%, 20 ml.) and acetic acid (10 ml.) was added zinc dust (5 g.) portionwise under warming. After two hours, the mixture was extracted with chloroform, and the residue, left after removal of the solvent, was warmed with acetic anhydride. After removal of the solvent, the residue was recrystallized from ethanol giving colorless plates (0.8 g.), m. p. 178°C.

Anal. Found: N, 7.22. Calcd. for $C_{11}H_{15}O_2N$ (XI): N, 7.25%.

12) Rowe et al.[3] report the m. p. 53°C.
13) Rowe et al.[3] report the m. p. 107~108°C.

***N*-Acetyl-4-methylmercapto-2, 6-dimethylaniline (XIV).**—Treatment of XIII (0.4 g.) by the same procedure as described above gave white needles (0.4 g.), m. p. 155~156°C [14].

Anal. Found: N, 6.80. Calcd. for $C_{11}H_{15}ONS$ (XIV): N, 6.69%.

Reaction of VIII with Ethyl Cyanoacetate.—A solution of VIII (2.4 g.) in a mixture of ethyl cyanoacetate (10 ml.) and *tert*-butanol (10 ml.) was treated by the same method as described in the reaction with nitromethane. Distillation gave solid distillate, which on recrystallization from ethanol gave orange leaflets (0.7 g.), m. p. 185°C. (Found: N, 6.35%). No melting point depression occurred when admixed with the authentic specimen V prepared by the condensation of II with ethyl cyanoacetate.

Reaction of VIII with Malonitrile.—A solution of VIII (2.4 g.) in a mixture of malonitrile (3 g.) and *tert*-butanol (15 ml.) was treated as described above. After refluxing for an hour, the mixture was poured into dilute hydrochloric acid and the yellow precipitate which separated out was collected. Yield, 1.7 g., m. p. 189°C. (Found: N, 15.99%.). No melting point depression occurred when admixed with the authentic specimen IV[1].

Reaction of XII with Malonitrile.—Into a suspension of XII (2.6 g.) in a mixture of malonitrile (1 g.) and *tert*-butanol (30 ml.) was added a hot solution of sodium *tert*-butoxide (0.47 g. of metallic sodium in 30 ml. of *tert*-butanol) under stirring and reflux. After refluxing for an hour, the mixture was poured into dilute hydrochloric acid and the precipitate which separated out was collected and recrystallized from ethanol giving yellow plates; m. p. 132~133°C.

Anal. Found: C, 60.14, N, 5.54; H, 12.87. Calcd. for $C_{11}H_{12}ON_2S$ (XVI): C, 60.00; H, 5.49; N, 12.72%.

The authors are indebted to Mr. Asaji Kondo for performing the microanalyses.

Laboratory of Organic Chemistry
Tokyo Institute of Technology
Meguro-ku, Tokyo

14) Kloosterziel et al.[5] report the m. p. 156.7~157.5°C.

Synthesis of 1,8(9)-p-Menthadien-10-yl-carbinol

By Kyoichi SUGA, Juichi ISHII and Shoji WATANABE*

(Received January 17, 1959)

The addition of formaldehyde to olefines is known as Prins reaction[1]. For the first time Ladenberg[2] discovered that formaldehyde can be added to terpenes and Kriewitz[3] researched this reaction with β-pinene. Lombard[4] obtained alcohol (IV) from *d*-limonene, using zinc chloride as a catalyst. The present authors investigated the addition reaction of *d*-limonene and formaldehyde, and prepared a limonenylcarbinol in high yields (30%), the structure of which was proved to be 1,8(9)-*p*-menthadien-10-yl-carbinol (III).

d-Limonene(I) and paraformaldehyde(II) scarcely reacted at all when the mixture was agitated in the presence of zinc chloride for 3 hr. at about 80°C; neither aluminum chloride nor ferric chloride in place of zinc chloride gave good results. When a mixture of one mol. each of I and II was heated for 12 hr. at 200~220°C in a sealed tube, a yellow viscous oil was obtained (yield, 11%). It gave a phenylurethan, m. p. 54~55°C, which was analyzed as the phenylurethan derived from an alcohol, $C_{11}H_{18}O$. As this procedure did not give satisfactory yields, a mixture of I, II and acetic anhydride was heated in an autoclave, and a limonenylcarbinyl acetate was obtained in a yield of 30%. The use of 0.5 mol. or more of acetic anhydride per one mol. of I, the reaction temperature 180~190°C, and the reaction time 4~5 hr., gave the best result. A limonenylcarbinol was prepared by the saponification of the acetate. The acetate could not be saponified by the action of 20% aqueous or alcoholic potassium hydroxide at 100°C, but the carbinol was produced almost quantitatively by heating the acetate with 20% aqueous potassium hydroxide for 3~4 hr. at 180~190°C in an autoclave. The carbinol is a colorless liquid and it smells like cineol. The analysis of its phenylurethan, m. p. 56~57°C, indicated that the alcohol was a limonenylcarbinol. The velocity of esterification of phenylacetic acid with the carbinol showed that the carbinol was a primary alcohol.

In the addition of formaldehyde to terpenes or other compounds[5], formaldehyde adds usually at an end methylene group[6] or an active methylene group[9] adjacent to a double bond. Thus it is considered that the limonenylcarbinol possesses one of structures III, IV, V, VI and VII.

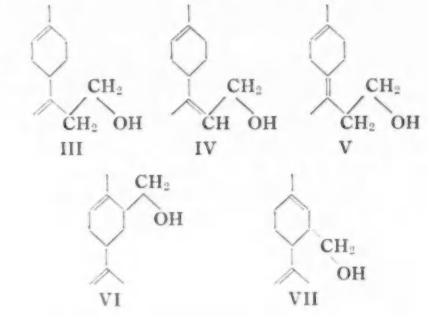

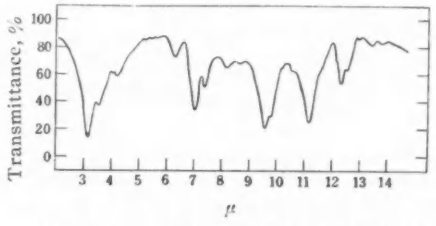

Fig. 1. The infrared absorption spectrum of the limonenylcarbinol(III).

The infrared absorption spectrum (Fig. 1) indicates the presence of a primary alcohol group (absorption peak at 9.6 μ) and an end methylene group (strong band at 11.25 μ), which excludes IV and V.

* Present address: Faculty of Technology, Chiba University, Iwase, Matsudo-shi, Chiba.

1) H. J. Prins, *Proc. Acad. Sci. Amsterdam*, **22**, 51 (1919), *J. Chem. Soc.*, **118**, 42 (1920).
2) A. Ladenberg, *Ber.*, **31**, 289 (1898).
3) O. Kriewitz, ibid., **32**, 57 (1899).
4) R. Lombard, *Bull. soc. chim. France*, No. **10**, C 24 (1953), No. **11**, C 1216 (1954).
5) E. E. Swissmann and R. A. Mode, *J. Am. Chem. Soc.*, **79**, 3447 (1957).
6) For example, β-pinene[7], 8(9)-*p*-menthene[4] and methylenecyclohexene[8].
7) J. P. Bain, *J. Am. Chem. Soc.*, **68**, 638 (1946).
8) E. Arundale and L. A. Mikeska, *Chem. Revs.*, **51**, 505 (1952).
9) For example, carvomenthene[10].
10) H. Yonetani and H. Yamabe, *Reports of Camphor Chemists' Society (Shono Gijitsu Kyokai Kogi)*, **20**, 109 (1955).

The optical activity ($[\alpha]_D^{10}$ +37.2) also makes V improbable. Formula III was concluded from the comparison of the infrared spectrum of the product(VIII), prepared by catalytic hydrogenation of the end methylene group of the carbinol, with that of 1(2)-*p*-menthen-6-yl-carbinol (IX) which was prepared from 1(2)-*p*-menthene and paraformaldehyde. The 1(2)-*p*-menthen-6-yl-carbinol (IX) showed remarkable doublet absorption peaks[11] at 7.2 μ (1390 cm^{-1}) and 7.3 μ (1370 cm^{-1}), and

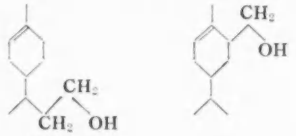

VIII IX

medium absorption peaks at 8.55 μ (1170 cm^{-1}) and 9.05 μ (1150 cm^{-1})[12] owing to an isopropyl radical (Fig. 2). On the other hand, the hydrogenation product from the limonenylcarbinol gave the strong single band of a methyl group at 7.25 μ, but no absorptions of an isopropyl group at 8.55 μ and 9.05 μ (Fig. 3). These results suggest the structure of 1,8(9)-*p*-menthadien-10-yl-carbinol (III) for the limonenylcarbinol.

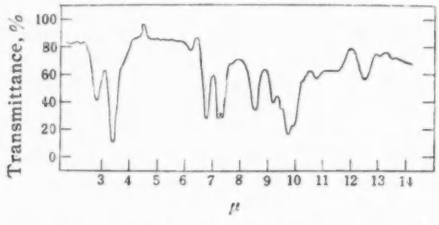

Fig. 2. The infrared absorption spectrum of 1(2)-*p*-menthen-6-yl-carbinol (IX).

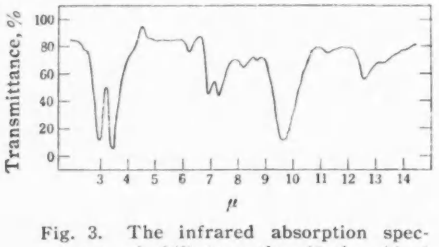

Fig. 3. The infrared absorption spectrum of 1(2)-*p*-menthen-10-yl-carbinol (VIII).

11) It was reported that the doublet absorption peaks of the isopropyl group are at 1362 cm^{-1} and 1378 cm^{-1}.

12) H. L. McMurry and V. Thornton, *Anal. Chem.*, **24**, 318 (1952).

Experimental

***d*-Limonene(I).**—Commercial *d*-limonene was distilled with a rectifying column. B. p. 64～65°C/15 mmHg; d_4^{15} 0.8494; n_D^{15} 1.4756; $[\alpha]_D^{10}$ +113°.

Reaction in a Sealed Tube.—A mixture of 20 g. (0.15 mol.) of I, 4.5 g. (0.15 mol.) of II and 10 g. of ethanol was sealed in a hard glass tube, and heated at 200～220°C for 12 hr. in an electric furnace. The reaction mixture was poured into water and extracted with ether, and the ethereal solution was washed with water and dried over anhydrous sodium sulfate. By fractional distillation, 14 g. of I and 2.8 g. of the limonenylcarbinol were obtained. B. p. 102～105°C/4 mmHg; d_4^{25} 0.9612; n_D^{25} 1.5069. Yield, 11%.

Phenylurethan.—It was prepared as usual and recrystallized from methanol. Colorless needles, m. p. 54～55°C.

Anal. Found: N, 4.79; Calcd. for $C_{18}H_{23}O_2N$: N, 4.91%.

Limonenylcarbinyl Acetate (1,8(9)-*p*-Menthadien-10-yl-carbinyl Acetate).—A mixture of 45.3 g. (0.333 mol.) of I, 10 g. (0.333 mol.) of II and 20 g. (0.196 mol.) of acetic anhydride was heated at 180～190°C for 4～5 hr. in an autoclave. The reaction mixture was washed with water and dried over anhydrous sodium sulfate. Fractional distillation gave 20.5 g. of the crude acetate. B. p. 96～106°C/4 mmHg Yield, 29.6%. It was redistilled for characterization. B. p. 103～107°C/5 mmHg; d_4^{25} 0.9618; n_D^{25} 1.4790; molecular refraction 61.38 (Calcd. for $C_{11}H_{17}O{\cdot}COCH_3$, F_2, 60.75).

Limonenylcarbinol (1,8(9)-*p*-Menthadien-10-yl-carbinol).—A mixture of 13 g. of the crude acetate and 6 g. of potassium hydroxide (20% aq. solution) was heated at 180°C for 4 hr. in an autoclave. After cooling, the reaction mixture was extracted with ether, and the extracts were washed with water and dried over anhydrous sodium sulfate. Fractional distillation gave 10 g. of the limonenylcarbinol in a yield of 96%. B. p. 102～106°C/4 mmHg; d_4^{17} 0.9603; n_D^{17} 1.5020; molecular refraction 51.04 (Calcd. for $C_{10}H_{13}CH_2OH$, F_2, 51.39) $[\alpha]_D^{10}$ +37.2.

Phenylurethan.—It was prepared as usual and recrystallized from methanol. Colorless needles, m. p. 56～57°C.

Anal. Found: N, 4.86. Calcd. for $C_{18}H_{23}O_2N$: N, 4.91%.

Velocity of Esterification of Phenylacetic Acid with the Limonenylcarbinol.—The nature of the hydroxyl group of the limonenylcarbinol was determined by Murahashi's method[13]. A small amount of the carbinol was heated with phenylacetic acid at 150°C for an hour in a sealed glass tube. The initial rate of esterification in an hour was found 63% showing the carbinol is a primary alcohol.

1(2)-*p*-Menthen-10-yl-carbinol (VIII).—In methanol solution 3.93 g. of the limonenylcarbinol was hydrogenated with Pd-$BaSO_4$ containing 3%

13) E. Funakubo, "Identification of Organic Compounds, I" (Yuki Kagobutsu Kakuninho I), Yokendo, Tokyo (1951), p. 11.

Pd, and absorbed 583 cc. of hydrogen (760 mmHg, 20°C) to give 3.0 g. of VIII. B. p. 100～103°C/4.5 mmHg; n_D^{13} 1.4923.

***d*-Limonene Hydrochloride**[14,15].—In a 200 cc. three-necked flask equipped with a mechanical stirrer, a thermometer and a gas inlet tube, 100 g. of I was placed. The flask was cooled to −5°C in an ice-salt freezing mixture. Anhydrous hydrogen chloride was passed into the solution for 2 hr. The reaction mixture turned deep purple in color and sticky. It was washed with water, dried over anhydrous sodium sulfate and fractionally distilled to give a fraction of b.p. 65～68°C/4 mmHg. By redistillation 84 g. of *d*-limonene hydrochloride was obtained. B. p. 73～75°C/5 mmHg; n_D^{12} 1.4850.

1(2)-*p*-Menthene[14,16]. — Sodium (40 g.) was added gradually in an hour to a mixture of 40 g. of *d*-limonene hydrochloride and 200 g. of absolute ethanol with ice cooling. After sodium ethylate was decomposed with water, the product was extracted with ether and the ethereal solution was washed with water and dried over anhydrous sodium sulfate. By fractional distillation, 22 g. of 1(2)-*p*-menthene was obtained. B. p. 50～54°C/3.5 mmHg; n_D^{12} 1.4766.

1(2)-*p*-Menthen-6-yl-carbinol (IX). — To a mixture of 12 g. of 1(2)-*p*-menthene, 3 g. of II, 17 g. of 95% acetic acid and 4 g. of ether, cooled to −2°C, a mixture of 7 g. of 95% acetic acid and 2.5 g. of 98% sulfuric acid was added, and the mixture was agitated for 5 hr. After being allowed to stand overnight, it was extracted with ether and the ethereal solution was washed with aqueous sodium bicarbonate and with water, dried over anhydrous sodium sulfate, and fractionally distilled to give 3 g. af 1(2)-*p*-menthen-6-yl-carbinyl acetate. B. p. 90～100°C/4 mmHg; n_D^6 1.4860.

A mixture of 3 g. of the acetate, 4 g. of potassium hydroxide, 40 cc. of methanol and 1 cc. of water, was refluxed on a warm water bath for 3 hr. The product was extracted with ether, and the ethereal solution was washed with water and dried over anhydrous sodium sulfate. Evaporation of the ether and fractional distillation gave 2 g. of the carbinol (IX). B. p. 95～97°C/3 mmHg; n_D^5 1.4896.

The authors are indebted to Shonan Aromatic Perfumery Co., Ltd. for *d*-limonene and to Mr. A. Matsuda for technical assistance.

Department of Applied Chemistry
Faculty of Technology
Chiba University
Matsudo-shi, Chiba

14) F. W. Semmler, *Ber.*, **36**, 1036 (1903).
15) H. Katsuragi, *Koryo*, No. **24**, 25 (1953).
16) F. W. Semmler, *Ber.*, **40**, 2959 (1907).

Distribution of Neptunium between TBP and Some Mineral Acids

By Tomitaro Ishimori and Eiko Nakamura

(Received January 20, 1959)

Tri-*n*-butyl phosphate*, an excellent solvent which plays an important role in the Purex process, attracts the attention of chemists. For example, the distribution of plutonium was studied by McKay et al.[1] in the TBP-nitric acid system. Peppard et al.[2-5] are aggressively studying the behaviors of both actinides and lanthanides in TBP-mineral acid systems.

Although the extraction of neptunium with TBP has caused deep concern in connection with the isolation of the element[6,7], systematic studies on the behavior of the element are not known. Besides, the existence of three kinds of oxidation states of the element, (IV), (V) and (VI) makes the study complicated.

In the present paper, extraction of neptunium with TBP is studied systematically with the emphasis on its oxidation states.

* Tri-*n*-butyl phosphate is denoted by "TBP" in the present paper.

1) G. F. Best, H. A. C. McKay and P. R. Woodgate, *J. Inorg. & Nucl. Chem.*, **4**, 315 (1957).
2) D. F. Peppard, G. W. Mason and J. L. Maier, ibid., **3**, 215 (1956).
3) D. E. Peppard, S. W. Moline and G. W. Mason, ibid., **4**, 344 (1957).
4) D. F. Peppard, W. J. Driscoll, R. J. Sironen and S. McCarty, ibid., **4**, 326 (1957).
5) D. F. Peppard, G. W. Mason, J. L. Maier and W. J. Driscoll, ibid., **4**, 334 (1957).
6) H. A. C. Mckay, "First United Nations International Conference on the Peaceful Uses of Atomic Energy", Vol. VII, P/441, United Nations Publication, New York (1956).
7) E. K. Hyde, ibid., Vol. VII, P/728.

Experimental

Sources of Materials.—Neptunium-239 tracer is prepared from uranyl nitrate hexahydrate irradiated by JRR-1 reactor for 2 hr. After cooling several hours, the irradiated uranyl salt is converted into chloride and dissolved in 0.5 M hydrochloric acid solution. After reduction by a small amount of granulated zinc**, neptunium is extracted by about 5% TTA***-benzene. After rinsing with a small portion of 0.5 M hydrochloric acid solution, the benzene layer is contacted with >3 N hydrochloric, nitric, perchloric or sulfuric acid according to preference. Neptunium is thus obtained as acid solution. The TTA which might go into the tracer solution is removed by contact with benzene. The radiochemical purity of the tracer is checked by both gamma spectrometry and the decay measurement. Separation from fission products is excellent. But a small remaining amount of uranium was still found by a color reaction with hydrogen peroxide.

Protactinium-233 is isolated from irradiated thorium nitrate by solvent extraction. Irradiation is carried out in conditions similar to those mentioned above. Protactinium is separated from thorium by contacting concentrated nitric acid solution with 10% TBP-toluene. In this separation protactinium is extracted into the organic phase leaving thorium in the aqueous phase. After washing with concentrated nitric acid, protactinium is recovered by shaking with water. The resultant solution of protactinium-233 gives no precipitate by adding aqueous ammonia, showing that practically thorium does not remain. The radiochemical purity of protactinium-233 thus prepared is checked again by both γ-spectrometry and the measurement of the decay curve.

Hafnium-181 received from Oak Ridge National Laboratory is used without further purification.

Thorium-234 is prepared according to Dyrssen's[8] method. The radiochemical purity is checked by determining its half life of 24.1 days.

Determination of Distribution Ratios. — In the determination of the distribution ratio, *Kd*, of a specific nuclide, defined as the concentration of nuclide in the organic phase divided by that of nuclide in the aqueous phase of two equilibrated liquid phases, a portion of aqueous acid of the indicated concentration containing a radioactive nuclide is equilibrated against a portion of solvent which is previously pre-equilibrated with respect to the corresponding barren aqueous acid. Every contact is carried out on a milliliter scale. For example, a 2.5 ml. portion of 10.1 M nitric acid containing approximately 10^5 cpm neptunium-239 is equilibrated with a 2.5 ml. portion of undiluted TBP which was previously contacted with three successive equal-volume portions of barren 10.1 M nitric acid. All solvent pre-equilibrations are made immediately before the use to avoid any complications arising from solvent hydrolysis. Aliquots of each phase are pipetted into small glass tubes for gamma counting. Gamma counting is made by means of Philips' scintillation counter with bed type head. Scrubbings are carried out both for aqueous and organic phases, if necessary. The *Kd* values are calculated dividing cpm of the organic phase by that of the aqueous phase after making a correction for natural counting.

Results and Discussion

Nitric Acid-TBP System. — Nitric acid solution of neptunium tracer prepared as mentioned above contains both neptunium (IV) and (V). The relative abundance between neptunium(IV) and (V) varies according to the treatment of the tracer solution. The freshly prepared solution contains only a very small amount of neptunium(V), whereas standing for a few days or warming in boiling water makes neptunium(V) rich.

Nitric acid solution containing both neptunium(IV) and (V) is contacted with TBP. The resultant organic or aqueous

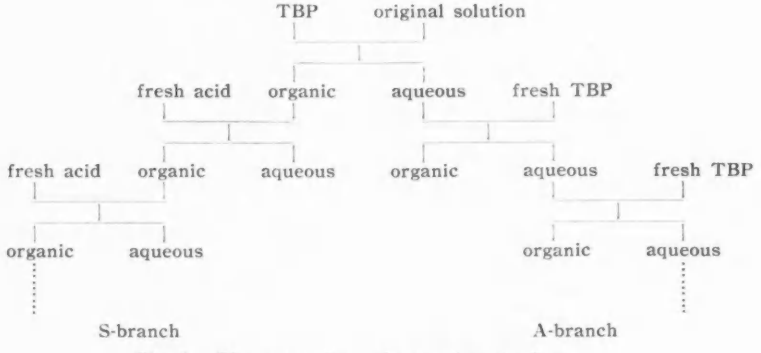

Fig. 1. The extraction scheme of neptunium.

** In order to avoid reduction of uranyl ion, reduction with zinc should be carried out at room temperature for only a few minutes.

*** Thenoyltrifluoroacetone

8) D. Dyrssen, *Svensk. Kem. Tid.*, **62**, 153 (1950).

phases are scrubbed with fresh acid solution or TBP, respectively. Scrubbings are carried out as shown in Fig. 1, until *Kd* values become practically constant, keeping the acidity of aqueous solution the same all through the procedures. Thus two values of *Kd*, Kd^{IV} and Kd^{V}, are obtained from S- and A-branches of the scrubbing scheme. Species which give Kd^{IV} and Kd^{V}, are assigned to neptunium (IV) and (V) respectively by the chemical behaviors against zinc, potassium bromate or TTA-benzene, to be mentioned below.

(*a*) *Oxidation with potassium bromate.* — The species which gives Kd^{IV} can not be oxidized with potassium bromate. At 0.5 N nitric acid Kd^{IV} value is 2.5. After adding the oxidant and scrubbing with a few portions of fresh acid, the *Kd* value remains almost constant, 2.7, showing that the species which gives Kd^{IV} is not practically oxidized.

On the other hand, Kd^{V} which is about 0.026 at 1 N nitric acid becomes about 16.3 after oxidation with potassium bromate and scrubbing with fresh acid solution. This change shows that the species which gives Kd^{V} is easily oxidized by potassium bromate. Besides that, the new third *Kd* value is also different from Kd^{IV} value of the same acidity. Accordingly this third value is supposed to be assigned to the hexavalent state. It is well known that neptunium(V) is easily oxidized by potassium bromate to neptunium(VI) state, whereas neptunium(IV) is not[9].

(*b*) *Reduction with zinc metal.* — Kd^{IV} value (6.92 at about 1 N) remains almost the same after adding zinc and heating on a water bath, whereas Kd^{V} value (0.026 at 1 N) becomes 7.8 after reduction with zinc metal****. This value almost coincides with that of Kd^{IV} at the same acidity, showing that the species which gives Kd^{V} is reduced to another species which gives Kd^{IV}.

(*c*) *Extraction with TTA.* — The comparison of extraction behaviors of the two species are given in Table I. The difference shown in the table again shows that the species which gives high Kd^{IV} in TBP-nitric acid system has high *Kd* in TTA extraction and is assigned to tetravalent[10], whereas another species which gives low Kd^{V} in TBP-nitric acid system has low *Kd* in TTA extraction and is assigned to quinquevalent[10].

TABLE I. THE BEHAVIOR OF NEPTUNIUM ON TTA EXTRACTION AT 1 N NITRIC ACID

Concn. of TTA in benzene (%, w/v)	*Kd* for the species which gives Kd^{IV} in TBP-HNO_3 system	Kd^{V} in TBP-HNO_3 system
5.0	4.11	0.017
2.5	0.95	0.021
1.25	0.31	0.011

The variation of Kd^{IV} or Kd^{V} caused by changing the acidity of aqueous phase is shown in Fig. 2. In Fig. 3 acid dependences of neptunium(IV) and (V) are compared with those of hafnium(IV), thorium(IV), protactinium(V) and plutonium(IV). The thorium line is written according to Peppard et al.[2] and that of plutonium(IV) is rewritten based upon the values of McKay et al.[1] The behavior of neptunium(IV) shows strong similarity to that of plutonium(IV). However, *Kd* value of neptunium(IV) always lies below that of plutonium(IV) at the same acidity. *Kd* values of neptunium(IV) and thorium are almost the same at acidities less than 10 N. But the neptunium(IV) curve shows a maximum at about 9 N while that for

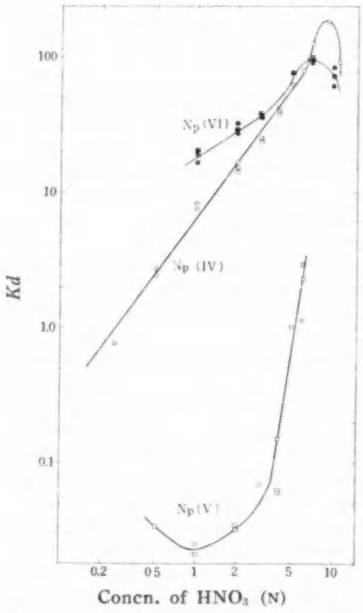

Fig. 2. The *Kd* values of neptunium in HNO_3–100% TBP.
—●— Np(VI) —○— Np(IV) —□— Np(V)

9) G. T. Seaborg and J. J. Katz, "The Chemistry of the Actinide Elements", Methuen and Co., Ltd., London (1957), p. 231.

**** The solution gives *Kd*=0.064 after heating on a water bath without zinc.

10) F. L. Moore, *Anal. Chem.*, **29**, 941 (1957).

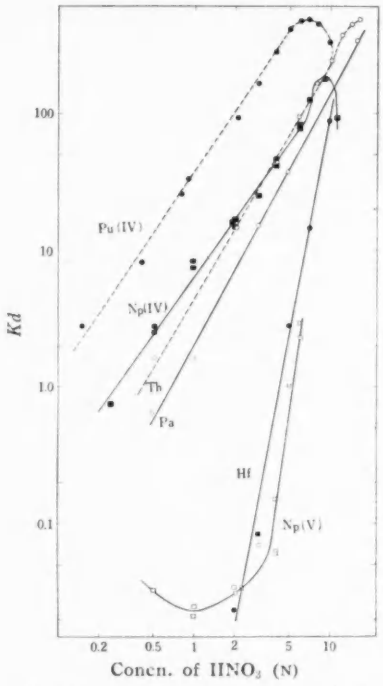

Fig. 3. The *Kd* values of neptunium, plutonium, thorium, protactinium and hafnium.
—●— Pu(IV) —■— Np(IV) —●— Hf
···○··· Th —□— Np(V) —○— Pa

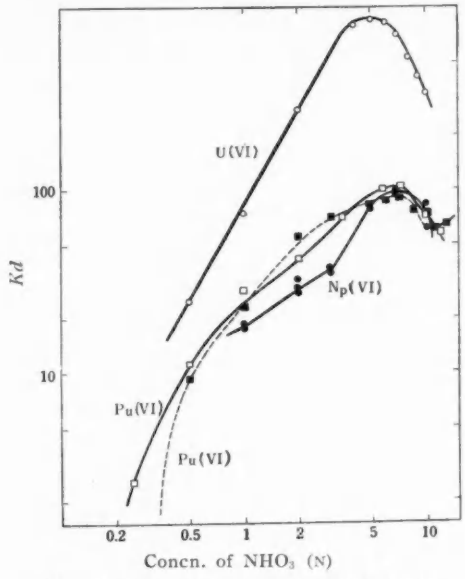

Fig. 4. The *Kd* values in HNO_3–100% TBP system.
—○— U(VI) —□— Pu(VI)
—●— Np(VI) —■— Pu(VI)

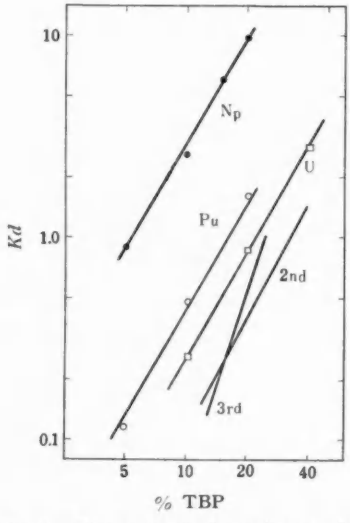

Fig. 5. The solvent dependence of *Kd* values in HNO_3–100% TBP system.
—●— Np(VI) at 10 N HNO_3
—○— Pu(VI) at 11.5 N HNO_3
—□— U(VI) at 0.27 N HNO_3

thorium does not. Hafnium shows a quite different behavior from that which neptunium(IV) does.

The behavior of neptunium(V) resembles that of hafnium(IV) more than that of protactinium(V).

As mentioned already neptunium(VI) is prepared easily by oxidation of neptunium (V) with potassium bromate and scrubbing of TBP phase with fresh acid solution in order to remove neptunium(V). Alternatively ceric ammonium nitrate works well as the oxidant in this case. The acid dependence of *Kd* value for neptunium(VI) is also given in Fig. 2. A comparison of *Kd* values for uranium(VI), neptunium(VI) and plutonium(VI) is also seen in Fig. 4. Naito[11] gave *Kd* values for macro amounts of uranium in 20% TBP in carbon tetrachloride-nitric acid system. He also found second power dependence of *Kd* in this system. Accordingly the present authors rewrite uranium (VI) curve of Fig. 4 multiplying Naito's *Kd* value with the factor of 25 in order to make it represent *Kd* values for 100% TBP-nitric acid solution system. Broken plutonium(VI) curve of Fig. 4 is rewritten

in a similar way correcting the values of McKay et al.[1] which were obtained with diluted TBP. The other plutonium(VI) curve represents values obtained by one of the present authors. As is known very well, correction with solvent dependence is not so satisfactory. Besides that, there might be some differences between behaviors of macro and micro amounts of actinide elements. Therefore, the comparison with each other of 3 curves in Fig. 4 will not be valid for a strict discussion. But it is remarkable that all of them show a maximum *Kd* value at about 6 or 7 N.

Solvent dependence of *Kd* value for neptunium is checked at 10 N nitric acid. As shown in Fig. 5, neptunium(VI) shows second power dependence. The figure shows also second power solvent dependences of uranium(VI) and plutonium(VI) according to the values obtained by Naito for uranium[11] and Mckay et al. for plutonium[1]. Here again strong similarity is shown among hexavalent uranium, neptunium and plutonium.

Hydrochloric Acid-TBP System. — Neptunium(VI) prepared by oxidizing neptunium(IV) and (V) with potassium chlorate and heating in boiling water shows *Kd* values as shown in Fig. 6. *Kd* values of uranium obtained by using uranium-233 as the tracer in the form of uranyl chloride are also show in the same figure in order to compare them with those for neptunium(VI). The acid dependences of these two elements are very similar in the shape indicating strong similarity in the chemical behaviors of these two species. However, neptunium(VI) is more extractable than uranium(VI) all through the acidity range investigated.

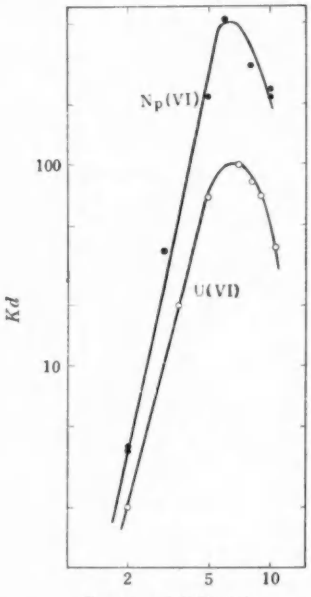

Fig. 6. The acid dependence of *Kd* values for neptunium and uranium.
—●— Np(VI) —○— U(VI)

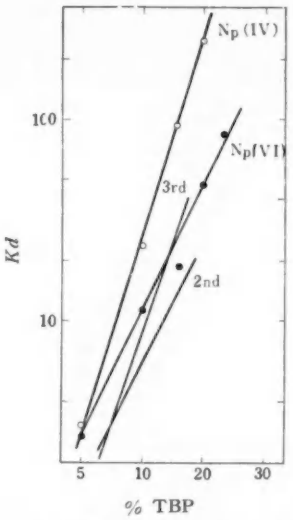

Fig. 7. The *Kd* values in diluted TBP-HCl system.
—●— Np(VI) at 6 N HCl
—○— Np(IV) at 8 N HCl

The solvent dependence of *Kd* for neptunium is studied at 6 N hydrochloric acid and found to be of second power as is seen in Fig. 7. Diluent used is toluene and TBP concentration is shown in volume per cent.

Neptunium(V) is prepared in hydrochloric acid solution by reducing neptunium(VI) with hydrazine sulfate. On the other hand, a solution of neptunium (IV) is prepared by recovering neptunium from TTA-benzene with hydrochloric acid (>3 N) and then treating it with hydroxylamine hydrochloride, granulated zinc or ascorbic acid in order to reduce neptunium(V) which comes into the solution in very small amount. Fig. 8 shows acid dependences of *Kd* values for both neptunium(V) and (IV) as well as those for hafnium, thorium and protactinium. The

11) K. Naito, In press.

neptunium(V) line is quite different from that of protactinium(V). In the range of 9~4 N, *Kd* of neptunium(IV) shows almost the same slope as those of thorium(IV) and hafnium(IV). It is notable that the acid dependence of neptunium(IV) shows a maximum at about 8 N.

The solvent dependence of *Kd* values for neptunium(IV) is studied at 8 N using toluene as the diluent. The result shows third power dependence as given in Fig. 7.

Sulfuric Acid-TBP System.—Neptunium (VI) in sulfuric acid solution is prepared by oxidation of the mixture of neptunium (IV) and (V) with ceric sulfate, while neptunium (V) is prepared by reducing neptunium (VI) with hydrazine sulfate. Variation curves of *Kd* values for both neptunium (V) and (VI) caused by the variation of the acidity in aqueous phases are given in Fig. 9. Extraction can not be carried out in the acidity range over about 20 N, because TBP becomes miscible with aqueous phase at such high acidity. Generally *Kd* values for both neptunium(V) and (VI) are small, their highest values being only about 2.5. The acid dependence of *Kd* values for protactinium is shown in Fig. 9 in order to compare it with that for neptunium(V).

Neptunium(IV) is prepared by contacting sulfuric acid solution with TTA-benzene which contains neptunium. In order to prevent contamination of neptunium (V), the resultant acid solution is treated

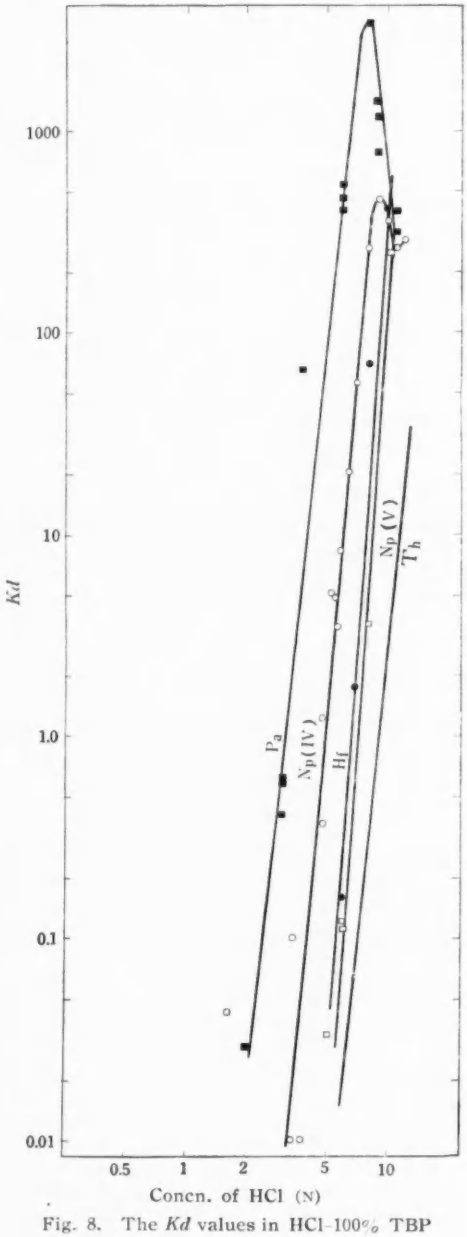

Fig. 8. The *Kd* values in HCl-100% TBP system.
—○— Np(IV) —□— Np(V) —— Th
—●— Hf —■— Pa

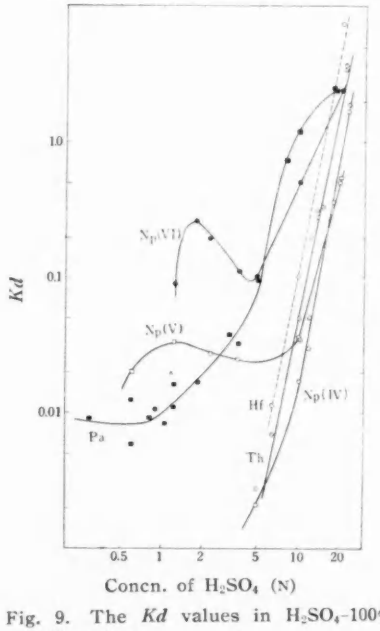

Fig. 9. The *Kd* values in H_2SO_4-100% TBP system.
—●— Np(VI) —■— Pa ---○--- Hf
—○— Np(IV) —□— Np(V) —⊙— Th

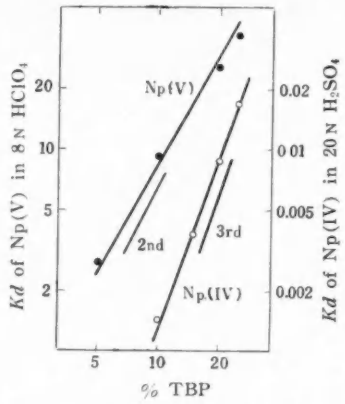

Fig. 10. The *Kd* values in diluted TBP-$HClO_4$ or H_2SO_4 system.
—●— Np(V) at 8 N $HClO_4$
—○— Np(IV) at 20 N H_2SO_4

with hydroxylamine hydrochloride and ferrous sulfate or 0.1 M hydroquinone and potassium iodide at higher acidities, while it is treated with granulated zinc at lower acidities. Acid dependence of *Kd* values for neptunium(IV) can also be seen in Fig. 9 where those for hafnium and thorium are added for comparison. These three curves resemble each other considerably. It is noted that in the range of lower acidities neptunium (IV) gives lower *Kd* values than neptunium(V) does.

The solvent dependence of *Kd* values for neptunium(IV) is studied at 20 N sulfuric acid and found as a third power. (Fig. 10).

Perchloric Acid-TBP System.—Perchloric acid (>3 N) solution obtained by contacting with neptunium solution in TTA-benzene contains only neptunium(V). This assignment is based on the following experiments:

(a) 3.4 N perchloric acid containing neptunium(V) is contacted with almost equal volume of TBP pre-equilibrated with 9 N hydrochloric acid. The resultant organic phase is equilibrated with many portions of 9 N hydrochloric acid successively. In this way, the system is converted to hydrochloric acid-TBP system. Finally *Kd* value approaches that of neptunium(V) at 9 N hydrochloric acid. (b) By oxidation with silver peroxide this species becomes another species which could be assigned to neptunium(VI).

The acid dependences of *Kd* values for both neptunium(V) and (VI) are given in Fig. 11 as well as that of protactinium.

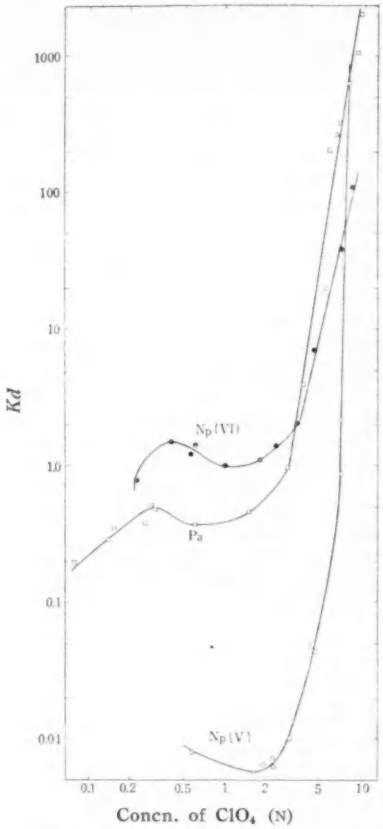

Fig. 11. The *Kd* values of neptunium and protactinium in $HClO_4$-100% TBP system.
—●— Np(VI) —□— Pa —○— Np(V)

It is characteristic that the neptunium(V) curve shows very rapid increase in *Kd* at the range of 3~8 N acidity. As will be shown later, this can be utilized for isolation of neptunium from irradiated uranyl nitrate.

As 8 N perchloric acid, the solvent dependence of *Kd* values for neptunium(V) is studied. The result is shown in Fig. 10.

The Reduction of neptunium(V) with hydroquinone and potassium iodide, hydrogen peroxide, granulated zinc or 3% zinc amalgam is not successful. Accordingly *Kd* values which could be assigned to the tetra-positive state can not be found.

Isolation of Neptunium from Irradiated Uranyl Nitrate.— As Fig. 11 shows, *Kd* for neptunium(V) in perchloric acid-TBP system varies from 800 at 8 N to 0.006 at 2 N. This is utilized in the isolation of

neptunium without introducing any other reagent.

Procedure. — Neutron irradiated uranyl nitrate hexahydrate is dissolved in a small volume of concentrated perchloric acid. The solution is heated under an infrared lamp in order to expel nitric acid. The residue is taken up by a few ml. of concentrated perchloric acid and the resultant solution is heated by dipping in boiling water for about 10 min. After cooling, it is shaken with 100% TBP. The organic phase contains neptunium(V) and uranium, while most of the fission products remain in the aqueous phase. The separated organic phase is shaken with 3 portions of 2 N perchloric acid. The resultant aqueous phase contains neptunium(V) and a small amount of uranium, while a large amount of uranium remains in organic phase. The resultant aqueous phase is washed with benzene in order to remove TBP, dried up under the infrared lamp, and dissolved into concentrated perchloric acid. The whole procedure is repeated as shown in Fig. 12.

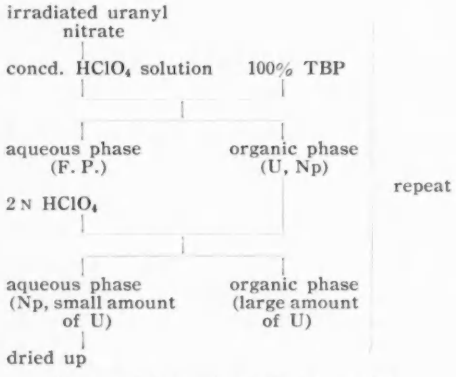

Fig. 12. Scheme for isolation of Np.

The yield of neptunium is 99%, and the decontamination of fission products is excellent. A very small amount of uranium remains.

Summary

Neptunium-239 is used as the tracer for studies on solvent extraction behaviors of neptunium in the following system:

1. Nitric acid solution and TBP.
2. Hydrochloric acid solution and TBP.
3. Sulfuric acid solution and TBP.
4. Perchloric acid solution and TBP.

Kd values are measured by combinations of scrubbing techniques and chemical treatments. In nitric, hydrochloric and sulfuric systems, neptunium gives three kinds of *Kd*, distribution ratio which could be assigned to oxidation states of (IV), (V) and (VI). On the other hand, in the perchloric system neptunium does not show *Kd* value which should be assigned to the oxidation state(IV).

Some of these results are compared with those of uranium, plutonium and other elements. In the nitric system, neptunium(VI) shows an acid dependence of *Kd* value similar to those of uranium (VI) and plutonium(VI). *Kd* values of neptunium(IV) and plutonium(IV) vary in almost the same way against the acid concentration of nitric acid. There is also a strong similarity between acid dependences of uranium(VI) and neptunium (VI) in the hydrochloric system.

Behavior of neptunium(V) are compared with those of protactinium.

Finally a simple method for isolation of neptunium from irradiated uranyl salt is stated.

The authors wish to express their sincere thanks to Dr. Kenjiro Kimura who afforded them convenience for this study in many ways.

Chemistry Division, Tokai Laboratory
Japan Atomic Energy
Research Institute
Tokai, Ibaraki

Spectrochemical Study of Microscopic Crystals. XIX[1] *The Structure and Absorption Spectra of Fremy's Salt*

By Shoichiro YAMADA and Ryutaro TSUCHIDA

(Received February 4, 1959)

In the nineteenth century, Fremy[2] isolated an interesting compound having an empirical formula of $ON(SO_3)_2K_2$, which is violet-blue in solution and yellow in the crystalline state. This phenomenon, which has been studied by a number of investigators[3,4] was eventually understood on the assumption that the compound might consist of monomeric ions in solution and of dimeric ions in the crystalline state[5-7]. Aside from the electronic structure of the monomeric ion involving a queer type of bonding, the structure of the dimeric ion was often discussed by the earlier investigators, but still remains in dispute. Although the compound has been studied from various sides, no spectral data have so far been reported. In an attempt to elucidate the structure of Fremy's salt, we have carried out a spectroscopic study with this salt and related compounds.

Experimental

Materials. — Potassium peroxylamine disulfonate, $K_2(O_3S)_2NO$, was prepared by the method of Haga[8] with slight modification. To a solution of 17.5 g. of sodium nitrite in 50 ml. of water were added 100 g. of crushed ice, a solution of 25 g. of sodium hydrogen sulfite in 50 ml. of water under continuous stirring, and finally 10 ml. of glacial acetic acid. After a few minutes the reaction mixture was rendered alkaline by the addition of 7 ml. of concentrated aqueous ammonia (*d*, 0.880), and then a solution of 6.3 g. of potassium permanganate in 200 ml. of water was added under stirring. The precipitate of manganese dioxide which was at once formed was removed by filtration. To the violet-colored filtrate was added 250 ml. of a saturated solution of potassium chloride. Orange-yellow crystals which precipitated were filtered by suction, and washed successively with a 5% solution of potassium hydroxide, ethanol and acetone. Recrystallization from water yielded orange-yellow crystals of Fremy's salt, which showed the typical reactions of Fremy's salt. Thus the crystals were dissolved in water to give a blue-violet solution, from which the orange-yellow crystals separated again on concentration. Potassium peroxylamine disulfonate thus prepared was found to form blue-colored mixed crystals with potassium hydroxylamine disulfonate, which was prepared in colorless crystals according to the method of Rollefson and Oldershaw[8].

The mixed crystals were prepared in the following way. Into 45 ml. of a 5% solution of potassium hydroxide were added 1 g. of potassium hydroxylamine disulfonate and 0.5 g. of potassium peroxylamine disulfonate at 45°C. The solution was filtered and cooled with crushed ice. After twenty hours large mixed crystals which were blue in color began to separate together with the crystals of potassium peroxylamine disulfonate. The blue mixed crystals were picked up from the mixture mechanically. Accurate determination of the $K_2(O_3S)_2NO$ content in the mixed crystal was not made, but approximate estimation from the intensity of the "NO band" showed it to be only a few per cent. The value seems to agree well with those reported earlier[5].

Measurements.—Quantitative dichroism measurements in the visible and ultra-violet regions were carried out at room temperature by Tsuchida and Kobayashi's microscopic method[9].

Absorption spectra of the compounds in aqueous solution were determined at room temperature by a Beckman DU spectrophotometer.

Infrared absorption spectra of the compounds in Nujol mulls and in potassium bromide discs were determined in the rock salt region by a Hilger H 800 infrared spectrophotometer.

The notations in the present paper are the same as those used in the former papers of this series.

Results and Discussion

Visible and Ultra-violet Absorption Spectra.—The mixed crystal formed from $K_2(O_3S)_2NOH$ and $K_2(O_3S)_2NO$ shows an absorption band at 52×10^{13}/sec., as seen

1) Part XVIII of this series, S. Yamada and R. Tsuchida, This Bulletin, **31**, 813 (1958).
2) E. Fremy, *Ann. chim. phys.*, **15**, iii, 408 (1845).
3) F. Raschig, *Ann.*, **241**, 223 (1887).
4) A. Claus, ibid., **158**, 205 (1871).
5) A. Hantzsch and W. Semple, *Ber.*, **28**, 2744 (1895).
6) T. Haga, *J. College of Sci. Imp. Univ. Tokyo*, **19**, No. 15 (1904); T. Haga and E. Divers, *J. Chem. Soc.*, **77**, 440 (1900).
7) R. W. W. Asmussen, *Z. anor. allgem. Chem.*, **212**, 316 (1933).
8) T. Haga, *J. Chem. Soc.*, **85**, 78 (1904); G. K. Rollefson and C. F. Oldershaw, *J. Am. Chem. Soc.*, **54**, 977 (1932).
9) R. Tsuchida and M. Kobayashi, "The Color and the Structure of Metallic Compounds", Zoshindo, Osaka (1944), p. 180 (in Japanese).

in Fig. 1. It has been found by the present measurements that for the band at 52×10^{13}/sec. the A-absorption in Fig. 1 is at least ten times stronger than the B-absorption. The difference in intensity between the two absorptions was so great that exact determination of the dichroic ratio could not be made.

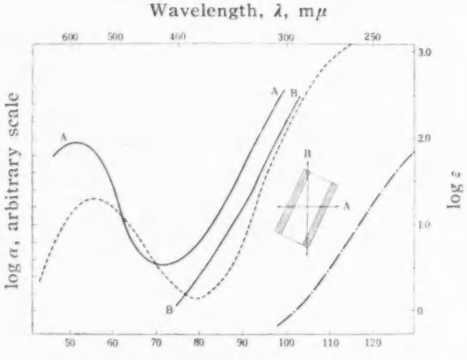

Fig. 1. Absorption spectra of a mixed crystal from $K_2(O_3S)_2$ NO and $K_2(O_3S)_2$·NOH, and its components: the mixed crystal in the solid state, ——: $K_2(O_3S)_2$·NO in 5% KOH solution, – – –: $K_2(O_3S)_2$·NOH in water, ·—·—.

Comparison of the absorption spectrum of the mixed crystal with the spectra of $K_2(O_3S)_2$NOH and $K_2(O_3S)_2$NO in solution (Fig. 1) reveals that the band at 52×10^{13}/sec. of the mixed crystal in the solid state may evidently be ascribed to the component, $K_2(O_3S)_2$NO, since the other component has no absorption in the neighborhood of this absorption band. It is presumed, in a similar way, that the state of the peroxylamine disulfonate ion in the mixed crystal is similar to that of Fremy's salt in water. Previously Asmussen[7] concluded from magnetic measurements that $K_2(O_3S)_2$NO in aqueous solution consists largely of monomeric ions; the three-electron bond is usually assumed to be involved in the bonding within the NO-group of the monomer. Therefore, it may be certain that Fremy's salt exists as a monomeric form when incorporated into the mixed crystal with $K_2(O_3S)_2$NOH. Thus the band at 52×10^{13}/sec. of the mixed crystal may be ascribed to the $(O_3S)_2NO^{2-}$ ions under the effect of the field by the surrounding ions. The band is, therefore, regarded as due primarily to the NO-group in the monomeric ion under small perturbation from the surrounding ions, although the bonding around the NO-group should not be considered, in a strict sense, to be isolated from the other part of the ion. The present measurements show that *the NO-band, in which the three-electron bond may be involved, is highly polarized.*

The effects of solvents upon the absorption band have also been examined. Formerly the "nitroso-band" at about 700 mμ of nitroso-derivatives and the band at about 350 mμ of a nitrite ion were reported to undergo a "blue solvent effect"[10]. This fact was then assumed to show that both the bands were due to $n-\pi^*$ transitions. On the contrary, the present measurements indicate that the absorption band at about 55×10^{13}/sec. (540 mμ) of the $ON(SO_3)_2^{2-}$ ion is displaced to longer wavelengths on changing a solvent from ethanol to water. The "red shift" of the band seems to show that the band may originate from a $\pi-\pi^*$ transition[10], although the intensity of the band is rather small for this type of transition. This appears to be consistent with the electronic structure of the NO group having a sort of three-electron bond, since the absorption band in question may originate from a transition of one of the three bonding electrons to an excited level.

It was reported earlier that the above mentioned bands, ascribed to the $n-\pi^*$ transition, were polarized perpendicularly to the plane of the NO-group in nitrosobenzene and its derivatives[11] or to the plane of an NO_2^- ion[12]. As for the band of the monomeric ion of $ON(SO_3)_2^{2-}$, which possibly originates from a $\pi-\pi^*$ transition and may be different in its origin from the above mentioned bands, we are inclined to regard it likely that the polarization of the band would be along the plane of the NO-group. Thus the A-absorption in Fig. 1 may correspond to the electric vector along the NO-group, and the B-absorption to the electric vector perpendicular to the NO-group. In order to confirm this suggestion, however, further study seems to be desirable.

Infrared Absorption Spectra. — Results of the present measurements are shown in Table I. Tentative assignment of the

10) H. McConnell, *J. Chem. Phys.*, **20**, 700 (1952); M. Kasha, *Discussions Faraday Soc.*, **9**, 14 (1950), etc.
11) K. Nakamoto and K. Suzuki, *J. Chem. Phys.*, **20**, 1971 (1952).
12) W. G. Trawick and W. H. Eberhardt, ibid., **22**, 1462 (1954); J. W. Sidman, *J. Am. Chem. Soc.*, **78**, 2911 (1956).

TABLE I. INFRARED ABSORPTION SPECTRA OF FREMY'S SALT AND RELATED COMPOUNDS IN THE SOLID STATE

Tent. Assign.	Mixed crystal $K_2(O_3S)_2NOH+K_2(O_3S)_2NO$*	$K_2(O_3S)_2NOH$	(presumed) $K_2(O_3S)_2NO$	$K_4[(O_3S)_2NO]_2$
O–N–SO_3	870 m	870 m	860~870 m	850 m
H–O–N	980 m	945 m		
SO_3	1030 s	1030 s		
SO_3	1050 s		1050 s	1050 s
SO_3	1085 m	1070 m	1080 m	1070 s
SO_3	1260 s	1255 s		
SO_3	1285 s		1285 s	1290 s
NO-str.	1620 m		1620 s	1260 s

* A very small amount as compared with the other component.
s: strong, m: medium intensity.

observed absorption bands to particular group-vibrations was made using the assignment by Drago[13] for $K_2(O_3S)(NO)_2$ and by Griffith and others[14] for Fremy's salt. Griffith and others have also reported the infrared absorption spectrum with Fremy's salt[15]. Unfortunately they did not state whether the measurements refer to the compound in the solid state, or in aqueous solution. Their measurements were probably made in the solid state in which the compound consists of the dimeric form, since their data agree with ours for the $[(O_3S)_2NO^{2-}]_2$ ion. They have not presented any detailed discussion about the infrared spectrum or the structure of the dimer, but mentioned the compound as having an N–N linkage. It seems, however, that no reports have appeared which may be regarded to establish the structure of the dimeric ion with certainty, as far as literatures accessible to us are concerned.

The infrared absorption bands of the monomeric $ON(SO_3)_2^{2-}$ ion were determined by comparing an absorption spectrum of the mixed crystal from Fremy's salt and potassium hydroxylamine disulfonate with the spectrum of the latter alone. Although some effects, such as hydrogen bonds, which possibly exist in the mixed crystal, are liable to complicate the spectrum and make the exact assignment of the absorption bands difficult, the interpretation of the absorption spectrum of $K_2(O_3S)_2NO$ has been possible. In a strict sense, the infrared absorption bands are not to be ascribed to particular groups within a molecule, but to a molecule or an ion as a whole. Nevertheless, the discussion, as is given here, may be correct for the nature and the purpose of the present work.

The vibrations which are ascribed to the $(O_3S)_2NO^{2-}$ ion in the mixed crystal are given in Table I, where the vibrations due to the sulfonate groups are added together, since the ion would certainly show the vibrations of the sulfonate groups. A rather strong band at 1620 cm^{-1} of the monomeric $(O_3S)_2NO^{2-}$ ion may be due possibly to an NO-stretching vibration. This assignment is regarded as reasonable, in view of the NO-frequencies which were formerly reported for other compounds: nitroalkyls[16] 1560~1500 and 1350~1300 cm^{-1}, dimeric nitrosomethane[17] 1282 cm^{-1}, nitrosamine 1455 cm^{-1} in a monomeric form and 1310 cm^{-} in a dimeric form[18]. Thus the rather high frequency of the NO-vibration for the monomeric $(O_3S)_2NO^{2-}$ ion is found to correspond to comparatively high bond-order of the NO-linkage, being in agreement with the assumption of the three-electron bond.

The Structure of the Dimeric Form of Fremy's Salt. — The structure of the dimeric form of Fremy's salt has formerly been examined by a number of investigators. Hantzsch and Semple[5] assumed that the violet-blue and the yellow form are, respectively, the monomeric and the dimeric form of Fremy's salt, comparing the relation between them to that between nitrogen dioxide and dinitrogen tetroxide. Investigating chemical property of Fremy's salt in aqueous solution, Haga and Divers[6] proposed a structure, $K_4(O_3S)_2NO\cdot ON(SO_3)_2$, for the monomeric form of Fremy's

13) R. S. Drago, ibid., **79**, 2049 (1957).
14) W. P. Griffith, J. Lewis and G. Wilkinson, *J. Inorg. Nucl. Chem.*, **7**, 38 (1958).
15) They denote Fremy's salt as $K(O_3S)(NO)_2$, but the compound should be represented by an empirical formula of $K_2(O_3S)_2NO$, as has usually been adopted for the compound.
16) L. J. Bellamy, "The Infrared Spectra of Complex Molecules", Methuen and Co., London (1954).
17) B. G. Gowenlock and J. Trotman, *J. Chem. Soc.*, **1955**, 4190.
18) R. n. Haszeldine and B. J. H. Mattinson, ibid., **1955**, 4172.

salt in solution and double the formula for the dimeric form. Much later, Asmussen[7] investigated the compound magnetochemically only to reaffirm Hantzsch and Semple's hypothesis, and regarded that Fremy's salt in aqueous solution exists as an equilibrium mixture consisting of a monomeric form in most part and a dimeric form in a very small amount. Neither Asmussen nor Hantzsch and Semple, however, presented a structural formula for the dimer after all. The structures, as proposed long ago for the dimer of Fremy's salt by Rasching[3] and by Claus[4], are not quite satisfactory, in view of insufficient materials available as well as because of poor knowledge at that time about the chemical bonds in general. Thus the problem of the structure of the dimer is not to be regarded as settled, but reexamination of the structure seems to be most desirable.

Examination of the possible electronic structures seems to indicate that the following three configurations (Fig. 2) may most probable for the dimer, the structures with resonance which involves the sulphonate-groups being omitted.

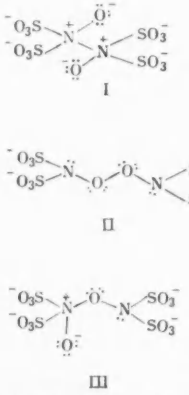

Fig. 2. Possible configurations for the dimeric form of Fremy's salt.

Examination of the steric requirements using molecular models shows that structure I seems to be very difficult, although it might not be quite impossible. Thus crowding of one oxygen atom and two sulfonate-groups around the nitrogen atom would hinder dimerization through an N–N linkage. Structure III is also difficult sterically, although this may not be impossible. On the other hand, structure II suffers no steric hindrance. Structure II, therefore, seems to be most probable from this standpoint.

The present measurements of UV spectra show that the electronic state of the dimer deviates greatly from the state of the monomer, since the UV absorption spectrum of Fremy's salt in the crystalline state is quite different from that of the monomer (Fig. 3). Thus the absorption band at about 55×10^{13}/sec., which is due primarily to the NO-group in the monomer, disappears with the dimer. Instead, the latter shows a few absorption

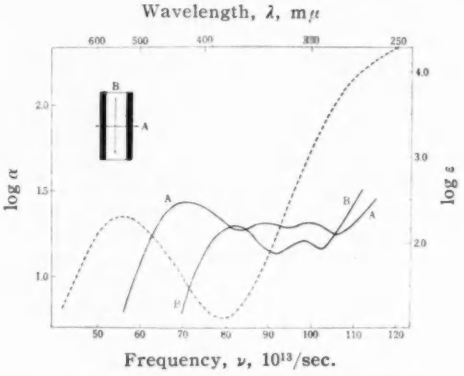

Fig. 3. Absorption spectra of Fremy's salt in the crystalline state (——) and in aqueous solution (----).

bands in the visible region and its neighborhood. If the dimer were represented by structure I, it would not exhibit an absorption band in the visible region, as is readily expected from absorption spectra of its related compounds. Previous data indicate that the dimer of nitrosomethane, which has a configuration similar to structure I, shows an absorption band at about 280 mμ (107×10^{13}/sec.) but no absorption band in the visible region, much less the "nitroso-band" at about 650 mμ (46×10^{13}/sec.). Since inspection of the structural formulae shows that structure I might involve N–O bonds with lower bond order than that of the N–O bond in the dimer of nitrosomethane, the ion represented by structure I would not show an absorption band in the neighborhood of the visible region. In fact, the present measurements indicate that the dimer of Fremy's salt has a few absorption bands in this wavelength range. Structure I, therefore, is rejected on the basis of the UV absorption spectra as well as of the steric requirements.

Absorption spectra of the compounds

which are somewhat similar to the compound represented by structure II have previously been studied. Thus Kortüm and Finckh[19] reported absorption spectra of sodium nitrite, pernitrite, hyponitrite and related compounds in solution, which were found to display absorption bands in the comparatively long wavelength region. Structure II, therefore, may not be inconsistent with the present observation that the compound in question displays absorption bands in the visible region and its neighborhood. Structure III, however, may not be excluded from the visible and ultra-violet spectrum alone.

The above discussion on the structure of the dimer of Fremy's salt is corroborated by the infrared absorption spectra. It is seen in Table I that the monomeric ion of $(O_3S)_2NO^{2-}$ shows a strong band at about 1620 cm^{-1} which is due to the N–O stretching vibration, whereas the dimeric ion shows the corresponding bands at 1260 cm^{-1}. Structure III would show the corresponding bands of high intensity due to the N–O stretching vibrations at wavenumbers smaller than the vibration of the monomer. Thus, at least a few absorption bands due to the N–O stretching vibrations might be observed in the infrared spectrum for structure III, since three kinds of the NO-groups are involved in this structure and those vibrations are all infrared active. The fact that there is observed only one absorption band of this sort for the dimer is not consistent with structure III, although a possibility might remain that some of the absorption bands would be hidden under strong bands due to the sulfonate groups.

On the contrary, structure II has only one kind of N–O bond, and the symmetric vibration due to the NO groups is infrared inactive. Only the symmetric vibration is infrared active, and may be regarded as corresponding to the band at 1260 cm^{-1}. Thus the infrared spectrum may be reconciled in a satisfactory way with structure II. Further evidence for this conclusion may be obtained by complete analysis of the infrared absorption spectra, which, however, requires data of the Raman spectrum with this compound. The determination of it would be enlightening in this respect. Based on the infrared spectrum alone, structure I might also be possible, but this structure has been shown in the preceding part of the present paper to be inconsistent with the UV spectra and steric requirements.

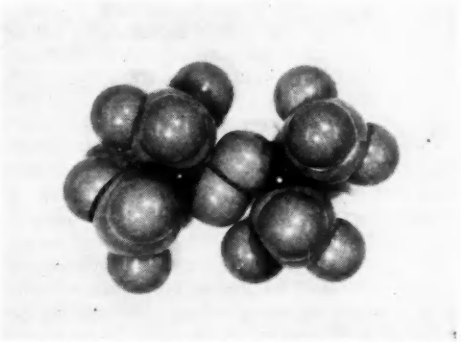

Fig. 4. Stuart model of $(O_3S)_2NO{\cdot}ON(SO_3)_2^{4-}$.

All the above materials combined seem to favour most strongly structure II having an O–O linkage. — A Stuart model representing structure II is shown in Fig. 4. This conclusion on the structure of the dimer seems to be noteworthy, since it is known that most nitroso-derivatives tend to form dimers involving a linkage of an N–N type.

Summary

Absorption spectra in the visible and ultra-violet region have been determined at room temperature by Tsuchida and Kobayashi's microscopic method with crystals of Fremy's salt and related compounds. Infrared absorption spectra have also been measured with these compounds.

The results of the measurements are discussed in relation to the structure of the compounds. A steric condition, visible and ultra-violet absorption spectra and infrared spectra are found to be in best agreement with a structure having a peroxide grouping.

The present authors wish to thank the Ministry of Education for a grant-in-aid, Mr. H. Nakamura for experimental assistance, and Mr. Ishikawa for infrared spectra.

Department of Chemistry, Faculty of Science, Osaka University
Nakanoshima, Osaka

19) G. Kortüm and B. Finckh, *Z. physik. Chem.*, **B48**, 32 (1941).

On the Difference between L-Forms and the Corresponding DL-Forms of Amino Acids in their Solid-State Infrared Spectra

By Masamichi TSUBOI and Tadao TAKENISHI

(Received February 6, 1959)

This paper is concerned with an interesting fact which led us to a conclusion that there are three different modes of composition of D- and L-molecules in so-called racemates of amino acids.

We have compared infrared spectra[1] of optically active forms in solid states with those of the corresponding racemates for a variety of amino acids, and have found that these results of the comparisons are grouped in three classes, A, B and C, as given below. It is remarkable that the distinction between these classes is sharp and that there is none intermediate between them.

(A) In class A, *the spectra of the L- and DL-forms are identical.*—Examples[1]: threonine, histidine hydrochloride monohydrate. Here, every band of the DL-form is observed at the same position with the same relative intensity as the corresponding band of the L-form, within the limits of experimental error.

(B) In class B, *the spectra of the L- and DL-forms are a little different from each other.*—Examples[1]: tyrosine (see Fig. 1), alanine, leucine, phenylalanine, asparagine, tryptophan. Here, as illustrated in Fig. 1, some of the bands of the DL-form are observed at different positions and/or with different relative intensities from the corresponding bands of the L-form, but all the bands of the DL-form are observed within 20 cm^{-1} from the corresponding bands of the L-form. Sometimes a band of the L-form splits into two in the DL-form, or a band of the DL-form splits into two in the L-form. But the splitting is mostly observed within a distance of 20 cm^{-1}.

(C) In class C, *the spectra of the L- and DL-forms are greatly different from each other.*—Examples[1]: aspartic acid (see Fig. 2), valine, isoleucine, serine, methionine, proline, lysine hydrochloride. Here, as illustrated in Fig. 2, many of the bands of the DL-form have no corresponding bands within 20 cm^{-1} in the spectrum of the L-form; and/or many of the bands of

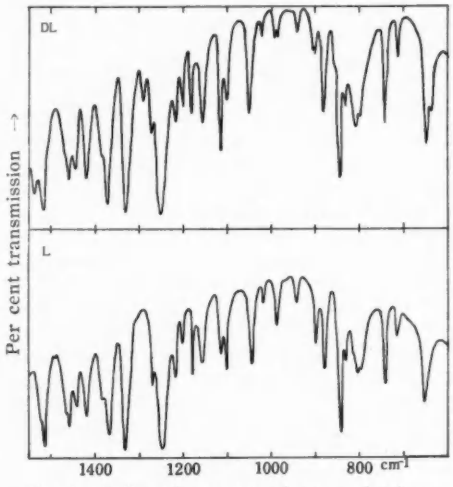

Fig. 1. Infrared spectra of DL- and L-forms of tyrosine in KBr disks.

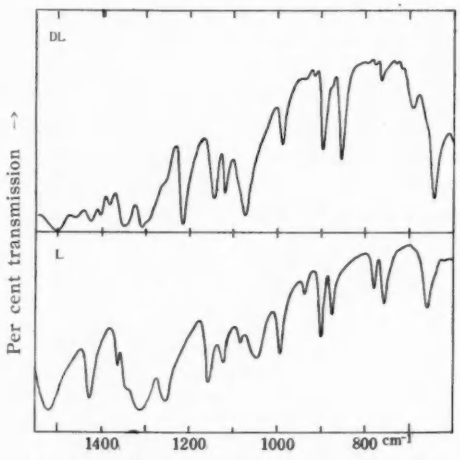

Fig. 2. Infrared spectra of DL- and L-forms of aspartic acid in KBr disks.

1) For the infrared spectra observed, see M. Tsuboi and T. Takenishi, *J. Japanese Chemistry* (*Kagaku-no-Ryoiki*), *Zokan*, No. 7, Nankodo Co. (1959).

the L-form have no corresponding bands within 20 cm^{-1} in the spectrum of the DL-form.

The comparisons of the infrared spectra in the solid states of optically active forms with those of the corresponding racemates have also been made by several authors[2-6] for several amino acids. All of these results, so far as is known to us, are grouped, without exception, in the same way as above.

From the above, we are led to consider that the three classes correspond to three different modes in which the D- and L-forms compose the DL-forms in solid states. Thus, in class A, the DL-form is merely a racemic mixture of the D- and L-forms; in class B, the crystal of the DL-form has a lattice composed of the D- and L-molecules, but the composing molecules are essentially identical in configuration with the molecules in the crystal lattice of the active forms; and in class C, the molecules composing the DL-form take different configurations from those in the D- and L-forms.

In the case where the crystal lattice of a racemate is composed of D- and L-molecules, the crystalline force field in it must of course be different from that in the lattice of the optically active crystal which is formed solely by the D- or L-molecules. This difference in the force field must be essentially of the same degree as that between different polymorphic forms of an ionic crystal[7], and must cause just as much difference in spectra as actually observed in class B.

On the other hand, no spectral difference is expected between a mechanical mixture of the D- and L-crystals and its component crystals, because all factors influencing the molecular and lattice vibrations must be exactly identical in the D- and L-crystals, as well as in their mixtures. Then, it may be concluded that the DL-form in class A is a mechanical mixture of the D- and L-crystals. For threonine, one of the examples for class A, Shoemaker et al.[8] reached, from X-ray examinations, a conclusion consistent with the above.

Considered on the basis of the accumulated knowledge on the internal rotations around the C–C and other single bonds[9,10] many of the amino acid molecules are expected to form rotational isomers with small energy differences. For such amino acids, the different crystalline force fields between the DL- and L-forms may result in occurrence of different rotational isomers[11]. Between these rotational isomers a great difference is expected in their infrared spectra. The great spectral difference actually observed in class C may be attributed to such rotational isomerism.

We wish to express our sincere thanks to Professor San-ichiro Mizushima, Dr. Takehiko Shimanouchi and Dr. Haruomi Oeda for their kind encouragements and valuable suggestions.

Department of Chemistry
Faculty of Science
The University of Tokyo
Hongo, Tokyo (M.T.)

Central Research Laboratory
Ajinomoto Company
Kawasaki, Knagawa (T.T.)

2) N. Wright, *J. Biol. Chem.*, **120**, 641 (1937).
3) N. Wright, ibid., **127**, 137 (1939).
4) G. B. B. M. Sutherland, *Discussions Faraday Soc.*, **9**, 319 (1950).
5) H. Brockman and H. Musso, *Chem. Ber.*, **89**, 241 (1956).
6) R. J. Koegel, R. A. McCallum, J. P. Greenstein, M. Winitz and S. M. Birnbaum, *Ann. N. Y. Acad. Sci.*, **69**, 94 (1957).
7) See, for example, M. Tsuboi, T. Onishi, I. Nakagawa, T. Shimanouchi and S. Mizushima, *Spectrochim. Acta*, **12**, 253 (1958).
8) D. P. Shoemaker, J. Donohue, V. Schomaker and R. B. Corey, *J. Am. Chem. Soc.*, **72**, 2328 (1950).
9) S. Mizushima, "Structure of Molecules and Internal Rotation", Academic Press, New York (1954).
10) M. Hayashi, T. Shimanouchi and S. Mizushima, This Bulletin, **29**, 802 (1956).
11) See, for example, J. Trommel and J. M. Bijvoet, *Acta Cryst.*, **7**, 703 (1954); A. McL. Mathieson, ibid., **5**, 332 (1952); M. Tsuboi, T. Takenishi and Y. Iitaka, This Bulletin, **32**, 305 (1959); M. Tsuboi, Y. Iitaka, S. Suzuki and S. Mizushima, ibid., **32**, 529 (1959).

Studies on the Graphitization. III. The Sub-Structure of Heat-Treated Coke*

By Haruo KURODA

(Received January 29, 1959)

Carbons made by carbonizing organic substances at a temperature lower than 1000°C are made up of minute crystallites of non-graphitic structure and disordered phase consisting of carbon, hydrogen and oxygen. The heat-treatment at a higher temperature causes in carbons the decrease of disordered phase and the crystallite growth as well as the improvement of the stacking order of the layer lattice in crystallites.

The progress of the structural change in the heat-treatment differs greatly depending on the characters of carbons even if they are heat-treated under the similar conditions. The crystal structure of carbons can be well defined by the analysis of their X-ray diffraction pattern[1]. Graphitization has been discussed hitherto mainly based on the knowledge concerning the crystal structure. The difference in graphitizability, however, can not be explained by comparing the crystal structure alone.

In the previous papers[2], we pointed out that the particular features in graphitization of carbon blacks are due to the substructure of carbon black particles. It might be natural that the graphitizability of carbon is strongly influenced by the character of crystallite boundaries, alignment of crystallites or other similar aspects of its structure which we shall call micro-structure distinguished from crystal structure. From such a point of view, we investigated the micro-structure and its change after heat-treatments in petroleum coke, which is known to be one of the well-graphitizable carbons.

Experimental and Results

Heat-Treatment and Crystal Structure.— Petroleum coke of Great Lake Co. was heat-treated in vacuo at several temperatures from 1000°C to 3000°C. X-ray diffraction was studied using a commercial X-ray diffractometer, with Cu K_α radiation. Diffractometer records of 10 diffraction are reproduced in Fig. 1. As seen in this figure, the raw coke has non-graphitic structure, and the improvement of the stacking order of layer lattice starts at a temperature around

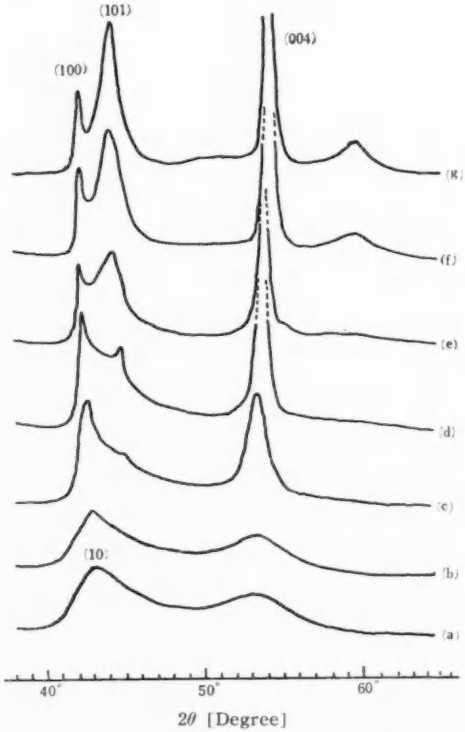

Fig. 1. X-ray diffraction pattern of petroleum coke. The effect of heat-treatment on the profile of (10) diffraction peak. (Cu K_α, Ni-filtered). (a) Raw state. (b) 1400°C. (c) 1850°C. (d) 1900°C. (e) 2040°C. (f) 2500°C. (g) 3000°C.

* This work is a part of a research project on carbons, supported by the 117 Committee in Nippon Gakujutsu Shinkokai, directed by Prof. H. Akamatu. Part I, This Bulletin, **29**, 574 (1956); Part II, ibid., **32**, 142 (1959).

1) J. Biscoe and B. E. Warren, *J. Appl. Phys.*, **13**, 364 (1942); C. E. Houska and B. E. Warren, ibid., **25**, 1503 (1954); R. E. Franklin, *Acta Cryst.*, **3**, 107 (1950); *Proc. Roy. Soc.* (*London*), **A209**, 196 (1951); H. Akamatu, H. Inokuchi, H. Takahashi and Y. Matsunaga, This Bulletin, **29**, 574 (1956).

2) H. Kuroda and H. Akamatu, "Proceeding of the 3rd Conference on Carbon", Pergamon Press, New York (1958), p. 381; This Bulletin, **32**, 142 (1959).

1900°C. When H.T.** is 2500°C, the observed value of layer spacing is 3.365 Å. This indicates that nearly 65% of layers are in graphitic orientation. It becomes 3.351 Å after the heat-treatment at 3000°C.

The crystallite sizes determined from the breadth of diffraction peak are given in Table I. At lower temperatures crystallite size increases only a little. The rapid growth starts at a temperature around 1900°C.

TABLE I. GROWTH OF CRYSTALLITE DIMENSION IN PETROLEUM COKE WITH HEAT-TREATMENT

H.T. (°C)	L_a (Å)	L_c (Å)
Original	38	37
1400	40	38
1550	42	49
1720	87	71
1850	110	93
2040	276	180
2500	392	202
3000	444	213

Grains of Coke Powder.—After the heat-treatment, coke was milled into a fine powder and observed under the electron microscope***. Minute flaky grains can be observed with the raw coke as shown in Fig. 2. They have a jagged outline and the appearance of the granular structure. Most of them are of several microns in transverse direction and less than 1000 Å in thickness. The granular appearance is removed by the heat-treatment. When H.T. is higher than 2000°C, it entirely disappears. After the heat-treatment with high H.T., the stepwise variation of electron transmission is seen at edges of grains. It can be found also at the inner part of grains when its thickness is very small. These facts indicate that each grain is a bundle of many thin lamellae. The thickness of one lamella seems to be in the order of 200~300 Å.

Fig. 2. Electron micrograph of coke grains, (raw state). (shadowed with Ge)

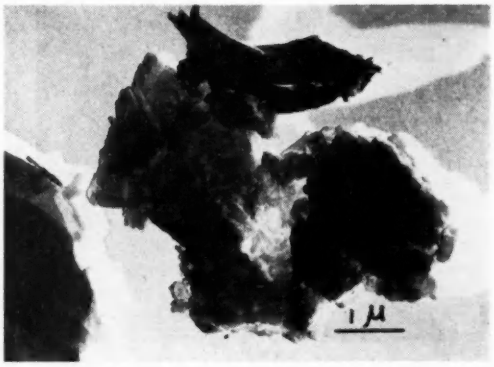

Fig. 3. Electron micrograph of coke grains, (H.T., 2500°C). (shadowed with Ge)

As can be seen in Figs. 3 and 6, in every coke grain are sub-boundaries, which are dividing it into smaller grains.

The electron diffraction pattern corresponding to each grain was studied by the method of selected-area electron diffraction. One of the typical results with the raw coke is given in

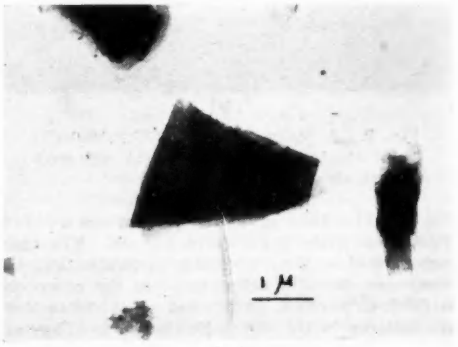

(a)

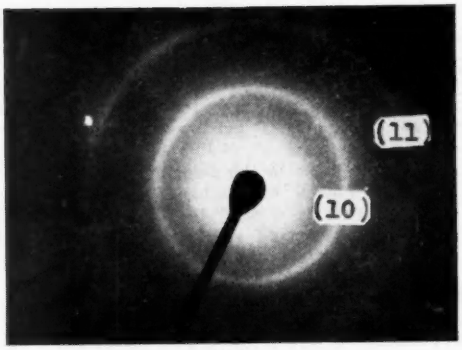

(b)

Fig. 4. A coke grain, (raw state): (a) electron micrograph. (b) selected-area electron diffraction.

** The temperature of heat-treatment is abbreviated to H. T.

*** Electron microscopic studies were made using Hitachi Electron Microscope, Model 10-A.

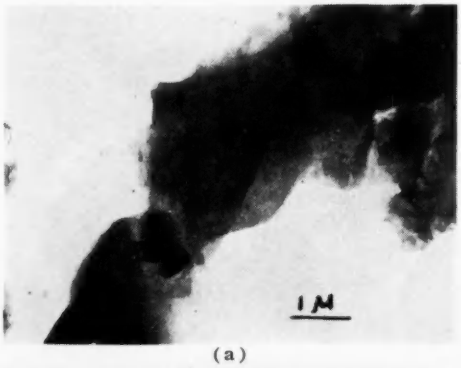

(a)

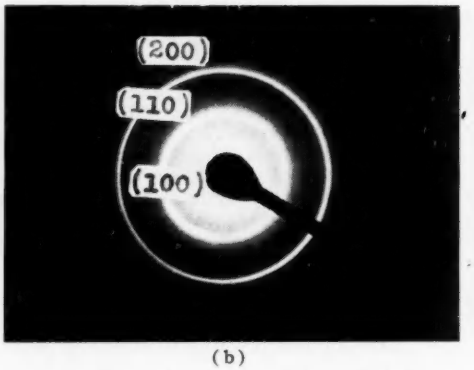

(b)

Fig. 5. A coke grain, (H.T., 1850°C): (a) electron micrograph, (b) selected-area electron diffraction.

(a)

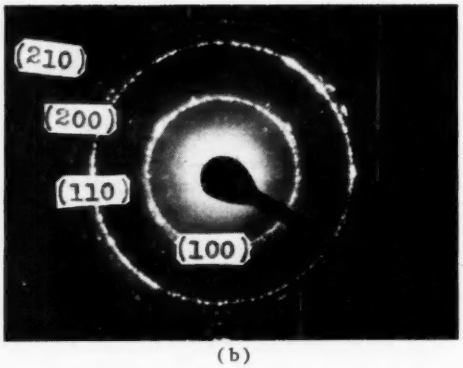

(b)

Fig. 6. A coke grain, (H.T., 3000°C): (a) electron micrograph, (b) selected-area electron diffraction.

Fig. 4. The flaky grain in Fig. 4a gives a diffuse diffraction pattern shown in Fig. 4b. The spacings related to the two halos indicate that the inner one is (100) diffraction and the outer one is (110) diffraction. (002) and (004) diffractions are missing in this diffraction pattern. They are always either missing or very weak in every selected-area electron diffraction pattern of the grain of the raw coke. After heat-treatment, diffraction rings become clear and sharp as seen in Figs. 5 and 6. In both of them, diffraction rings correspond to (100), (110),(200), (210) and (300) diffractions, respectively. Most of the grains give such a polycrystalline diffraction pattern consisting of $(h\,k\,0)$ diffractions alone. *c*-axis should be in the direction parallel to the incident electron beam, hence parallel to the direction that is normal to the surface of the grains, in order to give such diffraction patterns. Thus each coke grain is a group of many crystallites with a preferential orientation of *c*-axis. In Fig. 5a diffraction rings have homogeneous intensity distribution in all directions, hence *a*-axis direction is quite random in the plane of the grain. In Fig. 6b however, diffraction rings split into many spots. Many grains give such a pattern if H.T. is 2500~3000°C. There are some grains which give a diffraction pattern like that of a single crystal. They seem to be a quasi-single crystal. As shown in Table I, the crystallite size along *a*-axis determined from X-ray diffraction is only 400~500Å, even if H. T. is around 3000°C. From the selected-area diffraction, however, the average dimension of the area, in which *a*-axis direction is the same, seems to be very much larger than the crystallite size.

A grain shown in Fig. 7a has a round outline and looks quite different from those already shown. Its diffraction pattern is a single-crystal pattern with Kikuchi-lines as shown in Fig. 7b. This is a single crystal of graphite. Grains of this kind can be found in the powders of various heat-treated carbons if H.T. is very high. Their size and shape do not depend on the characters of the original carbons. It seems that they are due to the crystal growth from vapor[3]. Since the formation of such single-crystal grains has no essential role in the principal process of graphtiization, we shall not further discuss it in this paper.

3) The growth of graphite crystals by the dislocation mechanism was observed and discussed by T. Tsuzuku, *Tanso* (*Carbons*), **5**, 2 (1955); T. Tsuzuku and T. Komoda, *Acta Cryst.*, **9**, 90 (1956).

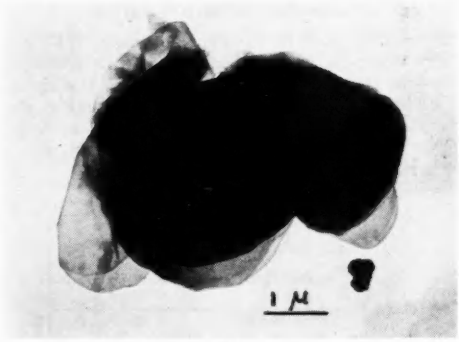

(a)

(b)

Fig. 7. A single-crystal grain: (a) electron micrograph, (b) selected-area electron diffraction.

Structure of Coke Grains.—If the direction of the incident electron beam is parallel to the texture axis, we can not find any difference between ($h\,k$) two-dimensional diffraction and ($h\,k\,0$) diffraction. This is the case in the diffraction patterns shown above. We studied the oblique diffraction pattern of coke grains in order to know their structure.

If coke grains have the textured polycrystalline structure, they should give oblique texture patterns[4]. The reciprocal lattice of non-graphitic structure consists of a series of (0 0 1) points along c-axis and ($h\,k$) lines parallel to it. Hence a grain should give an oblique pattern consisting of continuous ellipses if crystallites in it have non-graphitic structure. As the stacking order of layer lattice is improved, the structure factor has a periodic variation on each ($h\,k$) line in the reciprocal lattice. Thus the stacking order in the crysallites can be known from the intensity variation on the elliptical pattern in the oblique texture pattern.

Fig. 8 is one of the diffraction patterns obtained with the raw coke. The long arc-patterns are (10) and (11) diffractions and the short ones are (002) and (004) diffractions. It can be seen from this diffraction pattern that the direction of the texture axis, c-axis, has fluctuation around that which is normal to the surface of the grain. Most of the grains in the raw coke give such diffraction patterns. This is the case also in the heat-treated coke if H.T. is low. The fluctuation of c-axis direction decreases as H.T. is raised, and it almost disappears when H.T. is higher than 1850°C. The indication of the improvement of the stacking order, however, is not observed with the grains which have appreciable fluctuation of c-axis direction. The improvement of the crystallite alignment seems to proceed in advance of the change in the stacking order.

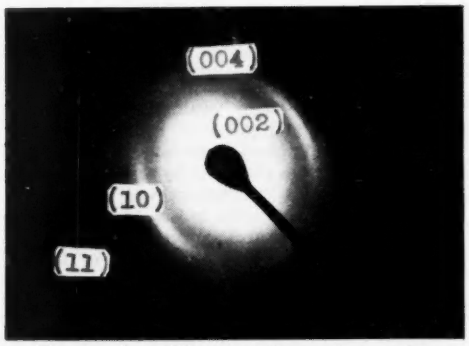

Fig. 8. An oblique pattern of a coke grain, (raw state). The oblique angle is larger than 80°.

In the X-ray diffraction pattern, the modulation of two-dimensional diffraction peak appears when H.T. is around 2000°C. The indication of the change in the stacking order can be observed also in electron microdiffraction from H.T. around 1900°C. One of the typical diffraction patterns corresponding to the earlier stage of graphitization is shown in Fig. 9. As H.T. is raised, the diffraction pattern becomes that of the textured polycrystalline structure of graphite. Some grains

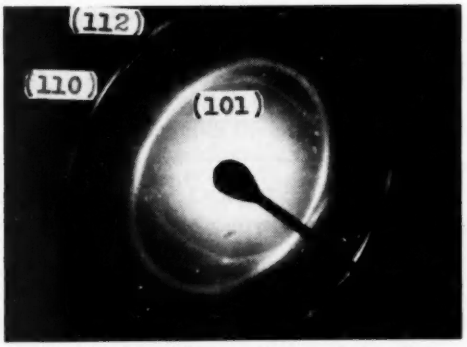

Fig. 9. An oblique pattern of a coke grain, (H.T., 1850°C). The oblique angle is 43°.

4) Z. G. Pinsker, "Electron Diffraction", Butterworths Scientific Publications, London (1953), p. 93.

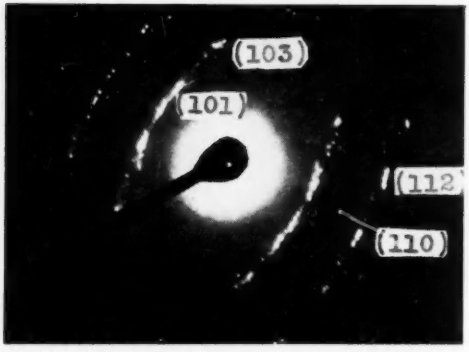

Fig. 10. An oblique pattern of a coke grain, (H.T., 2500°C). The oblique angle is 62°.

give a single crystal pattern. A typical diffraction pattern for coke grains heat-treated at 3000°C is shown in Fig. 10.

X-ray Small-Angle Scattering.—X-ray small-angle scattering was observed by the experimental procedures described elsewhere[5]. The observed intensity curves are given in Fig. 11. The small-angle scattering of petroleum coke is very weak, and, as H.T. is raised, the gradient of the intensity curve becomes very steep. It is difficult to make an accurate measurement when H.T. is high. As can be seen from Fig. 12, the intensity is nearly proportional to $h^{-2.3}\sim h^{-2.5}$ throughout the observed range of scattering angle. Such a relation can not be expected if the system is made up of spherical particles. The result seems to suggest that the structural units responsible for the observed scattering are thin plates.

Kratky and Porod[6] have derived an approximate formula for the scattering function of a thin disk of thickness $2H$ and diameter $2R$****.

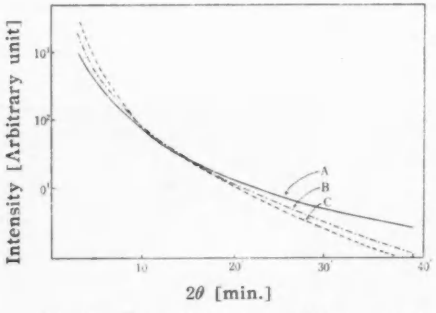

Fig. 11. Intensity curves of X-ray small-angle scattering: (A) raw state, (B) H.T., 1725°C, (C) H.T., 1850°C.

5) H. Kuroda, *J. Chem. Soc. Japan, Pure Chem. Sec.* (*Nippon Kagaku Zasshi*), **77**, 1298 (1956); *J. Colloid Sci.*, **12**, 496 (1957).

6) O. Kratky and G. Porod, ibid., **4**, 35 (1949).

**** $h=4\pi\sin\theta/\lambda$ and n is the number of electrons in the particle.

$$\overline{F^2(h)} = (2n^2/h^2R^2)\exp(-h^2H^2/3)$$

This can be used in the range of angle, $1/R<h<1/H$. When the system consists of thin plates of different sizes and random orientation, the small-angle scattering intensity might be roughly expressed by the following formula at the angle where h is large with respect to $1/\bar{R}$ but small with respect to $1/\bar{H}$.

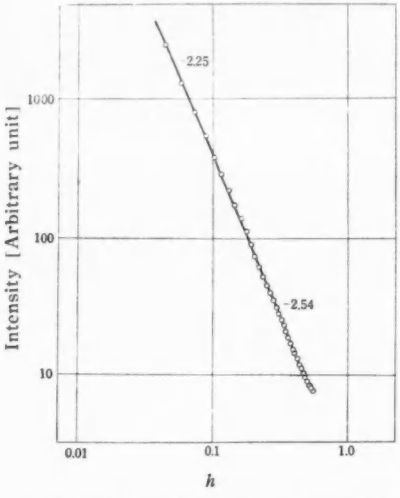

Fig. 12. Plot of $\log I(h)$ versus $\log h$, (raw state). The numbers on the curve indicate the inclination.

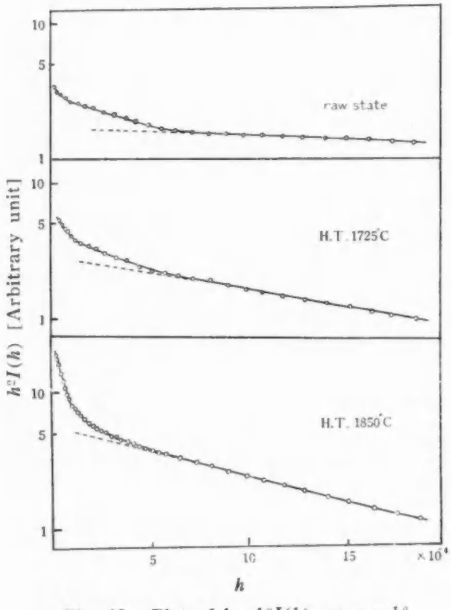

Fig. 13. Plot of $\log h^2I(h)$ versus h^2.

$$h^2I(h) = \text{const} \sum M(H_i) H_i \exp(-h^2H_i^2/3)$$

where $M(H_i)$ is the mass-fraction of plates with thickness of $2H$, and $\bar{R}$, $\bar{H}$ are the average value of R and H, respectively.

The curves of $\log h^2I(h)$ versus h^2 are shown in Fig. 13. There is a wide linear part in each curve. The value of $2H$ corresponding to the inclination of this part is given in Table II. They are of the same magnitude with crystallite size.

TABLE II. VALUES OF $2H$

H.T. (°C)	Range of the linear part (h)	Inclination of the linear part	$2H$ (Å)	L_c (Å)
Original	$>7.3\times10^{-4}$	3.48×10^2	49	37
1720	$>5.8\times10^{-4}$	10.72×10^2	86	71
1850	$>5.1\times10^{-4}$	14.51×10^2	100	93

$2H$ was calculated assuming that the inclination is equal to $-0.434H^2/3$.

Although we are not sure whether the structural units responsible for the observed small-angle scattering are the groups of crystallites or the voids between them, the results seem to suggest that petroleum coke has some kind of lamellar units in its structure even in the raw state and after heat-treatment at low temperatures.

Discussion

It has been found that petroleum coke can be disintegrated into minute flaky grains. When H.T. is high, it has been observed that each coke grain is made up of smaller grains or lamellae in which carbon crystallites are aligned so as to make their c-axes normal to the plane of the lamella. When H.T. is low, the lamellar structure can not be seen, but the alignment of crystallites is already not at random, c-axis direction being nearly perpendicular to the surface of grain. X-ray small-angle scattering suggests also the presence of lamellar units in the structure of petroleum coke.

It has been frequently presumed hitherto as the structural model for cokes that carbon crystallites are randomly linked to one another with chain-like molecules in disordered phase. Such a model, however, is not satisfactory for petroleum coke, since it is disintegrated into grains as mentioned above, and it must be made up of lamellar groups of crystallites with the preferential orientation concerning c-axis.

As mentioned already, the textured structure can be found even in the raw coke. It seems to have been formed during the carbonization process. If each crystallite is separated from the neighboring ones by a large amount of disordered phase, it might be difficult to form a large group of crystallites in which c-axis direction is nearly the same. The textured structure will be explained if we presume that there is a comparatively small amount of disordered phase between neighboring crystallites.

It has been known that the disordered phase is made up of mainly aliphatic C–C bonds, C–H bonds, C–O, bonds etc. Since these chemical bonds are thermally unstable compared with aromatic C–C bond, they can be broken at a lower temperature which can not provide a sufficient energy to break up residual bonds of aromatic character. Thus, when H.T. is low, the crystallite growth will proceed solely at the expense of disordered phase. This will cause only a slight increase of crystallite size. This is actually the case as seen in Table I. The crystallite alignment, however, is to be improved well in this stage. At the extreme of the crystallite growth of this mechanism, there should be only a very narrow disordered region or slight structural defects between the neighboring crystallites. The remaining residual bonds might be of aromatic character at this stage. If H.T. is high enough to provide sufficient energy to break them up, the rapid growth will proceed by the condensation of the neighboring crystallites. Actually it starts at a temperature around 2000°C which is known to be a temperature at which the plastic deformation can occur in various carbons. If we presume such a mechanism of crystal growth, the structural change in petroleum coke will be explained well.

In a carbon black particle, c-axis direction of crystallites is considered to be nearly normal to the surface of the particle. When crystallite grows well, a carbon black particle becomes polyhedrone. If the crystallite size increases too much, a stress will be created in the particle. As has been shown in the previous papers, this situation sometimes causes the disintegration of carbon black particle into smaller units. There is no situation like this in the crystallite growth in petroleum coke if it proceeds within each textured polycrystalline group.

The micro-structure pictured in this paper is not to be considered as the special one that can be found only in petroleum coke. The similar structure can be found widely in soft cokes. In hard cokes, the

textured polycrystalline group does not exist, or, if it exists, the crystals are of small dimension. The large difference in graphitizability seems to be due to such a situation.

The author wishes to express his thanks to Professor H. Akamatu for his kind direction, and to Dr. H. Takahashi for his valuable advice. He is also indebted to Mr. S. Sakata for his kind help in the experiment.

Department of Chemistry
Faculty of Science
The University of Tokyo
Hongo, Tokyo

Theoretical Study on the Mechanism of the Aromatic Substitution[1)]

By Saburo NAGAKURA and Jiro TANAKA

(Received July 30, 1958)

As is well known, the mechanism of aromatic substitution may be regarded as one of the most typical problems to which the quantum mechanical theory has been applied with succcss. Since 1940, a number of notable theoretical papers on this subject have already been published by several authors[2-8]. In these papers, some quantum mechanical concepts useful for interpreting chemical reactivity of the aromatic molecule have been introduced. They are such concepts as π-electron density, free valency, localization energy, frontier electron density, etc.[9)] By means of them, one has succeeded in explaining the orientation rule observed with some aromatic substitution reactions. It seems hasty, however, to consider that all the problems in this field have been settled completely. In fact, one can easily find some facts which can hardly be interpreted by any theory presented hitherto. For instance, the facts that the aliphatic hydrocarbon like methane is generally less susceptible to the electrophilic substitution than the aromatic hydrocarbon is, and that the silver cation is difficult to cause the substitution reaction with benzene while the nitronium cation is well known as a typical reagent for it, are not thought to be explained satisfactorily by the previous theories.

In the present paper, it is undertaken to study the mechanism of the aromatic substitution with reference to the relative heights of energy levels of the reagent to those of the aromatic molecule. From the consideration of these energy levels, it is concluded that a large electron transfer necessarily occurs from the aromatic molecule towards the reagent and in the reverse direction for the electrophilic and the nucleophilic substitution, respectively. On the basis of this electron transfer mechanism, conditions necessary for causing the aromatic substitution are reasonably introduced. It is shown, moreover, that the orientation in the aromatic substitution can properly be predicted by the free valency values evaluated with the aromatic cation, the neutral molecule and the anion for the electrophilic, the radical and the nucleophilic substitution, respectively.

1) Preliminary reports on this work have been published in *J. Chem. Phys.*, **22**, 563 (1954) and *J. Chem. Soc. Japan. Pure Chem. Sec.* (*Nippon Kagaku Zasshi*), **75**, 933 (1954).
2) T. Ri and H. Eyring, *J. Chem. Phys.*, **8**, 433 (1940).
3) G. W. Wheland, *J. Am. Chem. Soc.*, **64**, 900 (1942).
4) M. J. S. Dewar, *J. Chem. Soc.*, **1949**, 463.
5) C. A. Coulson and H. C. Longuet-Higgins, *Proc. Roy. Soc.*, **A191**, 39; **A192**, 16 (1947).
6) K. Fukui, T. Yonezawa and H. Shingu, *J. Chem. Phys.*, **20**, 722 (1952); K. Fukui, T. Yonezawa and C. Nagata, This Bulletin, **27**, 423 (1954).
7) R. S. Mulliken, *J. Phys. Chem.*, **56**, 801 (1952).
8) On this problem various excellent reviews have already been published. Some of them are as follows:
(a) C. A. Coulson, *Research*, **4**, 307 (1951).
(b) K. Higasi, *Monograph Ser. Research Institute of Applied Electricity, Hokkaido University*, **No. 4**, 307 (1951).
(c) R. D. Brown, *Quart. Revs.*, **6**, 63 (1952).
9) Some of these concepts are in intimate relations to one another. This problem has been discussed by Baba and also by Fukui et al. (cf. H. Baba, This Bulletin, **30**, 147, 154 (1957); K. Fukui, T. Yonezawa and C. Nagata, *J. Chem. Phys.*, **26**, 831 (1957)).

Determination of Energy Level Diagrams of Some Reagents and Aromatic Molecules

According to the authors' method described in the previous papers[10], the highest occupied (H) and the lowest vacant (V) orbital of a certain molecule can be determined by the aid of the experimental data on the ionization potential and the near ultraviolet absorption spectrum. The same method was applied to the determination of orbital energies of the neutral molecules and radicals considered in the present paper. Concerning electrophilic reagents, such as the nitronium (NO_2^+), chlorine (Cl^+), bromine (Br^+), iodine (I^+), and hydrogen cations[11], the lowest vacant orbital was set equal to the ionization potential of the corresponding neutral molecule or atom. On the other hand, the highest occupied orbital of the nucleophilic reagent, such as hydroxyl (OH^-) or chlorine (Cl^-) anion, was estimated from the electron affinity of the corresponding neutral radical or atom. The results thus obtained are shown in Fig. 1, where energy levels of the silver cation (Ag^+) and the iodine molecule are also given for the purpose of comparison. It is worthy of notice that both of them can form the stable charge transfer complex with the aromatic molecule[12-14] but are difficult to cause the substitution reaction.

Consideration of the Reaction Mechanism from Energy Level Diagrams[15]

First of all, let us consider the electrophilic substitution. It is evident from Fig. 1 that the lowest vacant orbital (hereafter abbreviated to V) of the typical electrophilic reagent lies definitely below the highest occupied orbital (hereafter abbreviated to H) of the aromatic molecule which is susceptible to the substitution reaction. On the other hand, the V orbitals of the silver cation and the iodine molecule, which can not act as the electrophilic reagent for the substitution, are apparently higher than the H orbitals of the aromatic molecules. This remarkable fact suggests that it may be necessary for the occurrence of the electrophilic substitution that the V orbital of the reagent is considerably lower than the H orbital of the aromatic molecule. Under this assumption, moreover, the fact that the simple aliphatic hydrocarbon like methane is attacked with difficulty by the electrophilic reagent can readily be understood. As is shown in Fig. 1, the H orbital of methane which exists at -13.0 eV. is clearly lower than or almost equal to the V orbitals for most electrophilic reagents. In this case, therefore, it is difficult to fulfil the necessary condition for causing the electrophilic substitution.

The above-mentioned fact probably gives an interesting suggestion concerning the mechanism of the electrophilic substitution. According to Mulliken's theory relevant to the intermolecular charge transfer phenomenon, the electron transfer occurs to some extent from a donor towards an acceptor when these two components approach each other[14]. For example, in the case of the molecular complex between benzene (electron donor) and iodine (electron acceptor), the magnitude of this electron transfer was estimated by Mulliken to be about 3%. On the basis of the molecular energy level diagrams shown in Fig. 1, this intermolecular charge transfer phenomenon can approximately be represented by the interaction of the H orbital of the electron donor with the V orbital of the electron acceptor. The simple LCMO treatment on this interaction leads to a qualitative conclusion that the magnitude of the electron transfer increases as the V orbital becomes lower or the H orbital higher if the resonance integral between these two orbitals remains almost constant. In fact, in the

10) S. Nagakura and J. Tanaka, *J. Chem. Phys.*, **22**, 236 (1954); S. Nagakura, ibid., **23**, 1441 (1955); J. Tanaka, S. Nagakura and M. Kobayashi, ibid., **24**, 311 (1956).

11) The reagent ion in solution is undoubtedly stabilized by the orientation of surrounding solvent molecules. In the present state of the study, however, it is difficult to make quantitative discussion on the solvation energy of the ion under actual conditions of reaction. Therefore, the effect of the solvent upon the orbital energies of the ion was not taken into account in the present treatment.

12) H. A. Benesi and J. H. Hildebrand, *J. Am. Chem. Soc.*, **71**, 2703 (1949).

13) L. J. Andrews and R. M. Keefer, ibid., **71**, 3644 (1949); **72**, 3113 (1950).

14) R. S. Mulliken, ibid., **72**, 600 (1950); **74**, 811 (1952); *J. Phys. Chem.*, **56**, 801 (1952).

15) The description in this chapter is an extention of the basic idea mentioned in the preliminary papers published in 1954[11]. The present authors' view on the importance of the electron transfer in the aromatic substitution is based on the energy level diagrams of the reagent and the aromatic molecule, which are determined by the use of the experimental data on the ionization potential and the near ultraviolet absorption spectrum. On the other hand, Fukui et al. have discussed a similar problem from the purely theoretical point of view and derived the equations representing the dependence of the electron density on the reagent upon the Coulomb and resonance integrals (K. Fukui, T. Yonezawa and C. Nagata, *J. Chem. Phys.*, **27**, 1247 (1957).

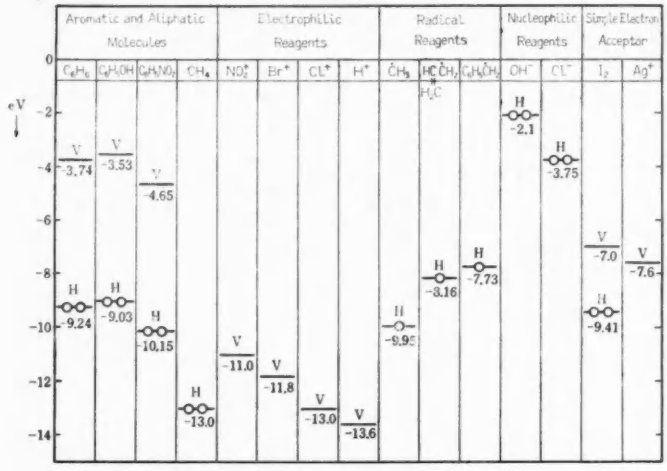

Fig. 1. Energy level diagrams for some reagents, and aromatic and aliphatic molecules.

The ionization potentials necessary for determining these diagrams were taken from the following references:

Benzene: W. C. Price and R. W. Wood, *J. Chem. Phys.*, **3**, 439 (1935).

Phenol and nitrobenzene: J. D. Morrison and A. J. C. Nicholson, ibid., **20**, 1221 (1952) and private communication from Dr. Morrison.

Iodine: J. D. Morrison, ibid., **19**, 1305 (1951).

Methane: R. E. Hornig, ibid., **16**, 105 (1948).

Nitrogen dioxide: E. C. G. Stueckelberg and H. D. Smyth, *Phys. Rev.*, **36**, 478 (1930).

Hydrogen, chlorine, bromine and silver atoms: Landolt-Börnstein, "Physikalische-Chemische Tabellen", 6-Auflage, I Band, 1. Teil, Springer-Verlag, Berlin (1951), p. 211.

Methyl, allyl and phenyl radicals: F. P. Lossing, K. U. Ingold and I. H. S. Henderson, *J. Chem. Phys.*, **22**, 621 (1954).

Electron affinities for hydroxyl group and chlorine atom are taken from Landolt-Börnstein, "Physikalische-Chemische Tabellen", 6-Auflage, I Band, 1. Teil, Springer-Verlag, Berlin (1951).

case of the iodine complex with triethylamine whose H orbital is much higher than that of benzene[16], the extent of the electron transfer certainly exceeds 50% as is revealed from the big dipole moment (11.3D)[17].

Applying the above consideration on the electron transfer to the system consisting of the aromatic molecule and the electrophilic reagent, one may be led to the conclusion that there necessarily occurs an extremely large electron transfer from the former towards the latter, because in this system the V orbital of the reagent is extraordinarily low and even lower than the H orbital of the aromatic molecule as mentioned above. This means that the electrophilic substitution proceeds passing through a stage at which the reagent cation robs almost one electron from the aromatic molecule and consequently the former changes nearly to the neutral radical and the latter nearly to the cation. On the present study of situation, it is difficult to ascertain whether or not this stage corresponds to the so-called transition state, namely the highest point in the potential energy curve for the reaction. According to our opinion, however, it is probably just before the transition state assumed by Wheland[2]. In other words, the above-mentioned large electron transfer may be accompanied by changes of the hybridizations and geometrical configurations in both the reagent and the aromatic molecule, and then a new σ bond may be formed between the former and a carbon atom of the latter

16) The ionization potential of triethylamine was determined as 7.50 eV. by Watanabe (K. Watanabe, *J. Chem. Phys.*, **26**, 542 (1957), whereas the ionization potential of benzene is 9.24 eV.

17) S. Nagakura, *J. Am. Chem. Soc.*, **80**, 520 (1958); H. Tsubomura and S. Nagakura, *J. Chem. Phys.*, **27**, 819 (1957).

(Wheland's activated complex, type II)[18]. This view is schematically shown in Fig. 2. In this figure, stages B and C correspond to the electron transfer state and Wheland's transition state, type II, respectively.

Spectrophotometric studies by Reid[19] and also by Gold and Tye[20] show that the aromatic carbonium ion $(ArH)^+$ can be formed by the interaction of the aromatic molecule with proton under suitable conditions. This kind of ion, which is called $b\pi$, $h\sigma$ inner complex and σ-complex by Mulliken[7] and by Brown[21], respectively, may be thought to take a structure similar to that of Wheland's activated complex, type II. Hence, the present theory may be said to clarify the necessary conditions for forming the inner complex.

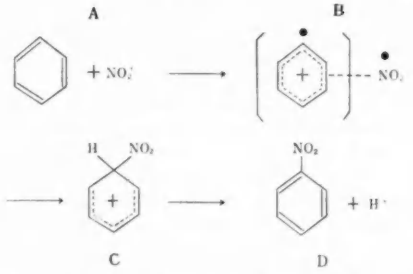

Fig. 2. Schematic diagram depicting the process of the substitution reaction between benzene and nitronium cation.

Let us now turn to the nucleophilic substitution. As is clearly seen from Fig. 1, the H orbital of the nucleophilic reagent is generally very high and may be regarded as comparable to the V orbital of the aromatic molecule. It is inferred from this that in this case a large electron transfer occurs from the reagent towards the aromatic molecule, and consequently the reaction takes place passing through the state in which the reagent becomes a nearly neutral radical and the aromatic molecule becomes an anion.

On the other hand, in the case of the radical substitution one may not expect such a large electron transfer as in the case of the heterolytic substitution, because unpaired electron levels of most radicals lie in an intermediate position between the H and the V orbitals of the aromatic molecule[22]. Thus in our opinion, the distinction between the heterolytic (electrophilic and nucleophilic) and homolytic (radical) substitutions is made in terms of the magnitude of the electron transfer between the reagent and the aromatic molecule. Furthermore, it is sure that in the electrophilic and the nucleophilic substitutions the directions of electron transfer are opposite to each other.

The present theory seems to have intimate relations with that presented by Weiss[23]. In 1946, Weiss emphasizes almost intuitively the importance of the electron transfer in many kinds of organic reactions. However, the grounds for his insistence concerning the aromatic substitution seem to be indefinite. The present theory has an advantage in that the necessity of a large electron transfer is reasonably concluded from the consideration of energy level diagrams of the reagent and the aromatic molecule.

Now, some consideration will be taken of the orientation in the aromatic substitution reaction, namely, the relative rate of substitution on various positions of the aromatic molecule. According to the present authors' view, in the heterolytic substitution the electron transfer takes place and consequently the reagent ion may be thought to attack the substrate as the radical. In other words, after the occurrence of the electron transfer, the mechanism of the heterolytic substitution may be regarded as similar to that of the homolytic substitution. Moreover, as is

18) The authors wish to express their sincere thanks to Professor Mulliken at Chicago and Professor Coulson at Oxford for their kindness in giving helpful suggestions on this respect. According to the present authors' opinion, Wheland's transition state, type II, corresponds to a basin in the potential energy curve for the substitution reaction.

19) C. Reid, *J. Am. Chem. Soc.*, **76**, 3264 (1954).

20) V. Gold and F. L. Tye, *J. Chem. Soc.*, **1952**, 2184.

21) H. C. Brown and J. D. Brady, *J. Am. Chem. Soc.*, **74**, 3570 (1952).

22) It is doubtful if the radical and the nucleophilic substitution proceed completely parallel to the electrophilic substitution. For example, the substitution of the hydroxyl radical for the hydrogen atom of benzene is considered to take place through the following procedures (G. Stein and J. Weiss, *J. Chem. Soc.*, **1949**, 3245):

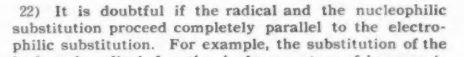

This mechanism is apparently different from that of the electrophilic substitution such as

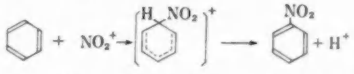

However, both reactions pass commonly through Wheland's type II transition state where the attacked point is clearly determined. Therefore, it seems reasonable to consider that concerning the orientation rule parallel treatment can be applied to the three types of aromatic substitution reactions.

23) J. Weiss, *Trans. Faraday Soc.*, **42**, 116 (1946).

well known, in the homolytic substitution the concept of free valency is very useful for explaining the orientation rule[23,24,25]. Hence, it is quite natural to consider that the orientation in the electrophilic and nucleophilic substitutions can be predicted on the basis of the free valency value of the aromatic cation and of the anion, respectively.

Calculation of the Free Valency and Consideration of the Results

Free valency of the r-th atom(F_r) can be evaluated with the aid of the following equation:

$$F_r = F_{\max} - \sum_s p_{rs}$$

where $F_{\max}$ is the maximum value of the total π bond order of the carbon atom and estimated at $\sqrt{3}$ [24], and p_{rs} is the π bond order of the r-s bond, where s denotes the adjacent atom to the r-th one. The value of p_{rs} can be calculated by the aid of the following equation:

$$p_{rs} = \sum_i n_i C_{ri} C_{si}$$

Here C_{ri} is the coefficient of the r-th atomic orbital in the i-th molecular orbital and n_i is the number of π-electron occupying it. The calculation of C_{ri} was made on the basis of the usual LCAO method under the assumption of orthogonality between adjacent $2p\pi$ atomic orbitals. Moreover, it was assumed that one electron is removed from the highest occupied orbital and is added to the lowest vacant one for the cation and the anion, respectively. In molecules containing hetero-atoms, evaluated values of free valency are rather sensitive to the assignment of the Coulomb and resonance integrals[26]. In the present calculation, the Coulomb integral for the hetero-atom was estimated with reference to its electronegativity and the resonance integral was set proportional to the corresponding overlap integral. By employing the self-consistent procedure which was certified to be useful for calculating the electron density for various molecules such as acetamide[27], tropolone[28], furan, pyrrole and thiophene[29], it was proved that the dependence of free valency upon the assignment of the Coulomb integral decreases considerably. The C_{ri} values for aniline, nitrobenzene, benzaldehyde and chlorobenzene were evaluated by the use of this iterative procedure. The C_{ri} values for phenol were calculated by Tsubomura[30]. The free valency values finally obtained in the present study are given in Tables I—III. In these tables, observed orientation rules are also given for the purpose of comparison.

It is seen from these tables that free valency values calculated for the aromatic cation, neutral molecule and anion can explain without contradiction the orientation observed with the electrophilic, radical and nucleophilic substitutions, respectively. Especially, it is worth notice that the free valency values calculated for the cations of the so-called *o*-, *p*-directing monosubstituted benzene molecules generally decrease in the order of $p > o > m$. This order is in complete accordance with the experimental results on the electrophilic substitution.

It is known that in some monosubstituted benzene molecules such as toluene[31] and styrene the radical substitution takes place in the side chain. In the case of styrene, this fact is coincident with the theoretical conclusion as is shown in Table II. The free valency of the carbon atom in the substituent group of benzaldehyde is also great compared with that of each atom in the benzene ring. This predicts the possibility that this molecule may be attacked on the carbon atom of the substituent group by the radical reagent.

The only exception in which the order of the free valency values does not agree with that of the observed reactivities in various positions is the case of radical substitution of biphenyl. In this case, free valencies decrease in the order of $2 > 4 > 3$, while the 4-position is most reactive from the experimental point of view. This descrepancy may be due to steric hindrance in the 2-position.

Such a satisfactory agreement between theoretical and experimental results as is seen from Tables I—III seems to support our view that at some stage of the heterolytic substitution reaction a large electron transfer takes place between the aromatic

24) H. H. Greenwood, ibid., **48**, 677 (1952).
25) F. H. Burkitt, C. A. Coulson and H. C. Longuet-Higgins, ibid., **47**, 553 (1951).
26) C. M. Moser, *J. Chem. Soc.*, **1953**, 1073.
27) S. Nagakura, This Bulletin, **25**, 164 (1952).
28) Y. Kurita and M. Kubo, ibid., **24**, 13 (1951).
29) S. Nagakura and T. Hosoya, ibid., **25**, 179 (1952).

30) The authors wish to express their thanks to Dr Tsubomura for his kindness in giving them information on these values.
31) J. H. Merz and W. A. Waters, *J. Chem. Soc.*, **1949**, 2427.

TABLE I. FREE VALENCY VALUES CALCULATED WITH VARIOUS AROMATIC CATIONS

Parent molecule	Free valency			Orientation	
				Theoretical	Experimental
	o	*m*	*p*		
Toluene	0.502	0.454	0.697	$p > o > m$	$p > o > m$
Aniline	0.494	0.395	0.495	$p > o > m$	$p > o > m$
Phenol	0.497	0.431	0.622	$p > o > m$	$p > o > m$
Chlorobenzene	0.472	0.405	0.488	$p > o > m$	$p > o > m$
Nitrobenzene	0.694	0.884	0.472	$m > o > p$	$m > o > p$
	o	*m*	*p*		
Styrene	0.502	0.407	0.518	$\beta > \alpha > p > o > m$	β
	α	β			
	0.517	1.055			
	α	β			
Naphthalene	0.545	0.447		$\alpha > \beta$	$\alpha > \beta$
	2	3	4		
Biphenyl	0.500	0.409	0.523	$4 > 2 > 3$	$4 > 2 > 3$
	1	2	3		
Phenanthrene	0.376	0.06	0.541	$9 > 4 > 3 > 1 > 2$	9
	4	9			
	0.768	0.814			

The experimental results given in this table are taken from the following references:

C. K. Ingold, "Structure and Mechanism in Organic Chemistry", G. Bell and Sons, Ltd., London (1953).

F. Bell, J. Kenyon and P. H. Robinson, *J. Chem. Soc.*, **1926**, 1239.

G. M. Badger, "The Structures and Reactions of the Aromatic Compounds", Cambridge University Press, London (1954).

TABLE II. FREE VALENCY VALUES CALCULATED WITH VARIOUS AROMATIC MOLECULES

Molecule	Free valency					Orientation	
						Theoretical	Experimental
	o	*m*	*p*				
Toluene	0.412	0.398	0.402			$o > p > m$	$o > p > m$
Aniline	0.433	0.396	0.415			$o > p > m$	—
Phenol	0.400	0.387	0.396			$o > p > m$	$o > p > m$
Chlorobenzene	0.420	0.389	0.409			$o > p > m$	$o > p > m$
Nitrobenzene	0.444	0.428	0.472			$p > o > m$	$p > o > m$
	o	*m*	*p*	α	β		
Benzaldehyde	0.438	0.396	0.457	0.870[a]	—	$\alpha > p > o > m$	—
Styrene	0.448	0.396	0.412	0.412	0.821	$\beta > o > \alpha = p > m$	β
	2	3	4				
Biphenyl	0.437	0.396	0.412			$2 > 4 > 3$	$4 > 2 > 3$

The experimental results given in this table are taken from the following references:

D. H. Hey and G. H. Williams, *Discussions Faraday Soc.*, **14**, 216 (1953).

J. I. G. Gadogan, D. H. Hey and G. H. Williams, *J. Chem. Soc.*, **1954**, 794.

O. Simamura and T. Migita, This Bulletin, **27**, 228 (1954).

O. Simamura and T. Inukai, ibid., **28**, 444 (1955).

T. Suehiro, *J. Chem. Soc. Japan, Pure Chem. Sec.* (*Nippon Kagaku Zasshi*), **72**, 301 (1951). (The experimental result on phenol referred to above is taken from this paper which is concerned with anisole).

a) This value was evaluated under the assumption that the π bond order for the C=O bond may be obtained with the aid of the same equation as for the C=C bond.

TABLE III. FREE VALENCY VALUES CALCULATED WITH NITROBENZENE AND CHLOROBENZENE ANIONS

Parent molecules	Free valency			Orientation	
				Theoretical	Experimental[a)]
	o	*m*	*p*		
Nitrobenzene	0.436	0.427	0.448	$p > o > m$	$p > o > m$
Chlorobenzene	0.669	0.648	0.409	$o > m > p$	$o > m > p$

The experimental results given in this table are taken from the following reference:
J. F. Bunnett and R. E. Zahler, *Chem. Revs.*, **49**, 273 (1951).

a) The orientation rules for nitrobenzene and chlorobenzene were deduced from the experimental results on dinitrobenzene and chloronitrobenzene, respectively, because it is difficult to replace a hydrogen atom of benzene directly by nucleophilic reagents such as Cl^- and OH^-.

TABLE IV. THE RELATIVE RATES OF RADICAL SUBSTITUTIONS IN *o*-, *m*- AND *p*-POSITIONS OF NITROBENZENE AND BENZOIC ACID

Molecule	Radical	Relative rate (%)		
		o	*m*	*p*
Nitrobenzene	OH[a)]	35.5	29.0	35.5
Nitrobenzene	C_6H_5[b)]	43.1	7.50	49.4
Benzoic acid	OH[c)]	40.0	40.0	20.0
Benzoic acid	OH[d)]	29.4	11.8	58.9
Benzoic acid ester	C_6H_5[e)]	44.1	8.30	47.5

a) H. Loebl, G. Stein and J. Weiss, *J. Chem. Soc.*, **1950**, 2704.
b) D. H. Hey and G. H. Williams, *Discussions Faraday Soc.*, **14**, 216 (1953).
c) H. G. C. Bates, M. G. Evans and N. Uri, *Nature*, **166**, 869 (1950).
d) H. Loebl, G. Stein and J. Weiss, *J. Chem. Soc.*, **1951**, 405.
e) O. Simamura, T. Inukai and T. Migita, unpublished data.

molecule and the reagent, and consequently the orientation in the substitution can be determined by free valency values of the aromatic cation, neutral molecule and anion for the electrophilic, radical and nucleophilic substitutions, respectively.

Finally it may be necessary to add a note on the reaction between the OH radical and the aromatic molecule. According to the measurement by Robertson[32], the ionization potential of the OH radical is determined as 13.75 eV. This means that the energy of its unpaired electron orbital is fairly low and a large electron transfer from the aromatic molecule may be expected for this radical as well as for the electrophilic reagent. From this it is inferred that the orientation rule for this radical becomes somewhat similar to that for the electrophilic reagent. In this respect, it seems interesting that in the radical substitution of nitrobenzene and of benzoic acid, the ratio of *m*-derivative to *o*- or *p*-derivative is conspicuously greater for the hydroxyl radical than for the phenyl radical (cf. Table IV). One of possible explanations for this is presumably that the hydroxyl radical partly possesses the characteristic of the electrophilic reagent.

32) A. G. B. Robertson, *Trans. Faraday Soc.*, **48**, 228 (1952).

Summary

The mechanism of the aromatic substitution was studied on the basis of the energy level diagrams determined for both the aromatic molecule and the reagent. From the consideration of the relative heights of the highest occupied and lowest vacant orbitals of the former to those of the latter, it was deduced that a large electron transfer occurs at some stage of the reaction from the aromatic molecule towards the reagent for the electrophilic substitution and in the reverse direction for the nucleophilic substitution.

In connection with this electron transfer mechanism, it was expected that the orientation rule observed with the aromatic substitution can be explained by free valency values of the aromatic cation,

neutral molecule and anion for the electrophilic, radical and nucleophilic substitutions respectively. It was shown that this expectation is fully satisfied for various aromatic substitutions.

The authors wish to express their sincere thanks to Professor K. Higasi and Professor O. Simamura for their kind advice. Their thanks are also due to Assistant Professor H. Baba and Mr. Y. Mizuno for their helpful discussion.

The Institute for Solid State Physics
The University of Tokyo
Komaba-cho, Meguro-ku, Tokyo

*The Crystal Structure of Bis(succinonitrilo)copper(I) Nitrate**

By Yukio KINOSHITA, Ikuo MATSUBARA and Yoshihiko SAITO**

(Received January 25, 1959)

It is well known that cuprous ion plays an important role in the dyeing of polyacrylonitrile fibers with anionic dyes; cuprous ion is readily absorbed by the fibers which then acquire an almost unlimited affinity for anionic dyes, which ordinarily can not be applied to this class of fibers.

Blaker et al.[1] suggested that the high affinity of cuprous ion for polyacrylonitrile is due to the inherent capability of nitrile groups in the fibers to absorb cuprous ion through formation of complexes analogous to those described by Morgan[2] for simple nitriles. These complexes, which may act as positive sites for fixation of dye anions, are considered to be of the type,

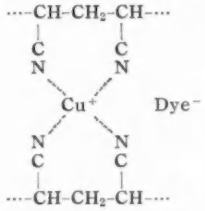

To verify this hypothesis, Rath et al.[3] have prepared similar complexes from nitriles of aliphatic dibasic acids. It would be of interest to determine the crystal structures of these compounds, since they would shed light on the mechanism of the dyeing.

The crystal structure of bis(succinonitrilo) copper (I) nitrate, $[Cu(NC{-}CH_2{-}CH_2{-}CN)_2]NO_3$, has been determined as a part of a program to establish the configurations of these complexes. Furthermore, the infrared spectrum of this complex has been investigated in relation to the crystal structure.

Experimental

Bis(succinonitrilo)copper(I) nitrate was prepared according to the directions of Morgan[2] by dissolving silver nitrate into succinonitrile at 60°C and adding an excess of copper powder. After black spongy silver was deposited, the mixture was filtered while warm and the filtrate was extracted with a mixture of ether and alcohol. On cooling, the clear extract deposited colorless crystals. This compound shows no definite melting point.

Anal. Found: C, 33.24; H, 2.99; N, 24.85; Cu, 22.12. Calcd. for $C_8H_8N_5O_3Cu$: C, 33.63; H, 2.82; N, 24.51; Cu, 22.24%.

Rotation and Weissenberg photograph showed the crystal to be monoclinic with

$a=11.62\pm0.03$Å, $b=5.31\pm0.01$Å, $c=9.53\pm0.03$Å, $\beta=98.8°\pm0.2°$.

Systematically absent reflections were $(h0l)$ for h odd, which indicated space groups $P2/a$ or Pa. The statistical method of Howells, Phillips and Rogers[4], when applied to the $h0l$ data, indicated the presence of a center of symmetry, which enabled us to adopt the space group $P2/a$ for the crystal. The density, determined by floatation, was found to be 1.634 g./cc., while

* Presented in part at the Symposium on the Chemistry of Complex Compounds, Tokyo, November 16, 1958.
** Institute of Polytechnics, Osaka City University, Kita-ku, Osaka.

1) R. H. Blaker, S. M. Katz, J. F. Laucius, W. R. Remington and H. E. Schroeder, *Discussions Faraday Soc.*, No. **16**, 210 (1954).
2) H. H. Morgan, *J. Chem. Soc.*, **123**, 2901 (1923).
3) H. Rath, H. Rehm, H. Rummler and E. Specht, *Melliand Textilber.*, **38**, 431, 538 (1957).
4) E. R. Howells, D. C. Phillips and D. Rogers, *Acta Cryst.*, **3**, 210 (1950).

that calculated assuming two formula units per cell was 1.633 g./cc.

Intensity data were obtained by visual estimation of *a*-, *b*- and *c*-axis zero-layer Weissenberg photographs taken with Cu $K\alpha$ radiation. A multiple-film technique was used and the intensity was corrected for geometrical and polarization factors. The final set of data consisted of 122 ($h\,0\,l$), 66 ($h\,k\,0$) and 54 ($0\,k\,l$) terms of measurable amplitudes. Absorption corrections were not made, but errors were minimized by selecting small and as well-formed crystals as were available.

The infrared absorption spectra of bis(succinonitrilo)copper(I) nitrate and succinonitrile in the wavelength region from 2 to 15 microns were obtained with a Perkin-Elmer model 21 spectrophotometer (with NaCl optics).

Structure Determination

Space group $P2/a$ contains fourfold general point positions. Since the unit cell contains only two formula units, the copper atom and the nitrate ion must lie either on a twofold symmetry axis or on a center of symmetry. The latter can be excluded since a tetrahedral coordination of a cuprous ion and trigonal configuration of a nitrate ion are to be expected. The copper atom and the central nitrogen atom(N_1) of the nitrate ion, therefore, must lie on twofold axes. The Patterson function was computed for the *b*-axis projection, which could be solved without difficulty, because of the occurrence of the copper atoms on special positions. Approximate *x*- and *z*-coordinates of all the lighter atoms were obtained at once.

A Fourier synthesis of the electron density projected along the *b*-axis was computed and this enabled all the *x*- and *z*-coordinates to be fixed. The Patterson function for the *a*- and *c*-axis projection could be solved successfully by trial

TABLE I. FINAL ATOMIC COORDINATES

Atom	x/a	y/b	z/c
Cu	0.250	−0.110	0.000
O_1	0.250	−0.359	0.500
O_2	0.155	−0.015	0.487
N_1	0.250	−0.123	0.500
N_2	0.340	0.108	0.143
N_3	0.153	−0.331	0.108
C_1	0.385	0.247	0.225
C_2	0.455	0.427	0.330
C_3	0.028	−0.607	0.262
C_4	0.100	−0.450	0.175

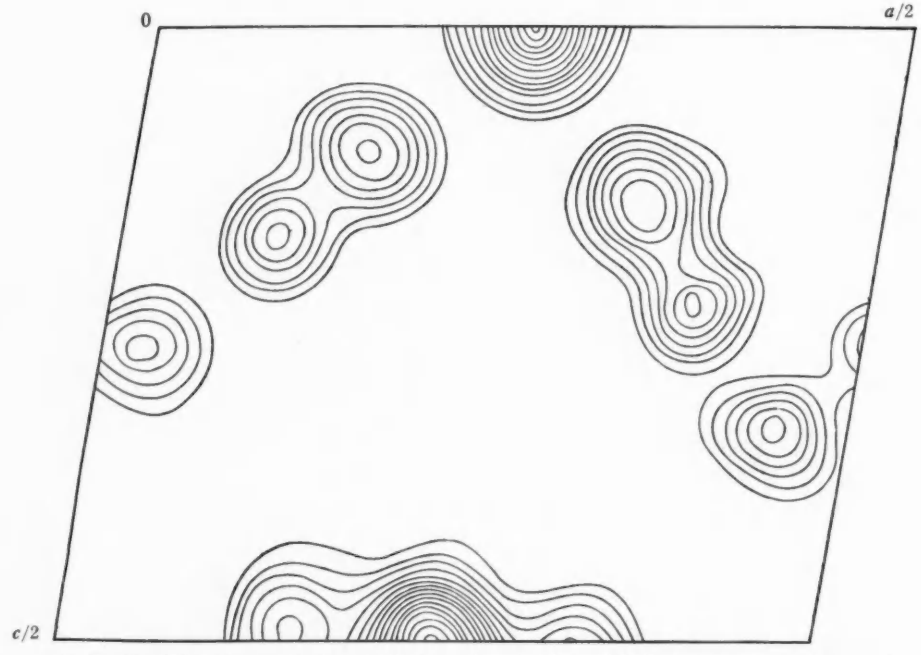

Fig. 1. Final Fourier projection of electron density along [0 1 0]. Contours are drawn at intervals of 3 eÅ^{-2} for copper and those for other atoms are at intervals of 1 eÅ^{-2}, the lowest being 2 eÅ^{-2}.

TABLE II. COMPARISON OF OBSERVED AND CALCULATED STRUCTURE FACTORS

Index	$F_o/4$	$F_c/4$	Index	$F_o/4$	$F_c/4$	Index	$F_o/4$	$F_c/4$
200	15.7	−15.8	601	6.1	− 5.6	40$\bar{1}$	2.6	+ 3.7
400	3.7	+ 3.5	602	7.3	− 6.9	40$\bar{2}$	17.5	+17.1
600	6.1	− 4.7	603	5.0	− 3.9	40$\bar{3}$	13.5	+14.2
800	9.8	+ 8.7	604	7.2	− 6.3	40$\bar{4}$	10.6	+ 9.6
1000	6.7	− 7.4	605	10.0	− 8.8	40$\bar{5}$	5.3	+ 4.4
1200	2.9	+ 3.2	606	6.1	− 5.1	40$\bar{6}$	7.0	+ 6.1
1400	2.6	− 2.3	607	<1.2	+ 0.2	40$\bar{7}$	4.8	+ 3.8
			608	1.1	− 1.5	40$\bar{8}$	8.1	+ 6.9
010	5.1	+ 5.6	609	2.2	− 1.7	40$\bar{9}$	2.4	+ 2.2
020	7.3	+ 7.4	6010	1.5	− 1.4	40$\bar{1}\bar{0}$	<1.1	+ 1.2
030	<0.9	+ 0.6				40$\bar{1}\bar{1}$	<0.9	+ 0.9
040	7.1	− 6.2	801	5.1	+ 4.3	40$\bar{1}\bar{2}$	1.2	+ 1.7
050	2.6	− 2.1	802	6.8	+ 6.0			
060	1.4	− 1.4	803	2.4	+ 1.8	60$\bar{1}$	4.0	− 5.4
			804	5.6	+ 5.1	60$\bar{2}$	7.2	− 6.5
001	7.2	+ 8.5	805	<1.2	− 0.2	60$\bar{3}$	13.9	−12.7
002	10.3	+11.0	806	2.3	+ 3.0	60$\bar{4}$	12.6	−10.9
003	6.4	− 6.7	807	2.6	+ 2.5	60$\bar{5}$	4.4	− 5.6
004	13.1	+14.3	808	2.4	+ 3.0	60$\bar{6}$	6.7	− 5.1
005	1.2	− 0.6	809	0.6	+ 0.4	60$\bar{7}$	4.4	− 4.5
006	12.0	+11.5				60$\bar{8}$	1.2	− 0.7
007	3.6	+ 2.5	1001	1.7	− 1.8	60$\bar{9}$	<1.2	− 1.1
008	7.2	+ 7.2	1002	6.8	− 5.7	60$\bar{1}\bar{0}$	1.8	− 2.1
009	2.9	+ 2.2	1003	2.4	− 1.5	60$\bar{1}\bar{1}$	0.8	− 1.5
0010	2.5	+ 2.6	1004	2.3	− 2.6			
0011	<0.9	+ 0.5	1005	<1.1	+ 0.8	80$\bar{1}$	4.7	+ 4.3
0012	1.8	+ 2.1	1006	1.9	− 2.0	80$\bar{2}$	7.1	+ 6.2
			1007	1.2	− 0.6	80$\bar{3}$	<1.1	+ 1.5
201	7.6	− 7.0				80$\bar{4}$	10.1	+ 8.7
202	26.9	−28.7	1201	1.6	+ 1.3	80$\bar{5}$	9.7	+ 7.9
203	3.4	− 3.9	1202	2.9	+ 3.5	80$\bar{6}$	3.4	+ 2.9
204	10.4	− 9.8	1203	<1.0	+ 0.4	80$\bar{7}$	1.2	− 0.8
205	5.1	− 5.0	1204	1.2	+ 1.5	80$\bar{8}$	2.0	+ 2.1
206	7.1	− 6.4	1205	1.3	+ 0.9	80$\bar{9}$	1.1	+ 1.8
207	3.9	− 3.2				80$\bar{1}\bar{0}$	1.8	+ 1.8
208	6.1	− 4.9	1401	1.4	− 1.6	80$\bar{1}\bar{1}$	1.4	+ 1.7
209	<1.2	− 1.3	1402	<0.5	− 0.4			
2010	<1.0	− 1.3				100$\bar{1}$	2.1	− 1.5
2011	0.8	− 1.3	20$\bar{1}$	11.2	−10.1	100$\bar{2}$	6.5	− 6.2
			20$\bar{2}$	24.7	−24.7	100$\bar{3}$	2.9	− 2.2
401	0.7	+ 1.9	20$\bar{3}$	6.5	+ 5.8	100$\bar{4}$	2.7	− 3.3
402	8.6	+ 7.5	20$\bar{4}$	11.2	−11.5	100$\bar{5}$	<1.2	+ 1.0
403	18.0	+16.8	205	2.1	− 1.9	100$\bar{6}$	4.1	− 4.9
404	14.8	+13.3	206	11.8	−11.6	100$\bar{7}$	1.1	− 1.9
405	5.7	+ 4.9	207	4.0	− 3.1	100$\bar{8}$	2.0	− 2.3
406	6.0	+ 4.4	208	6.0	− 6.5	100$\bar{9}$	1.7	− 1.0
407	4.8	+ 3.8	209	3.4	− 2.3	100$\bar{1}\bar{0}$	1.9	− 2.0
408	<1.2	+ 0.5	20$\bar{1}\bar{0}$	5.7	− 5.4			
409	<1.1	+ 0.9	20$\bar{1}\bar{1}$	<0.9	+ 0.1			
4010	2.5	+ 2.0	20$\bar{1}\bar{2}$	<0.6	− 0.1			
4011	1.3	+ 1.7						

TABLE II. (continued)

Index	$F_o/4$	$F_c/4$	Index	$F_o/4$	$F_c/4$	Index	$F_o/4$	$F_c/4$
$120\bar{1}$	2.3	+ 2.6	710	6.5	− 6.4	021	4.1	− 3.9
$120\bar{2}$	3.9	+ 4.3	720	4.0	− 3.7	022	5.2	+ 4.9
$120\bar{3}$	<1.1	− 0.9	730	7.5	− 8.2	023	1.7	− 0.8
$120\bar{4}$	1.1	+ 1.8	740	<1.2	+ 0.5	024	3.6	+ 2.6
$120\bar{5}$	<1.1	+ 0.2	750	<1.0	+ 0.8	025	<0.9	− 0.8
$120\bar{6}$	1.9	+ 2.8	760	<0.5	+ 1.3	026	5.8	+ 5.2
1207	2.4	+ 1.8				027	2.1	+ 0.8
$120\bar{8}$	2.5	+ 3.1	810	4.1	+ 4.0	028	<1.1	+ 0.3
			820	<1.2	− 0.4	029	<1.0	− 1.2
$140\bar{1}$	<0.8	− 0.2	830	1.8	− 1.2	0210	<0.9	+ 0.2
$140\bar{2}$	0.8	− 0.8	840	1.2	− 2.2	0211	<0.6	+ 0.4
$140\bar{3}$	1.6	− 1.4	850	1.3	− 1.5			
$140\bar{4}$	1.0	− 1.8				031	6.9	− 6.2
$140\bar{5}$	<0.6	− 0.9	910	3.5	+ 3.0	032	<0.8	+ 0.7
$140\bar{6}$	<0.4	− 1.4	920	3.8	+ 4.1	033	4.7	− 5.1
			930	1.2	+ 1.6	034	1.4	− 0.4
110	11.7	+10.7	940	1.6	+ 2.0	035	5.7	− 5.7
120	4.6	+ 4.4	950	0.8	− 1.1	036	2.6	− 2.4
130	8.5	+ 8.2				037	3.4	− 2.6
140	3.4	+ 3.1	1010	3.4	− 3.9	038	<1.0	+ 0.4
150	2.2	− 1.9	1020	1.3	− 1.4	039	<0.9	− 0.8
160	1.4	− 1.2	1030	<1.2	− 0.4	0310	<0.7	+ 0.1
			1040	2.4	+ 2.6			
210	19.2	−20.4	1050	0.5	+ 1.0	041	4.8	− 5.3
220	<0.8	− 0.3				042	4.8	− 4.1
230	2.4	+ 1.6	1110	2.9	− 3.5	043	4.4	− 3.9
240	5.0	+ 5.0	1120	<1.2	− 0.9	044	2.6	− 2.1
250	4.2	+ 4.1	1130	<1.1	− 1.3	045	<1.1	− 1.3
260	<1.0	− 0.2	1140	0.8	− 0.9	046	3.6	− 2.5
						047	2.4	− 3.1
310	15.0	−14.6	1210	2.7	+ 2.8	048	2.7	− 2.3
320	7.9	− 8.3	1220	1.1	+ 0.8	049	1.0	− 0.8
330	6.2	− 6.6	1230	0.9	− 0.3			
340	1.7	− 1.5	1240	<0.4	− 1.4	051	4.0	− 4.7
350	1.7	+ 1.3				052	3.7	− 2.9
360	<1.0	+ 1.0	1310	1.0	+ 1.3	053	1.5	− 1.7
			1320	0.9	+ 1.1	054	<1.0	− 0.3
410	4.4	+ 3.0	1330	1.1	+ 1.2	055	1.7	− 2.2
420	1.2	+ 1.1				056	1.5	− 1.5
430	3.5	− 3.9	1410	<0.7	− 0.2	057	1.8	− 1.9
440	5.9	− 6.9	1420	<0.6	− 0.2	058	<0.6	− 1.1
450	1.7	− 1.8						
460	0.9	− 1.0	011	4.2	+ 4.0	061	1.3	− 1.2
			012	20.9	+20.8	062	<0.8	+ 0.8
510	6.0	+ 6.0	013	<0.6	+ 0.8	063	1.2	− 1.4
520	12.5	+13.5	014	10.5	+ 9.1	064	<0.7	− 0.7
530	2.9	+ 3.9	015	5.3	+ 4.0	065	1.0	− 1.4
540	2.2	+ 1.7	016	7.7	+ 6.4			
550	1.2	− 1.3	017	4.2	+ 3.0			
560	<1.1	− 1.7	018	5.3	+ 4.5			
			019	1.8	+ 1.2			
610	1.3	− 1.0	0110	2.1	+ 1.8			
620	<1.0	+ 0.4	0111	<0.8	+ 0.1			
630	3.9	+ 4.9	0112	<0.3	+ 0.4			
640	3.0	+ 2.9						
650	1.6	+ 2.0						
660	<0.7	+ 1.1						

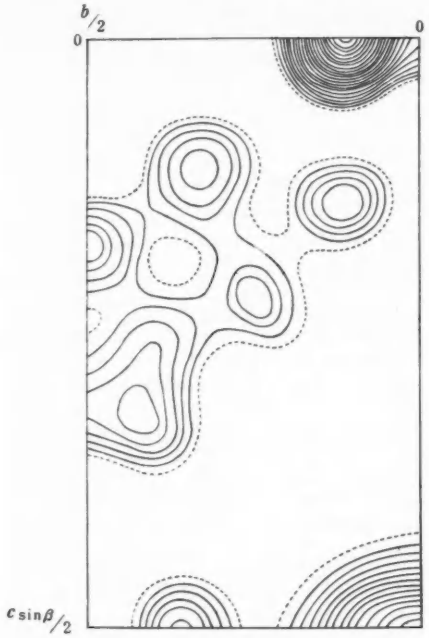

Fig. 2. Final Fourier projection of electron density along [1 0 0]. Contours are drawn at intervals of 2 eÅ^{-2} for copper and nitrate group except O_1. Those for other atoms are at intervals of 1 eÅ^{-2}, the lowest being 2 eÅ^{-2} (broken).

studies with models having suitable interatomic distances and bond angles. Approximate y-coordinates of all the atoms were thus obtained. Fourier projections of the electron density along [1 0 0] and [0 0 1] were then computed. Fourier refinements were repeated as usual. The final projections along [0 1 0] and [1 0 0] are shown in Figs. 1 and 2, respectively.

The final set of parameters is listed in Table I. This gave the reliability index $R=\Sigma||F_o|-|F_c||/\Sigma|F_o|$ of 0.124, 0.106 and 0.134 for $(h\,0\,l)$, $(h\,k\,0)$ and $(0\,k\,l)$, respectively. A mean isotropic temperature factor with B=4.0 Å^2 was found to be satisfactory for the three equatorial zones. Observed and calculated structure factors are shown in Table II.

Calculation of the structure factors as well as that of the electron density was carried out with Remington Rand UNIVAC 120 electronic computer quite effectively.

Description of the Structure

The interatomic distances and the bond angles calculated on the basis of the above parameter values are given in Table III. Calculation of the standard deviation of atomic coordinates by Cruickshank's

TABLE III. INTERATOMIC DISTANCES AND BOND ANGLES

Cu—N_2	1.96 Å	$\angle CuN_2C_1$	175°
Cu—N_3	2.02	$\angle CuN_3C_4$	177
C_1—N_2	1.14	$\angle N_2C_1C_2$	175
C_4—N_3	1.14	$\angle N_3C_4C_3$	180
C_1—C_2	1.53	$\angle C_1C_2C_3$	113
C_3—C_4	1.52	$\angle C_4C_3C_2$	107
C_2—C_3	1.49	$\angle O_1N_1O_2$	118
N_1—O_1	1.25	$\angle O_2N_1O_{2'}$	125
N_1—O_2	1.23		

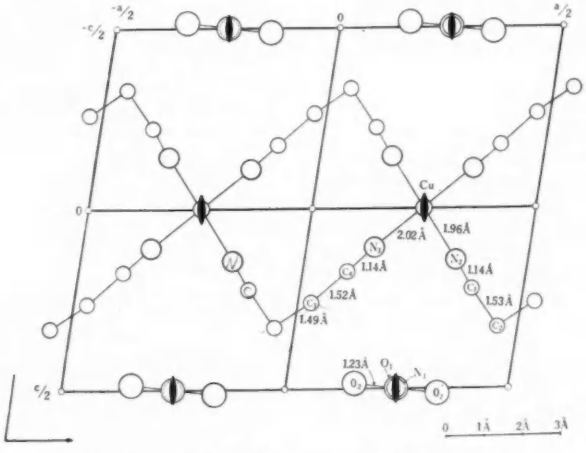

Fig. 3. Projection of the structure along [0 1 0].

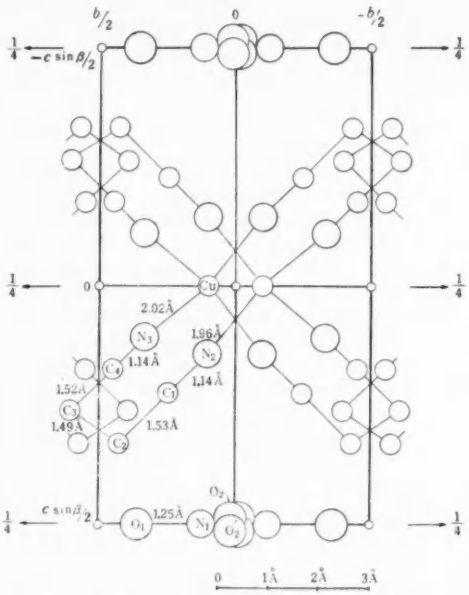

Fig. 4. Projection of the structure along [1 0 0].

method[5] for each projection gives 0.025Å for the resolved carbon and nitrogen atoms. This suggests a standard deviation of about ±0.04 Å in the Cu-N bond length determination.

The projections of the structure of bis-(succinonitrilo)copper (I) nitrate along [0 1 0] and [1 0 0] are shown in Figs. 3 and 4, respectively.

It is evident from the figures that the structure consists of nitrate ions and a polymeric chain of the composition,

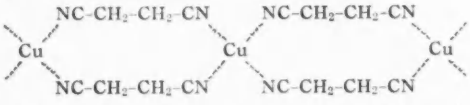

which runs parallel to the *a*-axis. A copper atom is surrounded tetrahedrally by four nitrogen atoms with Cu–N distances of 1.96 and 2.02 Å. A succinonitrile molecule in the complex takes a *gauche* configuration with respect to the central C_2–C_3 bond, the azimuthal angle of internal rotation being 127° with the *trans* position taken as the origin. The observed C–N distance of 1.14 Å is, within the limits of error, close to the value expected for triple C–N bond length. The N–C–C bond as well as the Cu–N–C bond is found to be approximately linear. It is possible accordingly that the bond character in the C–N group may be expressed as C≡N.

The nitrate ion exists on a twofold symmetry axis. The shape and size of the ion is as listed in Table III. These data are in good agreement with those obtained for other crystals.

Infrared Spectrum as Related to the Configuration of the Ligand Molecule

The vibrational spectrum of the free succinonitrile molecule was investigated by Fitzgerald and Janz[6], who concluded that this molecule exists as an equilibrium mixture of two rotational isomers, *trans* and *gauche*, the latter being the more stable configuration. Nakagawa and Tokumaru[7] also studied the vibrational spectrum of this substance and reached a similar conclusion. In considering the infrared spectrum of the complex compound it was first assumed that the interaction forces between ligand molecules are so small that the main features of the spectrum may be explained from consideration of an isolated succinonitrile molecule. The infrared spectra of bis-(succinonitrilo)copper(I) nitrate and free succinonitrile are shown in Fig. 5. In Table IV are listed the vibrational frequencies and the assignments for the infrared absorption bands of these substances in the region 1300~700 cm^{-1}. In fact, all the main bands of the complex in this region may be assigned to the vibrations of the

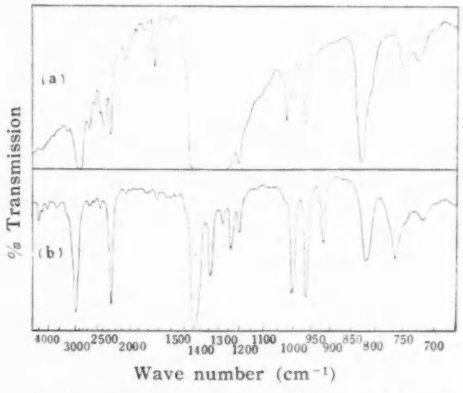

Fig. 5. Infrared spectra of (a) complex and (b) free succinonitrile.

5) D. W. J. Cruickshank, *Acta Cryst.*, **2**, 65 (1949).

6) W. E. Fitzgerald and G. J. Janz, *J. Molec. Spectroscopy*, **1**, 49 (1957).

7) I. Nakagawa, Private communication.

TABLE IV. INFRARED BANDS OF COMPLEX AND FREE SUCCINONITRILE

Wave numbers in cm^{-1}

Free[a]	Complex[b]	Assignments[c]			
1335	?	*gauche*	CH_2	wag	B
1271	—	*trans*	CH_2	wag	B_u
1231	1242	*gauche*	CH_2	wag	A
1198	1202	*gauche*	CH_2	twist	A
1020	1021	*gauche*	C-C	stretch	A
1001	1010	*gauche*	C-CN	stretch	B
962	965	*gauche*	CH_2	rock	A
917	—	*trans*	C-C	stretch	B_u
818	825	*gauche*	CH_2	rock	B
813	813	*gauche*	C-CN	stretch	A
761	—	*trans*	CH_2	rock	A_u

a) Solid film
b) In Nujol
c) Based on Nakagawa and Tokumaru's results

gauche configuration of succinonitrile, which is in complete agreement with the X-ray results.

The spectral features in the nitrile absorption region show strong evidence of tetrahedral coordination of the nitrile groups to the copper sp^3 orbitals; the complex compound shows two intense bands with peaks at 2278 cm^{-1} and 2381 cm^{-1}, instead of the one at 2257 cm^{-1} corresponding to the C≡N stretching vibration of the free succinonitrile. These two bands are certainly to be assigned to the C≡N stretching modes characteristic to the tetrahedral configuration of the complex compound, although the vibrational shifts towards higher frequencies with respect to the free nitrile may require further considerations.

The intense bands at 830 cm^{-1} and near 1380 cm^{-1} and a weak band at 749 cm^{-1} are assigned to the vibrations of the nitrate ion. A weak band at 1042 cm^{-1} may correspond to an infrared inactive frequency for the nitrate ion which is considered to become active because of the breakdown of the selection rule in the crystalline field.

Summary

The crystal structure of bis(succinonitrilo)copper(I) nitrate has been determined by two dimensional Fourier method. It is monoclinic $P2/a$ with two formula units in a cell of dimensions: $a=11.62\pm0.03$ Å, $b=5.31\pm0.01$ Å, $c=9.53\pm0.03$ Å and $\beta=98.8°\pm0.2°$. The crystal consists of nitrate ions and polymeric chains of the following composition:

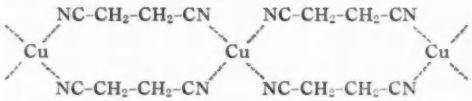

These chains run parallel to the a-axis. A succinonitrile molecule takes a *gauche* form with respect to the central C_2–C_3 bond. A copper atom is surrounded tetrahedrally by four nitrogen atoms with Cu–N distances of 1.96 and 2.02 Å. These facts are in close agreement with infrared spectral observations.

All the atoms in the group Cu–N–C–C lie almost on a straight line. This fact and the observed C–N distance of 1.14 Å suggest that the bond character in the C–N group may essentially be expressed as C≡N.

The authors wish to express their hearty thanks to Dr. K. Hoshino and Dr. K. Kato of the Central Research Laboratories of Toyo Rayon Co., Ltd. for their kind encouragement in the course of this study. They also wish to thank Mr. K. Yoshida of Toyo Rayon Co., Ltd. for carrying out the mechanical computations.

Central Research Laboratories
Toyo Rayon Co., Ltd.
Otsu, Shiga

Electron Diffraction Investigation on the Molecular Structure of n-Butane

By Kôzo KUCHITSU

(Received December, 27, 1958)

The structural parameters of normal hydrocarbons have not yet been thoroghly studied[1], except the simplest ones, methane[2] and ethane[3-5], though there are many investigations on their halogen derivatives[6]. The results which have so far been obtained, except the above two, are on propane by Pauling and Brockway[7], C–C=1.54±0.02A, and ∠C–C–C=111.5°±3°, and on *n*-butane by Wierl[8], C–C=1.51± 0.05A. As the technique has since been developed, more accurate results are expected to be given in the determination of the C–C distances and the C–C–C valence angles. Furthermore, the position of hydrogen atoms may be located with considerable accuracy, because these molecules do not include heavier atoms than carbon. Accordingly, it seems worth while to investigate the structure of *n*-butane.

Various spectroscopic and thermodynamic studies have shown that rotational isomers exist in the normal paraffins higher than propane[6]. As for *n*-butane, it was first noticed by Kohlrausch and Köppl[9] in their study of the Raman spectra. It was soon confirmed by Mizushima, Morino and Nakamura[10] in their study of the Raman spectra in the liquid and solid. They found that two forms exist in the liquid whereas only the *trans* form remains in the solid. The energy difference between the isomers was measured by Szasz and his co-workers in the liquid phase[11,12]. They obtained from the measurement of the temperature dependence of the Raman intensity the value of 770±90 cal./mol.[11], or 760±100 cal./mol.[12] (the *trans* form being the more stable). This result is in good agreement with the value of 800 cal./mol. which was estimated by Pitzer[13] from the entropy of *n*-butane[14] and used in the studies of the thermodynamic functions of hydrocarbons. Thus the rotational isomerism seems to be well established in the liquid phase, but no experimental evidence concerning the energy difference in the vapor is so far available[12]. While it seems probable that the magnitude is nearly the same as in the liquid because of the nonpolar nature of the molecule, the infrared spectrum of the vapor of *n*-butane was interpreted by Gates[15] in terms of a single form. However, as pointed out by Axford and Rank[16], his interpretation seems to rest on a rather insecure foundation and a further study on this point will make the situation clear. In the present study it is confirmed that two isomers exist, the *trans* and the *gauche* forms, in the vapor of *n*-butane, the energy difference being nearly equal to that in the liquid.

Experimental

The electron diffraction instrument used in this study was designed by Morino, Kimura and Iwasaki[17]. The details of the apparatus and procedure were reported previously[18-20]. Diffraction photographs were taken through an r^3-sector

1) M. H. Jellinek, "Physical Chemistry of Hydrocarbons," Vol. I, Chap. 2, Academic Press Inc., New York (1950).
2) G. Herzberg, "Infrared and Raman Spectra of Polyatomic Molecules", D. Van Nostrand Co., Inc., New York (1945).
3) G. E. Hansen and D. M. Dennison, *J. Chem. Phys.*, **20**, 313 (1952).
4) K. Hedberg and V. Schomaker, *J. Am. Chem. Soc.*, **73**, 1482 (1951).
5) A. Almenningen and O. Bastiansen, *Acta Chem. Scand.*, **9**, 815 (1955).
6) S. Mizushima, "Structure of Molecules snd Internal Rotation", Academic Press Inc., New York (1954).
7) L. Pauling and L. O. Brockway, *J. Am. Chem. Soc.*, **59**, 1223 (1937).
8) R. Wierl, *Ann. Physik*, **13**, 453 (1932).
9) K. W. F. Kohlrausch and F. Köppl, *Z. phys. Chem.*, **B26**, 209 (1934).
10) S. Mizushima, Y. Morino and S. Nakamura, *Sci. Papers Inst. Phys. Chem. Research (Tokyo)*, **37**, 205 (1940).
11) G. J. Szasz, N. Sheppard and D. H. Rank, *J. Chem. Phys.*, **16**, 704 (1948).
12) N. Sheppard and G. J. Szasz, ibid., **17**, 86 (1949).
13) K. S. Pitzer, ibid., **5**, 473 (1937).
14) K. S. Pitzer, ibid., **8**, 711 (1940); *J. Am. Chem. Soc.*, **63**, 2413 (1941).
15) D. M. Gates, *J. Chem. Phys.*, **17**, 393 (1949).
16) D. W. E. Axford and D. H. Rank, ibid., **18**, 51 (1950).
17) Y. Morino, M. Kimura and M. Iwasaki, The Sixth Annual Meeting of the Chemical Society of Japan (1953).
18) T. Ino, *J. Phys. Soc. Japan*, **8**, 92 (1953).
19) Y. Morino and K. Kuchitsu, *J. Chem. Phys.*, **28**, 175 (1958).
20) Y. Morino, K. Kuchitsu and E. Hirota, "Electron Diffraction by Gas", Maruzen Co., Tokyo (1957).

(in the case of the shorter camera length, 11.8 cm.) or an r^2-sector (in the case of the longer camera length, 27.9 cm.). The sectors were carefully cut to fit the proper shape within a hundredth of a millimeter[21]. They were mounted on a ball-bearing race and rotated rapidly during the exposure. In taking the diffraction photographs particular care was taken in regard to the constancy of the electron wavelength, the reducing of the extraneous scattering, and a good localization of the sample vapor.

The electron beam was focused to a spot of about 0.1 mm. in diameter. The fluctuation or the drift of the accelerating voltage was regulated within 0.1%. The wavelength of the beam was determined to be about 0.0556Å by a transmission pattern of gold foil. In order to reduce the extraneous scattering, a beam stopper of a shape similar to that described by Brockway[22] or Bastiansen[23] was mounted at the center of the sector[21]. The effect of the stopper on reducing the extraneous background was clearly seen on the photometer trace; the blank line of the photometer curve was nearly on the same level as the center line screened by the stopper, illustrating the fact that the extraneous background was not significant. Further evidence was given by a "blank test"[24] (taking photographs under the same condition as the experiment but without a sample jet), or by the "shadow test"[24] (taking photographs with the sample jet through a non-rotating sector) showing that there was no appreciable extraneous scattering caused by the main beam, nor by the scattering on the edge of the sector, of the slit, and of the nozzle aperture.

A "Research Grade" sample of *n*-butane of Phillips Petroleum Company was kindly furnished by Mr. T. Takatani of the Hitachi Central Research Laboratory. The sample (gas at room temperature) was introduced into a glass container of about 1 liter and the pressure was kept at about 20 mmHg. A liquid air trap was placed just over the nozzle to prevent the sample from diffusing through the camera. The flowing rate of the sample gas was carefully controlled, and diffraction photographs were taken with a long exposure time (a few minutes)[23,25]. A set of three photographs of different exposures were taken successively and developed at one time in the same bath. Two of the better photographs among them were used for the density-intensity calibration.

The photographs were scanned by a Riken B-type recording microphotometer of Nagoya University to measure the optical density as a function of the radius[18]. The photographic plate was rotated rapidly about the center of the pattern while being scanned by the photometer.

The measurement of the photometer curves was carried out with a Riken two-dimensional comparator in the interval of $\Delta q = 0.5$. Optical densities thus measured were converted into relative intensities either by Karles' method[26] or by Bartell's method[27] by using the set of two density curves. The resulting intensity curves were averaged respectively for each set. The agreement between the calibration curves obtained by either method was satisfactory. The curves obtained in both procedures were used in the analysis described below.

The averaged intensity curve was multiplied by $q^{1/2}$ to accentuate the molecular oscillations, and a smooth background line I_B was drawn through the curve. After a few steps of redrawing of the line, a reasonable background which satisfies Karles' criterion[24,26], that is, no fluctuation (0.0 through 0.7Å) and non-negativeness of the baseline of the radial distribution curve was obtained. The corresponding molecular intensity curve $qM(q)$ was readily calculated by using the following equation[26]:

$$qM(q) = q(I/I_B - 1) \tag{1}$$

The above procedures were repeated one by one for the three sets of plates taken with the shorter camera length, and finally five molecular intensity curves shown in Fig. 1 were obtained: two from the curves calibrated by Karles' procedure, two by Bartell's procedure, and one for which the density is nearly linear so that the same molecular intensity curve was obtained by both calibrations. The average deviations of the peak positions and intensities, listed in Table I,

TABLE I. AVERAGE DEVIATIONS OF THE PEAK POSITIONS AND INTENSITIES FOR FIVE OBSERVED MOLECULAR INTENSITY CURVES

Peak		Peak position[a]		Peak intensity[b]	
Max.	Min.	Average	Average dev.	Average	Average dev.
3		18.18	0.08	1.37	0.06
	3	23.02	0.06	−0.22	0.04
4		28.18	0.06	1.12	0.06
	4	35.07	0.04	−2.95	0.14
5		41.08	0.02	3.05	0.18
	5	50.19	0.07	−1.70	0.08
6		56.55	0.04	2.10	0.10
	6	61.31	0.05	−1.28	0.05
7		67.84	0.06	0.80	0.04
	7	75.14	0.09	−0.79	0.03
8		80.92	0.14	1.08	0.02
	8	87.60	0.16	−0.93	0.04
9		95.03	0.14	0.89	0.04
Average		—	0.08	—	0.07

a) in q-unit.
b) in absolute unit.

21) S. Shibata, Symposium on the Diffraction of X-ray and Electrons (1955).
22) L. O. Brockway and L. S. Bartell, *Rev. Sci. Instr.*, **25**, 569 (1954).
23) O. Bastiansen, O. Hassel and E. Risberg, *Acta Chem. Scand.*, **9**, 232 (1955).
24) I. L. Karle and J. Karle, *J. Chem. Phys.*, **18**, 963 (1950).
25) O. Bastiansen, L. Hedberg, and K. Hedberg, ibid., **27**, 1311 (1957).
26) J. Karle and I. L. Karle., ibid., **18**, 957 (1950).
27) L. S. Bartell and L. O. Brockway, *J. Appl. Phys.*, **24**, 656 (1957).

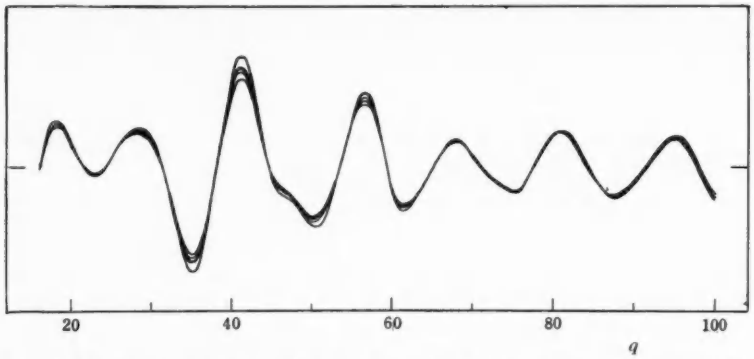

Fig. 1. Experimental molecular intensity curves for *n*-butane. Five experimental intensity curves are given in the same coordinate. The maximum average deviations among these intensities (near $q=40$) amounts to about 6%.

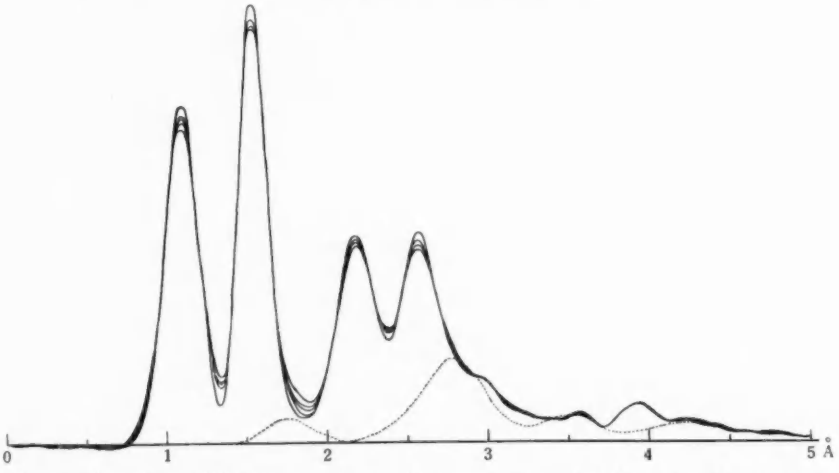

Fig. 2. Experimental RD curves. The RD curves computed from the five experimental intensity curves (Fig. 1) are illustrated in the same scale. The average deviations at the larger peaks are 1~2%. The dotted line denotes a minor contribution from the atomic pairs including hydrogen computed by use of a self-consistent model (see text). It is seen that the curves are non-negative everywhere within the experimental uncertainty.

are important measures for estimating the experimental errors of the structure analysis.

Analysis of the Radial Distribution Curve

Procedure.—Modified radial distribution curves[28] (they will be abbreviated as RD curves) were calculated from the molecular intensity curves, changing the Fourier integral into summation[29,30],

$$f(r)=\sum_{q=1}^{100} qM_c(q)\sin(\pi qr/10)\exp(-b\pi^2q^2/100) \quad (2)$$

where $qM_c(q)$ is the observed molecular intensity corrected for the non-nuclear scattering. Since the experimental intensity extends to $q=100$, a constant b was chosen to be 0.002333 to make the summation converge rapidly.

The summation was performed by the use of a punched-card machine[29]. The detail of the computation was given elsewhere[31]. Near the end of the study, a

28) Y. Morino and E. Hirota, *J. Chem. Phys.*, **28**, 185 (1958).
29) P. A. Shaffer, V. Schomaker and L. Pauling, ibid., **14**, 648, 659 (1946).
30) T. Ino, *J. Phys. Soc. Japan*, **12**, 495 (1957).
31) Y. Morino and K. Kuchitsu, *X-Rays*, **8**, 37 (1954).

TABLE II. SELF-CONSISTENT ANALYSIS FOR THE STRUCTURE (in Å unit)

Atomic pair	A		B		C	
	Distance	Mean amplitude	Distance	Mean amplitude	Distance	Mean amplitude
C-H	1.090	0.078	1.092	0.0830	1.092	0.0823
C-C	1.540	0.050	1.540	0.0534	1.539	0.0530
C-H (nonbonded)	2.163	0.110	2.178	0.1075	2.179	0.1005
C-C (nonbonded)	2.515	0.070	2.552	0.0739	2.553	0.0726
C-C (*gauche*)	2.949	0.160	(3.047)[a]	(0.160)[a]	3.12	0.125
C-C (*trans*)	3.876	0.070	3.906	0.0749	3.914	0.065

A: The model assumed at the first stage.
B: Result of the first analysis.
C: Result of the second analysis.
a) The *gauche* distance and its mean amplitude could not be measured accurately in the first analysis. Therefore, the values in brackets were used as the basis of the second analysis. The distance was calculated by using the result of the first analysis and the assumption that the azimuthal angle was 60°.

parametron digital computor became available at Department of Physics of the University of Tokyo. Some of the calculations were carried out by the use of this machine[32].

The RD curves thus obtained for the five molecular intensity curves are illustrated in Fig. 2; the agreement is satisfactory. A detailed analysis was made for the averaged RD curve.

Care was taken in the analysis in regard to the following points: a) the structure assumed in the analysis, b) a correction for the non-nuclear scattering, and c) minor contributions of hydrogen terms.

a) In the calculation of the RD curve, the inner region ($q=0\sim15$) of the molecular intensity curve was spliced by a theoretical intensity curve $qM_c(q)$ computed with an assumed model*. The model listed in the first column A of Table II was assumed at the first stage; in this model all angles were assumed to be tetrahedral and the mean amplitudes calculated theoretically (see section V) were used**. The result of the first analysis was used to calculate the second RD curve, and as shown in the second B and the last column C of the table the second-stage parameters were made self-consistent with the final result of the analysis.

TABLE III. SELF-CONSISTENT ANALYSIS FOR THE FRACTIONS OF THE ISOMERS

Series		A	B	C	D
I	*trans*	100%	65%	67%	65%
II	〃	0%	48%	57%	61%

Besides the assumptions on the structural parameters, assumptions had to be made for the rotational isomers, i.e., the configurations and the fractions of the isomers[19]. It was found that the shape of the RD curve beyond 2.3Å is sensitive to these assumptions, though they had no appreciable effect on the inner part of the RD curve. A method of analysis similar to that used by Iwasaki[33] was applied as follows. The process is shown in Table III. Theoretical curves were calculated first for 100% *trans* form (azimuthal angle 180°) (Series I), and for 100% *gauche* form (azimuthal angle assumed to be 60°) (Series II). The frame structure was based on the model C of Table II. The area under the *trans* C-C peak in the resulting RD curve was compared with the theoretical value and the fraction of the *trans* form was estimated from the ratio (IB and IIB). A theoretical curve of the mixture of two isomers in this fraction was then spliced to the experimental curve and the same analysis was carried out. This procedure was repeated until a self-consistent result for

32) Y. Morino, K. Kuchitsu and M. Shibuya, Symposium on Structural Chemistry, Kyoto, Japan, Oct. 1958.

* The contribution of the theoretical molecular intensity curve spliced in the inner region ($q=0\sim15$) to the RD curve is such a slowly fluctuating function that slight changes in the parameters have no essential influences on either the peak positions or the peak widths, though there may be considerable changes in the peak areas. Account was taken of this point for estimating the errors.

** The hydrogen atoms in the methyl groups were assumed to be at the staggered configuration in euqilibrium with respect to the hydrogen and carbon atoms in the methylene groups. See L. G. Smith, *J. Chem. Phys.*, **17**, 179 (1949), Refs. 4 and 5 for ethane, Ref. 50 for ethyl chloride, and K. S. Pitzer, ibid., **12**, 310 (1944), for propane.

33) M. Iwasaki, S. Nagase and R. Kojima, This Bulletin, **30**, 230 (1957).

the fraction of the isomers was obtained (C and D). Since both series gave nearly the same values, the fraction of the *trans* form was thus found to be 60~65% in this analysis. The area under the *gauche* peak in the final RD curve was found to be about 35~40% of the theoretical maximum value (that is, the area which could be expected if the *gauche* form only were present), also in agreement with this result.

In conclusion, the model used for calculating the final RD curve was made sufficiently self-consistent, so that the result of the following RD analysis is essentially free from any arbitrary assumptions.

b) A correction for the non-nuclear scattering was made by using the method of Bartell[34]. A minor correction term $\Delta M(q)$ was subtracted from the observed molecular intensity $qM(q)$ to obtain $qM_c(q)$. The function $\Delta M(q)$, which is defined as

$$\Delta M(q) = qM(q) - qM_c(q)$$
$$= \sum_{i,j}{}' (c_{ij}/r_{ij})(\mu_{ij}-1)\exp(-l^2_{ij}s^2/2)\sin sr_{ij} \quad (3)$$

where

$$\mu_{ij} = c_{ij}/c_{ij}$$
$$c_{ij} = (Z_i - f_i)(Z_j - f_j)/\sum[(Z_i - f_i)^2 + S_i]$$

and

$$c_{ij} = Z_i Z_j/(\sum Z_i^2 + Z_i)$$

was calculated theoretically on the base of an assumed model. As in the former case a), the structure first assumed was that listed in the first column of Table II; and then ΔM was calculated again by using the second column of the same table. The elastic scattering factors for carbon and hydrogen atoms, $f(s)$, were taken from the tables of Viervoll and Ögrim[35], McWeeny[36], and Berghuis[37]. For the inelastic scattering factor of carbon, $S_C(s)$, Bewilogua's function[38] was used; as pointed out in his paper, this function which is based on the Thomas-Fermi model is still a good approximation for carbon. The *S*-function for hydrogen, $S_H(s)$, is approximated by $S_H(s) = 1 - [f_H(s)]^2$ after the argument of Mott and Massey[39]. In order to make the magnitude of the ΔM-function smaller, the value Z_H in Eq. 3 was put equal to 1.25. It seems probable that uncertainties in these factors have a negligible effect on the final result as compared with the experimental errors.

c) As there are many non-equivalent C–C, C–H and H–H distances in *n*-butane, (twenty-seven in the *trans* form, and thirty-five in the *gauche* form), thorough analysis of all distances is obviously too

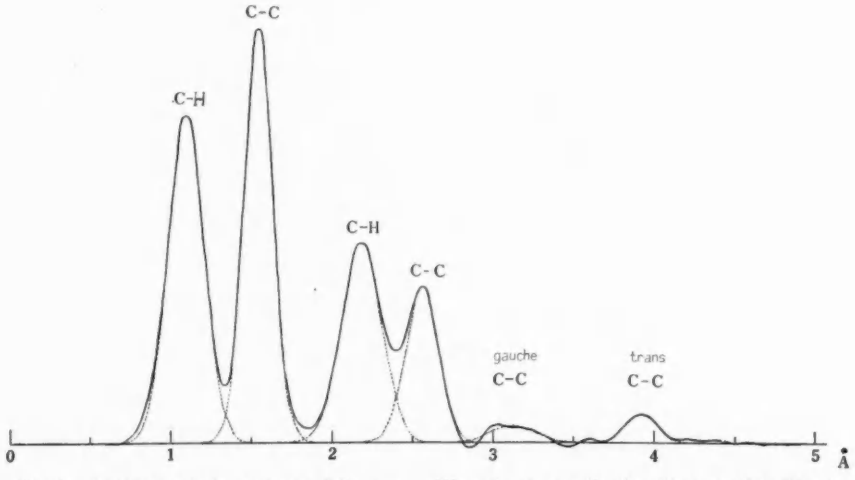

Fig. 3 Analysis of the average RD curve. The minor contribution illustrated in Fig. 2 is subtracted from the total curve. The dotted curves denote the best-fit Gaussian curves. The peaks represent (from left to right) the C–H, C–C, nonbonded C–H, nonbonded C–C, *gauche* C–C, and *trans* C–C distances, respectively.

34) L. S. Bartell, L. O. Brockway and R. H. Schwendeman, *J. Chem. Phys.*, **23**, 1854 (1955).
35) H. Viervoll and O. Ögrim, *Acta Cryst.*, **2**, 277 (1949).
36) R. McWeeny, ibid., **4**, 513 (1951).
37) J. Berghuis, et al., ibid., **8**, 478 (1955).
38) L. Bewilogua, *Physik. Z.*, **32**, 740 (1931).
39) N. F. Mott and H. S. W. Massey, "The Theory of Atomic Collisions", Oxford Univ. Press, London (1949).

complicated to be feasible. However, the structure of this molecule is principally determined by four main structure parameters, i.e., the C–H (average), C–C (average), C—H (average), and C—C distances. Since the contribution from these distances are exceedingly greater than that from the other distances, it is advantageous to subtract the minor contributions from the total RD, leaving the contributions from the principal parameters, which can then be analyzed uniquely. The minor contributions calculated by use of a self-consistent model are illustrated in Fig. 2 as a dotted line. The same procedure of obtaining such a self-consistent model as that discussed in a and b was undertaken. Tables II and III show that for the procedures a, b and c the model was simultaneously made self-consistent in two steps. The result is shown in Fig. 3.

Least-square Analysis of the Main Peak*.—The peak at 1.1Å in the RD curve (Fig. 3) corresponds to the C–H distance. The center of gravity which is equal to the mean distance was readily determined. The peak was found to be symmetrical with respect to the center, and accordingly, the curve could be fitted to a Gaussian function**.

The Gaussian function to be fitted is

$$y = y_0 \exp(-Hx^2), \quad x = r - r_g \tag{4}$$

where r_g is the center of gravity. By taking the logarithm of both sides, the following linear equation is obtained.

$$Y = q - pX \tag{5}$$

where

$$X = x^2, \quad Y = \log_{10} y, \quad p = H \log_{10} e$$
$$\text{and} \quad q = \log_{10} y_0 \tag{6}$$

About ten sets of the observed values X_i's and Y_i's were used to determine the parameter p, under the condition that

$$\sum_i (\mathrm{d}y_i)^2 = (\log_{10} e)^{-2} \sum_i y_i^2 (\mathrm{d}Y_i)^2 = \text{minimum} \tag{7}$$

Solving the equation for p,

$$p = \frac{[\sum y_i^2 X_i]\,[\sum y_i^2 Y_i] - [\sum y_i^2]\,[\sum y_i^2 X_i Y_i]}{[\sum y_i^2]\,[\sum y_i^2 X_i^2] - [\sum y_i^2 X_i]^2} \tag{8}$$

The parameter is related to the mean amplitude as

$$p = \log_{10} e/(4b + 2l^2) \tag{9}$$

and

$$l = (\log_{10} e/2p - 2b)^{1/2} \tag{10}$$

Since the standard error of the parameter p is given by

$$\sigma_p^2 = \frac{[\sum y_i^2]}{[\sum y_i^2]\,[\sum y_i^2 X_i^2] - [\sum y_i^2 X_i]^2} \cdot \frac{\sum (\mathrm{d}y_i)^2}{n-2} \tag{11}$$

the standard error of the parameter l is readily obtained as*

$$\sigma_l = -\frac{\log_{10} e}{4lp^2}\sigma_p \tag{12}$$

The second peak at 1.54Å corresponds to the C–C distance. Because of the separation of 0.45Å between the C–H and C–C distances, a similar least-square analysis could be made with no ambiguity. The peaks for the non-bonded C–H and C–C distances are in a slightly closer separation. However, they were resolved by using the left side of the C–H peak, and the same procedure was applied. The results are listed in Table IV.

In the region beyond 3Å, two peaks

TABLE IV. RESULT OF THE LEAST-SQUARE ANALYSIS OF THE MRD CURVE

	$r_g(1)$[a]	Apparent mean amplitude	Area[b]
C–H (average)	1.092	0.084_6	0.987
C–C (average)	1.539	0.054_0	0.994
C–H (average)	2.179	0.103_2	0.970
C–C	2.553	0.074_8	1.060
C–C *trans*	3.914	0.069_6	0.590[c]
∠C–C–H (average)	=110°40'[d]		
∠C–C–C	=112°6'		

a) in Å unit

b) the ratio with respect to the theoretical absolute value

c) to be regarded as the fraction of the *trans* isomer

d) the value derived from $r_g(1)$ by Eq. 24

* The least-square analysis of RD curve has been reported recently by Bastiansen and Cyvin (O. Bastiansen and S. J. Cyvin, *Acta Chem. Scand.*, **11**, 1789 (1957).). For a similar treatment of a $\sigma(r)$ curve, see the paper by Cruickshank et al. (D. W. J. Cruickshank and H. Viervoll, *Acta Chem. Scand.*, **3**, 560 (1949).).

** The middle points of the curve at various peak heights were constant to a third decimal place of an angstrom. Strictly speaking, an $f(r)$ peak is expressed as

$$f(r) = \frac{c(\pi H)^{1/2}}{2r_c}\exp(-Hx^2)(1 + ax + bx^2 + cx^3 + \cdots\cdots), \quad x = r - r_c$$

showing a slight distortion in trems of the parameters of anharmonicity and of the perpendicular amplitudes. However, the distortion is often so small that the curve can be interpreted as Gaussian. As will be shown later, the mean amplitude for $f(r)$ curve is almost the same as that for the probability distribution.

* The standard error is about 1%, being considerably smaller than the random errors estimated in section IV B.

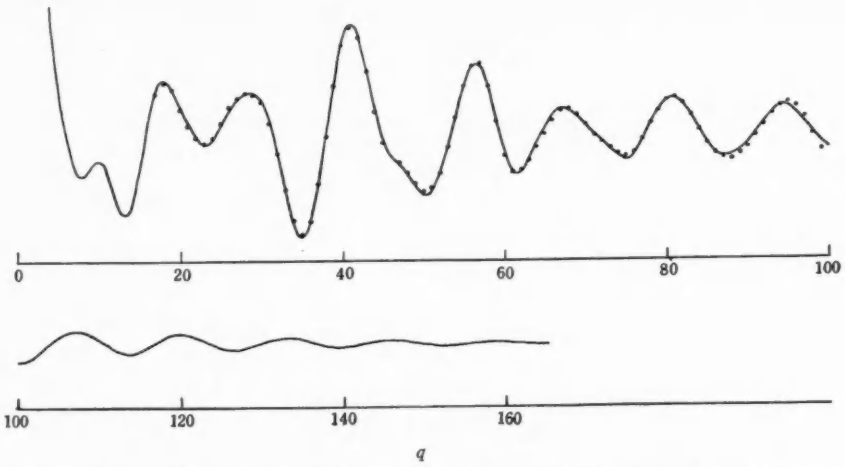

Fig. 4. Comparison of the observed and calculated molecular intensity curves. The solid line denotes the theoretical intensity calculated from the result of the MRD analysis (Table IV). The dots are the averaged experimental molecular intensity. These intensities fit within the experimental uncertainty illustrated in Fig. 1. The theoretical curve is extended beyond $q=100$, and is used in the UMRD analysis.
—— calculated ○ observed

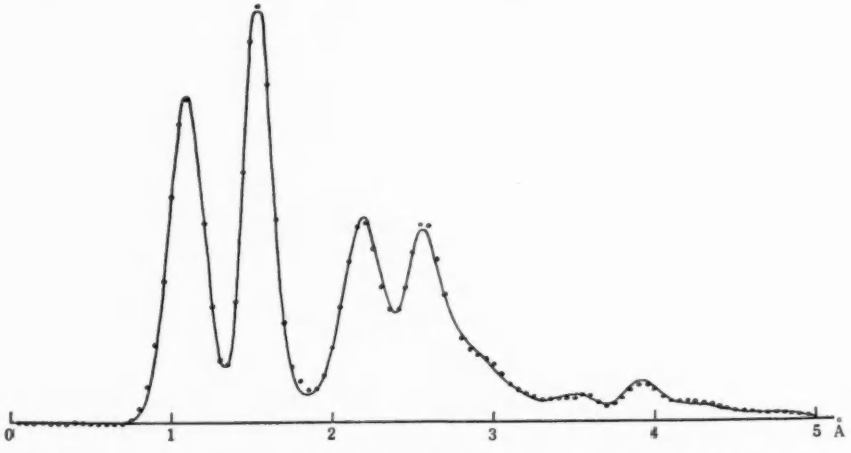

Fig. 5. Comparison of the observed and theoretical RD curves. The solid line represents the theoretical RD curve based on the result of the analysis assuming Gaussian distribution. The dots are the experimental MRD curve.
—— theoretical ○ observed (average)

appeared at 3.1Å and 3.9Å, corresponding to the *gauche* and the *trans* C–C distances, respectively. It affords a definite evidence for the rotational isomerism in this molecule. As the shape of the latter peak is practically Gaussian, the same procedure was applied, whereas only approximate values for the distance and its mean amplitude were estimated from the former peak. A theoretical intensity curve and an RD curve were calculated by the use of the result listed in Table IV. The agreement with the experimental curve is satisfactory, as shown in Figs. 4, 5 and Table V. The average index of resolution is about 99%.

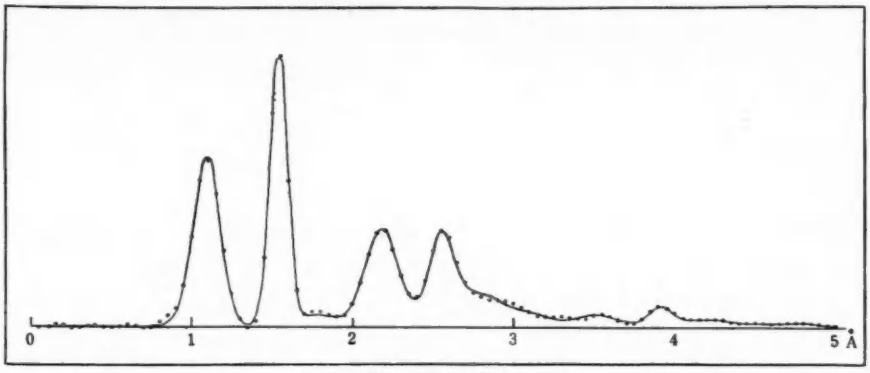

Fig. 6. Unmodified RD curve.
—— starting model (theoretical) ○ observed

TABLE V. COMPARISON OF THE OBSERVED AND THE CALCULATED INTENSITY CURVES

Max.	Min.	Peak position		Peak intensity	
		q_{calc}	q_{calc}/q_{obs}	I_{calc}	I_{obs}/I_{calc}
3		18.0	(0.990)	1.41	0.977
	3	23.1	1.004	−1.20	1.085
4		28.8	(1.022)	1.20	0.937
	4	34.9	0.995	−3.03	0.974
5		41.2	1.003	3.15	0.970
	5	50.0	0.996	−1.77	0.964
6		56.5	0.999	1.99	1.056
	6	61.4	1.001	−1.35	0.948
7		67.2	(0.991)	0.80	1.011
	7	75.3	1.002	−0.90	0.876
8		80.8	0.999	1.18	0.912
	8	87.2	0.996	−0.85	1.099
9		94.5	0.995	0.81	1.096
Average		—	0.998_8	—	0.993
Average Deviation		—	0.003	—	0.059

Unmodified Radial Distribution Curve.—By the same procedure as that described by Morino and Hirota[28], an unmodified radial distribution curve (UMRD), Eq. 13, was calculated for a further refinement of the analysis:

$$f(r)=\sum_{q=0}^{\infty}[w(q)qM_c(q)_{obs}+(1-w)qM_c(q)_{calc}]\times\sin\frac{\pi}{10}qr \qquad (13)$$

where $qM_c(q)_{obs}$ is the observed molecular intensity corrected for the non-nuclear scattering[34] and $qM_c(q)_{calc}$ is the calculated intensity based on the result of the analysis of the modified RD curve (Table IV and Fig. 4). The weight function $w(q)$ was so chosen that $w(q)\propto\exp[-c\Delta(q)^2]$, where $\Delta(q)$ is the amount of fluctuation among the observed intensity curves at a point q (Fig. 1), and c is a constant. The value $w(q)$ fluctuates somewhat irregularly with q between 100 and 80% for most of the experimental region ($q=17\sim95$), and is zero for the inner and outer parts. The UMRD curve is shown in Fig. 6. The analysis was carried out in the same way as that of the MRD curve (item 2). The results are given in Table VI and Fig. 6.

Estimation of the Errors in the Measurement of Interatomic Distances.—For the estimation of errors in the interatomic distances, sources of systematic errors in the scale factor and other errors in the observed RD curve must be considered. The main sources of systematic errors may be as follows.

a) The uncertainty in the scale-magnification ratio on the microphotometer trace, which is estimated to be about 0.1%.

b) The uncertainty in the camera length: it comes mainly from the difference between the position of the scattering center of the sample and that of the reference, and from the uncertainty in the position of the photographic plate. This error is about 0.1%.

c) The errors involved in the measurement of $L\lambda$: the product of the camera length L and the wavelength λ is determined by the measurement of the transmission pattern of gold foil. The standard error of the measurement is about 0.1%.

d) The drift of the wavelength: since a few minutes were required for exposure, the drift of the wavelength may be a cause of systematic error. In this experiment, however, the drift was controlled to within 0.05% by use of voltage stabilizers.

e) Errors in the determination of the

center in the photometric trace: they will cause error of less than 0.05%*. Assuming that these errors occur independently, a standard error in the scale factor is estimated to be about 0.2%.

f) A finite size of the light beam in the photometry: if the light beam has the rectangular shape of $a \times b$ on the photographic plate which is being measured (a being measured in the radial, and b in the perpendicular direction), the location of a halo of radius R on the plate suffers an inward shift of about $b^2/24R$. Since $a \times b = 0.1\,\text{mm.} \times 1\,\text{mm.}$ in this experiment, this shift has a uniform dependence on q, which is about 0.1% at $q=20$, and 0.01% at $q=60$. The correction was made for this effect though the magnitude is not important compared with other random errors.

For the standardization of the absolute scale factor, an analysis of carbon tetrachloride was made to check the apparatus and the method of analysis[19]. The C-Cl distance (the center of gravity of the $f(r)$ curve) was found to be 1.766Å, in good agreement with the results reported in the literature[34,40] within the experimental error.

Other errors were estimated from the variance of the results of the analyses for each of the five experimental RD curves, by using the standard statistical method on the assumption that this variance was caused by random errors. For the non-bonded peaks, possible sources of errors caused by the processes a, b and c stated in item 1 and the process of the decomposition of the composite peaks were also taken into account, the results of the above estimation are given in Table VI.

The Meaning of the Values Measured.— It is important to define clearly the meaning of the distances determined in this analysis, as pointed out by Bartell[41]. While the distance obtained above is the "center of gravity" or the "mean distance" of the $f(r)$ curve, it seems useful to correlate it to the $r_g(0)$ value, or the center of gravity of the probability distribution curve $P(r)$.

Including the anharmonicity in molecular vibrations[41] and the correction for the perpendicular amplitude, $P(r)$ may be expanded as (See f on page 756)

$$P(x) = (h/\pi)^{1/2} \exp(-hx^2) \times (1 + \alpha x + \beta x^2 + \gamma x^3 + \cdots\cdots) \tag{14}$$

where

$$x = r - r_e, \quad h = 1/2 < \Delta z^2 > \tag{15}$$

Then the mean value of the distance, $r_g(0)$, is expressed as

$$r_g(0) = \frac{\int_0^\infty r P(r)\,dr}{\int_0^\infty P(r)\,dr} = \frac{\int_{-\infty}^\infty (r_e + x) P(x)\,dx}{\int_{-\infty}^\infty P(x)\,dx}$$

$$= r_e + \alpha l^2 + \left(3\gamma - \frac{3}{2}\alpha\beta\right) l^4 + \cdots\cdots \tag{16}$$

where l^2 is the mean square amplitude, $< \Delta z^2 >$. On the other hand, the center of gravity of $f(r)$ is written by using the relation between $P(r)$ and $f(r)$,

$$f(r) = (\pi/16b)^{1/2} \int_{-\infty}^\infty [P(\rho)/\rho] \times \exp[-(r-\rho)^2/4b]\,d\rho \tag{17}$$

as

$$r_g(f) = \frac{\int_0^\infty r f(r)\,dr}{\int_0^\infty f(r)\,dr} = \frac{\int_0^\infty P(r)\,dr}{\int_0^\infty (P(r)/r)\,dr} \tag{18}$$

Therefore, it is equal to the center of gravity of the $P(r)/r$ curve, $r_g(1)$. By using Eq. 14, the difference between the above two is approximated by

$$r_g(0) - r_g(1) \cong \frac{l^2}{r_e} + \cdots\cdots \tag{19}$$

It amounts to a few thousandth of an angstrom; the second term is of the order of 10^{-5}Å. If a Morse-type potential function for the ground state of a diatomic molecule is assumed, as done by Bartell[41], the constants in Eq. 14 are in the following approximate relations,

$$\alpha = a, \quad \beta = 0, \quad \gamma = ah/3 \tag{20}$$

where a is a parameter of the Morse potential function, and Eqs. 16 and 19 agree with his expression (Eq. 4 of his paper). On the other hand, the center of gravity of the $rf(r)$ curve is given by

$$r_g(rf) = r_g(0) + 2b/r_g(1) \tag{21}$$

the difference being dependent on the damping factor b. The distance $r_g(0)$ can be obtained either from Eq. 19 or from 21. It is also obtained from the UMRD curve. The values of $r_g(0)$ obtained in this way are given in Table VI.

* The error due to an imperfect centering of the photographic plate during the scanning by the photometer is negligible, being of the order of a few ten thousandth of an angstrom, since the center was adjusted to within 5/100 mm. The error due to the deviation of the electron beam from the correct center of the sector during the exposure (which was within 5/100 mm.) is also negligible.

40) I. L. Karle and J. Karle, *J. Chem. Phys.* **17**, 1052 (1949).

41) L. S. Bartell, ibid., **23**, 1219 (1955).

TABLE VI. THE MEAN DISTANCES[a] AND ANGLES[b]

	MRD	UMRD	Standard error
C-H (average)	1.098	1.100	0.003
C-C (average)	1.540	1.539	0.003
C-H (nonbonded average)	2.182	2.181	0.005
C-C (nonbonded)	2.554	2.554	0.005
C-C (*gauche*)	3.12	3.13	0.02
C-C (*trans*)	3.913	3.911	0.009
∠C-C-H (average)	110°32′	110°22′	15′
∠C-C-C	112° 1′	112° 9′	9′

a) $r_g(0)$ in Å unit
b) the "mean angle" derived from $r_g(0)$ by Eq. 24

The mean square amplitude af a distance is defined by*

$$l^2(0)=\left[\int_0^\infty r^2P(r)\mathrm{d}r\right]\Big/\left[\int_0^\infty P(r)\mathrm{d}r\right]-[r_g(0)]^2 \tag{22}$$

whereas the mean square amplitude obtained from the radial distribution curve is

$$l^2(f)=\left[\int_0^\infty r^2f(r)\mathrm{d}r\right]\Big/\left[\int_0^\infty f(r)\mathrm{d}r\right]-[r_g(1)]^2 \tag{23}$$

A simple calculation using Eqs. 14 and 17 shows that the latter is equal to the mean square amplitude for the $P(r)/r$ curve, $l^2(1)$, plus $2b$, and the difference between $l^2(0)$ and $l^2(1)$ is only a minor correction as compared with the experimental error. (See f on page 756).

Determination of Valence Angles.—Following the above argument, the "mean angle" may be defined as the angle α derived by the following equation

$$\cos\alpha=(r_A^2+r_B^2-r_G^2)/(2r_Ar_B) \tag{24}$$

where r_A, r_B, and r_G are the mean values of the respective distances. The standard error of the angle is readily calculated to be

$$\sigma_\alpha=\left\{\left(\frac{1}{r_B}-\frac{\cos\alpha}{r_A}\right)^2\sigma_{r_A}^2+\left(\frac{1}{r_A}-\frac{\cos\alpha}{r_B}\right)^2\sigma_{r_B}^2+\left(\frac{r_G}{r_Ar_B}\right)^2\sigma_{r_G}^2\right\}^{1/2}\Big/\sin\alpha \tag{25}$$

The systematic error of the scale factor, 0.2%, is not included in σ_r's, because it has no effect on the angle. The result is given in Table VI.

Discussion Concerning the Longer Distances.—The *trans* C-C distance is calculated from the C-C distance $r_g(0)$ and the C-C-C angle assuming that the four carbon atoms are coplanar; it was found to be 3.926±0.003Å. On the other hand, the observed distance was 3.911±0.004Å*. The shortening, 0.015±0.005Å, can be interpreted as "significant", according to Cruickshank's definition[42]. It is likely that the shift is caused by a hindered rotation of the ethyl groups around the C-C axis taking the equilibrium position on the plane. The shift due to this effect was calculated theoretically by Karle and Hauptman[43]. It is calculated in a similar manner that the shift is 0.0120Å when the barrier V_0 is equal to 3.6 kcal./mol., and 0.0155Å when it is equal to 3.0 kcal./mol., in satisfactory agreement with the experimental shift. It is therefore inferred that the barrier height lies close to these values, in agreement with the value estimated by Pitzer, 3.6 kcal./mol.[14]

The azimuthal angle of the *gauche* form was calculated from the *gauche* C-C distance R_g(3.13±0.01Å) to be 67.5°±1.1°. The angle is thus nearly 60° as was usually assumed but possibly a little larger than that.

Estimation of Errors in the Mean Amplitude

The mean amplitudes listed in Table IV include both systematic and random errors. They were either corrected or estimated as shown in the following table.

A. Systematic errors
Experimental
a) effect of finite sample size: corrected,
b) multiple or extraneous scattering: negligible,
c) density-intensity calibration: estimated,
Theoretical
d) failure of Born approximation: corrected,
e) effect of the possible difference in length between non-equivalent bonds: estimated,
f) effect of perpendicular amplitude and of anharmonicity: negligible,
g) effect of series termination: negligible, (in the case of MRD)
B. Random errors*

* The definition corresponds to u_a used by A. Reitan (Ref. 53).

* The error of the scale factor is not included in this comparison.

42) D. W. J. Cruickshank, *Acta Cryst.*, **2**, 65 (1949).

43) J. Karle and H. Hauptman, *J. Chem. Phys.*, **18**, 875 (1950).

* Errors which could not be treated as systematic errors were simply regarded as random errors though they might not be purely random in a strict sense.

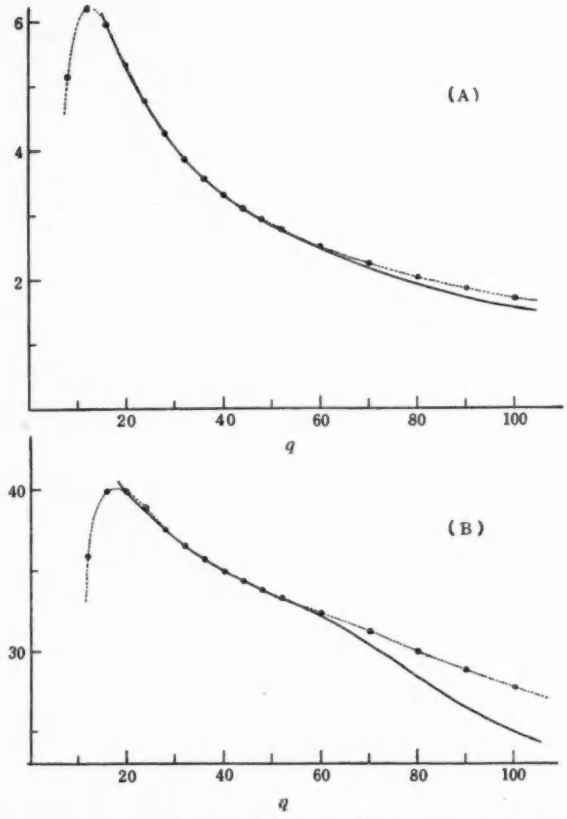

Fig. 7. Comparison of the background lines. Soild line: experimental; and dotted line: theoretical. The ordinate scales are adjusted in such a way that two curves coincide at $q=40$. (A) The background line obtained by use of an r^3-sector. (B) The curves shown in A are multiplied by $q^{1/2}$ to accentuate the difference; it amounts to about 10% at $q=100$.

Experimental: treated with a simple statistical method,
Computational: estimated.

These errors will be discussed as follows.

A. Systematic Errors.—*a) Effect of finite sample size.*—This effect was extensively studied by Karle[24], and also Harvey et al.[44] It is easily estimated if the distribution of the sample gas around the nozzle is known. The shape of the background line was found to be useful in this case for estimating the distribution. In Fig. 7 is shown a comparison of the observed background line with the calculated curve based upon the assumption that the diffracting molecules are located at an infinitesimal volume. The agreement is good in the inner region, whereas the deviation of the observed curve is clearly recognized beyond $q=60$. The nozzle used in this experiment is illustrated in Fig. 8. If this effect is attributed to the "screening" of the electrons at the nozzle edge, the distribution is estimated with the following simple assumptions:

1) The decrease in the observed background compared with the theoretical background is essentially caused by process in which a small fraction of the electrons scattered by the sample hit the wall of nozzle and do not reach the photographic plate (Fig. 8).

2) Since the beam diameter is much less than the nozzle aperture, a one-dimensional distribution of the sample gas, the area being normalized, is considered. Then the decrease is determined by the area of the shadowed region in Fig. 8.

44) R. B. Harvey, F. A. Keidel and S. H. Bauer, *J. Appl. Phys.*, **21**, 860 (1950).

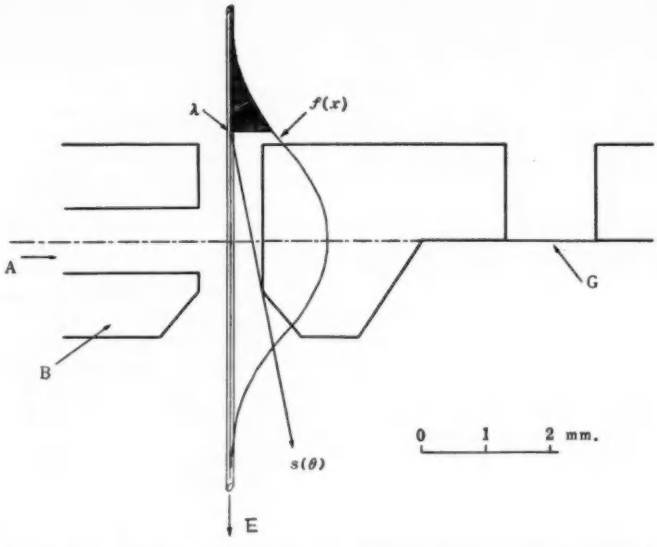

Fig. 8. "Screening effect" of the nozzle. An enlarged cross section of the drum-type nozzle is illustrated. A: gas inlet; B: nozzle body; E: electron beam (the cylinder represents a rough measure of the diameter); $f(x)$: normalized one-dimensional distribution of the gas; G: gold foil used as the reference. It is assumed that the electrons scattered at the point farther than the critical point $\lambda(\theta)$ (shaded region) in the direction of $s(\theta)$ are completely screened by the wall of the nozzle and do not reach the photographic plate, and that the scattered intensity undergoes a fractional decrease proportional to the shaded area.

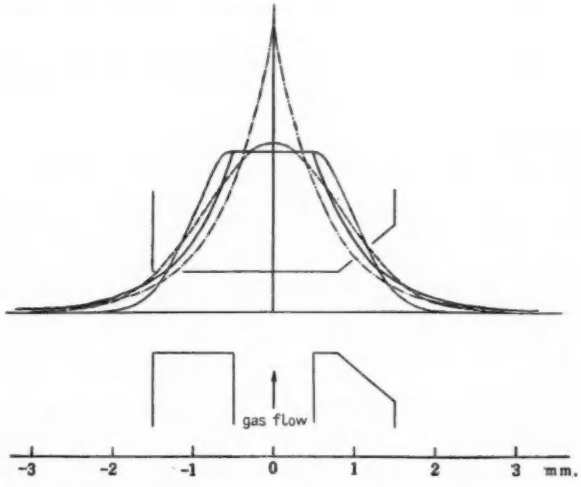

Fig. 9. Distribution functions of the gas spreading. It is assumed that they are symmetrical across the center of the nozzle inlet, and the areas are normalized. Solid line : flat and exponential; dotted line: flat and Gaussian; chain line: exponential; and broken line: Gaussian. It is seen that the distributions are all practically zero outside the nozzle.

3) The distribution is symmetrical across the center of the nozzle inlet.

In additon to these assumptions, the following simple analytical functions were assumed for the distribution, and parameters were determined to reproduce the experimental fractional decrease. The shapes of the distribution functions assumed are:

Exponential:

$$f(x)=\frac{1}{2}\rho\exp(-\rho|x|),\quad \rho=1.593 \tag{26}$$

Gaussian:

$$f(x)=(\sigma/\pi)^{1/2}\exp(-\sigma x^2),\quad \sigma=0.700 \tag{27}$$

Flat and exponential:

$$f(x)=c,\quad |x|\leq x_0,\quad c=0.45$$
$$f(x)=c\exp(-\alpha|x|),\ |x|>x_0,\ \alpha=1.636 \tag{28}$$

and Flat and Gaussian:

$$f(x)=c,\quad |x|\leq x_0,\quad c=0.45$$
$$f(x)=c\exp(-\beta x^2),\ |x|>x_0,\ \beta=2.103 \tag{29}$$

where x is the distance in millimeters measured from the center of the nozzle inlet, and $x_0=0.5$ mm. is the radius of the inlet. The distribution is illustrated in Fig. 9. It is seen that the density is practically zero outside the nozzle, though the localization is somewhat poorer than that of Karles' nozzle estimated in their paper[24].

The distribution function being assumed, the damping of the molecular intensity (a contribution of a particular atomic pair whose equilibrium distance is r) caused by the spreading of the sample is calculated by the following integration:

$$M=\int_{-\infty}^{\infty}M(s)f(x)\mathrm{d}x=\int_{-\infty}^{\infty}(\text{const.})\times\exp\left(-\frac{l^2}{2}s^2\right)\frac{\sin sr}{sr}f(x)\mathrm{d}x \tag{30}$$

where s is a function of the camera length L, which is the sum of L_0+x, L_0 being the camera length referred to the nozzle center. This may be expressed as:

$$s(x)=\frac{2\pi R}{\lambda}\frac{1}{(L_0+x)}\left[1-\frac{3}{8}\frac{R^2}{(L_0+x)^2}\right]$$
$$=\frac{2\pi R}{\lambda L_0}\left(1-\frac{3R^2}{8L_0^2}\right)\left(1-\gamma\frac{x}{L_0}\right) \tag{31}$$
$$=s_0\left(1-\gamma\frac{x}{L_0}\right)$$
$$\gamma=1-\frac{3R^2}{4L_0^2}\sim 1-7\times10^{-5}s_0^2 \tag{32}$$

where R is the radius on the photographic plate. Substituting Eq. 31 into 30 and remembering that $f(x)$ is assumed to be a symmetrical function of x, Eq. 30 is transformed into Eq. 33 giving the damping of the molecular intensity:

$$M/M_0=\int_{-\infty}^{\infty}f(x)\cos\alpha x\mathrm{d}x,\ \alpha=\gamma s_0 r/L_0 \tag{33}$$

where $M_0(s_0)$ refers to L_0 (the molecular intensity scattered by a point source).

TABLE VII. CORRECTION AND ESTIMATION OF ERRORS IN THE MEAN AMPLITUDES

		C–H_{av}	C–C_{av}	C–H_{av}	C–C	C–C_{trans}
Systematic errors (%)						
(a) Finite sample size	cor	+0.5	+2.1	+1.0	+3.0	+7.2
(b) Multiple or extraneous scattering	neg	—	—	—	—	—
(c) D-E calibration[a]	est	$<\pm3$	$<\pm5$	$<\pm4$	$<\pm3$	$<\pm3$
(d) Born approximation	cor	+2.3	—	+1.6	—	—
(e) Non-equivalent bonds	est	$<+0.2$	$<+1.6$	$<+0.4$		
(f) Perpendicular amplitude and anharmonicity	neg	—	—	—	—	—
(g) Series termination (in the case of MRD)	neg	—	+0.7	—	—	—
Random errors (%)	est	$\sim\pm4$	$\sim\pm3.5$	$\sim\pm4$	$\sim\pm8$	$\sim\pm7$
Total standard errors[b] (%)	est	$\sim\pm5$	$\sim\pm5$	$\sim\pm5$	$\sim\pm9$	$\sim\pm9$
Apparent mean amplitude (UMRD)		0.085_5	0.053_7	0.100_1	0.080_0	0.072_9
Corrected mean amplitude (A)		0.083_1	0.052_6	0.097_5	0.077_6	0.067_7
Standard error (A)		0.004	0.003	0.005	0.007	0.007

cor: corrected; est: estimated; neg: negligible

a) The meaning of the symbol $<\pm$ is that the sign may be positive or negative, but that the absolute value should not exceed the given figure.

b) The uncertainties involved in the corrections a and d are estimated to be $\pm70\%$ of the correction values.

On calculating the damping function (Eq. 33) analytically using Eq. 26 through 29 for $f(x)$*, it was found that all assumed distributions give nearly the same result, and it can be expressed in a good approximation in the form

$$M/M_0=\exp(-\varepsilon s^2) \tag{34}$$

An apparent increase in the mean amplitude is accordingly given by

$$(l+\Delta l)^2=l^2+2\varepsilon, \quad \Delta l\sim\varepsilon/l \tag{35}$$

The percentage correction for each interatomic distance is given in Table VII. It should be noted that the parameter ε is a function of r, and that the correction is greater for the longer distance, and for the harder distance (i.e., the distance which has a smaller mean amplitude), as already pointed out[24,44].

b) Effect of multiple or extraneous scattering.—This effect was considered to be negligible in view of the following argument.

1) No appreciable extraneous scattering was found to be present, as stated in the experiment part.

2) Care was taken in the experiment to reduce the sample pressure during the exposure[9]; the flow rate was sufficiently "slow" in the sense discussed by Harvey et at.[44] to avoid the multiple scattering.

3) The observed background line agrees well with the theoretical form, showing no appreciable multiple scattering present (Fig. 7).

4) The index of resolution is nearly unity, which affords another point of support.

5) It was shown by Karle[24] theoretically that even if a considerable amount of multiple scattering were present, it would raise the background uniformly and decrease the molecular intensity also in a uniform manner. Consequently it does not change the damping factor of the molecular term significantly.

c) Uncertainty in the density-intensity calibration curve.—This effect may be estimated in the following way. Suppose the calibration function $E(D)$, in which E and D denote the intensity and density, respectively, is obtained experimentally instead of the true function $E^0(D)$ which is unknown. Since the functions E^0 and E are both uniform functions of D, their ratio may be expanded as

$$E(D)/E^0(D)=c(1+\alpha D+\beta D^2+\cdots\cdots) \tag{36}$$

If the maximum or the minimum point of the intensity curve and the background intensity of the same point are denoted by E_1 and E_2 respectively, and the densities which correspond to E_1 and E_2 on the $D-E$ curve by D_1 and D_2, the fractional error R in the molecular intensity obtained from Eq. 1 is given by

$$\begin{aligned} R&=\left\{\frac{E_1^0(1+\alpha D_1+\beta D_1^2)}{E_2^0(1+\alpha D_2+\beta D_2^2)}-1\right\}\Big/\left\{\frac{E_1^0}{E_2^0}-1\right\} \\ &=1+\frac{E_1^0}{E_1^0-E_2^0}\{\alpha(D_1-D_2) \\ &\quad+(2\beta-\alpha^2)D_2(D_1-D_2)\} \end{aligned} \tag{37}$$

Since D is nearly proportional to E,

$$R\sim1+\alpha D_1+(2\beta-\alpha^2)D_1D_2 \tag{38}$$

On the other hand, the experimental measure of the uncertainty in the $D-E$ curve may be estimated 1) by the variance of the slope of the observed background lines, and 2) by the difference between the $D-E$ curve obtained by Karles' method and that obtained by Bartell's method using the same density curves.

It was found that the magnitude of the parameters α or β is about ±0.05. Since the maximum density in this experiment was about 0.8, the upper limit of the error in the molecular intensity was estimated to be 10%. Possible error in the mean amplitude caused by this effect is accordingly estimated for each distance by fitting roughly to an exponential function, and listed in Table VII.

d) Failure of Born approximation.—It is well known that the theoretical expression 4 for the scattering of electrons by molecules is derived by Born approximation, which is not always justified[39]. The failure of Born approximation was first pointed out by Schomaker and Glauber[45,46], and discussed by Hoerni and Ibers[47]. The effect on the mean amplitude, an apparent increase, was discussed by Bartell and

* For example, the use of Eq. 26 gives

$$M/M_0=\rho^2/(\alpha^2+\rho^2)$$

and the use of Eq. 27 gives

$$M/M_0=\exp[-\alpha^2/(4a)]$$

The latter formula corresponds to Eq. 13 of Karles' paper[24]. More strictly, the upper limit of the integral 30 should be the cut-off point, λ, shown in Fig. 8, which is a function of s. A detailed calculation shows, however, that the molecular term assumes an additional factor and a phase shift which are both of a negligible order of magnitude.

45) V. Schomaker and R. Glauber, *Nature*, **170**, 291 (1952).

46) R. Glauber and V. Schomaker, *Phys. Rev.*, **89**, 667 (1953).

47) J. A. Hoerni and J. A. Ibers, ibid., **91**, 1182 (1953).

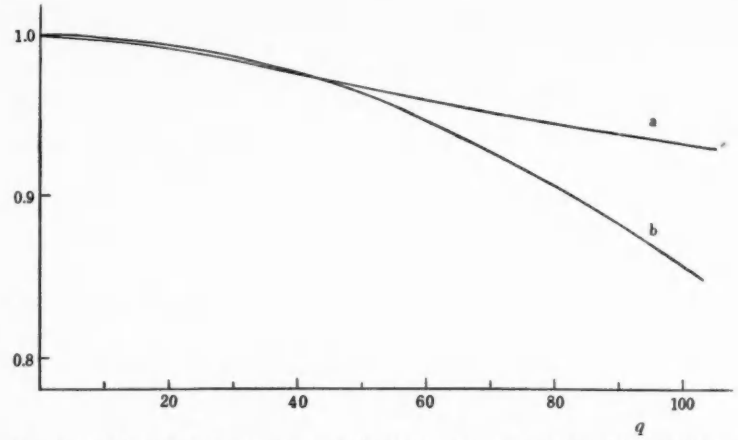

Fig. 10. Approximation of the phase shift $\cos \Delta\eta$ by an exponential function. a) $\cos \Delta\eta$ for the C–H pair: and b) $\exp(-\delta s^2/2)$ where $\delta = 3.096 \times 10^{-4}$. The deviation is about 7% at $q = 100$.

Brockway[48,34]. In the following a similar correction for this effect is carried out.

The expression is given by

$$sM(s) = \sum_{i,j}{}' (c_{ij}/r_{ij}) \exp\left(-\frac{l_{ij}^2}{2} s^2\right) \times \cos \Delta\eta_{ij} \sin s r_{ij} \quad (39)$$

$$\Delta\eta_{ij} = \eta_i(s) - \eta_j(s) \quad (40)$$

The C–H pairs are the only objects to be considered for this molecule, since the phase shift $\Delta\eta$ appears only for a pair of different atoms. The phase function $\eta(s)$ was calculated and tabulated by Ibers and Hoerni[49]. Since the values are based on the Thomas-Fermi model, they may naturally be a poor approximation for carbon and hydrogen. According to their argument[49], however, the phase shift $\Delta\eta$ is probably reliable, and in addition, the magnitude of η for hydrogen is very small. The Eq. 13 of their paper is available to convert the values to η for the accellerating voltage used in this experiment.

The damping function $\cos \Delta\eta_{C-H}$ was approximated by an exponential form, as discussed by Bartell,

$$\cos \Delta\eta_{C-H}(s) \sim \exp(-\delta s^2/2) \quad (41)$$

the value δ being derived numerically in the following average, taking the damping function (including the artificial temperature factor) as a weight $w(s)$

$$\int w(s) [\cos \Delta\eta - \exp(-\delta s^2/2)] \, ds = 0 \quad (42)$$

$$w(s) = \exp\left(-\frac{l^2_{C-H}}{2} s^2\right) \exp(-bs^2) \quad (43)$$

The value thus obtained is

$$\delta = 3.096 \times 10^{-4} \text{ Å}^2 \text{ for bonded C–H,}$$

and $\delta' = 3.431 \times 10^{-4}$ Å^2 for non-bonded C–H.

The maximum deviations of the exponential functions from the cosine functions were about 7% (Fig. 10). These deviations were further corrected by introducing a δM-function in a way similar to that discussed in the case of non-nuclear scattering[34],

$$\delta M(s) = M_{C-H}(s)\{1 - \cos \Delta\eta/\exp(-\delta s^2/2)\} + M'_{C-H}(s)\{1 - \cos \Delta\eta/\exp(-\delta' s^2/2)\} \quad (44)$$

The order of magnitude of this function is less than 1% of the molecular intensity, and therefore it barely contributes to the RD curve.

The percentage correction for this effect to the mean amplitude is given in Table VII.

e) Effect of the possible difference in the distances between non-equivalent bonds. — It should be noted that the C–H, C–H (non-bonded), and C–C distances observed are the average values of the two respective non-eqivalent distances, i.e., C–H (methyl) and C–H (methylene), and C–C (end) C–C (central). Should these distances differ slightly, as may be the case, observed mean amplitudes will show apparent increase.

This effect is readily treated as follows. Suppose there are two Gaussian peaks 1 and 2 (peak positions r_1 and r_2, and peak

48) L. S. Bartell and L. O. Brockway, *Nature*, **171**, 978 (1953).
49) J. A. Ibers and J. A. Hoerni, *Acta Cryst.*, **7**, 405 (1954).

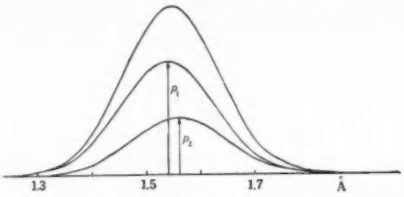

Fig. 11. A composite peak of non-equivalent C-C distances. The peak is slightly broader than each of the component peaks.

heights p_1 and p_2, respectively) close together (Fig. 11). Their mean amplitudes are assumed to be the same, l. The composite peak will then be given by

$$P=p_1\exp\{-H(r-r_1)^2\}+p_2\exp\{-H(r-r_2)^2\} \quad (45)$$
$$H=(2l^2+4b)^{-1}$$

If the origin of the distance r is chosen at the center of gravity, the composite peak is expresed as

$$P=\exp(-Hr^2)\,[\sum P_i\exp(2Hr_ir)] \quad (46)$$
$$P_i=p_i\exp(-Hr_i^2), \qquad i=1,2 \quad (47)$$

The term in the bracket being expanded,

$$\sum_{1,2} P_i\exp(2Hr_ir)=(P_1+P_2)+2H^2rp_1r_1(r_1^2-r_2^2)+2H^2r^2(P_1r_1^2+P_2r_2^2) \quad (48)$$

The second term is about a small percentage of the third term and does not affect the width. Therefore, the peak is expressed as a Gaussian function to a good approximation:

$$P=(P_1+P_2)\exp(-H'r^2) \quad (49)$$

where

$$H'=H-2H^2(P_1r_1^2+P_2r_2^2)/(P_1+P_2) \quad (50)$$

The coefficient H is related to l in Eq. 45, so that the apparent increase in l is calculated by Eq. 50.

The splittings of the distances are definitely too small to be detected in this experiment; the only available references seem to be the splitting of the C-H distances in ethyl chloride estimated in the microwave spectroscopy[50],

C-H(methyl) = 1.110Å

C-H(methylene) = 1.101Å

and the plausible values predicted by Glockler from the consideration of bond-energy data[51],

C-H(methyl) = 1.097Å

C-H(methylene) = 1.0985Å

C-C(end) = 1.559Å

C-C(central) = 1.564Å (in *n*-butane)

The maximum possible percentage apparent increases listed in Table VII are calculated by inserting in Eq. 50 the value:

r_1-r_2(C-H bonded) = 0.01Å

r_1-r_2(C-H non-bonded) = 0.02Å

and r_1-r_2(C-C bonded) = 0.02Å

It is seen that this effcet is possibly negligible.

f) The effect of perpendicular amplitude and of anharmonicity. — The probability distribution function of an interatomic distance including both parallel and perpendicular amplitudes was derived by Morino and Hirota[52]

$$P(r)=(h/\pi)^{1/2}\exp(-hx^2)\times(1+c_1x+c_3x^3+\cdots\cdots) \quad (51)$$

where

$$h=1/2<\Delta z^2>, \qquad x=r-r_e$$

and

$$c_1=(h/r_e)\,[<\Delta x^2>+<\Delta y^2>-6h(<\Delta z\Delta x>^2+<\Delta z\Delta y>^2)] \quad (52)$$
$$c_3=(4h^3/r_e)\,[<\Delta z\Delta x>^2+<\Delta z\Delta y>^2] \quad (53)$$

On the other hand, the following $P(r)$-function including anharmonic vibration was given by Bartell[41] and by Reitan[53].

$$P_{anh}(r)=(h/\pi)^{1/2}\exp(-hx^2)\times(1+a_1x+a_2x^2+a_3x^3+\cdots\cdots) \quad (54)$$

Since these effects introduce only slight modifications on the Gaussian distribution, the combined effect may be written in the first approximation,

$$P(x)=(h/\pi)^{1/2}\exp(-hx^2)(1+c_1x+c_3x^3)\times(1+a_1x+a_2x^2+a_3x^3) \quad (55)$$
$$=(h/\pi)^{1/2}\exp(-hx^2)\times(1+\alpha x+\beta x^2+\gamma x^3+\cdots\cdots) \quad (14)$$

The mean square amplitude for this distribution is readily calculated as

$$l^2(0)=<\Delta z^2>+\left(2\beta-\frac{3}{2}\alpha^2\right)(<\Delta z^2>)^2 \quad (56)$$

$l^2(0)$ can be obtained from $l^2(f)$ by the equation,

50) R. S. Wagner and B. P. Dailey, *J. Chem. Phys.*, **23**, 1355 (1955).
51) G. Glockler, ibid., **17**, 747 (1949).
52) Y. Morino and E. Hirota, ibid., **23**, 737 (1955).
53) A. Reitan, *Acta Chem. Scand.*, **12**, 131, 785 (1958).

$$l^2(0)=l^2(f)-2b+\left[\frac{1}{2}\alpha^2+\frac{3\alpha}{2r_e}-3\alpha\beta r_e+4\beta+4\beta^2r_e^2-\frac{1}{r_e^2}\right]l^4+\cdots\cdots \quad (57)$$

It is to be noted that a minor fractional correction is of the order of $l^2/2r_e^2$, which is less than 0.5%. Thus the effect of anharmonicity or the perpendicular amplitude are regarded as negligible, at least in obtaining the mean amplitude defined in Eq. 56.

Care should be taken, however, in the comparison of the amplitudes observed in this way with that calculated from the vibrational data. For the influence of anharmonicity on the mean amplitudes, interesting discussions were made by Reitan[53]. According to his calculation, apparent mean amplitudes of O-H and H-H bonds in water molecule based on the harmonic approximation are about 5% smaller than those which include the anharmonic effect. For heavier molecules such as Br_2, the correction was shown to be negligible.

g) Effect of series termination. — The MRD function was computed by use of Eq. 2 taking the upper limit of the integral as q_{max} instead of infinity. According to Waser and Schomaker[54], an exponential damping function $\exp(-bs^2)$ was adopted in the present analysis for the modification of the RD, the factor b being chosen following the usual convention that $\exp(-bs_{max}^2)=0.1$.

Since the intensity curve multiplied by the damping factor is given by a sum of the contribution of the component terms,

$$sM(s)=\sum_n sM_n(s)=\sum_n (c_n/r_n)\times\exp(-s^2/4H_n)\sin sr_n \quad (58)$$

the Fourier inversion is also expressed as a sum,

$$f(r)=\sum_n\int_0^\infty sM_n(s)\sin sr\,ds-\sum_n\int_{s_{max}}^\infty sM_n(s)\sin sr\,ds=f_0(r)-f'(r) \quad (59)$$

The RD function actually obtained is the sum of $f_0(r)$, the true RD function, and $-f'(r)$, additional ripples. Taking out the n-th contribution to $f'(r)$, and using Eq. 58, $f'_n(r)$ is given by

$$f'_n(r)=(c_n/2r_n)\left\{\int_{s_{max}}^\infty \cos s(r_n-r)\times\exp(-s^2/4H_n)ds-\int_{s_{max}}^\infty \cos s(r_n+r)\exp(-s^2/4H_n)ds\right\} \quad (60)$$

where the second term is usually negligible. At the center of the RD peak, i.e., $r=r_n$, the function $f'_n(r)$ has its maximum value, which is expressed in terms of the error integral, $\Phi(s_{max}/\sqrt{2H_n})$. Elsewhere, $f'_n(r)$ reveals itself as a ripple of the period of slightly less than $2\pi/s_{max}$. It is obviously symmetrical across the center of the peak and damps slowly as $|r-r_n|$ increases.

In the present example, $s_{max}=10\pi$, $H_n\sim66$ for the C-C bond which has the smallest damping factor, and $H_n\sim50-30$ for the other bonds. By the evaluation of the error integral, it was found that the maximum magnitude of f'_n is about 0.6% of the peak height for the C-C peak, and less than 0.1% for the others. The effect is thus unquestionable except for the C-C peak, and even in that case, it causes a slight symmetrical distortion of the C-C peak itself and an apparent increase of about 0.7% in its mean amplitude. A shift of the distance r_g of the adjacent peaks due to this effect amounts to only a few ten thousandth of an angstrom.

A similar, but more extensive discussion was carried out by Morimoto in his recent RD analysis of evaporated crystallites[55]. The result is in agreement with the estimation described above.

B. Random Errors.—The main origins of experimental random errors are 1) errors introduced in the photographic process (exposure, development, etc.), 2) errors of the microphotometry, 3) errors of the measurement of the photometer curve, and 4) errors introduced in the failure of drawing a proper background line, etc.

These errors are included in the molecular intensity and, being Fourier inverted, reveal themselves as random fluctuations or "ghosts" in the RD curve, which cause errors in the measurement of mean amplitudes.

The following features may be used as the measures of these fluctuations.

1) Fluctuations of the baseline in the regions where no interatomic distance should exist: as shown previously, there are no appreciable fluctuations in the baseline from 0 through 0.7Å (Fig. 3). Beyond 2.8Å of the RD curve, however, there

54) J. Waser and V. Schomaker, *Revs. Modern Phys.*, **25**, 671 (1953).

55) H. Morimoto, *J. Phys. Soc. Japan*, **13**, 1015 (1958).

appear small fluctuations, which probably come from the experimental errors together with the computational errors.

2) Difference among RD curves illustrated in Fig. 2, obtained by the independent procedure: the maximum deviation amounts to a small percentage of the peak height.

3) The standard errors given in the least-square analysis of the mean RD curve (Eq. 12): they were found to be about 1% of the mean amplitudes.

4) Deviations of the areas of the RD peaks from the theoretical values: the ratios listed in Table IV show that the deviations amount to a small percentage.

In order to estimate the random errors in the mean amplitudes, it seems possible to make use of one of the following methods:

1) Use of the variance in the results of the least-square analysis of the individual RD curves, which may correspond to the "mean square deviation between classes",

2) Use of the square sum of the residuals in the process 1, which may correspond to the "mean square deviation within classes",

3) Use of the difference among the RD curves to estimate the standard error at each point of the peak.

Each method was used in the present estimation together with Eqs. 11 and 12. Errors introduced in the computational process were also taken into account. Important ones among them would be 1) errors in the computation (rounding-up errors, etc.), 2) improper assumptions used in the analysis (structure, scattering factors, etc.), 3) ambiguity in the decomposition of the composite peak, and 4) improper correction for various systematic errors. A plausible estimation was made utilizing the experience in the self-consistent analysis described above. As for the effect 4, the corrections for systematic errors were considered to include ±70% uncertainties.

The results of the estimation of random errors are listed in Table VII. In the last row of the table are listed the mean amplitudes for which suitable corrections have been made, with their total standard errors which include all errors estimated in the above consideration.

Calculation of the Mean Amplitudes

In order to correlate the observed mean amplitudes to be spectroscopic data, a calculation of the mean amplitudes was carried out. Because of the lack of knowledge of the force constants, a simple and approximate treatment was made.

First the skeleton vibrations were considered by assuming a methyl or a methylene group as a particle for the *trans* and the *gauche* forms. The Wilson's G and F matrices for the *trans* form given as follows[56,58].

$$
\begin{array}{lll}
 & \mathbf{G} & \mathbf{F} \\
\mathrm{A}: & \begin{vmatrix} 2\mu_0 & & \\ 2\mu_0\cos\varphi & \mu_0+\mu & \\ -\sqrt{2}\,\rho_0\mu_0\sin\varphi & -2\rho_1\mu_0\sin\varphi & \rho_0^2(\mu_0+\mu)+4\mu_0(\rho_1^2-\cos\varphi) \end{vmatrix} & \begin{vmatrix} K_0+2a_0F & & \\ \sqrt{2}\,cF & K_1+a_1F & \\ \sqrt{2}\,\rho_1 d_0F & \rho_0 d_1F & H+bF \end{vmatrix} \\
\mathrm{B}: & \begin{bmatrix} \mu_0+\mu & \\ 0 & \rho_0^2(\mu_0+\mu) \end{bmatrix} & \begin{bmatrix} K_1+a_1F & \\ \rho_0 d_1F & H+bF \end{bmatrix}
\end{array}
\qquad (61)
$$

TABLE VIII. COMPARISON OF THE NORMAL FREQUENCIES FOR THE TRANS FORM

		Skeleton vibration	Observed (cm^{-1}) a	b	c	Calculated (cm^{-1}) A set	B set
A_g	ν_1	stretching	1059	1058	1056	1075	1068
	ν_2	mixed	837	835	833	835	909
	ν_3	deformation	425	432	(319?)	432	374
B_u	ν_4	stretching	—	970?	956.4	955	993
	ν_5	deformation	—	?	215.0	295	277

a: Ref. 60, b: Ref. 11, c: Refs. 9 and 15.

56) E. B. Wilson, Jr., *J. Chem. Phys.*, **7**, 1047 (1939); **9**, 76 (1941).

57) E. B. Wilson, Jr., J. C. Decius, and P. C. Cross, "Molecular Vibrations" McGraw-Hill, New York (1955).

TABLE IX. CALCULATED VALUES FOR THE MEAN AMPLITUDES (skeleton) (in Å unit)

Atomic pair	Observed (UMRD)	Calculated			
		trans Form		*gauche* Form	
		A set	B set	A set	B set
C-C (CH_2-CH_2)	$0.052_6 \pm 0.003$	0.048_7	0.049_8	0.049_1	0.049_9
C-C (CH_2-CH_3)		0.051_6	0.048_9	0.051_3	0.049_0
C-C (nonbonded)	$0.077_6 \pm 0.007$	0.069_2	0.079_4	0.068_2	0.078_2
C-C (*gauche*)	0.136	—	—	0.161_1	0.169_1
C-C (*trans*)	$0.067_7 \pm 0.007$	0.070_4	0.079_2	—	—

where the symbols have their usual meaning[57,59]. Two different sets of Urey-Bradly force constants were taken. One set A is that given by Shimanouchi[60], which was selected to the fit to Raman spectra of *n*-butane,

$K_0=4.0$, $K_1=3.2$, $H=0.11$, $F=0.96$ and $F'=0$

The other set B is that reported as the force constants of methyl and methylene groups[59], and taken by Hayashi in his calculation of the normal vibration of *n*-pentane molecule as a five-body problem[61].

$$K_0=3.7,\quad K_1=4.0,\quad H=0.20,\quad F=0.33$$
$$\text{and } F'=-0.1F$$

These force constants being inserted in Eq. 61, it is an easy and straightforward computation to obtain the normal frequencies[56,57] and the mean amplitudes[62,63]. A comparison of the frequencies for the *trans* form is given in Table VIII. The assignment of the skeleton frequencies was made by several authors[11,15,60,64], and there seems to be no difficulty except in the lowest B_u (bending) mode*. Although the band 215.0 cm^{-1} observed in the far infrared spectra was assigned to this mode by Gates, and no other band was found between 400 and 170 cm^{-1}, it seems likely that this mode has a little higher frequency. The agreemment of the calculated frequencies with the observed is much better for the A-set. Accordingly, the mean amplitudes calculated with the A-set may be the more reliable.

For the mean amplitudes of the *gauche* form the barrier against the torsional motion was assumed to be 3.6 kcal./mol.[14] An approximate method[63] was applied. These results are shown in Table IX. The larger amplitude obtained for the *gauche* C-C distance as compared with the *trans* C-C is just as expected.

For the mean amplitudes of the distances including hydrogen atoms, methyl groups were approximated by chlorine atoms, that is, the mean amplitudes of the H-H and C-H atom pairs in 1,2-dichloroethane were calculated, be cause the L matrices for this molecule calculated by Nakagawa[65] were available. Although this approximation apparently seems drastic, past experience on the calculation of mean amplitudes assures that it will give sufficiently correct values for this purpose[63]. The results obtained are listed in Table X. The mean amplitude of the C-C distance agrees with the previous values given in Table IX.

TABLE X. COMPARISON OF THE OBSERVED AND CALCULATED MEAN AMPLITUDES (FOR PAIRS INCLUDING HYDROGEN) (in Å unit)

Pairs	Observed	Calculated
(C-C)	$0.052_8 \pm 0.003$	0.050_3
C-H	$0.083_1 \pm 0.004$	0.078_3
C-H (nonbonded)	$0.097_5 \pm 0.005$	0.109_7
H-H (nonbonded)	—	0.126_8
H-H (*trans*)	—	0.128_2
H-H (*gauche*)	—	0.156_8

The comparison of the calculated amplitudes with the observed values is given in Table IX and X. The agreement is satisfactory, taking account of the experimental error, and of the uncertainty in the theoretical values (possibly a small

58) J. C. Decius, *J. Chem. Phys.*, **16**, 1025 (1948).
59) S. Mizushima, T. Shimanouchi, I. Nakagawa and A. Miyake, ibid., **21**, 215 (1953).
60) T. Shimanouchi, *Sci. Papers Inst. Phys. Chem. Research (Tokyo)*, **40**, 467 (1943); *Bull. Inst. Phys. Chem. Research (Tokyo)*, **23**, 371 (1944).
61) M. Hayashi, *J. Chem. Soc. Japan, Pure Chem. Sec. (Nippon Kagaku Zasshi)*, **78**, 222 (1957).
62) Y. Morino, K. Kuchitsu and T. Shimanouchi, *J. Chem. Phys.*, **20**, 726 (1952).
63) Y. Morino, K. Kuchitsu, A. Takahashi and K. Maeda, ibid., **21**, 1927 (1953).
64) R. S. Rasmussen, ibid., **16**, 712 (1948).
* Although Gates (Ref. 15) assigned the Raman line 319 cm^{-1} to the lowest A_g mode, this line should be assigned to the same mode of the *gauche* form (Ref. 16). The valence force constants determined by Gates are therefore not very reliable.
65) I. Nakagawa, *J. Chem. Soc. Japan., Pure Chem. Sec. (Nippon Kagaku Zasshi)*, **74**, 848 (1953); **75**, 60 (1954).

percentage), caused by the approximate nature of the calculation, the uncertainty in the force constants, and the neglect of anharmonicity in the vibration.

Analysis of the Intensity in the Small-angle Region

The intensity curve in a small-q region was analyzed for the purpose of obtaining further information on the rotational isomerism. The detail of the method was described in a previous paper[19,66].

Diffraction photographs were taken at the longer camera length through an r^2-sector with a multiple-layer stopper of the same type as that used by Bastiansen[23]. The density measured was converted into the intensity by Karles' procedure[26]. Independent observations gave good agreement with one another.

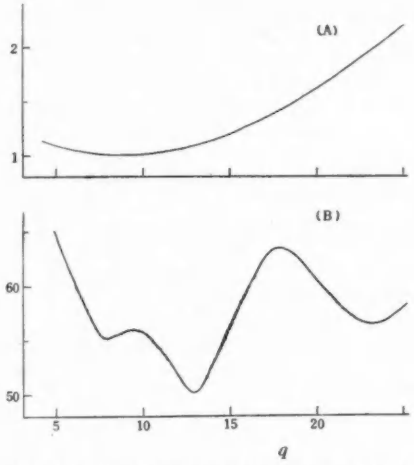

Fig. 12. Small-angle intensity curve of *n*-butane. (A) $f(q)$ curve; and (B) $f(q)I(q)$ curve.

The intensity $I(q)$ was multiplied by a smooth function $f(q)$ (Fig. 12) to make the background line nearly flat, where

$$f(q)=1+0.0054(q-9)^2+3\times10^{-6}(q-9)^4 \quad (62)$$

A background function $I_b(q)$ was calculated by the following equation,

$$I_b(q)=f(q)I(q)/(1+cM(q)_{\text{calc}}) \quad (63)$$

where $M(q)_{\text{calc}}$ is the theoretical molecular intensity divided by q, and c is the index of resolution[34,44]. A criterion that I_b should be a smooth function of q can be used to select a reasonable model[19].

The frame structure and the mean amplitudes determined by the analysis described on pages 750~757 was used to compute the theoretical molecular intensity, together with the same assumption discussed in *procedure* of that section. Two parameters of the rotational isomerism, the *gauche* azimuthal angle ϕ and the fraction of the *trans* form n_t, were varied systematically. The index of resolution was estimated to be 0.90±0.10.

It was found that when n_t was assumed to be less than 30% or more than 70%, the I_b functions (Fig. 13) showed such large fluctuations irrespective of the choice of angle ϕ, that the existence of both rotational isomers was definitely confirmed. It gives an independent support to the conclusion of the RD analysis.

For the estimation of the parameters and their limits, the maximum possible ripples caused by experimental errors or by theoretical uncertainties were regarded as about 1% of the I_b function*. The result of the analysis is

$$\phi=65°\pm10°, \text{ and } n_t=65\sim35\%$$

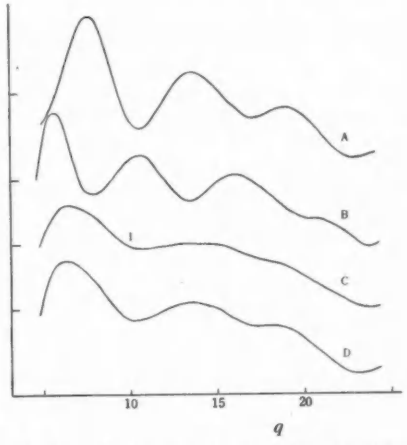

Fig. 13. I_b functions of *n*-butane for models (A) *trans* 100%; (B) *gauche* ($\phi=65°$) 100%; (C) a mixture of *trans* and *gauche* ($\phi=65°$) in 1:1; and (D) a mixture of *trans* and *gauche* ($\phi=50°$) in 1:1. The index of resolution is 0.90. The curve C is in the acceptable region. The vertical line denotes the amplitude of a one per cent fluctuation of the I_b curve.

* This estimation was based on a similar argument given in the previous paper on *n*-propyl chloride (Ref. 19), but a larger value should be taken for the uncertainty in this case, since the contribution of the internal rotation is less (being about 20% of the total intensity), and the uncertainty of the assumptions is more serious (particularly for the position of the hydrogen atoms).

66) K. Kuchitsu, This Bulletin, **30** 391, 399 (1957).

TABLE XI. COMPARISON OF THE STRUCTURES OF RELATED MOLECULES

Molecule	Ethane		Propane	Butane	
Method	Infrared	E.D.	E.D.	E.D.	E.D.
C–H(A)	1.102	1.114±0.027	1.107	(1.09)	1.100±0.003	1.107_5 ±0.005
C–C(A)	1.543	1.536±0.016	1.536	1.54±0.02	1.53_9±0.003	1.533 ±0.003
∠C–C–H	109°37′	110.5°±3.5°	109°32′	—	110°22′±15′	110.5°±0.7°
∠C–C–C	—	—	—	111.5°±3°	112°9′±9′	112.4°±0.4°
Reference	3	4	5	7	Present work	72

E.D.: electron diffraction investigation.

which is consistent with the result on pages 750~757 within the limit of uncertainty.

Discussion

The C–H and C–C distances were obtained with accuracies of better than 0.01Å (Table VI). These distances are the average values of two non-equivalent distances, but they may not differ more than 0.01Å. It is seen that the values are close to the "normal" bond lengths[67] accepted generally: C–H=1.09Å, and C–C=1.54Å. This result therefore gives some support for these standard values.

The average C–C–H angle was found to be slightly larger than the tetrahedral angle. The structures of methyl groups have been obtained by means of microwave spectroscopy for a number of simple molecules[68]; the angles C–C–H differ slightly from one molecule to another around the tetrahedral angle.

The structural data for normal paraffins comparable with the present result are those for ethane and propane (Table XI). The spectroscopic value r_0 is slightly different from $r_g(0)$ (probably about 0.01Å or less), and the values given by electron diffration may be $r_g(1)$, although not stated explicitly. The general agreement shows that there may be no conspicuous difference between the structures of these hydrocarbons.

It was confirmed that the angle C–C–C is definitely larger than tetrahedral (112°9′). A similar but not so accurate result was obtained in propane (111.5°±3.5°)[7]. It is interesting to note that a similar fact was known for higher normal paraffin crystals studied by the X-ray diffraction; it was first noticed by Bunn[69], and confirmed in a recent study of Shearer and Vand[70], who found that ∠C–C–C=112°1′± 21′ for $C_{36}H_{74}$. This fact is consistent with the earlier theoretical prediction of Ingold[71] based on organic reactions.

As for the rotational isomerism, it was definitely confirmed that there are two isomers, the *trans* and the *gauche* forms, in the gaseous phase. The fractions of these forms were found to be about 60% for the *trans* form and about 40% for the *gauche* form. Since the complete assignment of the vibrational frequencies is not available at present, the partition functions can not be calculated. If the ratio of the functions is assumed to be unity, (the statistical weight for the *gauche* form being 2), then the energy difference between the two forms is about 650 cal./mol., the *trans* form being the more stable. This value is close to that of liquid *n*-butane[11,12], as expected. The azimuthal angle of the *gauche* form was found to be slightly larger than 60°. The effect of hindered internal rotation around the *trans* position was observed in the shift of the *trans* C–C distance. An evaluation of the barrier height gave a rough but reasonable order of magnitude for this value.

A precise measurement of the structure of *n*-butane has been made by Bartell[72]. His result is in satisfactory agreement with the present result, except slight discrepancies in atomic distances (less than 0.7%) which may be partly due to uncertainties in the scale factor.

Summary

The molecular structure of *n*-butane has been investigated by means of the sector-microphotometer method of electron diffraction. The least-square analysis of the radial distribution curve has been carried out both for modified and unmodified curves giving the internuclear

67) L. Pauling, "The Nature of the Chemical Bond", Cornell University Press, Ithaca, N. Y. (1940), p. 160.
68) W. Gordy, W. V. Smith and R. F. Trambarulo, "Microwave Spectroscopy", John Wiley and Sons, Inc., New York (1953). C. H. Townes and A. L. Shawlow, "Microwave Spectroscopy" McGraw-Hill, New York (1955).
69) C. W. Bann, *Trans. Faraday Soc.*, **35**, 482 (1939).
70) H. M. M. Shearer and V. Vand, *Acta Cryst.*, **9**, 379 (1956).
71) C. K. Ingold, *J. Chem. Soc.*, **1921**, 305.
72) L. S. Bartell, private communication (1958).

distances as well as their mean amplitudes and the bond angles. The estimation of experimental standard errors has been made by examining various sources of errors. Important results are the following:

a) The average distance of the C–C bonds is 1.539±0.003Å.

b) The angle C–C–C is 112°9′±9′, is considerably greater than the tetrahedral angle.

c) The position of hydrogen atoms is located with considerable accuracy; C–H =1.100±0.003Å and ∠C–C–H=110°22′±15′.

d) The mean amplitudes measured are in agreement with the calculated values within the limit of error.

e) The existence of rotational isomers, the *trans* and the *gauche* forms, are confirmed. The structure and the fraction of the isomers are determined. The result is consistent with the spectroscopic results.

The author wishes to express his sincere gratitude to Professor Yonezo Morino for his kind guidance and encouragement throughout this work. He is also indebted to Mr. H. Morimoto of Nagoya Univesity and to Dr. M. Iwasaki of the Government Industrial Research Institute of Nagoya for their help in the microphotometry, to Mr. R. Tsunoda in the Division of Health and Welfare Statistics, Welfare Ministries Secretariat for the use of the punched cards machines, and to Mr. T. Takatani of Hitachi Central Research Laboratory for his kind supply of the *n*-butane sample. This research was financially supported by the Scientific Grant from the Ministry of Education.

Department of Chemistry
Faculty of Science
The University of Tokyo
Hongo, Tokyo

SHORT COMMUNICATIONS

Far Infrared Spectrum of Gaseous Formic Acid

By Kozo Hirota and Yasuo Nakai

(Received April 20, 1959)

Since the first report of Bonner and Kirby-Smith[1] on a Raman line of formic acid, low frequency vibrations of the acid have not been studied till recently. However, it is interesting to investigate the vibrational bands in relation to the anomalous band features of OH groups due to hydrogen bonding found in both near infrared and infrared regions[2]. Sato and Nagakura explained their results by the motion of the proton in the double minimum potential. Oshida, Ooshika and Miyasaka[3] also explained these phenomena theoretically by the same model, and predicted appearance of new bands in the far infrared region. However, though Pitzer et al.[4] observed two bands of gaseous formic acid at 237 cm^{-1} and 160 cm^{-1}, they ascribed[5] them to the intermolecular vibrations between the two monomers making up formic acid dimer by hydrogen bonding.

In the course of studies[6] on chemisorption of gaseous formic acid HCOOH to the silver surface, the present authors also found two bands independently[7]. In connection to this measurement they extended their research over the region 85~300 cm^{-1} not only on formic acid HCOOH but also on formic acid-d HCOOD, and found some new knowledge, the essential point of

1) L. Bonner and J. B. Kirby-Smith, *Phys. Rev.*, **57**, 1078 (1940).

2) Y. Sato and S. Nagakura, *Sci. of Light*, **4**, 120 (1955); *J. Chem. Soc. Japan, Pure Chem. Sec.* (*Nippon Kagaku Zasshi*), **76**, 1007 (1955): Y. Sato, ibid., **79**, 358, 1384 (1958).

3) I. Oshida, Y. Ooshika and R. Miyasaka, *J. Phys. Soc. Japan*, **10**, 849 (1955).

4) R. C. Millikan and K. S. Pitzer, *J. Am. Chem. Soc.*, **80**, 3515 (1958).

5) T. Miyazawa and K. S. Pitzer, ibid., **81**, 74 (1959).

6) K. Hirota, K. Kuwata and Y. Nakai, This Bulletin, **31**, 861 (1958).

7) K. Hirota and Y. Nakai, *J. Chem. Soc. Japan, Pure Chem. Sec.* (*Nippon Kagaku Zasshi*), **80**, 70 (1959).

which will be reported.

Formic acid of chemically pure grade (Edogawa Kagaku Kogyo Co.) was repeatedly vacuum-distillated, crystallized, and dehydrated with unhydrous copper sulfate. Formic acid-d was prepared by the reaction of sodium formate, whose degree of purity was the same as formic acid, with sulfuric acid-d D_2SO_4 (36%). Method of purification was the same as described on formic acid. It was confirmed that formic acid-d thus obtained does not include H_2O and HCOOH so much as can be detected by use of the NMR method (Apparatus: Varian V 4800 B).

The spectrometer made by Yoshinaga et al.[8], Engineering Faculty of Osaka University, was used. During the measurement, the apparatus was kept constant at 21°C, while the pressure of the acid in the measuring cell was about 30 mmHg. Gratings, light sources, reststrahlen filter and width of slits were changed according to the spectrum range as shown in Table I.

TABLE I

Wave number (cm^{-1})	Light source	Reststrahlen filter	Slit width (mm.)
300~190	Pt-source	NaCl	0.36
190~155	Hg lamp	NaCl	0.50
160~130	〃	KCl	0.47
140~105	〃	KBr	0.68
110~ 85	〃	KBr	1.30

The experimental results are shown in Figs. 1 and 2 and in Table II, where the data of Pitzer[4] and Simova[9] are compared for the sake of discussion. However, Simova's values seem to be of less confidence, because they were estimated from the combination bands of a Raman line.

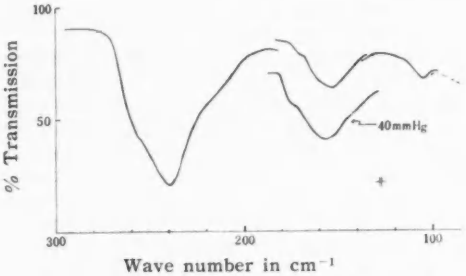

Fig. 1. Far infrared spectrum of HCOOH
Pressure 30 mmHg; Temp. 21°C.

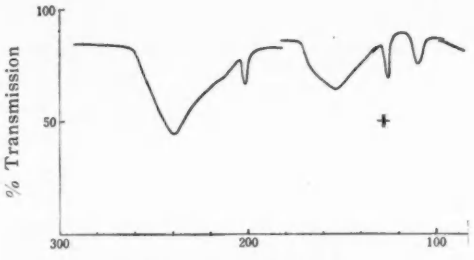

Fig. 2. Far infrared spectrum of HCOOD
Pressure 30 mmHg; Temp. 21°C.

TABLE II. FAR INFRARED BANDS OF FORMIC ACID (cm^{-1})

The present work		Pitzer	Simova	Other researchers
HCOOH	HCOOH	HCOOH	HCOOH	HCOOH
ca. 270 (sh.)				
240±5 (vs)	240±5 (vs)	237	230	232[a]
	202 (m)		200	
175 (sh.)			170	
155 (s)	155 (s)	160		
			145	
	126 (m)			
109 (m)	111 (m)			110[b]

a) Cf. G. Herzberg, "Infrared and Raman Spectra", D. Van Nostrand Co., New York (1945).

b) L. M. Sverklow, *Izv. AN. USSR*, **17**, 567 (1953).

The important point obtained from the present data is as follows. Strong bands are observed at 240 cm^{-1} and 155 cm^{-1} in both acids, but it is noteworthy that their feature differs markedly; i.e., (a) in case of HCOOH the 240 cm^{-1} band is broad and begins at 278 cm^{-1}, making a sharp contrast with the beginning at ca. 258 cm^{-1} in case of HCOOD, and (b) small bands can be detected at ca. 270 cm^{-1} and 175 cm^{-1} as shoulders of the 240 cm^{-1} and 155 cm^{-1} bands, respectively, in case of HCOOH. These shoulders become conspicuous if the pressure of formic acid is increased to ca. 40 mmHg as shown in Fig. 1. The second point to be mentioned is appearance of sharp bands at 202 cm^{-1} and 126 cm^{-1} in case of HCOOD. Besides, a new band is observed at ca. 110 cm^{-1} in both acids. Their nature, however, will not be discussed in the present note*),

8) Y. Yoshinaga, S. Fujita, S. Minami, A. Mitsuishi, R. A. Oetjen and Y. Yamada, *J. Opt. Soc. Am.*, **48**, 311 (1958).

9) P. Simova, *Izv. Bulgar. Akad. Nauk. Otdel. Fiz. Mat. i Tekh., ser. Fiz.*, **2**, 107 (1951).

*) Their frequency is too high if they are the lowest infrared active band predicted by Miyazawa and Pitzer.

except to mention that a Raman line has been observed in the neighborhood of this band (110 cm^{-1}).

The strong and broad bands at 240 cm^{-1} and 155 cm^{-1} seem to correspond to those at 238 cm^{-1} and 160 cm^{-1} observed by Pitzer et al. and can be assigned to the bands produced by the intermolecular vibration between the two monomers making up formic acid dimer as already done by Miyazawa and Pitzer. They may be two higher frequency bands of the three infrared active ones which are expected from the symmetry of the dimer (C_{2h}). It is necessary, therefore, to introduce another cause in order to explain the appearance of two bands of the similar form at 270 cm^{-1} and 175 cm^{-1} in case of HCOOH. Taking the fact into consideration that the ratio of their wave number to that of the sharp bands at 202 cm^{-1} and 126 cm^{-1} in case of HCOOD nearly equals $\sqrt{2}$, respectively, it may presumably be reasonable to assign them to the bands due to the motion of the proton in the double minimum potential, as proposed several years ago[2,3,10].

In conclusion, the present authors express their sincere thanks to Professor H. Yoshinaga and the members of his laboratory (Dr. S. Fujita, Dr. Y. Yamada and Dr. A. Mitsuishi) without whose assistance the present research could not be carried out, and they are much indebted to Professor S. Nagakura of the University of Tokyo and also to Associate Professor S. Seki of Osaka University for helpful discussion of the problem here considered.

Department of Chemistry
Faculty of Science
Osaka University
Kita-ku, Osaka

10) *Discussions Faraday Soc.*, **9**, 210–212 (1950).

Poly-p-halostyrenes. I. Preparation of Crystalline Poly-p-chlorostyrene

Kazuo NAGAI, Masamichi KOBAYASHI and Eiichi NAGAI

(Received May 12, 1959)

Recently Natta et al. reported[1] that while some substituted polystyrenes prepared by Ziegler catalyst were crystalline, others were amorphous. To the contrary of Natta et al.'s results that poly-*p*-chlorostyrene is not crystalline, we find that a small part of poly-*p*-chlorostyrene prepared by Ziegler catalyst is crystalline.

p-Chlorostyrene (4.4 g.) prepared by an usual method[2], enclosed in a glass tube with $Al(C_2H_5)_3$ (0.53 g.), $TiCl_4$ (0.18 g.) and *n*-heptane (20 cc.) is polymerized at 70°C

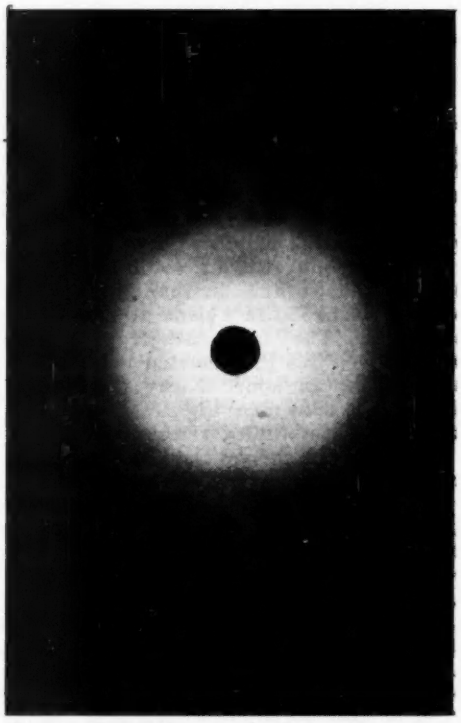

Fig. 1. X-ray diagram of poly-*p*-chlorostyrene (PCIS-IS)

1) G. Natta, F. Danusso and D. Sianesi, *Makro. Mol. Chem.*, **28**, 253 (1958).
2) R. Adams and C. R. Noller, "Organic Syntheses", Vol. 5, John Wiley & Sons, New York (1925), p. 17; W. Kern and D. Braun, *Makro. Mol. Chem.*, **27**, 23 (1958).

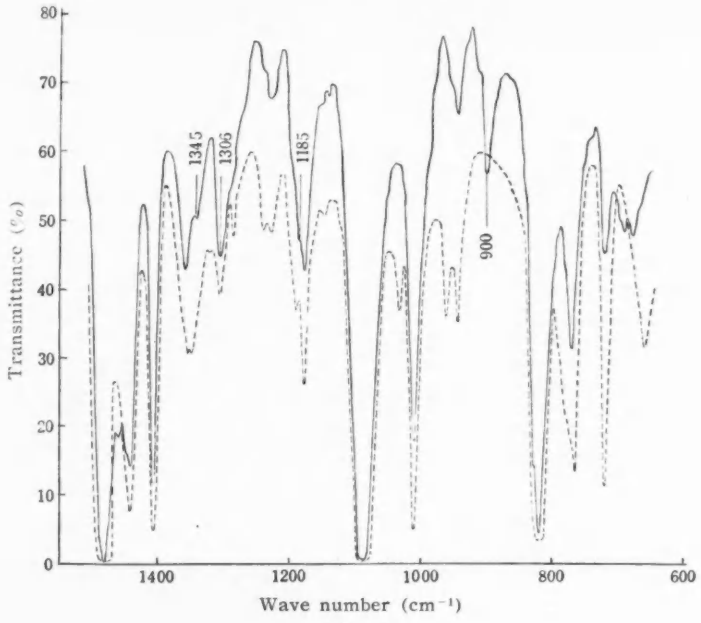

Fig. 2.

for about 10 hr. The product washed by hot ethanol and then boiled in water is dissolved in boiling xylene and the solution is filtered to separate from titanium oxide. By centrifuging this solution kept at room temperature the polymer is devided into two parts; one (2.20 g.) soluble (refered as to PClS-S) and another (0.13 g.) insoluble (PClS-IS) in xylene at room temperature. The film cast from toluene solution of PClS-IS is heated in silicon oil at 160°C for an hour. X-ray diagram of this film is shown in Fig. 1, manifesting moderate crystallinity of this sample.

In Fig. 2 are shown the infrared spectroscopic data of PClS-IS (full line) and radically polymerized poly-*p*-chlorostyrene (PClS-At) (dashed line), both previously heated at 160°C for an hour. It is expected that in the crystalline region and in the amorphous region, so far as the short portion of the polymer chain is concerned, the skeletal chain of PClS-IS has a helical structure, although whether 3-fold helix as in the case of polystyrene is still kept or not is not obvious, owing to the steric effects of chlorine atoms. Recently Tadokoro et al.[3,4] showed that the absorption bands ascribed to deformation vibrations of CH_2 and CH groups of the skeletal carbon chain, and to C-C stretching vibration were affected by the configurations of the skeletal chain, and bands at 1364, 1314, 1297 and 1185 cm^{-1} of isotactic polystyrene and *p*-deuterostyrene were assumed to be characteristic to 3-fold helical structure. Moreover, in our investigations on the infrared spectroscopy of the crystalline poly-*p*-fluorostyrene, we found[5] the bands at 1330 and 1302 cm^{-1} as to be charasteristic to the helical structure of the skeletal chain. From these results, the bands 1345, 1303 and 1185 cm^{-1} of PClS-IS are assumed to be characteristic to the helical structure. A band at 900 cm^{-1} probably corresponds to crystallization sensitive band. The spectroscopic data of PClS-S are almost similar to those of PClS-At. Investigations are in progress on the bands appearing at near 700 cm^{-1} and longer wavelength region.

We thank Mr. S. Kuribayashi for his preparation of X-ray diagram.

The Osaka Industrial Research Institute
Daini-Nishi 2-Chome, Oyodo-ku, Osaka

3) H. Tadokoro, S. Nozakura, T. Kitazawa, Y. Yasuhara and S. Murahashi, This Bulletin, **32**, 313 (1959).
4) S. Murahashi, S. Nozakura and H. Tadokoro, This Bulletin, **32**, 534 (1959).
5) K. Nagai, M. Kobayashi and E. Nagai, Presented at the 8th Annual Meeting of the Society of Polymer Science of Japan, held in Tokyo, May, 1959.

On the Magnetic Susceptibility of Hexabenzocoronene and Triphenylene

By Hideo Akamatu
and Minoru Kinoshita

(Received May 15, 1959)

Hexabenzocoronene is an extremely stable, pale yellow hydrocarbon. Clar and Ironside suggested that it contains exclusively benzenoid rings interlinked by quasi-single bonds[1]. Afterwards, however, they found an asymmetric effect of the electronic interaction between benzenoid rings, and proposed a formula of hexabenzocoronene consisting of a triphenylene complex and 4 benzenoid rings[2]. Magnetic susceptibility of hexabenzocoronene would be interesting for these points of view, as the effect of the aromatic conjugation should reflect on its value. We measured the magnetic susceptibility of hexabenzocoronene and triphenylene; the samples were provided by C. T. Ironside and M. Zander, respectively.

The purification of the specimens was made by sublimation in vacuo at about 490°C for hexabenzocoronene, and at about 120°C for triphenylene. The magnetic measurement was made by the Gouy method at room temperature. The observed values are as follows. Hexabenzocoronene (M.W. 522.6, density 1.57[3]):

$-\chi_g \times 10^6 = 0.562 \pm 0.002$ per gram,

$-\chi_M \times 10^6 = 346.0$ per mole.

Triphenylene (M.W. 228.3, density 1.30).

$-\chi_g \times 10^6 = 0.686 \pm 0.001$ per gram,

$-\chi_M \times 10^6 = 156.6$ per mole.

The magnetic susceptibilities of related compounds are as follows.

Phenanthrene:

$-\chi_g \times 10^6 = 0.718$; $-\chi_M \times 10^6 = 127.9$

Benzene:

$-\chi_g \times 10^6 = 0.712$; $-\chi_M \times 10^6 = 55.6$

Atomic susceptibility of hydrogen;

$-\chi_M(\mathrm{H}) \times 10^6 = 2.93$

1) E. Clar and C. T. Ironside, *Proc. Chem. Soc.*, **1958**, 150.
2) E. Clar, C. T. Ironside and M. Zander, *J. Chem. Soc.*, **1959**, 142; E. Clar, *Tetrahedron*, **5**, 98 (1959); Private communication.
3) A. Halleux, R. H. Martin and G. S. D. King, *Helv. Chim. Acta*, **41**, 1177 (1958).

Hexabenzocoronene can be presumed as being made of seven benzenoid rings interlinked by quasi-single bonds (Formula 1), or consisting of triphenylene and four benzenoid rings. The expected value of each formula will be respectively,

$$-\chi_M \times 10^6 = 7\chi_M(\text{Benzene}) - 24\chi_M(\mathrm{H}) = 318.9$$

$$-\chi_M \times 10^6 = \chi_M(\text{Triphenylene}) + 4\chi_M(\text{Benzene}) - 18\chi_M(\mathrm{H}) = 326.3$$

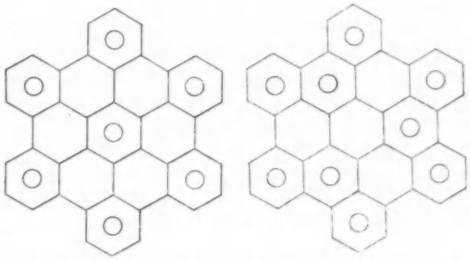

Formula (1) Formula (2)

Fig. 1. Hexabenzocoronene

The observed value is higher than those of anticipated formulae. The other formula which is conceivable consists of three phenanthrene rings connected by contact bonds (Formula 2). This leads to the expected value as,

$$-\chi_M \times 10^6 = 3\chi_M(\text{Phenanthrene}) - 12\chi_M(\mathrm{H}) = 348.5\,; \quad -\chi_g \times 10^6 = 0.667$$

This value is very near to the observed one. It is likely that a small effect of the electronic interaction takes place between benzenoid rings, its amount is in the same order as the aromatic conjugation in phenanthrene molecule.

The mean susceptibility of triphenylene was measured by Honda and Ouchi[4]. Their observed value is $\chi_g = -0.685 \times 10^{-6}$, which is in good agreement with the present result. From the observed susceptibility and using the empirical formula[5], the principal diamagnetic susceptibilities of triphenylene molecule can be estimated as $K_1 = -95.6 \times 10^{-6}$ and $K_3 = -278.6 \times 10^{-6}$, where K_1 is in the plane of molecule and K_3 is perpendicular to it. This leads to the diamagnetic anisotropy of $\Delta K = -183.0 \times 10^{-6}$. This value is 3.4 times of the diamagnetic anisotropy of benzene, ΔK (Benzene) $= -54 \times 10^{-6}$. The molecular

4) H. Honda and K. Ouchi, *Reports of the Resources Research Institute, Japan*, No. 1, 8, (1952).
5) H. Akamatu and Y. Matsunaga, This Bulletin, **26**, 364 (1953); **29**, 800 (1956).

orbital calculation[6], however, gave 4.08 for this ratio, which is too large compared with the above value.

Our estimated values of the principal diamagnetic susceptibility are likely to be reasonable from the following reason. Triphenylene crystal is orthorhombic, and its principal susceptibilities along the crystal axes were measured by Banerjee and Guha[7]. Their observed values are $\chi_a = -150.1\times10^{-6}$, $\chi_b = -149.5\times10^{-6}$ and $\chi_c = -174.2\times10^{-6}$. Using these values combined with the above values for K_1 and K_3, we can estimate the orientation of the molecule to the crystal axes. The procedure has been given by Lonsdale and Krishnan[8]. This gives the result that the plane of molecule makes the angle of 50°20′ to the *ab*-plane. This value is in good agreement with the observed angle, 50°30′, by Klug[9] who made the X-ray crystal analysis of triphenylene.

The authors wish to express their thanks to Dr. E. Clar and his school who provided them with the samples of hexabenzocoronene and triphenylene.

Department of Chemistry
Faculty of Science
The University of Tokyo
Hongo, Tokyo

Added in Proof:

E. Clar proposed* the other possible formula for hexabenzocoronene, after we had made our communication. He suggested that the induced sextet in the center ring of triphenylene may rotate or oscillate through the ring system of hexabenzocoronene, as if the Formulae 1 and 2 are overlapping with each other. In this case, the induced sextet in triphenylene (the center ring) has magnetic susceptibility of

$$\chi_M(\text{Triphenylene}) - 3[\chi_M(\text{Benzene}) - 2\chi_M(\text{H})] = -7.4\times10^{-6}$$

Three times this value (-22.2×10^{-6}) added to the value for Formula 1, it leads to -341.1×10^{-6} which is near to the observed value.

6) G. Berthier, M. Mayot, A. Pullman and B. Pullman, *J. Physique Rad.*, **13**, 15 (1952).
7) S. Banerjee and A. C. Guha, *Z. Krist.*, **96**, 107 (1936).
8) K. Lonsdale and K. S. Krishnan, *Proc. Roy. Soc.*, **A156**, 597 (1936).
9) A. Klug, *Acta Cryst.*, **3**, 165 (1950).
* Private communication.

Isodelphinine, a New Alkaloid from Aconitum miyabei, Nakai

By Nobukatsu KATSUI

(Received May 26, 1959)

Recently a third new alkaloid, sachaconitine, and a fourth probably new alkaloid (I)[1], base D, having the same empirical formula, $C_{33}H_{45}O_9N$, as that of delphinine (II)[2] but different m.p. and $[\alpha]_D$, were isolated from Aconitum *miyabei*, Nakai. As described below, I has the same empirical formula and the same functional groups as II, but differs distinctly from II as shown by the mixed m. p. and infrared spectra. Thus the name isodelphinine was assigned to I. This substance, m. p. 167~168°C, $[\alpha]_D^{20}$ +20.1°, gave a perchlorate, m. p. 171~172°C, $[\alpha]_D^{20}$ −2.38°. (*Anal.* Found: C, 56.35; H, 4.97; Cl, 4.87. Calcd. for $C_{33}H_{45}O_9N\cdot HClO_4$: C, 56.55; H, 5.19; Cl, 5.06%). The aurichloride crystallized from chloroform-ethanol in prisms, m. p. 228~229°C. (*Anal.* Found: Au, 20.96. Calcd. for $C_{33}H_{45}O_9N\cdot HAuCl_4$: Au, 20.94%). Other salts of I, for example, acid oxalate or hydrochloride, did not crystallize although the corresponding salts of II had been obtained[3] as crystals.

On acetylation with acetyl chloride I gave a monoacetate, m.p. 188~190°C. (*Anal.* Found: C, 65.43; H, 6.81. Calcd. for $C_{35}H_{47}O_{10}N$: C, 65.55; H, 6.76%). Saponification of I gave benzoic acid which was identified with an authentic sample, and acetic acid which was confirmed as silver salt. (*Anal.* Found: Ag, 64.49. Calcd. for $C_2H_3O_2Ag$: Ag, 64.67%). The presence of four methoxyl groups was determined by the micro-Zeizel determination. (*Anal.* Found: OCH_3, 20.11. Calcd. for $C_{29}H_{33}O_5N\cdot 4(OCH_3)$: OCH_3, 20.63%). In the Herzig-Meyer *N*-alkyl determination, I gave methyl iodide which was confirmed as tetramethylammonium iodide. (*Anal.* Found: I, 67.46. Calcd. for $(CH_3)_4\cdot NI$: I, 67.86%).

Above evidences show that the formula of I may be extended as follows in the same way as that of II:

1) H. Suginome, N. Katsui and G. Hasegawa, This Bulletin, **32**, 604 (1959).
2) R. H. F. Manske and H. L. Holmes, "The Alkaloids", Vol. IV, Academic Press Inc., New York (1954), p. 275.
3) T. Walz, *Arch. Pharm.*, **260**, 9 (1922); W. A. Jacobs and L. C. Craig, *J. Biol. Chem.*, **127**, 301 (1939).

$(OCH_3)_4$
OH
$C_{19}H_{21}$ $OCOCH_3$
$OCOC_6H_5$
$N\text{-}CH_3$

The infrared spectra of I and II were quite similar except for the region due to ester carbonyl groups: compound I showed two bands at 1720 cm^{-1} and 1702 cm^{-1}, whilst II one band[4] at 1720 cm^{-1}.

On the basis of the same extended formula and the resemblant spectra, it may be reasonable to consider that I possesses a skeletal formula closely related to that of II. Furthermore, the same ring structure has been suggested for several alkaloids[5] of two genera, Aconitum and Delphinium, in which oxygen atoms are similarly located although the substituents are different. And then it may be considered that the substituents of I and II are also similarly located. On the other hand, it is well known[6] that the benzoyl group in II covers a secondary hydroxyl group which is vicinal to a free *tert* hydroxyl group.

If above consideration is correct, a simple explanation of the difference in infrared spectra of I and II may be that the free hydroxyl and the benzoyl group have *trans* orientation in II against *cis* in I.

In the *cis* orientation, an ester carbonyl band displacement[7] to lower frequencies due to hydrogen bonding is considerable. An experiment to clarify the relation of I and II is in progress and will be reported in a later paper.

The author is grateful to Professor Harusada Suginome, President of Hokkaido University, for his unfailing kindness in encouraging this work, and to Dr. S.W. Pelletier for his courtesy in sending the sample of delphinine.

Depariment of Chemistry
Faculty of Science
Hokkaido Univerity, Sapporo

4) Schneider has reported that the spectrum of II showed one band due to two ester groups at 5.78 μ, *Ann.*, **590**, 155 (1954).

5) R. C. Cookson and M. E. Trevett, *J. Chem. Soc.*, 1956, 3121; R. Anet, D. W. Clayton and L. Marion, *Can. J. Chem.*, **35**, 397 (1957); F. Sparatore, R. Greenhalgh and L. Marion, *Tetrahedron*, **4**, 157 (1958); O. E. Edwards, L. Marion and K. H. Palmer, *Can. J. Chem.*, **36**, 1097 (1958); E. Ochiai, T. Okamoto and M. Kaneko, *Chem. Pharm. Bull. Japan*, **6**, 730 (1958).

6) W. A. Jacobs and Y. Sato, *J. Biol. Chem.*, **180**, 479 (1949); K. Wiesner, F. Bickehaupt and Z. Valenta, *Tetrahedron*, **4**, 418 (1958).

7) R. N. Jones, P. Humphries, F. Herling and K. Dobriner, *J. Am. Chem. Soc.*, **74**, 2820 (1952).

Visible Absorption Spectra of Colored Solutions Produced by Adding Alkali to Nitro-, Dinitro-, and Trinitro-substituted Benzenes in Acetone

By Takehiro Abe

(Received May 28, 1959)

In the course of my visible absorption studies on the color reactions of polynitrobenzenes with alkali, it has been found that nitrobenzene, *o*-, *m*-, and *p*-dinitrobenzene, and 1,3,5-trinitrobenzene, all in acetone give intense absorption bands at the visible region when they are treated with a few drops of dilute aqueous solution of sodium hydroxide at room temperature, as shown in Fig. 1. Dinitrobenzenes slowly yield reddish-violet colors. Trinitrobenzene at once gives a red color, while a red color can be observed by standing the nitrobenzene solution containing sodium hydroxide (in a brown desiccator to avoid light) for a long time. These red colors show the maximum

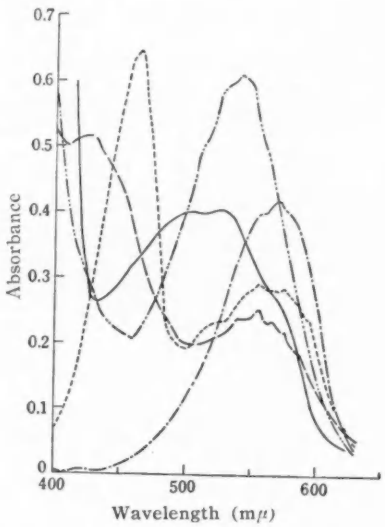

Fig. 1. Absorption spectra of the colored solutions produced by adding a few drops of dilute sodium hydroxide solution to nitrobenzene (——), *o*-dinitrobenzene(——), *m*-dinitrobenzene (— — —), *p*-dinitrobenzene (— · — · —), and 1,3,5-trinitrobenzene (----), in acetone at room temperature.

absorption bands at longer wavelengths as compared with the maximum absorption bands observed for the solutions that are obtained by adding sodium hydroxide into aqueous solutions of polynitrobenzenes[1]. There is no simple relation between numbers of nitro group and the positions of the absorption maxima, although the aromatic nitro compounds show the absorption bands at longer wavelengths in the aqueous solutions of sodium hydroxide as the number of nitro group increases[1].

The absorption curve of the red-colored solution produced by treating trinitrobenzene in acetone with sodium hydroxide solution, giving the intense maximum absorption band at about 460 mμ and several bands at 510~590 mμ, is greatly different from that of the red complex of trinitrobenzene with ammonium hydroxide[2]. Fig. 2 shows the absorption curves of the red solutions produced by adding a few drops of dilute sodium hydroxide solution, of dilute calcium hydroxide solution, or of concentrated ammonia water into the acetone solutions of 1,3,5-trinitrobenzene. It may be known from Fig. 2 that the absorption curves of the colored solutions produced by treating with strong alkalies (sodium hydroxide and calcium hydroxide) is different from that of the red solution obtained by addition of a weak alkali (ammonia). The maximum absorption band of the red complex of trinitrobenzene with ammonium hydroxide lies at the longer wavelength in acetone than in ethanol and in water[2].

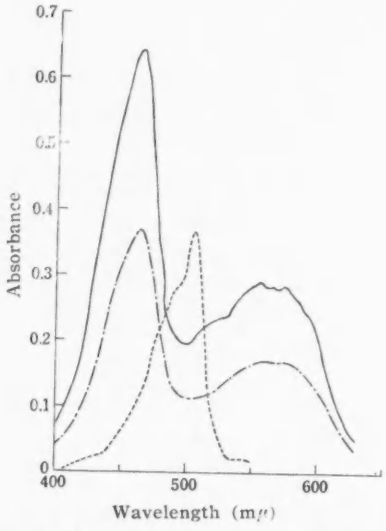

Fig. 2. Absorption spectra of the colored solutions produced by adding a few drops of dilute sodium hydroxide solution (——), of dilute calcium hydroxide solution (– – –), and of concentrated ammonia water (- - - -) to 1,3,5-trinitrobenzene in acetone at room temperature.

Although weak alkali and strong alkali give different absorption curves, all the above red colors seems possibly to be owing to formation of the same transition complexes of Meisenheimer's type as the intermediates presented for the color reactions of trinitrobenzenes and dinitrobenzens with alkalies[1-8].

The author is particularly indebted to Professor Y. Nomura for his suggestion and encouragement through this work.

Department of Chemistry
Defense Academy
Yokosuka

1) A. Abe, This Bulletin, **31**, 901 (1958); **32**, 339 (1959).
2) T. Abe, ibid., to be published.
3) J. Meisenheimer, *Ann.*, **323**, 205, 214, 241 (1902).
4) D. L. Hammick and R. Foster, *J. Chem. Soc.*, **1954**, 2153.
5) R. Schaal, *Compt. rend.*, **239**, 1036 (1954).
6) R. Foster, *Nature*, **175**, 746 (1955).
7) J. B. Ainscough and E. F. Caldin, *J. Chem. Soc.*, **1956**, 2528.
8) S. Nagakura and S. Oosawa, Presented at the 12th Annual Meeting of the Chemical Society of Japan, held at Kyoto in April, 1959.